PROPERTIES AND PERFORMANCE OF POLYMER MODIFIED CEMENTS AND MORTARS

MAT KHAIR SALBIN

Doctor of Philosophy

THE UNIVERSITY OF ASTON IN BIRMINGHAM

May 1996

The University of Aston in Birmingham

PROPERTIES AND PERFORMANCE OF POLYMER MODIFIED CEMENTS AND MORTARS

Submitted by **Mat Khair Salbin** for the degree of PhD
May 1996

THESIS SUMMARY

Polymer modified cements and mortars have become popular for use as patch repair materials. General evidence suggests that these materials offer considerable improvements compared to traditional mortars although the mechanisms for this are not fully understood. This work elucidates the factors which govern some properties and performance of different polymer systems.

In view of the wide range of commercial systems available, investigations concentrated on the use of three of the most commonly available groups of polymers. These were: (1) Styrene Butadiene Rubber (SBR), (2) Acrylics and, (3) Ethylene Vinyl Acetates (EVA). The later two were in the form of both emulsions and redispersible powders.

Experiments concentrated on:

(1) Rheological behaviour of polymer modified cement pastes
(2) Workability of polymer modified mortars
(3) Influence of curing conditions on the pore size distribution and diffusion of chloride ions
(4) Bond strength of polymer modified cement and mortar patches
(5) Microscopic examination and semi-quantitative analyses of the bulk and interfacial microstructures

The following main conclusions were reached:

(1) The addition of polymer emulsions can have a considerable influence on the workability of fresh cement pastes, the extent of this depending on the type of system used.

(2) The rheological parameters of fresh polymer modified mortars can be established using a two-point workability test which may be used when comparing the properties of different systems at constant workability.

(3) Curing conditions affect the properties of polymer modified systems and a wet/dry curing regime was essential for good adhesion of these materials to mortar substrates.

(4) In contrast, the wet/dry curing regime resulted in a curing affected zone at the surface of patch materials. This can result in a much coarser pore structure and enhanced diffusion of e.g. chloride ions.

(5) The microstructure of polymer modified systems was very different compared with the unmodified cement/mortar and varied depending on curing conditions. A non-uniform distribution of polymer, intimately associated with cement hydration products was found and there was little evidence for the presence of a distinct polymer film phase.

KEY WORDS: Cement, polymer modified, rheology, porosity, bond, microstructure.

Dedicated to my wife and children

ACKNOWLEDGEMENTS

I would like to thank the following people and organisations for their support and assistance during the course of my research;

Dr Neil Short: For excellent supervision and helpful suggestions throughout my research and during writing of this thesis.

The staff of the Civil Engineering Department, Research Fellows, Research Assistants and friends.

Doverstrand Ltd, Hercules Ltd, Rhom and Haas Ltd, Vinamul Ltd and Wacker Chemicals Ltd.

Finally, to the Government of Malaysia for financial support and SIRIM for granting study leave.

LIST OF CONTENTS

8 BOND STRENGTH AND MICROSTRUCTURE OF INTERFACES

9 GENERAL DISCUSSION, CONCLUSIONS AND FUTURE WORK

LIST OF TABLES

LIST OF FIGURES

1 INTRODUCTION AND AIMS

1.1 INTRODUCTION

Concrete structures should have sufficient durability to withstand environmental conditions for the duration of their design life, which may be in excess of 60 years. In practice there are many causes that may limit durability. These include, for instance, exposure to weathering, impact damage, attack by chemicals, alkali-aggregate reactions etc. Many of these will change the microstructure of the material in such a way that leads to failure. An essential feature in the long term durability of a reinforced concrete structure is the protection of the steel reinforcement to avoid cracking, spalling and ultimate failure.

Traditional mortar or concrete has high compressive strength but low tensile, flexural and impact strengths. The presence of voids, gel and capillary pores makes concrete a permeable material. The permeability of concrete will determine whether aggressive agents and water can penetrate. A damaged structure may be reinstated by application of a patch repair material. However, lack of adhesion of new mortar or concrete to the old is also a problem. Furthermore, ordinary mortar or concrete used for this repair material may not last very long as it will be exposed to the same environment as the original.

Various methods have been used to improve the properties of cements, mortars and concretes and in this respect the incorporation of polymers, to produce what might be termed polymer-cement composites, has received considerable international attention.

There are three principal routes for the production of polymer-cement composites:

(i) Polymer-modified cement, mortar and concrete (PMC)

(a) Starting with an essentially standard fresh mix, polymers are incorporated as an aqueous dispersion (latex). As the concrete cures, the polymer particles in the latex flocculate and coalesce to form a continuous film which binds hydrates and aggregate together.

(b) A variation on the above involves addition of liquid monomer to a fresh mix followed by in-situ polymerisation which occurs at the same time as cement hydration.

(ii) Polymer impregnated mortar and concrete (PIC)

Polymer impregnated mortar and concrete consists of a hardened Portland cement concrete that has been impregnated with a monomer which is subsequently polymerised in-situ. A low viscosity monomer is introduced into the concrete by either atmospheric or pressure soaking. The polymerisation process may be initiated by thermal catalysis, promoted catalysis or gamma-ray radiation. The resulting composite consists of hardened concrete and a continuous polymer network that fills most of the voids. This will generally result in a less permeable matrix but the quality of the final product depends very much on the quality of impregnation and polymer used.

(iii) Polymer mortar and concrete (PC)

In these systems polymers are used to replace Portland cement as the binder for mineral aggregates. Monomer is combined with well graded fillers such as ground calcium carbonate, silica, fly ash, and mixed so that the monomer coats the surface of the aggregate. The monomer resin is then cured shortly after placement as a result of polymerisation reactions. The final properties of the composites are dominated by the quality of binders and properties of aggregates used.

The relative importance of these three types of polymer-cement composites has changed with time but from a practical point of view types (i) and (iii) are used far more widely than type (ii). Type (iii) tends to be more expensive.

This present work is concerned only with type (i) - polymer modified cements / mortars.

1.2 POLYMER MODIFIED CEMENTITIOUS MATERIALS

The use of polymer dispersions as additives to modify the properties of cement mortar and concrete has increased rapidly in recent years. Applications include patch repair of concrete structures, grouts, bridge deck overlays and flooring. Polymer modified cements, mortars and concretes may be prepared by adding the polymer in the form of either a latex or redispersible powder.

(a) Latex: The polymer is in the form of a fine aqueous dispersion which is added to the mixing water. A wide variety of forms are available e.g.

Elastomeric -

- Styrene-Butadiene Rubber (SBR)
- Chloroprene Rubber (CR)
- Acrylonitrile -Butadiene Rubber (NBR)

Thermoplastic -

- Acrylics (Ac)
- Styrene-Acrylic (SAc)
- Vinyl Acetate (VA)
- Ethylene-Vinyl Acetate (EVA)
- Vinyl Chloride-Vinylidene diChloride- (VCdC)

(b) Redispersible Powders: In the case of redispersible powder polymers (originally from a polymer dispersion) all the dry ingredients are pre-blended followed by mixing with water. During wet mixing the powdered polymers are re-emulsified and behave in a similar manner as the lattices. However, the particles in a polymer dispersion which has been made from redispersible powder tend to be larger than in the case of an emulsion and hence the properties of the final products may be different. Examples include:

Acrylics (Ac)

Ethylene-Vinyl Acetate (EVA)

Vinyl acetate-Vinylversatate (VaVe)

Vinyl acetate-Vinylversatate-Acrylic (VaVeAc)

In both cases polymer compositions vary widely and all dispersions include other constituents with surfactant, bactericide, anti-oxidant and anti-foaming agent being the most common.

The addition of polymers to mortars and concretes results in modification of both the fresh and hardened characteristics. In general terms:

- The same level of workability can be achieved at lower water/cement ratios compared to the unmodified mix.

- Hydration characteristics and setting of the cement may be modified as a result of possible interactions between cement minerals and polymer.

- The products of cement hydration include an agglomeration of calcium silicate hydrates, calcium aluminate hydrates and calcium hydroxide which in the case of polymer modified cement becomes an even more complex matrix including a polymer network. This network

modifies the hardened cement matrix in such a way that allows a polymer film to bridge microcracks, improving mechanical properties.

There is a large amount of general evidence that concrete polymer composites offer improvements to traditional concrete with regard to enhancing durability, resistance to chemicals and other physical properties. Improved durability results from reduced penetration of carbon dioxide, chloride ions, water and freeze thaw damage.

Finally, an improved bond is found with existing substrates.

1.3 SCOPE FOR FURTHER IMPROVEMENTS

The specific properties of materials depend very much on the formulation of the polymer dispersion, mortar mix design and curing procedures used. There are numerous proprietary polymer emulsions and redispersible powders available. Polymer compositions vary widely and all dispersions include other constituents such as surfactant, bactericide, anti-oxidant and anti-foaming agent. Little information is available on mix procedures, a primary aim being to use the minimum water/cement ratio for the required workability. This information or requirements are very often recommended by the supplier.

Workability of mortars can be characterised by its flow properties. For a Bingham material, measurements must be made at not fewer than two different shear rates (two-point) in order to measure yield value and plastic viscosity. Thus any test in which only one measurement is made, that is a single-point test, is incapable of providing sufficient information to describe the flow properties of a Bingham material. Methods used to date have been predominantly the single point type of test e.g. slump or flow.

The kinetics and mechanisms of hydration of polymer modified cements are not understood. (This aspect is being looked at in an associated project, Zeng, 1996).

Interactions between polymers and hydrating cement are known to occur e.g. saponification, release of chloride ions etc. although their extent is not fully understood. (Again, this aspect is being looked at in an associated project, Zeng, 1996).

Curing regimes involving wet-dry cycles are often recommended for these materials since they result in good mechanical properties. This type of regime goes against that normally considered as suitable for good durability.

The nature of the polymer phase and its effect on mechanical properties and bond to existing substrates is not fully understood.

1.4 THE AIMS OF PROJECT

The present investigation deals only with polymers in the form of latex or redispersible powders. Chapter 2 covers the general literature for these types of system. The materials used are given in Chapter 3 but details of the experimental techniques used are covered in the relevant chapters.

The main aims of the investigations are as follows:

(i) To establish suitable methods and procedures for describing the workability of polymer modified cements and mortars in terms that reflect their true flow behaviour. These tests could then be used when comparisons are being made of the properties of different polymer-cement systems at constant workability.

The rheological behaviour of fresh cement pastes and mortars have been investigated using a coaxial cylinder viscometer with ribbed sensor and cup, and a two-point workability apparatus respectively. The influence of different polymer

systems, mix proportions and water/cement ratios has been determined (Chapters 4 and 5).

(ii) To study the influence of curing conditions on, porosity, pore size distribution and the resistance to chloride ion diffusion, for hardened polymer modified cement pastes.

The influence of different curing regimes, particularly a wet-dry one, on pore structure at different distances from the curing surface have been investigated using Mercury Intrusion Porosimetry (Chapter 6). The influence of different polymer systems, polymer contents and water/cement ratios was determined. A limited study has been made of the diffusion of chloride ions in polymer modified cements (Chapter 7).

(iii) To investigate the bond strength between a new polymer modified cement / mortar patch and an old mortar substrate.

Adhesion in tension and flexural tests were used to determine bond strength of the polymer modified patch. The influence of curing conditions, polymer content and types of polymer were investigated (Chapter 8).

(iv) To investigate the morphology of the bulk polymer-cement composites and the loci of failure after mechanical debonding between a new polymer modified patch and an old mortar substrate.

Scanning Electron Microscopy (SEM) with Energy Dispersive X-Ray Analysis (EDXA) and Thin Section Microscopy (TSM) along with visual examination were used to determine the type and loci of failure and interfacial microstructure between polymer cement composites and old substrates (Chapter 8).

2 LITERATURE REVIEW

2.1 INTRODUCTION

The incorporation of polymers in concrete started early this century. The initial use of a latex-hydraulic cement involved incorporation of natural rubber latex with cement and was used as a paving material. The first patent on the use of polymers in concrete was issued to Cresson (1923). Further developments included patents issued to Lefebure (1924), Kirkpatrick (1925) and Bond (1932).

More patents were issued in the 1940's and 1950's on the use of modified systems which incorporated synthetic latexes, such as polychloroprene rubber, polyacrylic, polyvinyl acetate and other synthetic resins. The Concrete Society Technical Report No. 39 (1994), reported that it was only in the last 10 years that polymer additions had become commercially significant. This was mainly due to a strong interest by engineers to utilise these materials for repair and restoration of damaged reinforced concrete structures.

It can be seen that polymer modified cement composites have now become widely accepted throughout the world. This was reflected in the development of standards for materials and test methods and similar efforts are actively being pursued by various organisations in Europe, United States and Japan.

2.2 HYDRATION OF ORDINARY PORTLAND CEMENT

Hydration of Portland cement is a sequence of overlapping chemical reactions between clinker components, calcium sulphate and water, leading to cement paste stiffening and then hardening. The stiffening process is the consequence of a change from concentrated

suspension to a viscoelastic skeletal solid. The subsequent decrease in porosity and formation of complex hydration products is called hardening, which leads to the development of mechanical strength. The hydration reactions continue until no more water is available to react with cement components.

The process is very complex involving dissolution-precipitation and the various hydration reactions proceed simultaneously at differing rates. Immediately after mixing, a large amount of heat is evolved followed by nucleation and slow growth of C-S-H gel and $Ca(OH)_2$. The subsequent decrease in the Ca^{2+} concentration triggers acceleration of alite dissolution, and further heat is evolved. Overall porosity of the paste decreases due to continuous deposition of C-S-H gel and other hydration products (Jawed *et. al.*, 1983). The C-S-H gel and $Ca(OH)_2$ are in the form of a continuous skeleton. The C_3A reacts with sulphates to form ettringite (AF_t phase) or in the case of insufficient sulphate, ettringite dissolves and reacts with $Al(OH)_4^-$ to form monosulpho-aluminate hydrate (AF_m phase). In the case of low C_3A contents, but an excess of calcium sulphate, the AF_m phase may not form at all.

The product of these hydration reactions gives a structure of high specific surface area namely cement gel. The relevance of these chemical processes to mechanical properties have been discussed by Jawed *et. al.*, (1983) and are given in Table 2.1.

2.3 HYDRATION OF INDIVIDUAL CEMENT COMPOUNDS

The most abundant compounds in Portland cement are listed below and expressed by various empirical formulae and their abbreviations:

1) Tricalcium silicate, $3CaO \cdot SiO_2$ C_3S

2) Dicalcium silicate, $2CaO \cdot SiO_2$ C_2S

3) Tricalcium aluminate, $3CaO \cdot Al_2O_3$ C_3A

4) Tetracalcium aluminoferrite, $4CaO . Al_2O_3 . Fe_2O_3$ C_4AF

The hydration of Portland cement in the early stages is usually dominated by the hydration of C_3S (alite). This produces amorphous material, C-S-H gel, and calcium hydroxide and can be described by the following equation:

$$2C_3S + 7H \longrightarrow \underset{\text{(CSH gel)}}{C_3S_2H_4} + \underset{\text{(Portlandite)}}{3CH} \qquad (2.1)$$

Similar hydration products are formed by the hydration of C_2S. However, the hydration and development of microstructure are very slow compared to C_3S. The reaction of dicalcium silicate can be shown as follows:

$$2C_2S + 5H \longrightarrow \underset{\text{(CSH gel)}}{C_3S_2H_4} + \underset{\text{(Portlandite)}}{CH} \qquad (2.2)$$

The proportion of C_3A in Portland cement is comparatively small but it is the most reactive component towards water. In order to slow down its reaction and control cement setting, gypsum is added to the cement. Gypsum ($CaSO_4.2H_2O$) combines with C_3A in the presence of water to form insoluble calcium sulphoaluminates (ettringite), until all the gypsum is consumed. The reaction can be shown as follows:

$$C_3A + 3C\bar{S}H_2 + 26H \longrightarrow \underset{\text{(ettringite)}}{C_6A\bar{S}_3H_{32}} \qquad (2.3)$$

or

$$C_6A\bar{S}_3H_{32} + 2C_3A + 4H \longrightarrow \underset{\text{(monosulpho-aluminate hydrate)}}{3C_4A\bar{S}H_{12}} \qquad (2.4)$$

The remaining fraction of cement composition is a solid ferrite solution referred to as C_4AF, which also reacts with gypsum. Jawed *et. al.*, (1983) suggested that the rates at

which the individual clinker compounds react with water are different and much more complex than shown in the general equations.

Hydration products are deposited in the pore space, large hexagonal $Ca(OH)_2$ crystals engulf parts of previously formed C-S-H gel, and overall the morphology becomes featureless with microcracks clearly visible.

2.4 POLYMER DISPERSIONS

A polymer consists of long molecular chains made up of many repeat units. The single unit from which the chains are made is known as a monomer, and contains unsaturated double bonds which are capable of reacting. A polymer with different characteristics may be formed by incorporating a second monomer into the chain to become a co-polymer. The length of the polymer chain is specified by the number of repeat units, and chains are usually very much coiled or entangled. An example of chain addition polymerization to produce the co-polymer styrene-butadiene rubber (SBR) is as shown in Section 2.4.1.

The polymers used in mortars and concretes are available in various forms including powders, solution, dispersions, and also as expanded solids. A dispersion is a two-phase system, comprising very fine polymer particles (the disperse phase) suspended in a non-solvent liquid (the continuous phase), usually water. Surfactants are added during manufacture of the emulsion and attach themselves to the surface of the latex particles. Other compounding ingredients are also added, such as bactericides, antioxidants, ultraviolet protectors, and antifoaming agents (ACI 548.3R-91, 1991).

Lattices are divided into three different classes according to the type of electrical charge on the particles, which is in turn determined by the type of surfactants used to disperse them. The three classes of lattices are cationic (positive), anionic (negative) and non-ionic (no

charge). Anionic and non-ionic surfactants may be used with cement (Dennis, 1992), although those most widely used are non-ionic (ACI 548.3R-91, 1991).

Typical polymer lattices used in modifying mortars or concrete are polyvinyl acetate (PVA), polyacrylates and natural rubber. Copolymers used include styrene butadiene rubber (SBR), styrene acrylates, ethylene vinyl acetate (EVA) and vinyl acetate/vinyl versatate. The solids content in water is around 45 - 70% but 45 - 50% is most commonly used. Lower solids contents of 20 - 25% are reportedly (Concrete Society Technical Report No. 39, 1994) being used on site in conjunction with pre-blended bags of aggregates and cement where no further addition of water is required.

2.4.1 Styrene Butadiene Rubber Co-polymers

Styrene butadiene rubber (SBR) is a synthetic latex which has been used as an admixture to Portland cement mortar in the United States & UK since 1950s (ACI 548.3R, 1991). The combination of styrene and butadiene with water, a surfactant and an initiator causes styrene and butadiene to polymerise as follows:

Step 1:

$$R^* + CH_2 = CH-CH = CH_2 \longrightarrow CH_2-CH = CH-CH_2^*$$
$$\qquad\qquad\qquad\qquad\qquad\qquad\qquad\quad |$$
$$\qquad\qquad\qquad\qquad\qquad\qquad\qquad\quad R$$

Butadiene

Step 2:

$$CH_2-CH = CH-CH_2^* + CH_2 = CH \longrightarrow CH_2-CH = CH-CH_2-CH_2-CH^*$$
$$\quad | \qquad\qquad\qquad\qquad\quad | \qquad\qquad\quad | \qquad\qquad\qquad\qquad\qquad\quad |$$
$$\quad R \qquad\qquad\qquad\qquad\quad C_6H_5 \qquad\quad R \qquad\qquad\qquad\qquad\qquad\quad C_6H_5$$

Styrene

* = reactive valence

R* = free radical

Both monomers are hydrophobic and it is claimed that (ACI 548.3R, 1991 and CSTR No. 39, 1994) this enables a Portland cement concrete modified with SBR to have superior water resistance and other physical/mechanical properties. Surfactants, unsaturated carboxylic acids (such as methacrylic and acrylic acid), antifoaming agents, antioxidants, bactericides and ultraviolet protectors are the most common compounding ingredients used in the production of SBR latex.

Carboxylate groups are incorporated in the polymer chain to the extent of about 1% expressed as monomer ratio, by e.g. acrylic acid as shown below:

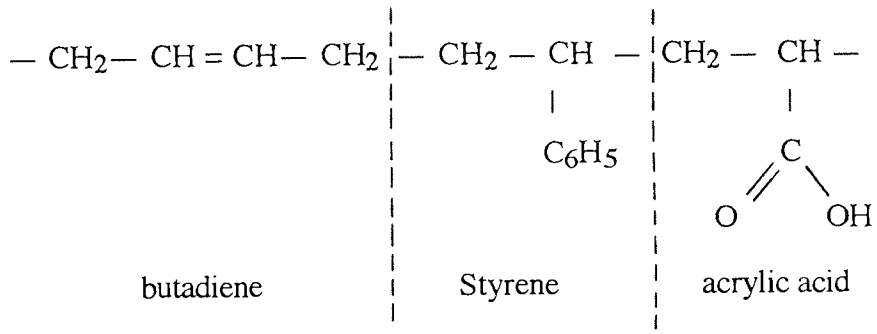

(2.5)

In alkaline conditions the carboxyl groups on the polymer particle produce a negative charge that may provide links between the polymer and the calcium ions from cements. These polar groups improve the physical and chemical stability of the dispersion, and improve its adhesion to many types of background.

2.4.2 Acrylics

Acrylics are a widely varying family of polymers, resulting from the polymerization of derivatives of acrylic acid. Acrylic polymers used with Portland cement are composed mainly of polyacrylates and polymethyl acrylates. Polymerization of acrylic monomers can be in bulk, by solution polymerization or emulsion polymerization.

Acrylics are not easily attacked by chemicals and generally have excellent durability. Acrylic monomers however are more expensive than other monomers. Cheaper acrylics

were later developed by incorporating the styrene co-monomer but their properties are slightly poorer than the unmodified acrylics.

2.4.3 Polyvinyl Acetate (PVA)

Polynivyl acetate is a thermoplastic polymer and was used extensively in the 1960s and 1970s as a versatile bonding agent. PVAs have many features that make them compatible to produce polymer-modified mortars. However, PVAs have proved unreliable in long-term performance for outdoor applications. They are readily hydrolysed in the alkaline conditions to give polyvinyl alcohol and acetic acid, both of which are water-soluble. Significant improvement in wet environments and resistance to hydrolysis can be achieved by introducing a variety of hydrophobic monomers. For example, VeoVa (a vinyl ester) and VA can polymerised to produce superior performance in wet environments.

Ethylene was introduced as a hydrophobic co-monomer to modify VA. At high pressures, VA and ethylene copolymerize to give high molecular weight products. The resulting co-polymer of VAE with optimum ratio of ethylene/vinyl acetate and emulsifier can give superior performance not only in dry conditions but can maintain good performance in wet conditions.

2.4.4 Redispersible Polymers

A further development of polymer dispersions for use with cement is the introduction of redispersible polymer powders. Most of the polymers of this type are ethylene vinyl acetate (EVA), VA/VeOVa copolymer systems and acrylics. Redispersible polymer powders are produced by spray drying an emulsion polymer. Generally a colloid such as polyvinyl alcohol (PVOH) is incorporated to improve redispersibility and as a stabilising agent. An inert filler is also blended as an anti-caking agent.

Redispersible polymer powders are increasingly popular for factory produced proprietary pre-packed polymer modified mortars where polymer powders are first blended with cement and aggregates. This is followed by mixing with the required amount water at the point of application. During mixing the powdered polymers are re-emulsified and behave in a similar manner as the lattices for cement modifiers. The particles in polymer dispersions which have been made from powder polymers are much larger than the original dispersion, hence the properties of the final product may not be as good as they would have been if the original dispersion had been used. However, it was reported that the performance of redispersible powdered polymers is nearly equivalent to that of the percursor emulsion (CSTR, 1994, Afridi *et. al.*, 1994).

2.5 CHEMICAL INTERACTIONS BETWEEN POLYMER AND OPC

When polymer is added to a fresh mix of cement, water and aggregate, interactions may take place during the hydration of cement. The actual mechanisms of interactions between polymer and cement during the hydration process are not fully understood.

A review by Chandra and Flodin (1987a) on the interactions of polymers and organic admixtures with Portland cement suggests two possible theories. The first theory suggests that there is no interaction between polymer and cement minerals. The second theory suggests that polymer interacts with the components of Portland cement hydration products and creates a type of reinforcement in the cement phase.

The review showed that most investigations involved looking at interactions of various types of polymer mixed with $Ca(OH)_2$ solution or other hydration products such as C_2S and C_3S. However, when polymer and cement are mixed in the presence of water, multiple reactions of various constituents will occur simultaneously. Certain types of polymer are

known to react chemically with cements, thus substantially changing the nature of the polymer phase.

Significant loss of compressive strength for wet cured cement pastes modified with PVA was reported by Wagner (1966). The strength reduction was attributed to the chemical reaction involving polymer. Ohama (1984), Øye (1989) and Øye & Justnes (1991a) reported that polyvinyl acetate (PVA) which is usually used as tile slip adhesive may saponify in wet conditions resulting in irreversible chemical change and poor water resistance. The reactions can be shown in the following manner:

$$-(-CH-CH_2-)- + OH^- = -(-CH-CH_2-)- + R-C-O^- \qquad (2.6)$$

(O, C–R, ||, O) (OH) (O)

both products are soluble in an alkaline environment

In the case of polyvinyl chloride (PVC) and polyvinylidene chloride (PVDC) hydrolysis occurs in the alkaline interior of mortar and concrete, releasing free chloride ions, shown by Wagner & Grenley (1978), Øye (1989), Justnes & Øye (1990a) and Larbi & Bijen (1990) to be as follows:

$$-(CH_2-CH)- + OH^- = -(CH_2-CH)- + Cl^- \qquad (2.7)$$

(Cl) (OH)

PVC PVA

or

$$-(CH_2-CH)- + OH^- = -(CH_2=CH)- + H_2O + Cl^- \qquad (2.8)$$

(Cl)

PVC

The chloride ions released from the hydrolysis or decomposition process could initiate corrosion of the embedded steel.

When carboxylic groups are hydrolysed in an alkaline environment of $Ca(OH)_2$ the calcium salt can form which may then react by ionic bonding with other constituents. This may then inhibit polymer film formation (Chandra and Flodin, 1987a & b). The reaction is shown as follows:

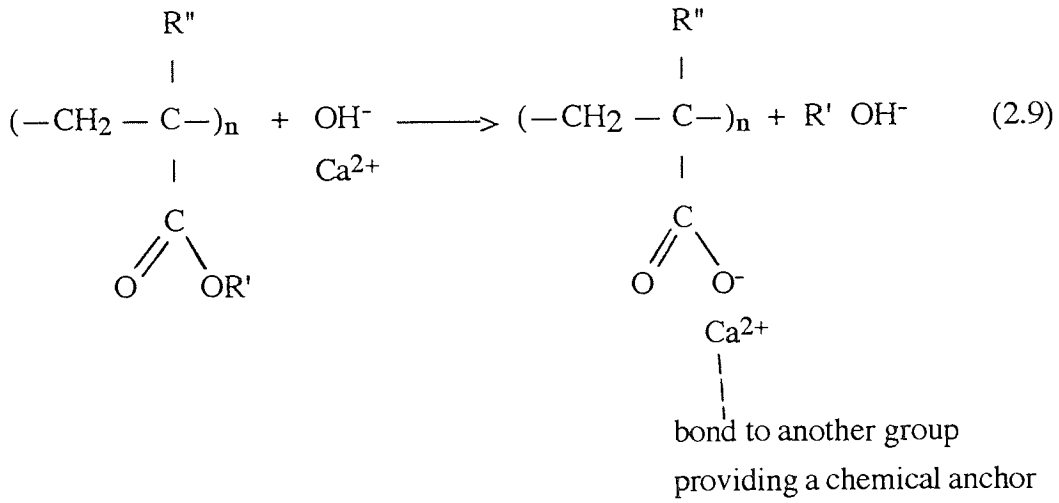

(2.9)

Links may be made with $Ca(OH)_2$, calcium silicates and tricalcium aluminate. The cross-linking of polymer particles (equation 2.9) from the carboxylate groups with solid $Ca(OH)_2$ is illustrated as follows (Chandra and Flodin, 1987a):

(a) by divalent Ca^{2+}

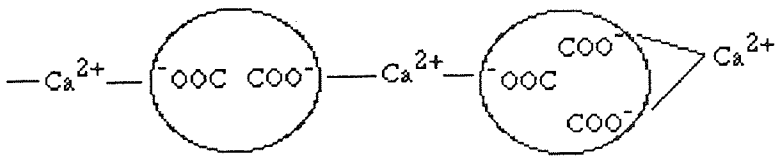

(b) by $Ca(OH)_2$

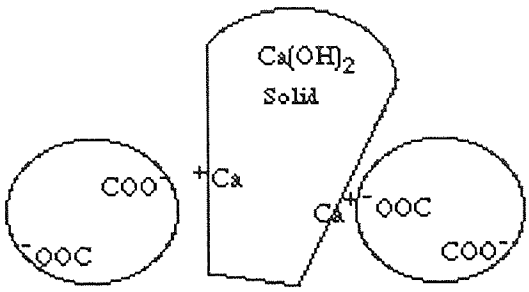

However, the review by Chandra and Flodin (1987a) indicates that chemical interactions only occur between individual components of Portland cement with certain type of polymers. The review suggested that the mechanisms of interactions between polymers and Portland cement during their reaction with water and hydration are very difficult to explain and not fully reported by other workers.

Justnes and Dennington (1988) suggested that it is possible to design polymers that will improve the flexural strength of cement mortars and concrete regardless of curing and exposure conditions. They reportedly combine n-butylacrylate (BA), methyl methacrylate (MMA) and a functional monomer. A functional monomer is added to give the base polymer some special properties, for example to act as 'chemical anchor' between the polymer and cement gel. The resulting terpolymer can be shown as follows:

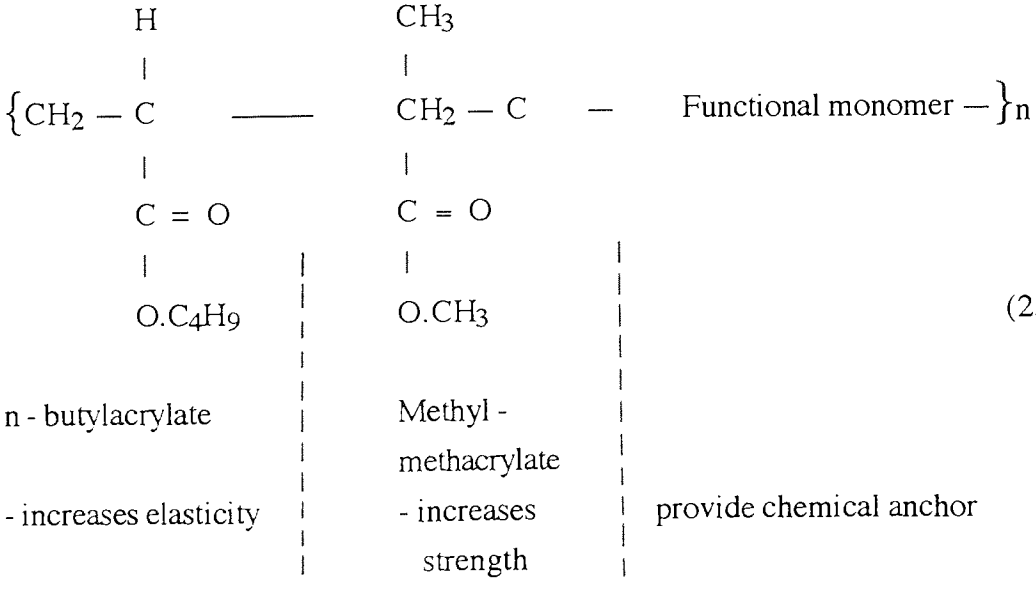

It was suggested that the functional monomer may couple together either by self-reaction or through chelate formation with polyvalent elements from the cement. From the latter mechanism, larger molecules and clusters may be formed and thus lead to further improvement in mechanical properties. However, the type of functional monomer was not given, but Shaw's (1989) work suggests that this functional monomer could be acrylic or methacrylic acid which are capable of bonding strongly to cements.

2.6 PRINCIPLE OF POLYMER MODIFICATION

According to Ohama (1984), latex modification of cement mortar and concrete is governed by first the hydration of cement, followed by formation of polymer film. He suggested that the final structure consists of cement gel with the polymer film acting as a binder. The process of hydration and film formation is simplified into three steps as described below, and shown in Fig. 2.1:

Step 1:

Polymer particles are uniformly dispersed in the cement phase when lattices are mixed with fresh cement mortar or concrete. The cement gel is gradually formed by cement hydration and the water phase is saturated with calcium hydroxide. Polymer particles are deposited on unhydrated cement particles, cement gel and aggregate.

Step 2:

As the cement hydration proceeds, the water is consumed, and polymer particles flocculate to form a continuous close-packed layer of polymer particles on the surfaces of unhydrated cement particles and aggregate.

Step 3:

Finally, when water demand is reduced or lost during hydration, the close-packed polymer particles finally coalesce into a continuous film which binds the cement hydrates together to form a monolithic network. This network is thought to interpenetrate throughout the cement hydrate phase.

The formation of a polymer film within the cement paste should in theory increase the bonding within the paste structure and at the paste/aggregate interfaces.

The model of polymer film formation put forward by Ohama (1984) was very much a simplified version of a hypothesis developed earlier by Isenburgh and Vanderhoff (1974). The hypothesis was deduced after examining the fracture surface of plain mortar and mortar modified with vinylidene chloride and stryrene-butadiene copolymer latexes using the scanning electron microscope. With the support of electron micrographs, they suggested that microfibres from styrene-butadiene polymer mortar were capable of bridging the microcracks and adhering to the mortar substrate. The microstructure of non-film forming latexes (vinylidene chloride) was significantly different compared with plain mortar which showed typical microcracks due to shrinkage. Based on the above observation, they presented the following hypothesis:

i) Latex substitutes for all or part of the water in the mix to give fluidity at lower water/cement ratio.

ii) Latex particles coalesce in a thin layer around each unhydrated cement grain and aggregate particle to form an interpenetrating network of polymer throughout the structure.

iii) Microcracks form throughout the structure to relieve the strains introduced by the shrinkage of hydrated Portland cement that occurs at a relative humidity of less than 100%.

iv) A propagating microcrack intersects the interpenetrating polymer network which results in microfibres spanning the microcrack, halting propagation and holding the faces of the microcrack together.

Neither of the above hypotheses explains the mechanism of structure development but rather explains the performance of polymer modified mortars. Evidence of the polymer layer coalescing into a continuous film and bridging microcracks is very difficult to find. The most common technique used involves a study of the fracture surfaces of polymer modified cement or mortars using scanning electron microscope and comparing it with the one without polymer. Attempts by many workers to locate or spot this discrete polymer film in the cement matrix have proved futile. The only evidence of polymer film bridging the microcracks is the micrograph from the work of Isenburgh and Vanderhoff (1974), although this has been reproduced and published many times, e.g. Riley & Razl (1974), Dennis (1985), Kuhlmann, (1987) and ACI 548.3R (1991).

The difficulty of locating a discrete polymer film in the mortar matrix was reported by Øye (1989). Scanning Electron Microscope with backscatter electron imaging, which was linked to an energy dispersive x-ray (EDXA) analyser was used in the study. Polymer phase was found only in the PVAc/PE/PVC and epoxy modified mortars where high carbon and chlorine peaks were obtained from epoxy and PVC respectively. Other elements such as calcium, silicon and iron were also detected. Justness and Øye (1990b, 1992a) concluded that the simplified polymer film formation model shown in Fig. 2.1 was basically correct. This was demonstrated by SEM photographs of the etched surfaces of polymer modified mortars with 15 volume percent of acrylate. A continuous network of polymer film may be achieved by using 5 - 10 volume percent of polymer at water/cement ratio of 0.5. However, the suggestion of polymer network was not supported by the EDXA and details of the etching technique were not reported.

2.7 PROPERTIES OF FRESH MIX

2.7.1 Workability

Polymer modified cement and mortars can produce an exceptionally good workable mix compared with an ordinary mix of the same water/cement ratio. Thus, for equivalent workability the water/cement ratio may be reduced.

This improved workability is thought to be mainly due to the dispersing effect of components in latex. According to Ohama (1984), improved consistency is due to the ball bearing action of the polymer particles, entrained air and dispersing effect of surfactants. He demonstrated that a SBR latex significantly improved workability even at the solids-cement ratio of 0.05. Fig. 2.2 shows how the water reducing effect of a concrete mix can be achieved by the addition of latex.

Øye (1989) measured the flow and slump of PVAc/PE/PVC, PVAC/VeOVa, SBR and epoxy modified concretes. At a water/cement ratio of 0.4 and polymer content of 10 and 20%, results showed that PVAc/PE/PVC, PVAc/VeOVa and SBR produced collapse slump and self-levelling concrete, but epoxy showed a marked thixotropic behaviour. SBR mixes showed the best all round workability. He concluded that the highest workability obtained is probably due to surfactants used in the latex. The findings are in agreement with the trends reported by Ohama (1984), ACI 548.3R (1991) and CSTR No. 39 (1994).

2.7.2 Air content

A large quantity of entrapped air in polymer modified mixes is common compared to that in unmodified mortar and concrete. This is because of the action of the surfactants used as emulsifiers and stabilizers in the manufacture of latex. The air content of most latex modified mortars is in the range of 5 - 20%. Although some entrained air is useful to

improve workability and resistance to freezing, an excessive amount causes a significant reduction in strength. The amount of entrained air can be controlled by adding a suitable anti-foaming agent in the latex or during mixing.

2.7.3 Setting

It is important to differentiate between the setting time and working time of polymer modified mortar and concrete. The setting time is a function of the hydration of the cement but working time is the time needed to place, work and finish before drying of the surface will hinder proper finishing. Ohama (1984) reported that the setting time of latex modified mortar and concrete is either equal or slightly delayed compared to the ordinary mix depending on the type of polymer and polymer/cement ratio. Further delay in the setting time may occur as the polymer content increases. The delayed setting is probably due to the surfactants in the latex which inhibit the hydration of cement.

2.7.4 Water retention

The recommended curing of polymer modified concrete is moist cure for 24 - 48 hours followed by air drying. During curing, the latex will immediately form a layer of polymer film on the evaporation surface that acts as a barrier for further evaporation. This will allows proper hydration of cement followed by coalescence of polymer film. The water retention ability can be monitored by measuring weight loss of specimens during curing.

Excellent water retention of concrete modified with SBR, NBR, PAE and PVAC compared to ordinary mix was reported by Ohama (1984). However, this may vary depending on the types of polymers used. Øye (1989) reported that some rapid loss of water through evaporation occurred as a result of retardation of the hydration caused by polymers containing acetate and acrylate groups. The water loss from SBR modified mortar was similar to the unmodified.

2.8 TYPICAL PROPERTIES OF HARDENED POLYMER MODIFIED MORTAR AND CONCRETE

2.8.1 Compressive strength

Improvement in compressive strength is not an objective when adding lattices to ordinary concrete because it known that many systems produce similar compressive strengths when compared to unmodified systems (Emberson and Mays, 1990a). At the same workability, compressive strength can be increased by the low water/cement ratio and reduced entrained air. Low air content can be obtained by adding appropriate amount of suitable anti-foaming agent.

2.8.2 Tensile and Flexural strengths

For polymer modified concrete, the type and duration of curing have significant influence on the tensile and flexural strengths. Maximum strength can be achieved by wet cure (100% RH) for the first 24 - 48 hours, followed by dry curing at ambient temperature and humidity (Ohama, 1984, ACI 548.3R, 1991). Initial wet curing allows proper hydration of cement, and dry curing allows excess water to evaporate and formation of polymer film.

Considerable increases in tensile and flexural strengths can be achieved by the inclusion of polymer to Portland cement concrete. Emberson and Mays (1990a) reported that out of nine generically classified repair systems, tensile strength of resinous materials and polymer modified systems were significantly higher than the unmodified. This was attributed to the high tensile strength of polymer film and improvement in the cement hydrate-aggregate bond.

Factors such as curing conditions, polymer/cement ratio, cement, aggregates and testing procedures also affect the tensile and flexural strengths (Ohama, 1984, Emberson & Mays,

1990a & b, ACI 548.3R, 1991). In general, tensile and flexural strengths of polymer modified mortars reduced significantly when exposed to wet curing.

2.8.3 Impact and Abrasion Resistance

Latex-modified mortar or concrete has an excellent impact and abrasion resistance compared with the unmodified concrete. The impact and abrasion resistance generally increase with increasing polymer/cement ratio and depend on the type of polymers added (Ohama, 1984). The impact resistances of the latex modified mortars with elastomers are reportedly superior to those of the mortars with thermoplastic resins. Excellent abrasion resistance has resulted in polymer modified mortar and concrete being successfully used for repairing and protecting parking structures, bridge decks and concrete floors (Kuhlmann, 1987, ACI 548.3R, 1991).

2.8.4 Permeability and Durability

Water absorption

The resulting morphology of polymer cement composites is such that micropores and voids may be partially filled by polymers or sealed by the three dimensional polymer network, thus increasing resistance to water penetration compared with ordinary mortar and concrete. Thus the polymer film is partly responsible for reduced permeability and water absorption by acting as barrier due to its hydrophobic nature. Ohama (1987) suggested that increase in pore diameters of less than 75 nm is further responsible for improvement in the impermeability. Methods such as water absorption, water vapour transmission, carbonation resistance and chloride permeability are commonly used to measure these properties.

Generally the water absorption is considerably reduced as the polymer content increases except in the case of polyvinyl acetates which hydrolyse under alkaline environment

(Ohama, 1984, Walters, 1990). Improved water resistance can be obtained by using ethylene vinyl acetate. Banfill *et. al.* (1993) reported that water permeability (measured by the Figg Test) of mortars modified with ethylene vinyl acetate and blended cements was reduced by a factor of more than 10 as polymer/cement ratio increases. They only speculate that this was probably due to blocking of pores by the coalesced polymer.

Chloride ion penetration

The low water permeability of latex modified concrete also contributes to the low chloride penetration. However, the reported performance of chloride penetration may vary depending on the type of polymers and test methods. Typical values of chloride ion diffusion coefficient which is estimated as a result of exposure to 2.4 % NaCl content is shown in Table 2.2. The values shown both for mortars and concretes are probably marginally better than those of the unmodified mortars and concretes.

Large reduction in the effective diffusivity of chloride ions using specially formulated shrinkage compensating mortar was reported by McCurrich (1993). The materials used are based on aluminate binder systems modified with appropriate plasticisers, redispersible polymer powder, shrinkage compensation and other additives. However, the type of polymer used was not mentioned. Justnes & Øye (1990a) and Øye & Justnes (1991b) reported that chloride penetration of polymer modified concrete is greatly influenced by the effect of lowering its water/cement ratio (but maintaining a constant workability) and the presence of chemical anchors.

Carbonation

Carbonation occurs when CO_2 in the air diffuses through the pores and voids of the concrete and reacts with the cement paste forming $CaCO_3$. This reaction causes

neutralisation of alkaline environment which reduces the pH to < 9. This destroys the passivity of the steel and leads to possible corrosion of reinforcement.

The carbonation resistance of latex modified mortars and concretes is either improved or not significantly improved depending on the types of polymers, water/cement ratio and exposure conditions. Most of reported work on carbonation was performed on laboratory samples. Ohama (1984, 1987) reported that carbonation resistance of most latex modified mortars remarkably improved. The carbonation depths of polymer modified mortars under a CO_2 pressure of 0.3 MPa and long term outdoor exposures were reportedly low compared with the control mortars. Significant improvement of carbonation resistance of a specially formulated shrinkage compensating polymer modified mortar was also reported by McCurrich (1993).

However, Øye (1989) and Øye & Justnes (1991a) reported that the carbonation resistances of polymer modified mortars were not significantly improved. The tests were performed on several types of polymers using mortar prisms of 40 x 40 x 160 mm, subjected to 3% CO_2 at 50 - 70% RH and temperature of 20°C for up to 36 weeks. The carbonation resistance of different systems varies significantly. This was partly due to the different amount of air contents produced by the different polymers which allows different rates of CO_2 diffusion into interconnecting capillaries of the mortars.

Freeze-thaw resistance

The performance of latex modified concrete to the freeze-thaw cycles varies depending on the types of polymers and exposure conditions. The freeze-thaw durability is generally improved due to the less permeable matrix and the effect of entrained air. Damage due to freezing and thawing is minimised because less or no water penetrating into the matrix. Entrained air will relieve the expansive forces when freezing occurs. A study was carried out on the adhesion and flexural strength of mortars modified with two different acrylic

polymers (Lavelle, 1988). The specimens were exposed in the north-eastern part of the US, and subjected to at least 70 freeze-thaw cycles and 1300 mm rain per year. The results indicate that adhesion and flexural strengths are retained and all adhesives tests showed cohesive failure for the acrylic modified mortars but adhesive failure for the unmodified controls.

High retention of flexural strength of polymer modified mortar prisms after 25 cycles of freeze-thaw by alternating temperatures every 24 hours at -10°C and 24°C was reported by Walters (1990). Poor performance was recorded from PVA which as expected, caused by the hydrolysis of the vinyl acetate group (see section 2.5).

Chemical resistance

Mechanisms of deterioration caused by acids, sulphates, solvents and chloride attacks to hardened mortars and concretes are described in detail elsewhere (CEB, 1992, Lees, 1992 and Neville, 1993). Some improvement in the chemical resistance of LMC is probably due to good water impermeability that reduced the ingress of deleterious chemicals. However, most LMC are attacked by organic or inorganic acids and sulphates. This is simply because the hydrated cement is attacked by these chemicals. Some elastomeric latexes are attacked by solvents. Generally, the chemical resistance of LMC very much depends on the chemical compositions of latexes to initiate reactions with acids, alkalis and solvents.

2.9 ADHESION OR BOND STRENGTH

2.9.1 Bonding of Fresh Mortar to Substrate

The adhesion or bond strength of the polymer modified mortars is one of the important properties required in practical applications. Superior bond performance is crucial for applications such as floor toppings, water proofings, deck coverings, coatings and patch

repairs. The moment fresh polymer modified cement or mortars are placed onto the old concrete (substrate), chemical interactions at the interface, surface diffusion and intermolecular action occur in stages. It is important that the two phases must be in contact as close as possible. Strong bonding at the interface of the two phases is possible through chemical bonds (strong polar interactions) and physical bonds (via van der Waals forces). It is obvious that when two phases are brought into contact, bonding may occur in a number of ways.

A good bond is likely to be achieved by taking steps to minimise shrinkage and ensuring good contact with the dampened substrate (Tabor, 1992). According to Naderi *et. al.* (1987) good bond strength achievement depends on the:

i) Degree of roughness of the substrate surface
ii) Wetting characteristics of the repair mortar
iii) Cleanness of the substrate
iv) Method of application (shotcreting etc.)
v) Degree of porosity and absorptivity, and
vi) Curing regimes

The placing of patch repair is preceded by wetting the substrate with water. Standing water should be removed by compressed air or by other suitable means. Bonding may be enhanced by applying a thin coat of latex mortar grout or slurry before the patch or overlay (Kuhlman, 1987, ACI 548.3R, 1991). The repair or overlay should be placed whilst the bond coat is still in a wet condition. Adhesion properties were further improved by using a slurry coat of SBR modified cement as a bonding aid with polymer solids of between 40 - 50% by weight of cement (Perkins, 1984, Judge *et. al.*, 1986). It is also important to obtain a pH close to 10.

However, not all polymer systems improve adhesion strength. Work by Su & Bijen (1990) and Su *et. al.* (1991a & b) showed that pull-off adhesion strength of styrene acrylate (SA), vinyl-propionate-vinyl chloride (VVC) and acrylate with coupling agent (ACA) polymer modified cement pastes to limestone and granite vary depending on polymer content and curing conditions compared with the unmodified paste. The increase in adhesion strength of SA modified paste at longer age was obtained but not for the VVC and ACA modified pastes.

Further caution is required in order to avoid short and long term problems as a result of incompatibility and property mismatch of repair and old substrates (Emberson and Mays, 1990a). They suggested that for structural repairs, the property of repair materials should meet certain requirements and be compatible with the old concrete, see Table 2.3. However, in practical situations it is difficult to obtain a perfect match simply because lack of data available on the property of substrates or old concrete.

A difference in elastic modulus will influence the stress concentration at the bond plane in the patch repair and substrate because of the difference in lateral deformation in the bond area. A low modulus patch may suffer high stress concentration that will lead to failure. This was demonstrated by the experimental and analytical predictions for nine different types of repair materials (Emberson and Mays, 1990b). Austin *et. al.* (1995) demonstrated that the difference in shrinkage causes the stress variation along the bond line. At the edge of the bond plane, the principal stress diverts from a horizontal direction and a tensile stress component acting on the bond plane is generated. This tensile stress tends to lift the overlay causing debonding of the new patch.

2.9.2 Adhesion or Bond Failure

A good bond between polymer modified mortars and mature hardened concrete substrate can readily be achieved in controlled conditions or with good working practice (Naderi *et.*

al., 1987). Surface preparation of concrete substrate prior to receiving fresh mortar should include removal of all loose and unsound concrete particles or contaminated areas either by mechanical, thermal or pneumatic pressure. The common methods used for surface preparation include sand-blasting, wire-brushing, high pressure water jet cleaning or vacuum blasting.

For polymer modified mortars, the development of adhesion is attributed to the high adhesion of the polymer to the substrate. However, the data on adhesion properties are often vary depending on the testing methods, service conditions, porosity of substrates and types of polymers (Ohama, 1984). The general trend suggests that the adhesion of most LMC tends to increase with the increase in polymer solids content.

The bond failure or adhesive failure often occurs when early preparation is not sufficient. Others are due to weaknesses in the two phases or at the interfacial region. According to Sasse and Fiebrich (1983) three types of adhesion failures often occurred to the patch repair. The types of failures are cohesion failure in the patch repair, cohesion failure within the concrete (near the surface) and adhesion failure in the contact zone between concrete and patch repair. Although there are variations in the equipment and methods of carrying out bond strength test, interpretation in assessing types of adhesion failures are similar. This is best illustrated by Mcleish (1993) and shown in Fig 2.3.

Cohesion failures within the patch occur probably due to tensile and shear stresses, air inclusion within the patch, stress variations during curing and incompatibility of patch. Cohesion failure of concrete substrate normally occurs due to low quality concrete near the surface, improper surface preparation and further deterioration as a result of chemical attacks or physical damage. Adhesion failure normally occurs due to poor chemical or physical bond between the two phases. Plum (1990) suggested that, for cosmetic or small patch repairs, failures may occur as a result of; i) high shrinkage due to inadequately cured patch, leading to cracking or curling, ii) high local stresses leading to debonding, iii) high

expansion due to temperature, moisture or thermal shock. Other reasons are associated with the surface preparation of the substrate (Marosszeky *et. al.*, 1991) and the property mismatch (Emberson and Mays, 1990a), between the new and old concrete.

2.9.3 Test Methods

Several test methods have been used to test the bond between new patch material and old concrete. For bond strength measurement, the most commonly reported procedures are; 1) Adhesion in tension, 2) Shear strength, 3) Pull-off strength, and 4) Adhesion in flexure. Various test methods have been used by Ohama *et. al.* (1986) to study the bond between polymer modified mortar and ordinary cement mortar, Fig 2.4. The test on various polymer modified systems suggest that each test produced similar trends of adhesion results. The failure mode however, varies markedly between the test methods and polymer cement ratio.

The slant shear test described in BS 6319 (1984) was initially devised to test the adhesive bond of resins, but is now widely used to test the bond strength of patch material. The standard also describes the procedures for preparing substrates with an inclination angle of 30°. Patch material is then cast to make a complete prism. The prism is then tested in compression which gives shear bond strength of the patch material. However, a considerable scatter of results was obtained by Eyre and Domone (1985) when the specimens were tested at inclination angle of 30°, 45° and 50°. The failure normally occurs either to the patch or substrate and not at the interface. This test has been criticised as not really measuring the bond strength at the interface but it is a combination of compressive, shear and bond strengths.

In an attempt to standardise a large number of different tests, CIRIA Technical Note 139 (McLeish, 1993) produced a technical report that listed a variety of pull-off tests including the types of equipment used to test repair materials and coatings for concrete. Some of the tests have been adopted as standard by various countries and organisations. However, not

all pull-off tests are relevant for bond test of patch materials. Furthermore, the pull-off tests should be conducted with care as partial debonding could occur due to the development of stress concentrations during pull-off (Robins and Austin, 1995). This may reduce the actual tensile bond strength of patch materials.

As mentioned earlier, most procedures adopted do have limitations. Very often the results of adhesion or bond test showed a considerable scatter. Therefore strength measurement requires a set of specimens so that the results can be analysed statistically. Apart from statistical analysis, the types of failure at the interface are examined and assessed physically and microscopically.

Microstructure at the failure interface can be examined by using optical microscopy, scanning electron microscopy (SEM), transmission electron microscopy (TEM), infrared spectroscopy (IP), X-ray photoelectron spectroscopy (XPS), X-ray fluorescence and other associated SEM and TEM techniques as described by Barnes and Ghose (1983).

2.10 TYPICAL APPLICATIONS OF POLYMER CEMENT COMPOSITES

2.10.1 Adhesives

Polymer dispersions combined with thickeners and inert fillers are commonly used for fixing tiles, gluing objects and other applications in the construction industry. The use of polymer dispersions in combination with hydraulic cements is widely practiced as an adhesive to fix brick slips, glass blocks, kerb, ceramic floors and wall tiles.

Polymer dispersion/cement mixtures also give good protection to steel, and are therefore used to protect steel reinforcement and as primer/undercoat on structural steelworks. The mixtures are also used between the floor slab and the screed topping to avoid the risk of

debonded screeds due to shrinkage (Tabor, 1992). The most commonly used water-borne adhesives to bond concrete are polyvinyl acetate (PVA), vinyl acetate copolymers, polyacrylic esters and styrene butadiene copolymers (ACI 503, 1992).

2.10.2 Cement slurries and grouts

Cement slurries are normally used as levelling compound before laying sheet flooring materials. They may also be used as a damp-proof membranes or to replace the more conventional polythene sheet. The thickness of polymer cement slurries usually varies from 1 to 5 mm.

Polymer/cement grouts are used as a protective coating to steel sheet and reinforcement. These grouts are also being used successfully with tar macadam in the resurfacing of airfield runaways and hard standings (CSTR, 1994). Polymer/cement grouts are vibrated into the first laid macadam to fill all the voids. The resulting composites were reportedly more economic due to shorter time of construction, flexibility compared to concrete and fuel resistance.

2.10.3 Mortars

Normal cementitious mortars used as patch repair materials often suffered from early cracking, debonding, high porosity, rapid carbonation and are susceptible to frost damage. One method of improving the performance of patch cementitious repair mortars is by the introduction of polymer emulsions. Careful selection of polymers such as SBRs, acrylics, styrene acrylics and various vinyl acetate copolymers could improve bond and increase tensile strength, and so reduced the tendency for cracking and debonding. Polymer also acts as a water reducing agent which results in strength increase, low porosity and improved workability.

The use of LMC is restricted to a thickness of between 6 to 25 mm. Although there are examples of floor screed or toppings up to 100 mm thick, the cost may be too high and drying out process for latex particles will be too slow (Dennis, 1985). SBR latex modified concrete has been reported to give a good all round performances as overlays for bridge decks and parking garages (ACI 548.3R, 1991). Other applications (Dennis, 1992) of polymer modified cementitious mortars include:

i) bonding agents
ii) floor screeds, underlayments and toppings
iii) fixing brick slips and ceramic tiles
iv) bedding paviour
v) bricklaying mortars and external renders
vi) renders over external insulation
vii) sprayed coatings
viii) pipe coatings, etc.

Further applications of polymer modified patch repair mortars are; reprofiling mortars and flexible cement coatings. The fairing coat or reprofiling mortars can be applied between 3 to 4 mm thick after the patch repair (McCurrich, 1993). The fairing coat is used to minimise the problem of long term drying shrinkage and to act as a very effective chloride and carbonation barrier.

A further development (CSTR, 1984) has been the use of redispersible powder polymer which can be factory blended with sand, cement and other additives, to give mortars simply by adding water at the point of applications. Recent trends (Tabor, 1992) suggest that a number of systems became available using the preblended proprietary mix which were supplied with a bottle of polymer dispersion. A suitable amount of water is then added on site to give a required workability.

Table 2.1: Physical meaning of basic Portland cement hydration reactions (Jawed *et. al.*, 1983)

Reaction stage	Chemical processes	Physical processes	Relevance to mechanical properties
First minutes	Rapid initial dissolution of alkali sulphates and aluminates; initial hydration of C_3S; formation of AFt	High rate of heat evolution	Changes in liquid phase composition may influence the subsequent setting
First hours (induction period)	Decrease in silicate but increase in Ca^{2+} ion concentration; formation of CH and C-S-H nuclei begins; Ca^{2+} concentration reaches a supersaturation level	Formation of early hydration products; low rate of heat evolution; continuous increase of viscosity	Formation of AFt and AFm phases may influence setting and workability. Hydration of calcium silicates determines initial set at end of induction period
Approximately 3-12 h (acceleration stage)	Rapid chemical reaction of C_3S to form C-S-H and CH; decrease of Ca^{2+} supersaturation	Rapid formation of hydrates leads to solidification and decrease in porosity; high rate of heat evolution	Change from plastic to rigid consistency (initial and final set); early strength development
Post-acceleration stage	Diffusion-controlled formation of C-S-H and CH; recrystallisation of ettringite to monosulphate and some polymerisation of silicates possible. Hydration of C_2S becomes significant	Decrease in heat evolution. Continuous decrease in porosity. Particle-to-particle and paste-to-aggregate bond formation	Continuous strength development at diminishing rate. Decrease in creep. Porosity and morphology of hydrated system determine ultimate strength, volume stability, and durability

Table 2.2: Apparent chloride ion diffusion coefficient of latex modified mortars and concretes (after Ohama, 1987)

Type of mortar	Polymer content (%)	Apparent chloride ion diffusion coefficient (x 10^8 cm^2s^{-1})	Type of concrete	Polymer content (%)	Apparent chloride ion diffusion coefficient (x 10^8 cm^2s^{-1})
Unmodified	0	6.4	Unmodified	0	2.2
SBR	10	6.4	SBR	10	1.9
	20	3.9		20	9.3
EVA	10	4.4	EVA	10	7.9
	20	2.4		20	1.0
PAE	10	3.8	PAE	10	6.2
	20	4.4		20	5.8

Table 2.3: General requirements of patch repair materials for structural compatibility, (Emberson and Mays, 1990a)

Property	Relationship of repair mortar (R) to concrete substrate (C)
Strength in compression, tension and flexure	$R \geq C$
Modulus in compression, tension and flexure	$R \approx C$
Poisson's ratio	Dependent on modulus and type of repair
Coefficient of thermal expansion	$R \approx C$
Adhesion in tension and shear	$R \geq C$
Curing and long term shrinkage	$R \leq C$
Strain capacity	$R \leq C$
Creep	Dependent on whether creep causes desirable or undesirable effects
Fatigue performance	$R \geq C$

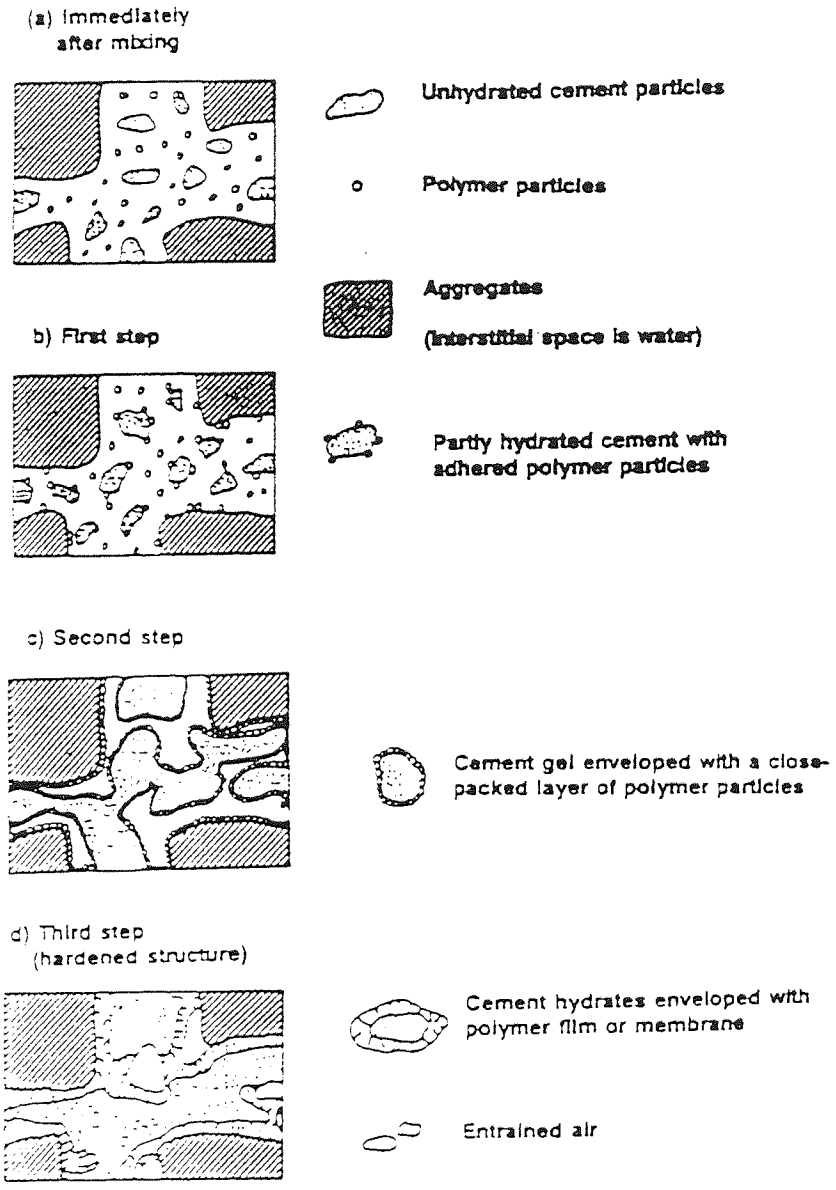

Fig. 2.1: The process of polymer film formation (Ohama, 1984)

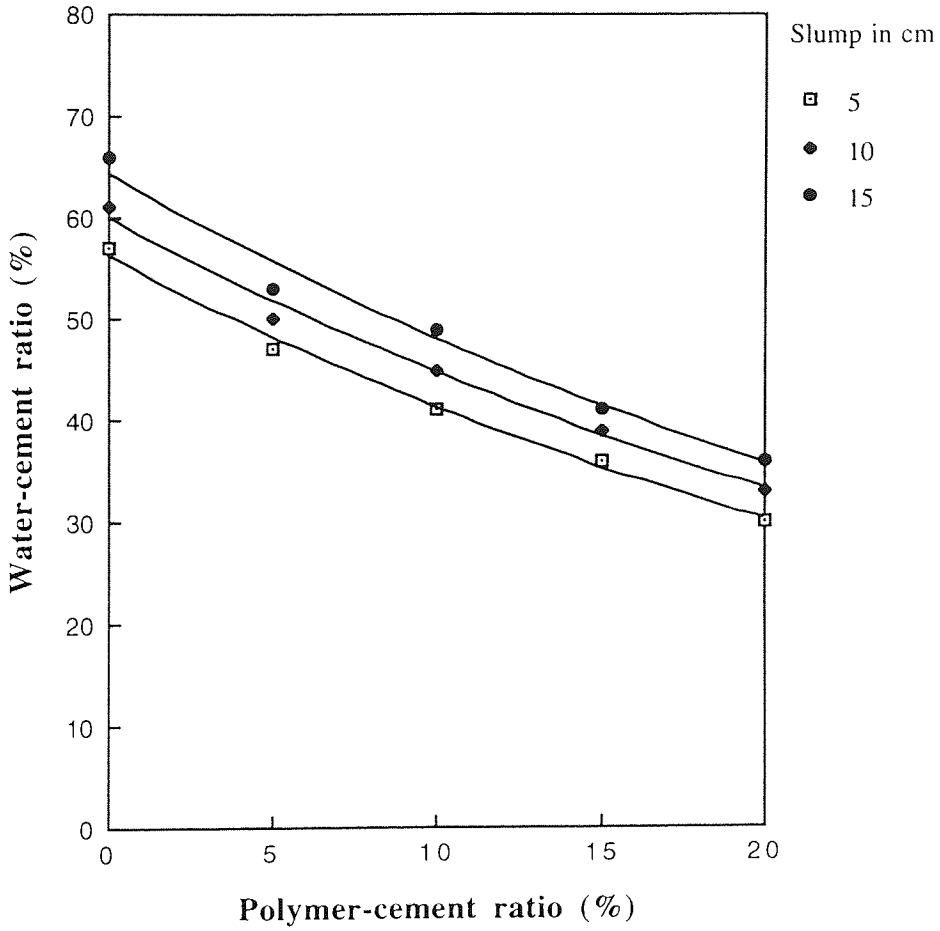

Fig. 2.2: Relation between polymer-cement ratio and water/cement ratio of SBR-modified concretes to give slumps of 5, 10 and 15 cm (after Ohama, 1984).

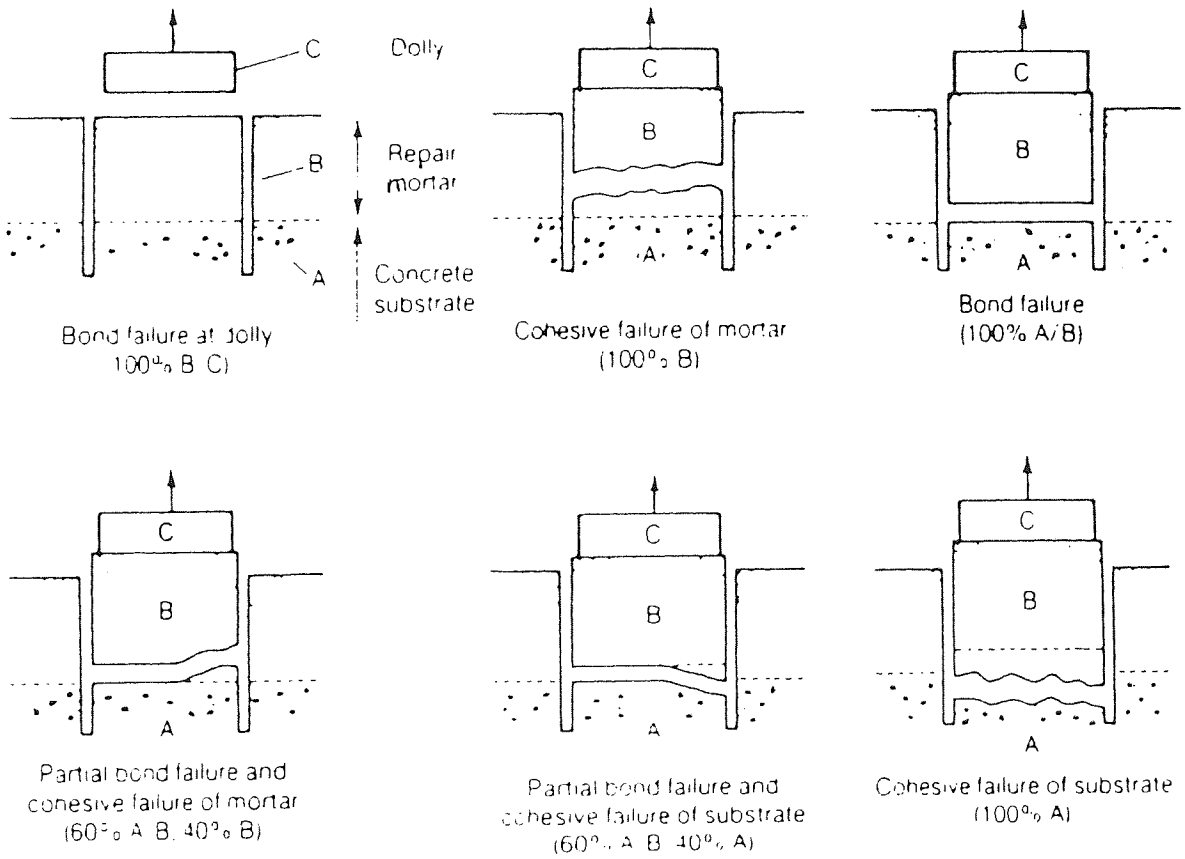

Fig. 2.3: Types of failure for pull-off test (Mcleish, 1993)

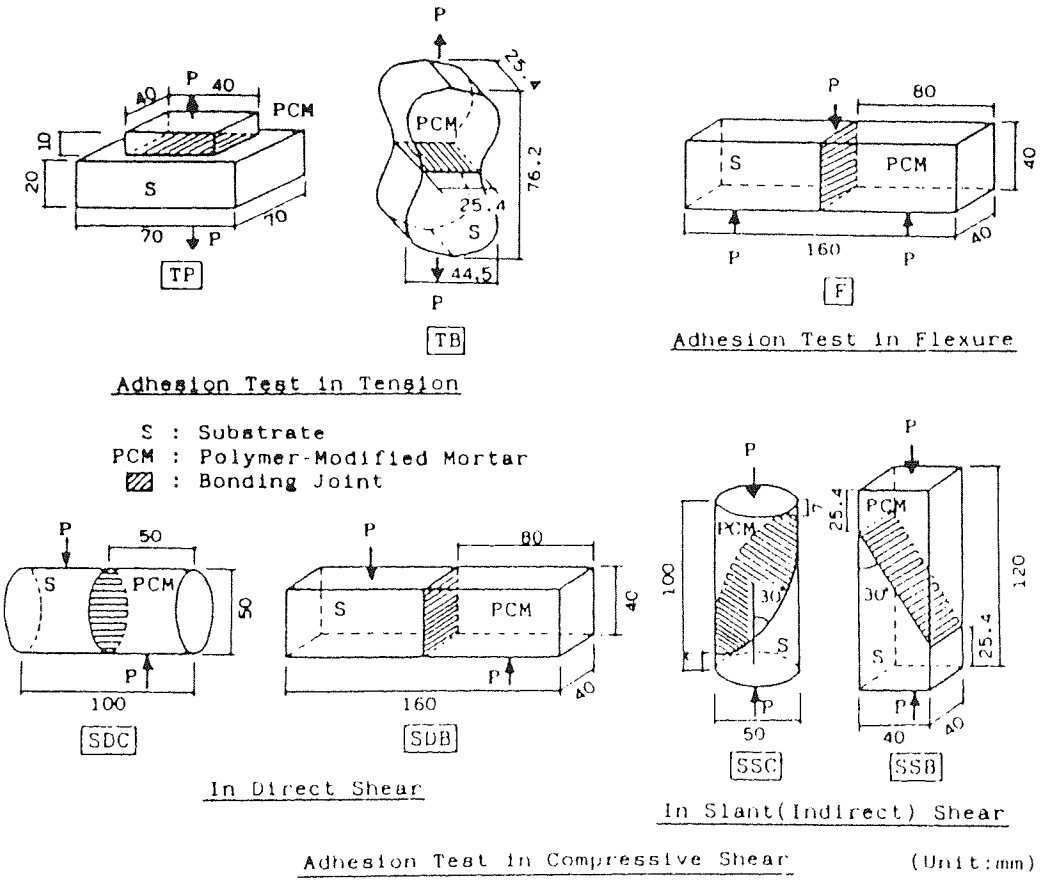

Fig. 2.4: Adhesion test configurations (Ohama *et. al.*, 1986)

3 MATERIALS

3.1 CEMENT

The cement used was an ordinary Portland cement, (Aston Standard 3) for which the chemical composition, expressed in percentages by weight of the constituent oxides is shown in Table 3.1.

3.2 AGGREGATES

The sand used was washed quartzite from the Upper Trent Terrace with a maximum size of 5 mm and conforming to Zone 2 of BS 882: 1990. Sands 1 and 2 shown in Table 3.2 were obtained by sieving and discarding particles larger than 850 μm and 2.36 mm respectively.

3.3 POLYMERS

The polymers used (see Table 3.3) included Styrene-Butadiene Rubber (SBR) latexes, acrylics and ethylene vinyl acetate (EVA) copolymers. These were chosen since they are the most commonly used in practice. Acrylics and EVAs were in the form of emulsions and redispersible powders. Redispersible powders are becoming more popular since they are supplied in easily disposed paper bags compared with latexes which are supplied in non-returnable plastic drums.

The SBR emulsions used were a standard carboxylated SBR (designated SBR 1), and a special carboxylated SBR (designated SBR 2). Both contained 47% polymer solids, non-ionic stabilisers, and anti-foaming agents; particle sizes were in the range 50 - 200 nm, the pH value was 9.5 and specific gravity was 1.01 in each case. The essential difference was that the amounts of carboxylic acid chemically bound in SBR 1 and SBR 2 were

1% and 5% respectively, expressed as monomer ratios. The aqueous component of SBR 2 (designated Aq. Comp), which included the stabilisers and anti-foaming agent but not the polymer solids was used only in the rheology tests.

Two types of acrylics were used, one in the form of an emulsion and the other was a redispersible powder. The acrylic emulsion used (designated Ac 1) contained 47% polymer solids, the pH value was 9.5 - 10.0 and specific gravity was 1.0 - 1.02. The redispersible acrylic powder (designated Ac 3) had a bulk density of 450 ± 100 g/l. Ac 3 was only used in the rheology test. Anti-foaming agents were not present in either case.

Three types of ethylene vinyl acetates were used; a redispersible powder - Vinamul 10166 (designated EVA 1), a Vinamul 3281 emulsion (designated EVA 2) and a second redispersible powder from a different supplier - Elotex 1080 (designated EVA 3). Particle size of EVA 1 was 10 - 250 μm and upon dispersion was 0.7 - 1.5 μm. For EVA 2, the polymer solids was 55%, the particle size was 1 - 3 μm, density of 1.07 g/cm^3 and the pH value was 4.0 - 5.0. All ethylene vinyl acetates contained a stabilising system of polyvinyl alcohol (PVOH).

Note: It was not always possible to get exact details of formulations from suppliers.

3.4 DEFOAMER

The defoamer (anti-foaming agent) used was a hydrophobic silica hydrocarbon oil; Hercules 1512M. It was added, during mixing, to all systems except the SBR 1 & 2 latexes which already contained a standard amount of defoamer.

3.5 EXPERIMENTAL TECHNIQUES

All experimental techniques will be discussed in the relevant chapters.

Table 3.1: Chemical analysis of cement and proportions of compounds

Oxides (weight %)

CaO	SiO_2	Al_2O_3	Fe_2O_3	SO_3	MgO	Na_2O	K_2O	LOI*
65.3	20.6	5.32	2.58	3.03	1.20	0.09	0.75	0.72

* Loss on ignition

C_3S	C_2S	C_3A	C_4AF
61.14	13.02	9.74	7.84

Bogue Compound

Table 3.2: Particle size distribution of sands (% passing BS sieve)

Sand	Sieve size						
	2.36 mm	1.18 mm	850 μm	600 μm	300 μm	150 μm	<150 μm
1	-	-	100.0	94.4	63.5	11.0	0
2	100.0	88.8	-	79.8	53.7	13.3	0.02

Table 3.3: Polymer systems

Code	Type	Form	Supplier & code
SBR 1	Styrene-Butadiene-Rubber copolymer, 1% carboxylic acid	Emulsion	Doverstrand - Revinex 29Y40
SBR 2	Styrene-Butadiene-Rubber copolymer, 5% carboxylic acid	Emulsion	Doverstrand - 6486
Aq Comp	Aqueous component of SBR 2	Solution	Doverstrand
Ac 1	Acrylic copolymer	Emulsion	Rohm Haas - Primal E330S
Ac 3	Acrylic copolymer	Powder	Wacker - Vinnapas LL512M
EVA 1	Ethylene-Vinyl-Acetate copolymer	Powder	Vinamul - 10166
EVA 2	Ethylene-Vinyl-Acetate copolymer	Emulsion	Vinamul - 3281
EVA 3	Ethylene-Vinyl-Acetate copolymer	Powder	Elotex A G - 1080
De	Defoamer	Oily liquid	Hercules - 1512M

4 RHEOLOGICAL BEHAVIOUR OF FRESH POLYMER MODIFIED CEMENT PASTES

4.1 INTRODUCTION

The relative performance of the wide range of modified mortar systems that are becoming available is difficult to assess and will depend on the actual procedures used (Dennis, 1985). Usually this involves comparison at the same percentage of dry polymer by weight of cement and using either the same water/cement ratio or sufficient water to give the same workability. For modified cement systems the same workability as the unmodified cement is normally achieved at lower water/cement ratios.

Comparisons have been made at constant workability using empirical tests such as slump, flow table and flow cone. However, the flow properties of fresh cements, mortars and concretes are quite complex. Flow properties are usually expressed in terms of relationships between shear stresses, shear strains and time. Typical relationships are as shown in Fig. 4.1.

Thus for a Newtonian liquid such as water or oil,

$$\tau = \eta\dot{\gamma} \tag{4.1}$$

where η is viscosity.

It is known that most mortars and concretes conform to the Bingham plastic model of behaviour (Banfill, 1987) as given by equation (4.2), relating shear stress τ, to shear rate $\dot{\gamma}$. Two parameters, the yield value τ_o, and the plastic viscosity μ, are then needed to characterise such materials.

$$\tau = \tau_o + \mu\dot{\gamma} \qquad (4.2)$$

Cement pastes are best described as conforming to shear thinning type of behaviour, where $n < 1$ as given by equation 4.3.

$$\tau = A\dot{\gamma}^n \qquad (4.3)$$

Equation (4.3) is also applicable to pseudoplastic or power law liquids which can give shear thickening behaviour, where $n > 1$.

Although the rheological behaviour of cement pastes and mortars/concretes are different, it is often assumed that the rheological behaviour of mortars / concretes is strongly influenced by the behaviour of fresh cement paste. It is the cement hydration reactions and associated microstructural changes which lead to setting of mortar / concrete.

The **main aim** of the present investigation was to compare the rheological behaviour of cement pastes mixed with various polymer systems using a viscometric technique. Cement pastes were investigated since it may be easier to interpret the influence of polymer additions without the presence of aggregate.

4.2 PREVIOUS WORK

The rheological behaviour of cement paste is complex and the most appropriate method of measuring it is by using a viscometer. It is possible to study the flow behaviour of cement paste under the action of a steady shear, its relationship between shear stress, shear rate and water/cement ratio.

Using various mathematical models and a Weissenberg rheometer with cone-and-plate geometry, Jones and Taylor (1977) investigated the flow curves of cement pastes with water/cement ratio of 0.3 to 0.5. The results of shear stress and shear rate have been used to develop empirical equations to construct the flow curves of a cement paste. The model developed was basically a combination of Bingham and power law models with additional constants which were suitable for that particular rheometer.

A specially built couette rheometer with fixed inner cylinder and a rotating outer cylinder was successfully used by Berg (1979). Serrated cylinders were used with the inner cylinder radius of 37 mm, outer cylinder radius was 38 mm and the height of inner cylinder was 100 mm. Equilibrium flow curves of cements with different particle sizes and concentration of solids were examined. Yield values were reported to increase with increasing specific solid surface at constant solids concentration. Shear thickening increased with the increase in solids concentration. The range of water/cement ratio used was 0.4 to 0.8. It was reported that cement paste with water/cement ratio of 0.4 was too stiff and could not be loaded into the apparatus. Flow curves were evaluated at mean shear rates of up to 1800 s^{-1}. However, Berg (1979) only analysed the flow curves in the region of shear thinning where the results were consistent. This was done simply to avoid complicated mathematical formulae to describe flow curves of cement pastes.

A comprehensive review on the structure and rheology of fresh cement paste by Helmuth (1980) suggested that the flow behaviour of cement pastes depend very much on the paste composition and testing conditions. The fineness of the cement and the water/cement ratio were said to be the major factors affecting the flow behaviour of fresh pastes. Additions of water-reducing and other organic admixtures to concrete made the rheological behaviour of cement pastes simpler compared to that of plain mixes. Admixture molecules become attached to the surface of the cement grains, increasing inter-particle repulsive forces, thus allowing cement to be fully dispersed. However, a well defined yield value from the shear strain rate versus shear stress were often not very clear. It depends

very much on the shear history and paste compositions. The review suggested that the flow behaviour of fresh cement pastes may indicate any of the trends shown in Fig. 4.1 except Newtonian.

Three types of viscometers with different geometries namely MVIIP, S13/15 and H/MVS were used by Banfill (1981) to study the flow behaviour of cement paste containing superplasticizers. Two types of admixtures used were sulphonated melamine fomaldehyde resin (type M) with solids content of 20%, and sulphonated naphthalene fomaldehyde resin (type N) with solids content of 37%. Three different flow curves were obtained but the down curves were characteriastic of a typical Bingham plastic material. The three different flow curves obtained were due to differences in geometry of the equipment used, shear rate applied and the degrees of structural breakdown which occurred in the pastes.

The effect of mixing, type of cement, equipment and shear cycle on hysteresis curves were reported by Banfill and Saunders (1981). In their work, shear cycle was immediately started after 2.5 minutes from the first addition of water. Rotational speed was increased to 200 rpm (176 s^{-1}) and decreased to zero again. It was reported that the time to complete a cycle varied from 2 to 36 minutes. From the hysteresis curves, they suggested that a short cycle time of less than 2 minutes should be used in rheological test. This suggests that the flow behaviour of cement paste is rather complex once many variations of test methods were introduced.

Different types of devices to study the flow behaviour of fresh pastes were used by Lapasin *et. al.* (1983). The hysteresis cycles of cement pastes were determined using the rotating coaxial cylinder viscometers of Haake Rotovisco RV3 with sensor systems of MVI, MVII, MVIIP and SVI. Four experimental procedures used were; *1)* tests at constant shear rate, *2)* step-wise decreasing shear rate *3)* step-wise increasing shear rate and *4)* hysteresis cycles. One type of cement and water/cement ratio of 0.3 to 0.4 were used. Lapasin *et.al.* (1983) suggested that procedure *(2)* should be used because cement

paste structure has already broken down once the cement paste has passed a sequence of low to high shear rate. This will produce a set of a steady data of shear stress and shear rate since the kinetics of structural rebuilding is negligible. However, the hysteresis loops obtained from different sensors were significantly different. This was attributed mainly to the dissimilarity in geometry of sensor systems.

Apart from the differences in the techniques and equipment used, the rheological behaviours of fresh pastes can be presented together with their mathematical models. Various mathematical models were applied and fitted into the data of shear stress and shear rates obtained from the rheological experiment using viscometer (Atzeni *et.al.*, 1985). Tests were conducted using Haake Rotovisco with SVIIP sensor. The data of second cycle of the hysteresis curves were used in the regression analysis and fitted into various models described by earlier workers namely Herschel & Bulkley (1926) and Eyring (1936). It has been suggested that the following models are the most suitable:

Eyring	$\tau = \text{asinh}^{-1}(Db)$	(4.4)
Herschel & Bulkley	$D = a(\tau - c)^b$	(4.5)

where τ is shear stress, D is shear rate, a, b and c are constants.

Basically the models shown in Equations (4.4) and (4.5) are capable of describing the rheological behaviour of cement pastes which is a combination of Newtonian, Bingham plastic and pseudoplastic. The simple derivations from Equation (4.5) will eventually explain a typical well-known rheological behaviour as shown in Fig. 4.1.

Improved workability of polymer modified mortars was partially due to polymer particles acting as 'ball bearings' in the mix (Ohama, 1984, ACI 548.3R, 1991). This characteristic in a way reflects the rheology of fresh polymer modified cement. Atzeni *et. al.* (1989) investigated the rheology of cement paste mixed with aqueous dispersions of acrylic, vinyl

and epoxy using coaxial cylinder viscometer. Shear stress against time was monitored at constant shear rate of 42.77 s^{-1}. Hysteresis cycles were performed by varying shear rates between 2.75 and 385 s^{-1}. It was found that the acrylic latex gives a plasticizing effect at polymer content of 5 - 10%. However, vinyl and epoxy latex produce a considerable stiffening even at 5% polymer content.

A rather complex rheological investigation using stress relaxation and oscillation techniques was reported by Gregory and O'Keefe (1991). The stress relaxation involves a rapid application of small strain which is held constant. The decay of generated stress is monitored as a function of time. Oscillation involves the fresh cement paste being subjected to sinusoidally varying strain with measurement of the resultant stress response. The results of a rheological study on cement paste modified with styrene-butadiene resin (SBR) with sodium dodecyl benzene as stabiliser and ethyleneoxy ethanol as surfactant suggests that the complex interactions do occur within the cement paste due to the effect of adding latex and surface active agent.

Chappuis (1991) suggested that inter-particle forces play a very important role in determining the flow properties of cement pastes. The stiffening behaviour of two aluminous cements during the first 90 minutes of hydration was reported. Water/cement ratios were varied from 0.225 to 0.60. Cement pastes were prepared by mixing for 3 minutes in a laboratory mixer, then transferred into viscometer. Shear stress was taken at rotational speed of 5 rpm for 5 seconds and at 15 minutes thereafter. The first reading was started 5 minutes after addition of water. At 15 minutes intervals the internal structure of paste could recover, and then destroyed by shearing and the paste fludified. As a result of chemical reactions and structure build-up, the stiffening behaviour of different cements during the first 90 minutes could be compared. It was reported that the shear stress increase was exponential with time.

4.3 EXPERIMENTAL

4.3.1 Description of the Viscometer

The rheological measurements were performed with a rotating coaxial cylinder viscometer, Haake Rotovisco RV 20 with measuring system M10. This system was capable of providing a range of shear stress and shear rate of up to 11500 Pa and 40000 s^{-1} respectively. The sensor system consisted of a MVP cup radius 21 mm, a MVIIP rotor, the geometry of which was 60 mm in height, and radius 18.4 mm (see Fig. 4.2). The gap of 2.6 mm between the inside of the cup and outer radius of the rotor was sufficient to provide laminar flow and continuity in the flow curves at low shear rates (Lapasin, *et. al.*, 1983).

The cup and cylinder were both profiled with ribs 0.1 mm high by 0.1 mm wide, spaced 2 mm apart running parallel to the rotor axis. These were used since the grooves improved the adhesion and thus avoided slippage between the test substance and the surfaces of the sensor system.

Temperature was controlled by means of a water jacket that was linked to a constant temperature bath set at 25 ± 0.5°C.

4.3.2 Cement Paste

The cement pastes were prepared by mixing OPC with the appropriate amount of deionised water. Redispersible powdered polymer was dry blended with OPC prior to adding the water. Latexes were added to deionised water and thoroughly mixed to give the correct water/cement ratio, taking into account the water content of the latex. Anti-foaming agents, when added, were also thoroughly mixed with the water. Mixing was carried out by hand in a plastic beaker for three minutes, followed by a one minute pause prior to testing.

4.3.3 Test Methods

Two different types of test methods were used:

(a) ***Hysteresis cycle***, which measures the behaviour of τ vs $\dot{\gamma}$, the latter varying stepwise from 0 to a maximum value (the up curve) and back (the down curve). This method enables rapid determination of the rheological parameters τ_o and μ of a system. Whilst it is recognised that behaviour is a combination of shear thinning and Newtonian, preliminary analysis of results showed that use of the Bingham model was adequate.

(b) ***Transient***, which measures the behaviour of shear stress τ with respect to time t, at a constant $\dot{\gamma}$. This method is suitable for interpreting the effect of the different forces existing between the particles of the system on viscometric flow conditions.

Hysteresis Cycle

The following procedures were chosen since cement paste is known to undergo structural breakdown until it reaches equilibrium in about 1 or 2 minutes (Helmuth, 1980). For a shear thinning substance, further breakdown will occur under continuous shearing until equilibrium shear stress has been achieved over a short period of time. The choice of the second hysteresis cycle to determine rheological parameter was to allow more consistent and reproducible measurements (Atzeni, *et. al.*, 1985).

(i) Following Section 4.3.2, the paste was then carefully poured into the viscometer cup and the cup loaded into the measuring system

(ii) The test was started 5 minutes after addition of the water and/or emulsion component by increasing the shear rate in the following steps: 7.92, 13.2, 23.8, 39.6, 66.9, 112.6, 188.3, 315.9 and 527.1 s^{-1}, each being maintained for 5 seconds. These

shear rates correspond to the speed of the rotor at 9, 15, 27, 45, 76, 128, 214, 359 and 599 rpm. The shear rate was then decreased in a similar fashion, giving a total time of 85 seconds for this first cycle.

(iii) After this first cycle was completed, the sample was allowed to stand for 2 minutes.

(iv) A second cycle of increasing/decreasing shear rate was performed as in (ii).

(v) The whole procedures starting at (i) was in some cases repeated three times in order to assess reproducibility of the results.

Transient

The following procedures were used:

(i) Following step (i) mentioned in the hysteresis cycle procedures above.

(ii) A constant shear rate of 112.6 s^{-1} was applied 5 minutes after addition of the water/emulsion to the cement. This shear rate was chosen since it was sufficient to provide flow continuity and avoid slippage due to the formation of a flocculent structure that normally occurs at low shear rates (Lapasin, *et. al.*, 1983). The readings were taken at 10s intervals until a constant shear stress (equilibrium shear stress) was achieved. The viscometer was then stopped.

(iii) At 15 minute intervals the viscometer was restarted at the constant shear rate of 112.6 s^{-1} and shear stress readings were taken. Throughout the test, the top of the cup was sealed with cling film to avoid evaporation of water.

(iv) At each interval, shear stress readings were measured immediately (τ_i), after 5s (τ_5) and after 10s (τ_{10}). The viscometer was then stopped.

(v) Procedures (iii) and (iv) were carried out until significant stiffening had occurred so that the measured shear stress was about 700 Pa. Further shearing resulted in the instrument automatic cut-off being triggered.

4.4 RESULTS AND DISCUSSION

4.4.1 Hysteresis cycles

Unmodified OPC

Typical hysteresis curves for an unmodified OPC paste with a water/cement ratio of 0.35 are shown in Fig. 4.3. Shear rate was varied stepwise from 0 to the maximum value of 527.1 s^{-1} (up curve 1) and back (down curve 1). This was followed, after a 2 minute pause, by a second cycle giving up curve 2 and down curve 2. The two minute pause allowed the temperature in the cup to regain equilibrium and provides time for potential reformation of paste structure.

The results show that cement pastes exhibit shear thinning behaviour. To aid in describing this behaviour, the following parameters were identified, (see Fig. 4.3). The initial yield stress τ_i is interpreted as the minimum force required to initiate flow of cement paste in the viscometer. It is given by the start of up-curve 1.

The equilibrium yield stress τ_{eq} was obtained by extrapolating the intercept of down curve 2 on the shear stress axis. The plastic viscosity after completion of cycle 1, μ_{1st} and at equilibrium, μ_{eq} was the reciprocal of the slope of the down curves 1 and 2 respectively. It should be noted that the slope was derived from the linear portion before

it deviates at the low shear stress. Values for these parameters are given in Tables 4.1 & 4.2, for a wide range of systems. Values obtained were typical of those found for similar systems by other workers (Lapasin *et. al.*, 1983 and Domone & Thurairatnam, 1991).

The higher shear stress found during increasing shear rate compared to that when decreasing the shear rate (cycle 1) suggests that the initial mixing by hand for 3 minutes was not sufficient to completely break down the cement paste structure. That, the up and down curves on cycle 2 are more or less coincident suggests that structural breakdown of cement was complete by the end of cycle 1. This demonstrates that the paste structure was not reformed during the two minute pause. This also suggests that the kinetics of the structural reformation at the end of cycle 1 was negligible compared with the kinetics of structural breakdown.

The influence of water/cement ratio on rheological behaviour is shown in Fig. 4.4. For clarity only the down curve 2 (the equilibrium curve) is shown. Parameters are given in Tables 4.1 and 4.2. As the water/cement ratio increases, the difference between τ_i and τ_{eq} diminishes showing that structural breakdown becomes easier. Values of τ_{eq} and μ_{eq} also become less as the water/cement ratio increases.

SBR 1 Modified OPC

Typical hysteresis curves for OPC + SBR 1 with water/cement ratio of 0.35 are shown in Fig. 4.5a & b. At 10% SBR 1 content, shear stresses of the up curve in the first cycle are higher than both the down curve and the second cycle. The first down and the second cycle curves are approximately coincident, suggesting that the paste was completely broken down at the end of the first cycle. At 20% SBR 1 content, the initial shear stresses were much lower compared with 10% SBR 1. By the end of cycle 1, the paste was completely broken down and its shear stresses with cycle 2 are almost coincident. Furthermore, the time taken to achieve equilibrium was quicker as the water/cement ratio

increases. Any structural reformation during the 2 minute pause at the end the first cycle was negligible for both 10 and 20% polymer contents. Similar relationships were apparent at all water/cement ratios.

SBR 1 modified cement also shows thixotropic behaviour. However, the equilibrium curves as shown in Fig. 4.6 suggest that all mixes were so dispersed that the relationships between $\dot{\gamma}$ and τ are almost linear. At high water/cement ratio and 20% polymer content, the paste becomes virtually Newtonian. The loop of the first and second cycles becoming smaller and less curvatures at low shear rates were observed.

It can be seen that the value of the τ_i for both SBR 1 contents was about 2.5 - 3.0 times higher than τ_{eq} (see Table 4.2). However, the plastic viscosity of both polymer contents, at the end of cycle 1 and at equilibrium was virtually similar except for 10% polymer content and water/cement ratio 0.3. This indicates that the entire volume of SBR 1 pastes flows apparently uniformly once the structure was completely broken down.

SBR 2 Modified OPC

A significantly different rheological behaviour has been observed for SBR 2 at 10% and 20% polymer content (see Fig. 4.7). At 10% polymer content and water/cement ratio 0.35, it was not possible to use the higher shear rates owing to the very high initial shear stresses produced, at which the equipment was automatically cut-off. Therefore the test was performed at low shear rates with a maximum value of 52.1 s^{-1} or 59.9 rpm.

Hysteresis curves (Fig. 4.7a) showed that high shear stresses occurred at low shear rates on the down curves of cycles 1 and 2. The initial shear stress was 350 Pa but reduced to 275 Pa at the end of cycle 1. After 2 minutes rest, shear stress was approximately at 375 Pa, then reduced to 325 Pa at the end of cycle 2. This shows that rapid structure

build-up has occurred, giving high shear stresses particularly at low shear rates of the second cycle.

Increasing SBR 2 content to 20% with w/c 0.35 was not workable. The mix was very stiff and difficult to place into the viscometer. It exerts very high shear stress at very low shear rate of 5.27 s^{-1} or 5.99 rpm, resulting in automatic cut-off, so that the rheological parameters could not be measured.

However, at w/c 0.4 and 20% SBR 2, it was possible to test using maximum shear rate of 527 s^{-1}. The result shows that higher shear stresses occurred at low shear rates on the down curve 2 than on the up curve (see Fig. 4.7b). Initially the mix was quite fluid with initial yield stress of 10 Pa and at the end of cycle 1 was about the same. The initial yield stress of cycle 2 was 25 Pa, but had increased considerably to 125 Pa by the end of cycle 2. It also can be seen that the loop of cycle 2 shifted to the right. Both 10 and 20% polymer content produced high shear stresses at low shear rates at the end cycles 1 and 2. Quick thickening was evident after only 2 minutes rest before the second cycles (curve 2 down) even at 20% polymer content and water/cement ratio of 0.4. The hysteresis curves depicted in Fig. 4.7 for SBR 2 may be explained by some forms of polymer-cement interaction during the early part of hydration.

A possibility for this behaviour is that the carboxyl groups that are chemically bound in SBR, ionise and react with calcium ions in solution, or bind to calcium ions at the surface of cement grains (Chandra and Flodin, 1987a). These interactions may, in the early stages of hydration, lead to an increased degree of flocculation and thickening of cement paste. Because of this interaction, SBR particles are unable to disperse uniformly in the cement paste phase and flocculate to much larger cement particles (see Fig. 4.8). It has been shown by Zeng, Short & Page (1996) that the concentration of carboxyl groups is very influential in determining hydration kinetics of cement paste.

Influence of the Aqueous Component (Aq Comp)

For this study, the equivalent amount of Aq Comp (aqueous component of SBR 2) that was contained in latex, together with the required amount of water was added to cement.

The equilibrium flow curves along with OPC and modified OPC at the same w/c ratios are shown in Fig. 4.9. Compared to unmodified cement, it can be seen that Aq Comp does not significantly affect τ_{eq} but affects μ_{eq} slightly. These values are shown in Table 4.2. The results suggest that the presence of Aq Comp does not significantly influence the flow behaviour of OPC compared to that of polymer solids. Thus free surfactant etc. is not as significant as the presence of polymer particles and their degree of carboxylation.

Acrylic 1 & 3 Modified OPC

Ac 1 modified pastes were much more fluid than those modified with SBR 1. The structural reformation during the 2 minute pause at the end the first cycle was negligible for both 10 and 20% Ac 1 content. The down curve 2 (the equilibrium curves) are shown (see Figs. 4.10a & b) and the rheological parameters are given in Tables 4.1 and 4.2. Results suggest that all mixes were well dispersed and the lines drawn were almost linear, becoming nearly Newtonian except that it slightly curved in the region of shear rates of 45 s^{-1} and lower. It can be seen that τ_{eq} and μ_{eq} decrease significantly as the w/c ratio and Ac 1 content increases.

Significantly different equilibrium curves were obtained from redispersible powder of Ac 3 compared with Ac 1 (see Fig. 4.10c). At the same polymer content and water/cement ratio, the equilibrium curves obtained were at very much higher shear stresses than Ac 1. It can be seen that addition of Ac 3 at 10% was worse than plain OPC. Addition of 20% Ac 3 makes the mix even less workable. Possible explanations are: *i)* A combination of the

actions of surface active agent and anti-foaming agent resulting in more disperse suspension of cement paste compared with Ac 3, *ii)* They may have different chemical compositions (especially carboxylation)as both polymers came from different sources and, *iii)* In the case of powdered Ac 3, water was in contact with the surface active agent and stabilising system first before the polymer particles compared with Ac 1 which was in the form of emulsion.

EVA 1 & 2 Modified OPC

Similar thixotropic behaviour was found for both EVA 1 & 2 in the sense that by the end of first cycle the structure was almost completely broken down. The down curves obtained for both cycles at the respective w/c ratio and EVA contents were almost coincident. It can be seen that equilibrium curves for EVA 1 and EVA 2 (see Fig. 4.11) were higher than plain OPC, SBR 1 and Ac 1. Fig. 4.11a & b show that at low w/c ratio (0.3), the EVA 1 mix was very stiff and produced very high shear stress compared to the other mixes.

It can be seen that at 20% EVA content, the equilibrium curves of EVA 1 (redispersible powder) were higher than EVA 2 (emulsions) but not significantly different at 10% polymer content. The low shear stress shown by EVA 2 compared with EVA 1 was probably due to combination of dispersive effect of stabilising system present in the emulsion and anti-foaming agent added in the mix.

Furthermore, the increase in surface activity of EVA 1 also results in a very high viscosity suspension as polymer particles disperse; the particle size initially was between 10 - 250 μm and, upon dispersion, it reduced to 0.7 - 1.5 μm. The protective surface layer of PVOH around polymer particles also absorbed water. As polymer content increases, more water is needed to disperse polymer particles and at the same time initial hydration of cement proceeds. This effect can be seen at 20% EVA 1 and w/c ratio 0.3 in which the plastic viscosity was significantly higher than other mixes. It also can be seen that further increase in EVA 1 was not beneficial in terms of rheological point of view.

4.4.2 Effect of polymers and water/cement ratio on τ_{eq} and μ_{eq}

For illustrative purposes, the values of τ_{eq} and μ_{eq} shown in Tables 4.1 & 4.2 are plotted against water/cement ratio and polymer content respectively. The effect of water/cement ratio and polymer content on equilibrium yield values and plastic viscosity are depicted in Figs. 4.12 & 4.13 respectively. It can be seen that τ_{eq} and μ_{eq} increased as water/cement ratio decreases, approximately exponentially.

In the case of SBR 1 and Ac 1, τ_{eq} and μ_{eq} were further improved when the concentrations of polymer were increased to 20%. These improvements were probably due to the influence of their formulations, e.g. the type of surfactant and surface chemistry of the polymer that influences the degree of flocculation. The combinations of actions of these chemicals are believed to give maximum dispersive effect during shearing. Furthermore the surface chemistry of these polymers probably reduced the attractive forces between particles and slightly delayed cement hydration during the first 10 minutes from the first addition of water until completion of the second cycle.

Overall it can be seen that SBR 1 and Ac 1 demonstrate quite clearly a potential for improving workability. EVA 1 and 2 seemed to have very little effect on workability, whilst Ac 3 seemed to be worse.

4.4.3 Transient behaviour

The rheological behaviour of cement paste during the dormant period of hydration was obtained for unmodified OPC and OPC modified with 20% SBR 1 and SBR 2. Shear stress readings were taken at a constant shear rate of 112.6 s^{-1}, and the water/cement ratio was 0.4. The curves of shear stress against time were plotted and are shown in Fig. 4.14. The three curves in each system represent shear stresses: *(i)* immediately after starting the rotovisco τ_i, *ii)* after 5 seconds τ_5 and, *iii)* after 10 seconds τ_{10} of shearing.

At the start of the test, the initial yield stress of all systems was high and the time taken to achieve equilibrium varied. These initial parameters for the different systems (see Table 4.3) suggest that the state of flocculation is related to the internal structure of the paste, which can be destroyed during shearing. These parameters may vary significantly depending on the method of paste preparation (Lapasin *et al.*, 1983). Vigorous mixing using a mechanical stirrer can lower the initial shear stress and shorten the time taken to achieve equilibrium compared to hand mixing.

Initially the shear stress values increase approximately linearly with time and $\tau_i \approx \tau_5 \approx \tau_{10}$. Eventually the rate of increase becomes greater and $\tau_i > \tau_5 > \tau_{10}$. At this stage loss of fluidity of the paste during shearing can be observed and is equivalent to the onset of setting. This suggests that the useful life of the fresh paste was ending and the stiffening of the mix was the result of C_3S hydration to form CSH gel.

Increase in shear stress during the dormant period for OPC was approximately 120 Pa (from 80 to 200 Pa) and SBR 1 was 80 Pa (from 20 to 100 Pa). The increase was relatively the same but the time taken for SBR 1 was much longer than OPC. Different rheological behaviour can be observed for SBR 2 in which at the beginning it shows lower equilibrium shear stress than OPC but increases steadily similar to OPC until approximately 80 minutes after the first addition of water. The initial shear stress (τ_i) and τ_5 was higher than for OPC. However, after 125 minutes, τ_{10} was similar to that for OPC. This suggests that continuous shearing will further break the structure down.

The time taken for deviations of the curves and the corresponding shear stresses for all systems depicted in Fig. 4.14 is shown in Table 4.4, along with the setting time data obtained by the conduction calorimetry (Zeng, Short & Page, 1996). The results show that for OPC and SBR 1, the values correlate well with the calorimetry test (w/c ratio 0.5 and polymer content 20%). However, the rheological parameters of SBR 2 show that an early thickening, i.e. analogous to initial setting occurred but the initial setting time

from calorimetry suggests that the setting time was longer than SBR 1 (Zeng, Short & Page, 1996).

The present work has shown that possible interactions between polymer latexes and cement particles occur which may result in retardation of setting time for SBR 1 mix and increase destabilisation of cement suspension for SBR 2. Increase in degree of flocculation of SBR 1 means the delay in the formation of hydration product making the mix more workable over a longer period of time. It also shows that SBR 1 prolongs the induction time (see Fig. 4.14b). This phenomenon was probably due to: *(i)* lower surface area for hydration, *(ii)* reducing the formation of calcium hydroxide crystals and, *(iii)* binding between polymer particles and surfaces of cement grains that reduces the number of sites available for calcium dissolution and hydration.

In the case of SBR 2, a complex surface activity between cement particles, surface active agent, aqueous component, carboxylic acid and polymer particles are thought to be the major contributing factors that quicken structure formation. The results confirm the chemical interactions in which carboxyl groups can react with calcium ions in solution or bind to calcium ions at the surface of cement grains.

4.5 CONCLUSIONS

(1) The present investigations confirm the rheological behaviour of unmodified OPC paste is typical of a thixotropic / Bingham plastic material depending on shear history.

(2) The flow behaviour of the polymer modified fresh paste is similar in character to that of the unmodified paste. However, for SBR 1 and Ac 1 increasing water/cement ratio and polymer content results in a significant reduction of yield and plastic viscosity values to an extent that their behaviour becomes almost Newtonian.

(3) EVA 1 and 2 had a very similar effect on workability demonstrating that there is little difference in adding the polymer as an emulsion or redispersible powder. However, overall they showed a decrease in workability, particularly at the higher concentrations. It is thought that this was the result of water being adsorbed initially by the stabilising system used to coat the powdered polymer particles.

(4) The behaviour of Ac 3 was quite different to that of Ac 1 showing no improvement in workability at additions of 10% and becoming significantly worse at greater additions. This demonstrates that not all acrylics behave in the same manner and a real understanding of their behaviour is only possible if the latexes are well characterised.

(5) Increasing the degree of carboxylation of the SBR was shown to have a very significant effect on rheological properties. SBR 2 showed anti-thixotropic behaviour demonstrating the importance of ionisable groups at the surface of the polymer particles which are capable of interacting with other constituents of the mix.

(6) Transient behaviour shows that for both OPC and SBR 1 modified OPC the time to accelerated stiffening of the cement paste is co-incident with the acceleratory stage of cement hydration. However these times are different owing to the retardation effect in the case of SBR 1. In contrast, accelerated stiffening of the SBR 2 modified OPC occurs much earlier than the acceleratory period for cement hydration. This latter effect is related to the much larger interaction forces between polymer and cement particles as a result of increased carboxylation.

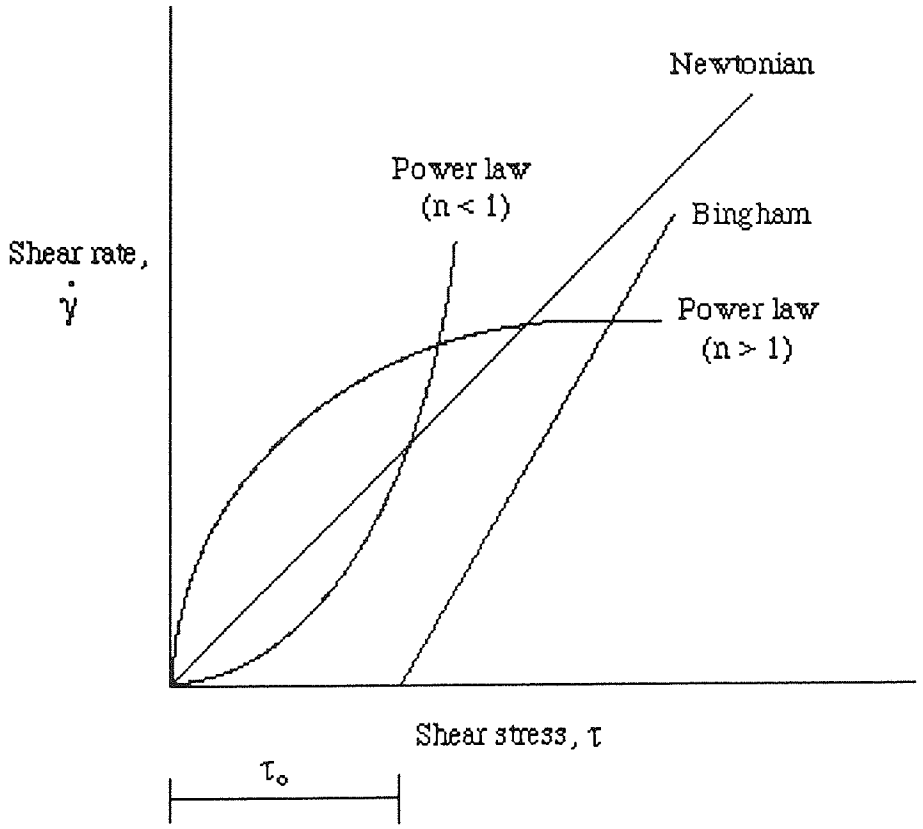

Fig. 4.1: Typical flow curves, showing relationships between shear rates ($\dot{\gamma}$) and shear stress (τ).

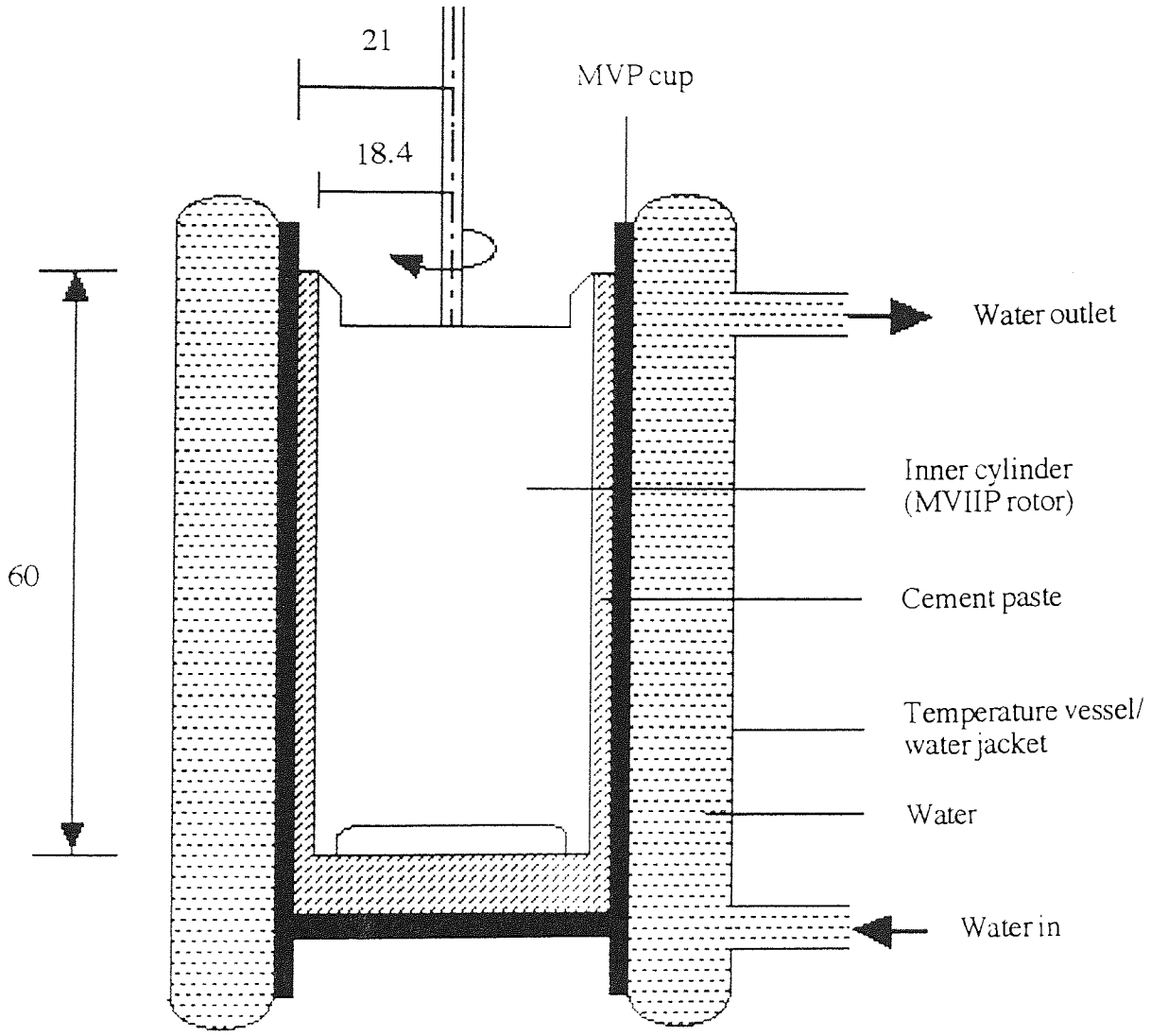

Fig. 4.2: Sensor system of MVIIP

Table 4.1: Initial and equilibrium shear stress values for different systems

(i) Cement paste with 0 & 10% polymer content and Aq Comp

W/C	Shear Stress (Pa)	OPC	SBR 1	SBR 2	Ac 1	Ac 3	EVA 1	EVA 2	Aq Comp
0.30	τ_i	135.0	170.0	-	140.0	-	160.0*	-	-
	τ_{eq}	84.0	51.0		43.5		135.0		
0.35	τ_i	97.0	44.0	350.0*	35.0	110.0	70.0	130.0	105.0
	τ_{eq}	37.0	15.0	325.0	17.5	40.0	53.0	45.7	45.0
0.40	τ_i	60.0	15.0	-	17.5	-	40.0	65.0	-
	τ_{eq}	20.0	5.8		9.0		20.0	25.1	
0.45	τ_i	30.0	-	-		-	25.0	-	-
	τ_{eq}	16.0					16.0		

* Maximum shear rate 52.7 s^{-1}

(ii) Cement paste with 0 & 20% polymer content and Aq Comp

W/C	Shear Stress (Pa)	OPC	SBR 1	SBR 2	Ac 1	Ac 3	EVA 1	EVA 2	Aq Comp
0.30	τ_i	135.0	34.0	-	37.5	-	312.0	-	-
	τ_{eq}	84.0	13.6		15.5		120.0		
0.35	τ_i	97.0	17.0	10.0	17.5	100.0	190.0	110.0	75.0
	τ_{eq}	37.0	4.6	125.0	8.5	55.0	57.0	26.4	27.5
0.40	τ_i	60.0	11.0	-	8.0	-	100.0	60.0	-
	τ_{eq}	20.0	1.7		4.8		32.6	18.9	
0.45	τ_i	30.0	-	-	-	-	58.0	-	-
	τ_{eq}	16.0					20.5		

Table 4.2: Plastic viscosity of different systems

(i) Cement paste with 0 & 10% polymer content and Aq Comp

W/C	Plastic viscosity (Pa.s)	OPC	SBR 1	SBR 2	Ac 1	Ac 3	EVA 1	EVA 2	Aq Comp
0.30	μ_{1st}	0.80	0.72	-	0.53	-	1.75	-	-
	μ_{eq}	0.68	0.54		0.41		1.74		
0.35	μ_{1st}	0.40	0.26	NM	0.24	0.72	0.61	0.66	0.60
	μ_{eq}	0.38	0.23	NM	0.23	0.64	0.26	0.55	0.45
0.40	μ_{1st}	0.25	0.11	-	0.13	-	0.30	0.29	-
	μ_{eq}	0.23	0.12		0.13		0.20	0.25	
0.45	μ_{1st}	0.17	-	-	-	-	0.18	-	-
	μ_{eq}	0.14							

NM = not measurable

(ii) Cement paste with 0 & 20% polymer content and Aq Comp

W/C	Plastic viscosity (Pa.s)	OPC	SBR 1	SBR 2	Ac 1	Ac 3	EVA 1	EVA 2	Aq Comp
0.30	μ_{1st}	0.80	0.41	-	0.33	-	19.2	-	-
	μ_{eq}	0.68	0.41		0.35		16.8		
0.35	μ_{1st}	0.40	0.19	-	0.18	2.13	2.05	1.22	-
	μ_{eq}	0.38	0.19		0.18	1.90	1.90	1.20	
0.40	μ_{1st}	0.25	0.11	0.12	0.10	-	0.75	0.68	0.34
	μ_{eq}	0.23	0.10	0.12	0.10		0.70	0.58	0.29
0.45	μ_{1st}	0.17	-	-	-	-	0.41	-	-
	μ_{eq}	0.14					0.40		

μ_{1st} is taken from the down curve of cycle 1

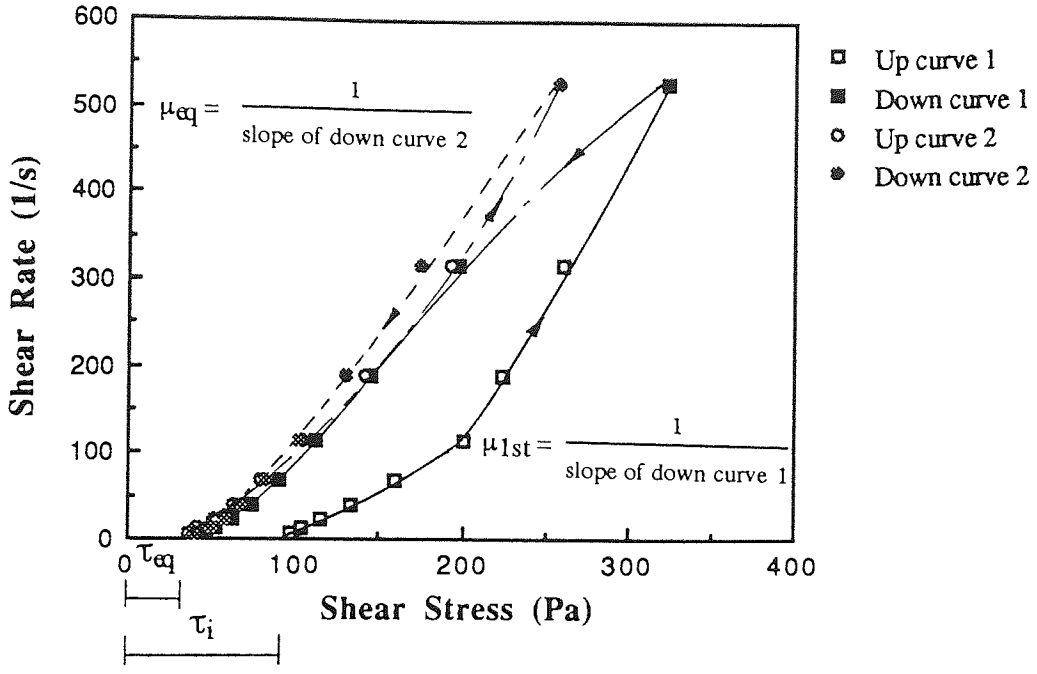

Fig. 4.3: Hysteresis curves for OPC, w/c 0.35

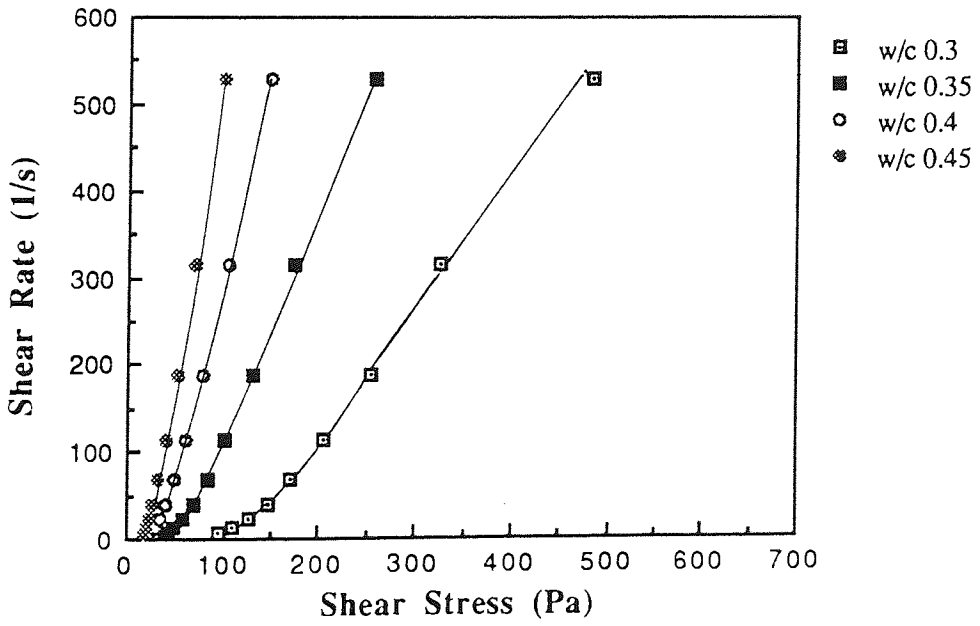

Fig. 4.4: Equilibrium curves for OPC

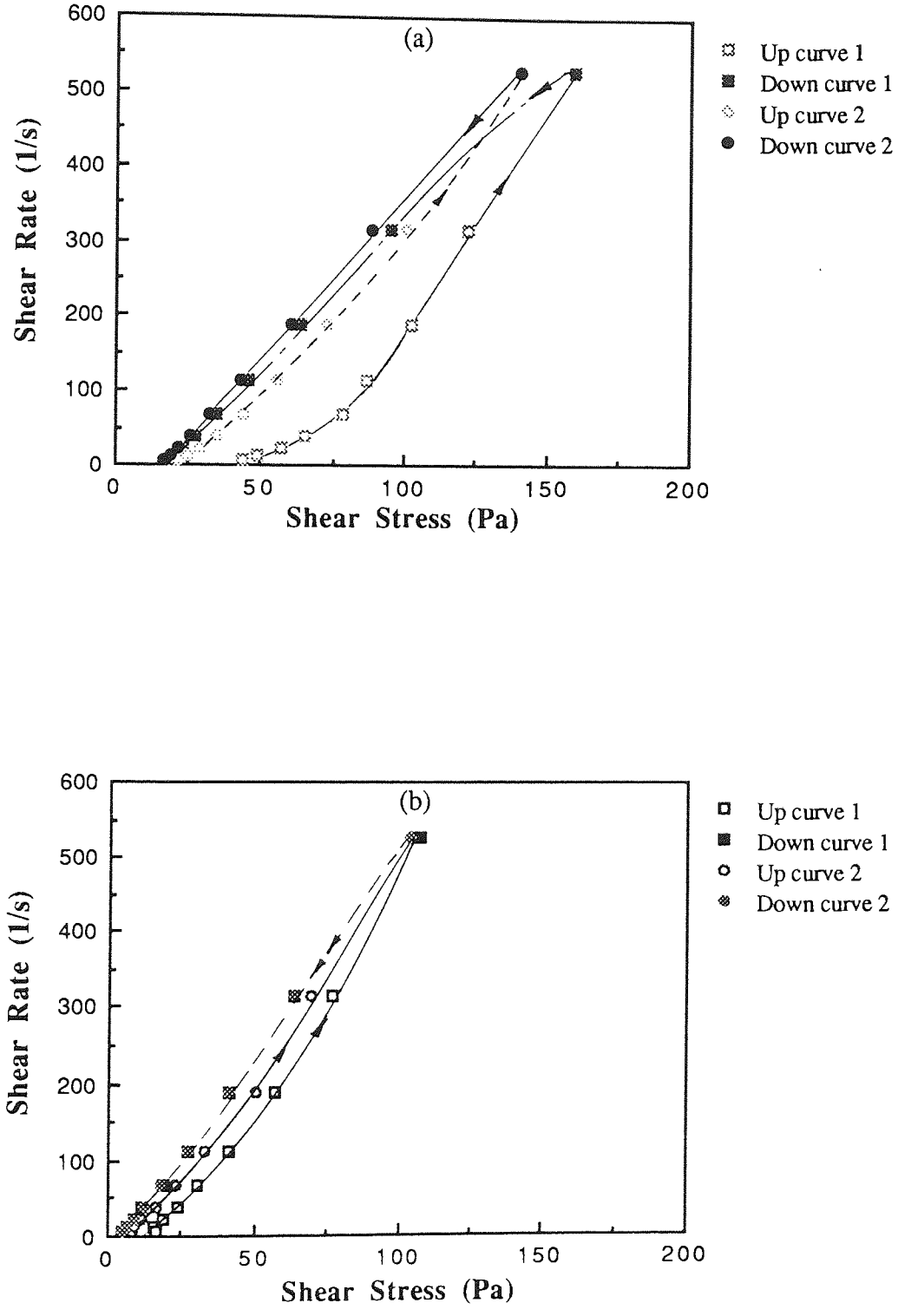

Fig. 4.5: Hysteresis curves for; (a) OPC + 10% SBR 1, (b) OPC + 20% SBR 1 with w/c 0.35

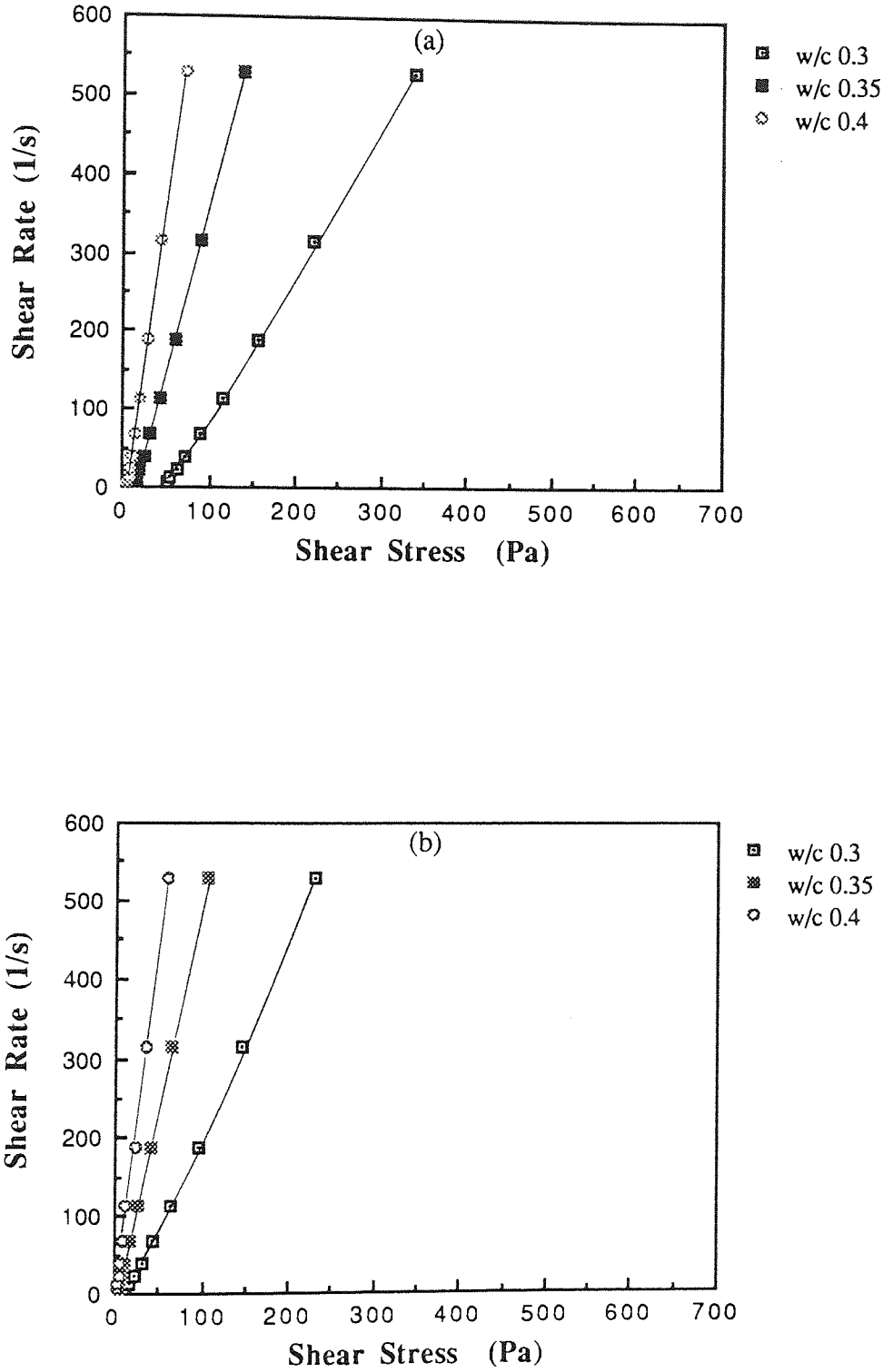

Fig. 4.6: Equilibrium curves for; (a) OPC + 10% SBR 1, (b) OPC + 20% SBR 1

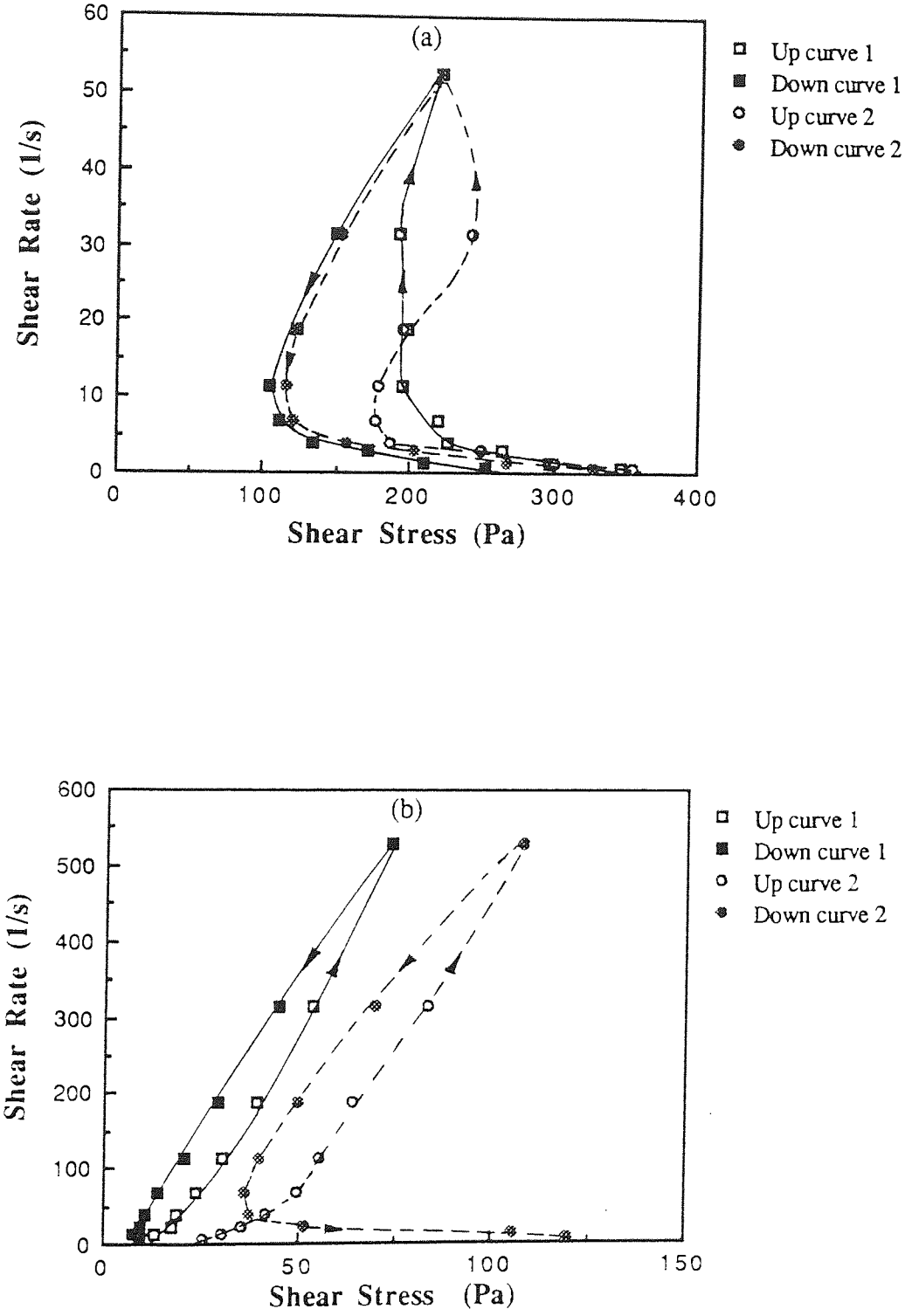

Fig. 4.7: Hysteresis curves for, (a) OPC + 10% SBR 2, w/c 0.35, (b) OPC + 20% SBR 2, w/c 0.4

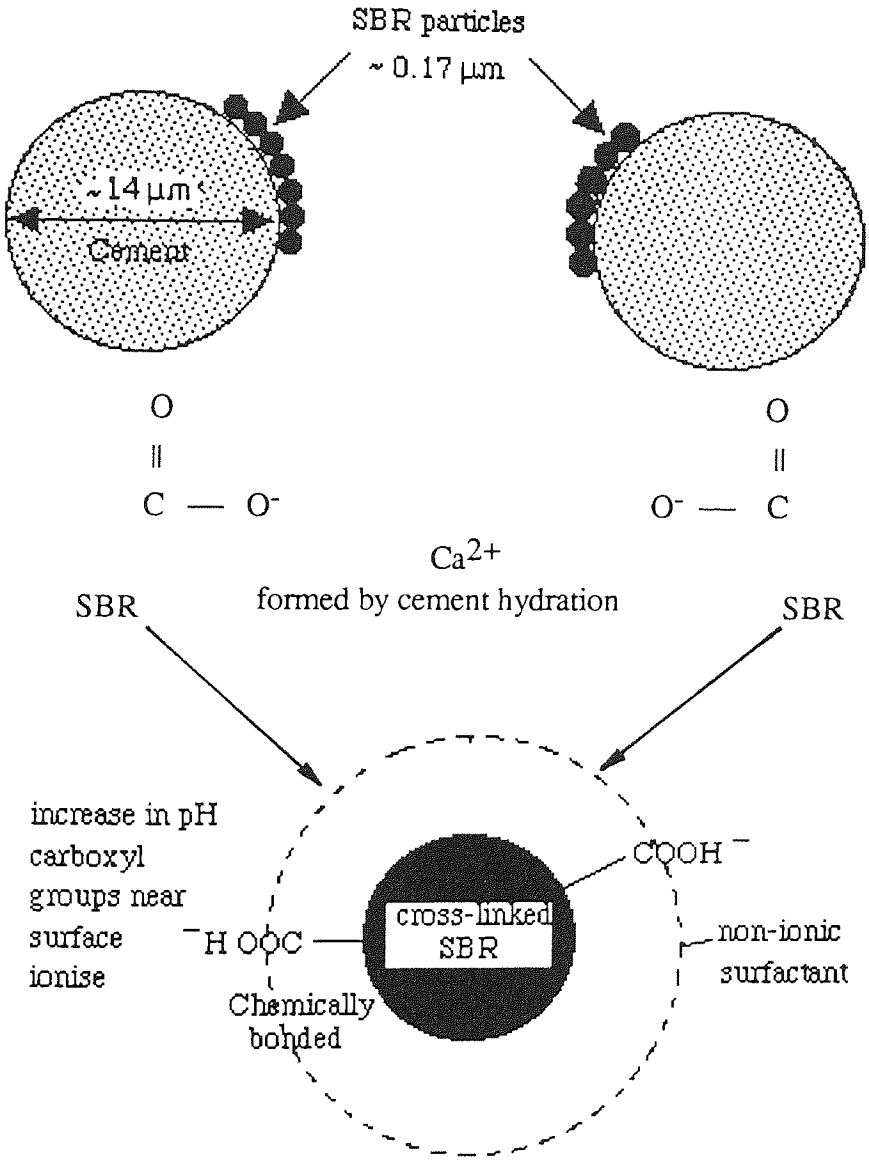

Fig. 4.8: Schematic illustration of mechanisms of anti-thixotropic as a result of carboxylation of carboxyl groups

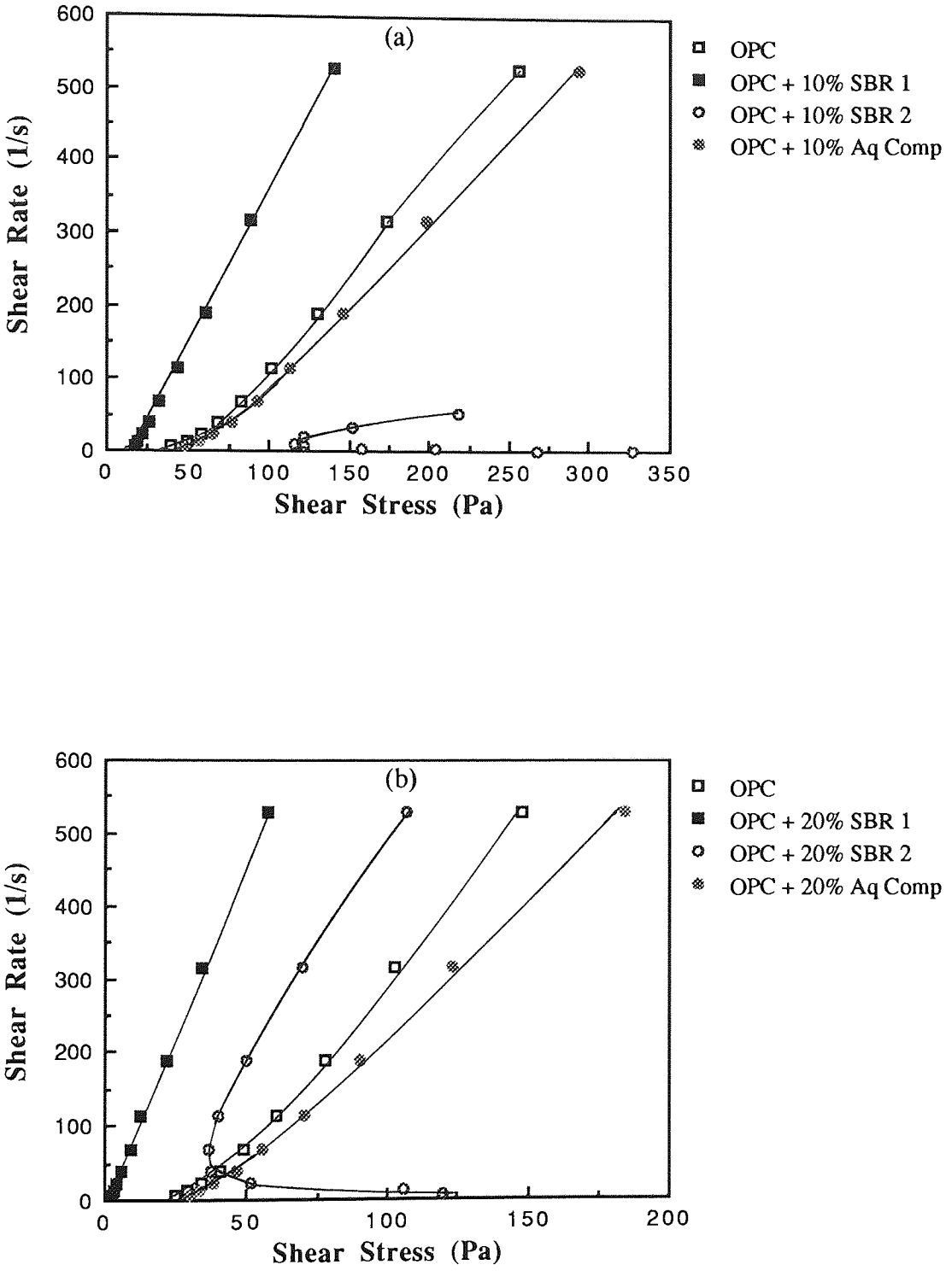

Fig. 4.9: Equilibrium curves for pastes with (a) w/c 0.35 and (b) w/c 0.4

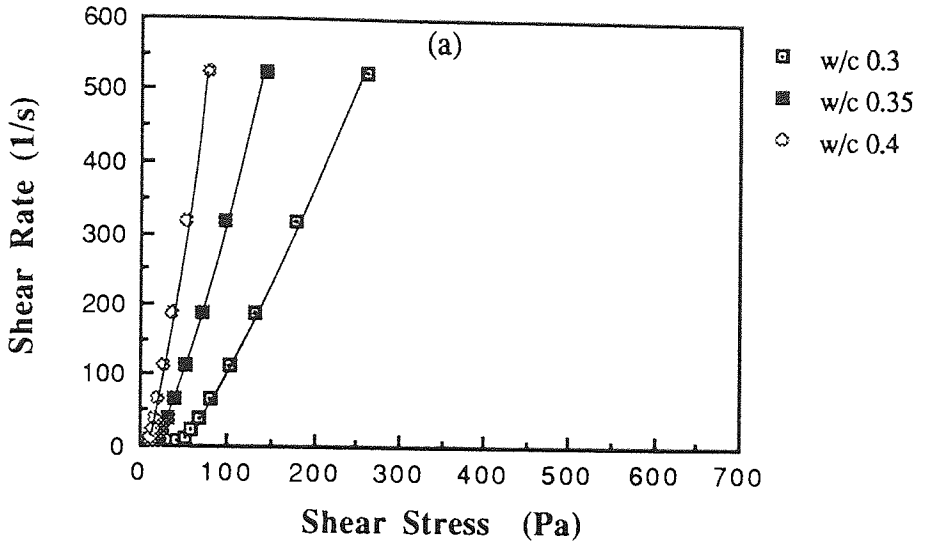

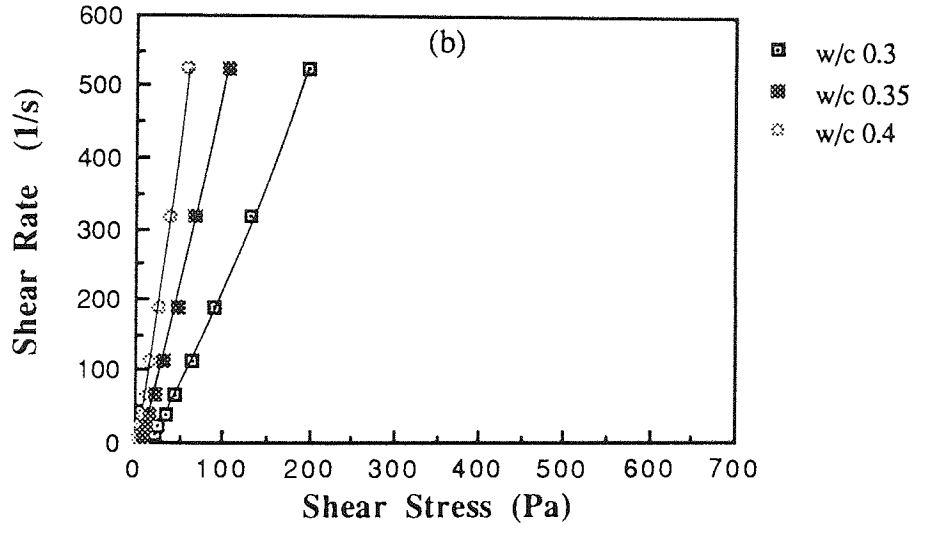

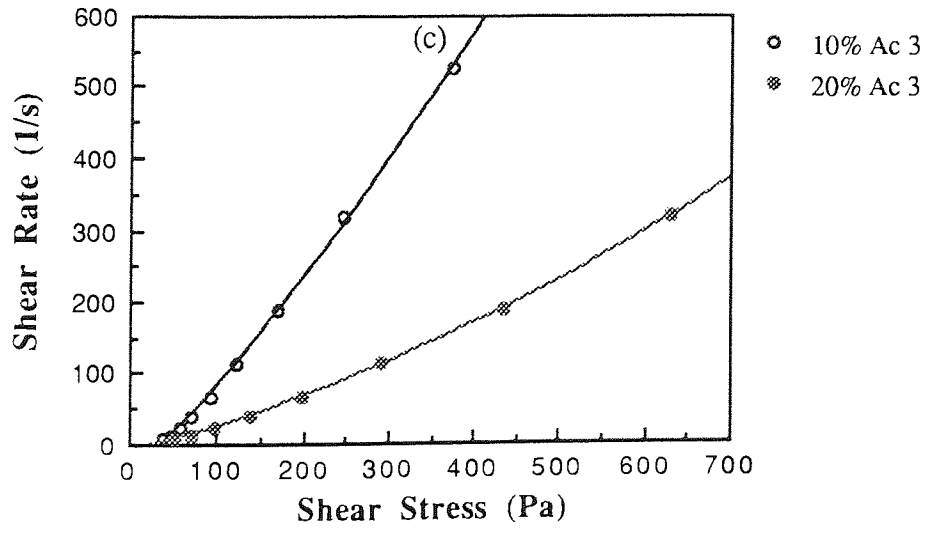

Fig. 4.10: Equilibrium curves for; (a) OPC + 10% Ac 1, (b) OPC + 20% Ac 1, (c) OPC + Ac 3 with w/c 0.35

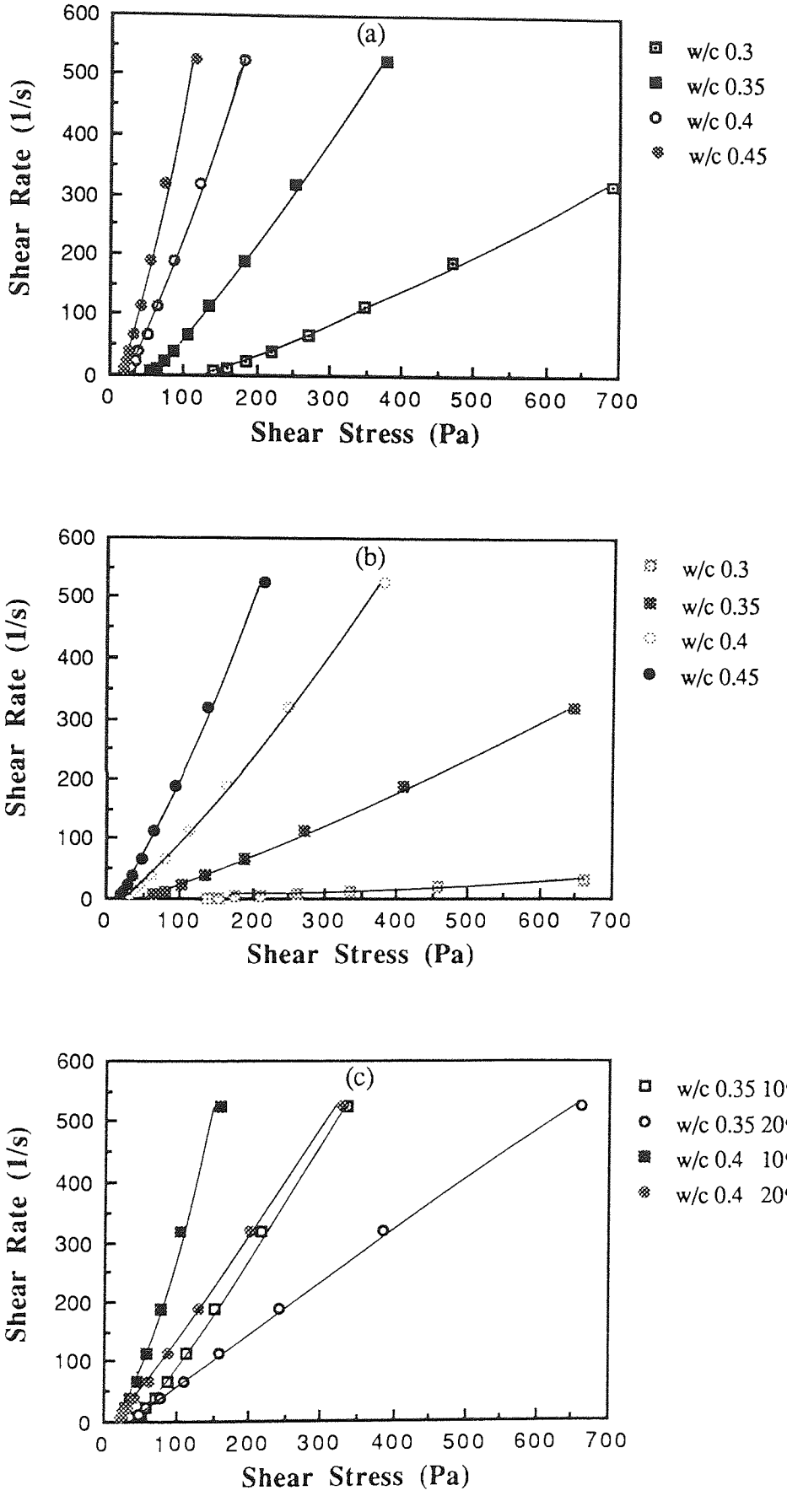

Fig. 4.11: Equilibrium curves for; (a) OPC + 10% EVA 1, (b) OPC + 20% EVA 1, (c) OPC + 10% & 20% EVA 2

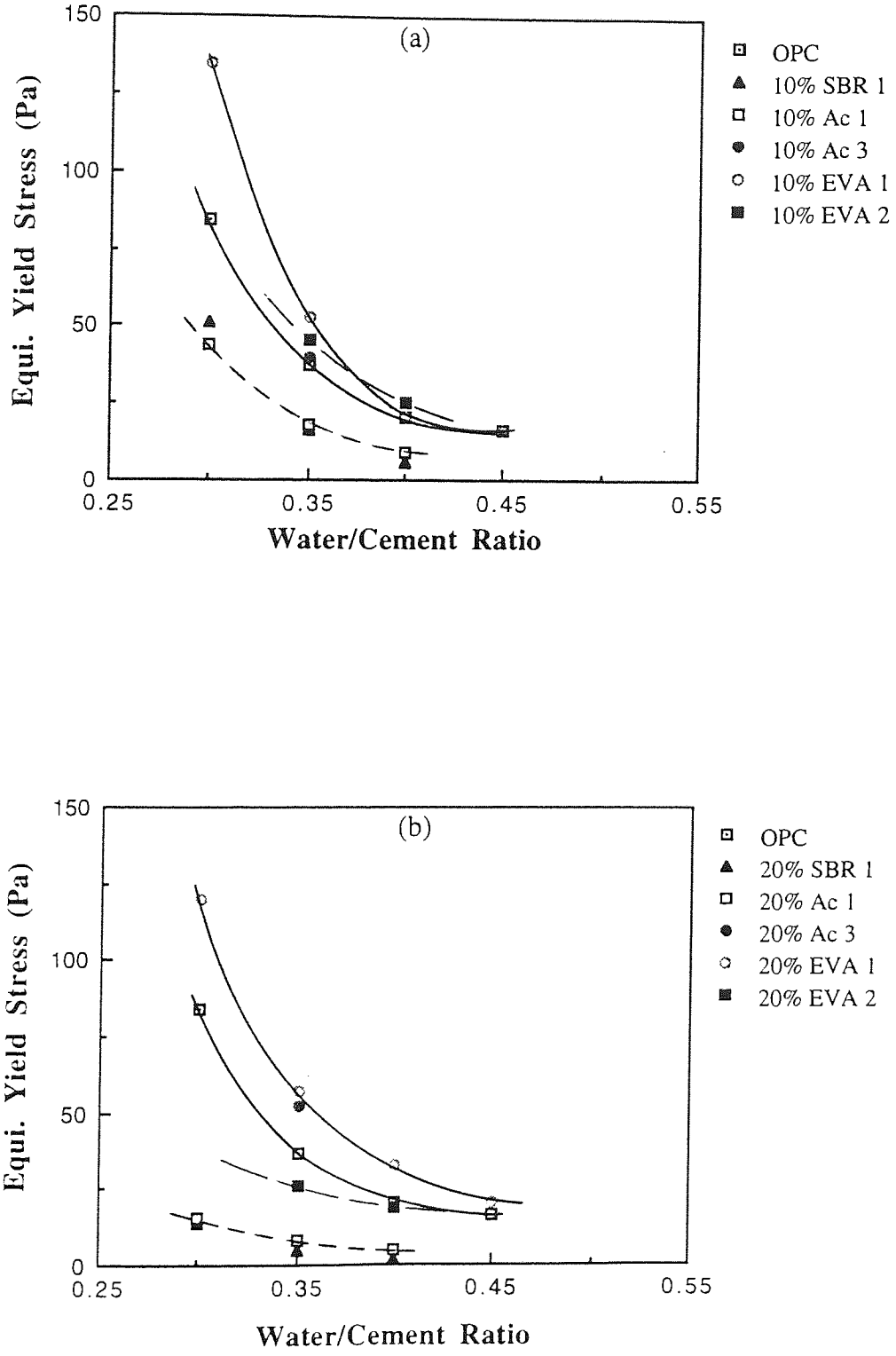

Fig. 4.12: Effect of water/cement ratio and polymer content on equilibrium yield stress; (a) 10% polymer, (b) 20% polymer

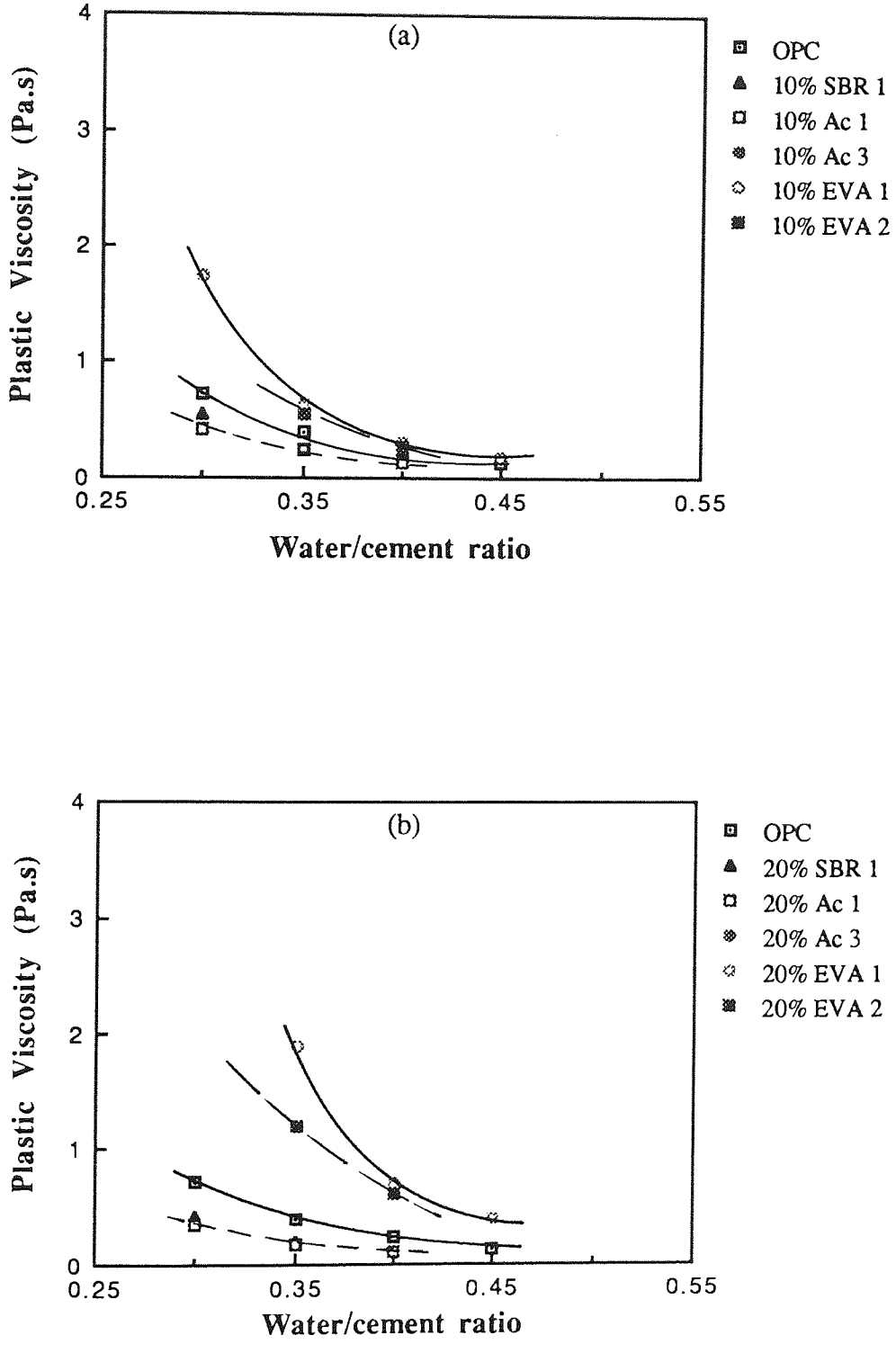

Fig. 4.13: Effect of water/cement ratio and polymer content on equilibrium plastic viscosity; (a) 10% polymer, (b) 20% polymer

Table 4.3: Initial rheological parameters

System	τ_i (Pa)	τ_{eq} (Pa)	Time to achieve τ_{eq} (min)
OPC	160	80	6
OPC + 20% SBR 1	80	20	4
OPC + 20% SBR 2	45	25	1

Table 4.4: Early setting parameters

System	Time of deviation (min)	τ_{eq} (Pa)	Initial setting time from calorimetry* (min)
OPC	80 - 120	200 - 300	75 - 115
OPC + 20% SBR 1	300	100	330 - 440
OPC + 20% SBR 2	80 - 120	200 - 300	440 - 500

* w/c ratio 0.5 (Zeng, S., Short, N.R. and Page, C.L., 1996)

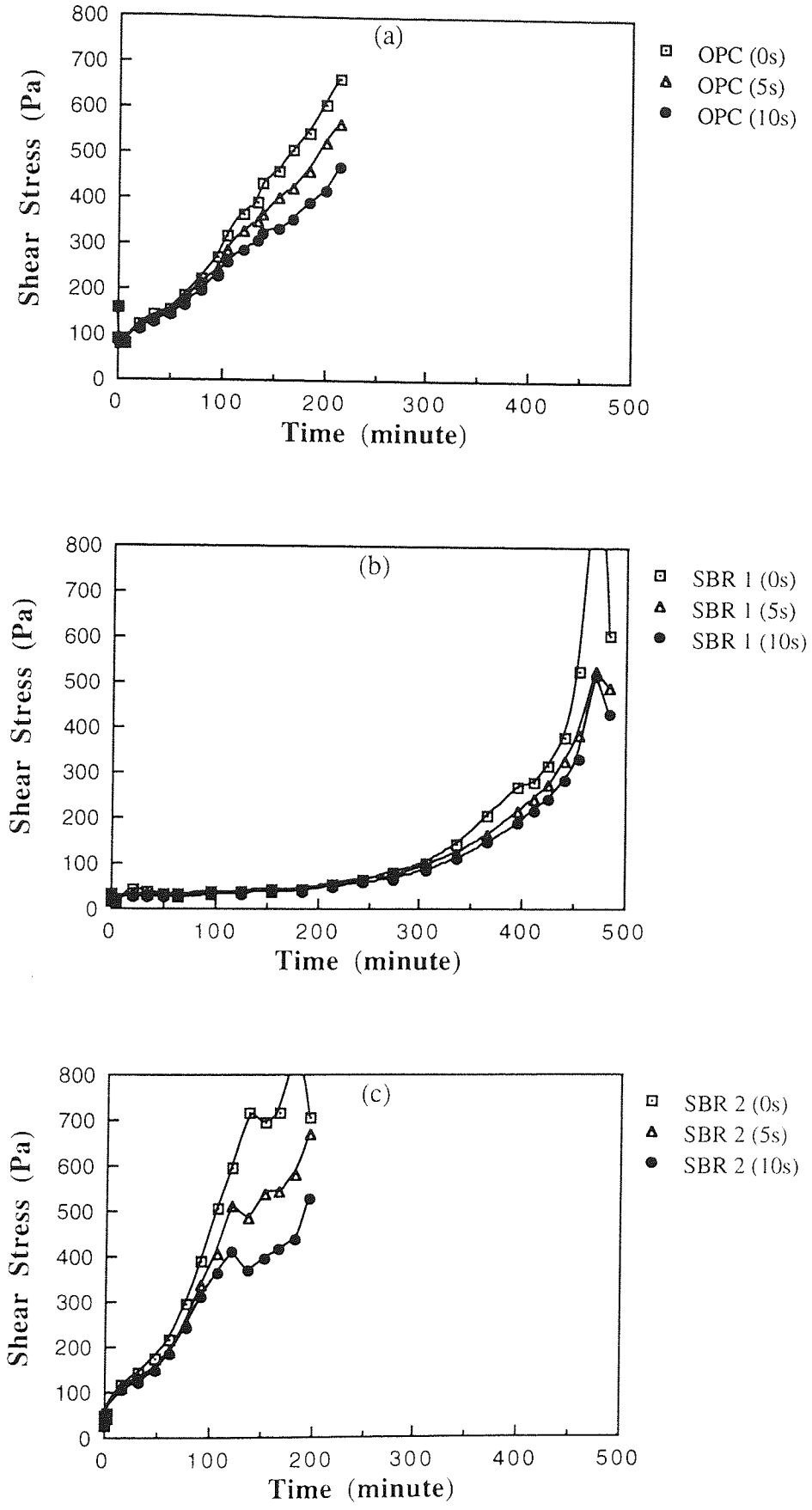

Fig. 4.14: Transient behaviour of pastes , w/c 0.4; (a) OPC, (b) OPC + 20% SBR 1, (c) OPC + 20% SBR 2

5 RHEOLOGICAL BEHAVIOUR OF FRESH POLYMER MODIFIED MORTARS

5.1 INTRODUCTION

The **main objective** of this investigation was to establish whether the Visco-Corder is capable of determining the rheological parameters needed to fully characterise fresh polymer modified mortar systems. In addition it was hoped to establish the sensitivity of measurements to changes in mortar mix design, especially in relation to the formulation of latex system used.

5.2 PREVIOUS WORK

A large number of empirical tests have been developed to measure the workability of concretes and many of them have been adopted as standard tests. These include slump, compacting factor, Ball-penetration, standard consistency, Vebe and flow table. They are fully described in the literature, see for example Tattersall (1991).

In the case of mortar, existing empirical tests used to determine the workability include flow and determination of consistence (BS 4551, 1980). For a very high workability or self-levelling repair mortar, the flow cone method (ASTM C 939 - 87) is probably very useful to quantify the workability providing that the time for flow is less than 35 s. This test is a standard test for cement grouts containing sand < 2.36 mm and is used for preplaced-aggregate concrete. For this application, a high fluidity mix is essential to allow the cement grout to fill the gaps of the preplaced-aggregate. If the flow is more than 35 s, the flow table test that measures the spread should be used.

Another method of determining workability of a superfluid microconcrete is by using a flow trough test specified by the Department of Transport (1986). This method specifies various minimum flow characteristics and simulated repair trials in terms of the time taken for the concrete to flow 750 mm along the trough. However, the flow test itself requires a large quantity of mortar and each test requires six readings, three taken immediately after mixing and three taken 30 minutes later. For compliance, the time taken for repair mortar to flow along a distance of 750 mm should not exceed 30 s.

However, most empirical tests only have a narrow range of suitability and they are known to measure only one parameter (Tattersall 1991). These empirical tests may no longer be suitable to measure workability of fresh mixes. For example the slump test described by BS 1881: Part 102 (1983) is not suitable for concrete where the workability is such as to give slumps of more than 180 mm or zero. Similar setbacks may be encountered for the other types of empirical test mentioned earlier where the tests are no longer valid to fully characterise the fresh properties of all types of mix.

Tattersall (1973) determined the properties of fresh concrete using the two-point test. He used a modified Hobart food mixer (MK I) to characterise the properties of concrete in terms of yield value and plastic viscosity. The technique involved measuring the torque (T) produced on an impeller rotating in fresh concrete at various speeds (N). It was shown that the rheological behaviour of concrete conformed to the Bingham plastic model (see also Chapter 4, equation 4.2 and Fig. 4.1) given by:

$$T = g + hN \qquad (5.1)$$

where g is a constant related to yield value, and h is a constant related to the plastic viscosity. According to Tattersall (1973) low and high workability concrete can be characterised by its yield value and plastic viscosity using the two-point test.

Since its introduction the MK 1 instrument has been developed, MK II, by incorporating an interrupted helical impeller which is rotated uniaxially in the concrete (Tattersall and Bloomer, 1979). Other modifications to the two-point equipment, Wallevik and Gjørv (1990), include improvements to the instrumentation to measure torque and rotating speeds. A segregation factor was introduced that can be used if segregation occurred during the test, which may happen at high speeds.

The two-point test equipment (MK II) used by Tattersall and Bloomer (1979) was calibrated using relevant flow theories and techniques. The calibration allows determination of various constants that are unique to a particular piece of equipment. Later they showed that the rheological behaviour of fresh concrete, i.e. yield value and plastic viscosity can be reported in fundamental units.

Since the flow behaviour of mortar conforms to the Bingham model, its rheological behaviour can be measured using the two-point test principle. Attempts were made by Banfill (1987) to measure the rheological parameters of mortar using the same measuring system used in the MK II equipment. A cylindrical impeller was used with inner radius of 101 mm, bowl of 126 mm radius and height of 157 mm, mounted on the drive shaft. Later, to avoid mortar sticking to the wall during rotation, the bowl and impeller were modified by sticking a vertically ribbed rubber sheet on the inner and outer surfaces of the bowl and impeller respectively. Although considerable difficulties were reported, the rheology of mortars is nevertheless characterised by the Bingham model and the rheological paramerters of mortar were reported in fundamental units.

Work on the two point test was further extended by determining the workability of mortar using a smaller version of the above apparatus, which was called the Visco-Corder. This equipment has been used in Germany as a single point test to determine the rheometric behaviour of fresh mortars (Lewandowski and Wolter, 1981). The equipment was used to measure the stiffening behaviour of mortar, using various types of cement, over a

specified period of time. The change in shearing resistance of the mortar in the Visco-Corder was recorded automatically at a constant rotational speed of 120 rpm.

Similar work was reported by Wolter (1985), using a more sophisticated Visco-Corder to study the relative viscosity and stiffening of various mortars mixed with fly ash and plasticiser. The experimental mortars consisted of standard sand with a particle size of less than 1 mm. It was reported that the Visco-Corder was sensitive and capable of detecting small changes in characteristics of each mix.

Rheological work on fresh mortars using the Visco-Corder was reported by Banfill (1990). He demonstrated that the Visco-Corder was capable of measuring the rheological parameters of mortars according to the two-point principle, and using the same type of cement and sand as reported by Lewandowski and Wolter (1981). It was shown that the flow curves obtained conformed to the Bingham plastic model in which the down curve was a good straight line given by Equation (5.1). Similar calibration principles as reported by Tattersall and Bloomer (1979) were used to calibrate the Visco-Corder. The rheological properties of mortar were then reported in fundamental units.

Further refinements to the mixing of mortar and testing procedures were reported by Banfill (1991). The work involved varying the mixing and testing procedures of various mortar compositions. He suggested that there was no practical advantage in using long cycle times to obtain the flow curves as the down curves of different test procedures were very similar.

However, the procedures reported by Hornung (1991) were different to those of Banfill (1991), whereby the test was started at a constant rotational speed of 120 rpm. Once a constant torque had been observed (completion of structural breakdown), the speed was reduced in steps to 80, 40 rpm and then stopped. The torques corresponding to these speeds (120, 80 and 40 rpm) were then used to construct the down curve. The rheological parameters reported were not converted into fundamental units. Hornung (1991) reported

that the equipment was capable of detecting changes in mortar components, such as changes in water/cement ratio, type of sand and cement.

5.3 EXPERIMENTAL

5.3.1 Description of the Two-point Workability Apparatus

The Visco-Corder used in this work (shown in Fig. 5.1) consisted of a cylindrical container which was mounted on a turntable of adjustable height. It could be rotated at speeds of up to 350 rpm, measured using a digital tachometer. A concentric paddle was mounted so that the gap between its outer tips and the inner wall of the cylinder was 3 mm, other dimensions being as shown in Figs. 5.1 & 5.2. As the cylinder rotates, the force resulting from the friction of the mortar flowing through the blades of the paddle is transferred through a lever arm that presses against the spring of a load gauge microprocessor (Micromesin UK).

The Haake Rotovisco described in Chapter 4 with sensor MV 2 was used in the calibration of this equipment.

5.3.2 Calibration

A series of procedures described by Tattersall and Bloomer (1979) were used to calibrate this Visco-Corder so that the rheological parameters of modified mortars may be reported in fundamental units. These procedures were used to determine the equipment constant G, a constant of proportionality K and power fluid constants p, q, r and s, which are unique to this instrument.

Equipment Constant, G

To determine G a Newtonian fluid is tested first in the Rotovisco to give a plot of shear stress against shear rate, the slope of which allows calculation of its viscosity η. It is then tested in the Visco-Corder to give a plot of torque against speed. The relationship between the two tests is then given by the following equation:

$$\frac{T}{N} = \eta G \qquad (5.2)$$

where: T is torque, N is rotational speed, η is viscosity and G is the equipment constant. In the present work G was determined by measuring the flow curves of castor oil and standard oil 102 at a slightly varying room temperature. The oils were tested in the Haake Rotovisco RV 20 using MVII cup and rotor (smooth surface) at several temperatures. Shear stress was determined at nine or ten shear rates. In the Visco-corder the torque was measured at increasing speeds of 130 - 250 rpm for castor oil, and 30 - 200 rpm for the standard oil.

Proportionality constants

A 4.5% carboxymethyl cellulose solution, which gives a typical power fluid response, was prepared and tested in the Visco-Corder and Haake Rotovisco. The torque was measured as the speed was increased in steps between 30 - 200 rpm. The solution was then tested in the Haake Rotovisco RV 20 using MVII cup and rotor (smooth surface) at several temperatures. Shear stress was determined at nine or ten shear rates. The data was analysed using the following equations:

For a pseudoplastic liquid that obeys the power law:

$$\tau = r\dot{\gamma}^{s} \qquad (5.3)$$

For the two-point apparatus,

$$T = pN^q \tag{5.4}$$

The shear rates $\dot{\gamma}$ for the power law fluid in the Haake Rotovisco were calculated at the inner cylinder using the expression described by Krieger and Maron (1951):

$$\dot{\gamma} = \frac{2N\Omega}{1-S^{-2N}}\left(1+\frac{N'}{N^2}f(\tau)\right) \tag{5.5}$$

where $S = R_2/R_1$ (R_1 = 18.4 mm and R_2 = 21 mm), R_1 is the radius of rotor and R_2 is the radius of the cylinder cup. The values of N' and $f(\tau)$ are rarely significant unless the slope N of logarithmic plots of log Ω (rotational speed) and log $\dot{\gamma}$ (shear stress) is not constant. For the purpose of this calibration, the following expression was used as the value of N obtained for the power law relationship is almost constant. Futhermore, the values of the second derivatives relating N' and $f(\tau)$ are too small (Sherman, 1970, Lenk, 1978). Therefore the following shear stress calculation was used:

$$\dot{\gamma} = \frac{2N\Omega}{1-S^{-2N}} \tag{5.6}$$

Further mathematical derivations by Tattersall and Bloomer (1979) and using constants p, q, r and s led to the use of constant of proportionality K which is shown as:

$$K = \left(\frac{p}{rG}\right)^{1/(s-1)} \tag{5.7}$$

Determination of the above equipment and proportionality constants allow the yield value and plastic viscosity of mortar given in equation (5.1) to be expressed by the following formulae respectively:

$$\tau_o = \left(\frac{K}{G}\right)g \qquad (5.8)$$

$$\mu = \left(\frac{1}{G}\right)h \qquad (5.9)$$

5.3.3 Mixing and Testing Procedures

Mortars were prepared using a standard Hobart three speed planetary mortar mixer, using an open paddle as described elsewhere (Banfill, 1990 & 1991). The water and SBR 1 or Ac 1 emulsions were placed in the bowl and mixing commenced at a shaft speed of 140 rpm. The cement was added and mixed for 30 s, followed by the sand with mixing continuing for a further 30 s. Mixing speed was then raised to 250 rpm and continued for a further 60 s giving a total mixing time of 2 minutes. When using EVA 1, the redispersible powder was first dry blended with the cement.

The amounts of polymer added were in the range 0 - 20% dry polymer solids by weight of cement. In the case of the Ac 1 and EVA 1, defoamer (De) was added by mixing 1% by weight of dry polymer solids to the water.

The mortar mix was then immediately poured into the Visco-Corder cup and tested. The speed of rotation of the cup was held constant at 50 rpm to allow structural breakdown to occur, during which time the load decreased and became nearly constant. The time for breakdown depended on the water/cement and polymer/cement ratios of the mortar mix, but it usually occurred within 3 - 5 minutes. Preliminary trials were carried out to determine breakdown time and its reproducibility.

Speed was increased in steps to give 100, 150, 200 and 250 rpm. At each step the speed was held constant for 10 seconds and the force recorded. The speed was then reduced in steps to give 200, 150, 100 and 50 rpm, and again the force was recorded at each step.

The recorded value of the force was then converted to give the torque in Nmm. All the tests were carried out at 20 ± 2°C.

The test procedures described above differed slightly from those used by Banfill (1990 & 1991) and Hornung (1991). For comparison, preliminary experiments were also carried out following these other procedures.

5.3.4 Test Programme

The work was carried out in five series of experiments:

1) Calibration of the Visco-Corder was carried out to determine the series of constants, discussed in Section 5.3.2. Following this, the rheological parameters could be determined in fundamental units using equations 5.8 & 5.9 and hence compared with work carried in other laboratories and after subsequent modifications of the instrument.

2) The influence of using the test procedures described by Banfill (1990 & 1991) and Hornung (1991) was investigated.

3) A mortar M1 was used which had an aggregate/cement ratio of 1.5 : 1 and utilised sand 1 which had a relatively fine grading. This mix was chosen for its similarity to that used in other work and to define the limitations of the equipment. The polymer employed was SBR 1 at concentrations of 0, 5, 10 and 20%, this later value representing the upper limit used in practice. The water/cement ratios used (0.3 - 0.55) depended on polymer content and were adjusted so that a range of workabilities could be obtained. These were determined by trial and error and ranged from wet, high workability to dry, low workability mixes.

4) Three mortar mixes were used, each containing 20% SBR 1:

M1 - Sand 1, aggregate/cement ratio 1.5 : 1

M2 - Sand 1, aggregate/cement ratio 2.5 : 1

M3 - Sand 2, aggregate/cement ratio 2.5 : 1

The mortar M2 was used to determine the effect of increasing aggregate/cement ratio, whilst use of mortar M3 showed the effect of using coarser sand, this latter mortar being more representative of those used for polymer modified mortars in practice. For plain mortars, Hornung (1991) has shown that increasing the aggregate/cement ratio gives an increase in τ_o and μ, whilst decreasing the percentage of fines in the aggregate gives a decrease in τ_o and μ.

5) Mortar M3 was used with polymers SBR 1, SBR 2, Ac 1 and EVA 1 at concentrations of 10% and 20% in order to compare the influence of different polymer systems on mortar workability.

5.4 RESULTS AND DISCUSSION

5.4.1 Calibration of the Visco-Corder

The plots of torque, T against rotational speed N of the Visco-Corder for the two Newtonian fluids are shown in Fig. 5.3. The equations for these lines are given in Table 5.1. Since the oils are Newtonian fluids, the straight lines drawn should pass through the origin, and since they do not a small zero error exists in the equipment. The average value of the intercept and therefore error was - 4.9 Nmm. This value was then added to all subsequent values obtained using this equipment.

The viscosities of these oils were obtained from the plot of shear stress against shear rate using the Haake Rotovisco, Fig. 5.4 and the values are shown in Table 5.1. All plots

show good straight lines through the origin with correlation coefficients of not less than 0.995. The results were then used to determine the equipment constant G using equation (5.2) and values are given in Table 5.1. The mean value of G was $3.81 \pm 0.39 \times 10^{-3}$ m^3.

To determine the proportionality constants a pseudo-plastic solution, carboxymethyl cellulose was tested in the Rotovisco, and the plot of $\ln \tau$ against $\ln \dot{\gamma}$ is shown in Fig. 5.5. The plot of ln T versus ln N of a similar solution tested in the Visco-Corder is shown in Fig. 5.6. By applying equations 5.3 & 5.4, the values of p, q, r and s were obtained and are given in Table 5.2. The constants r and p are the intercepts whilst s and q are the slopes of these plots respectively.

Mean values of the constants obtained in this work are comparable with those obtained by Banfill (1990), Table 5.3, any discrepancies in the figures obtained probably arising from minor equipment differences, e.g. geometry of the paddles. For the calibration theory to apply, the ratio (q-1)/(s-1) should be equal to unity (Tattersall and Bloomer, 1979). The value of this ratio obtained for the equipment used in the present work was 1.04 compared to 1.02 for testing concrete (Tattersall and Bloomer, 1979) and 1.2 for testing mortars (Banfill, 1990), thus it was considered that the calibration procedures were correct and the equipment used in the present investigation was suitable for testing mortars.

Using data given in Tables 5.1 & 5.2, it was then possible to calculate the proportionality constants relating τ_o to g (given by equation 5.8) and μ to h (given by equation 5.9), and these were calculated to be 4.1 and 0.26 respectively. Thus for the present equipment, the yield values, τ_o (Nm^{-2}), and plastic viscosity μ (Nsm^{-2}), can be found from the following equations:

$$\tau_o = 4.1g \qquad (5.10)$$

$$\mu = 0.26h \qquad (5.11)$$

5.4.2 Comparison with Different Test Procedures

The flow curves (down curves) for mortars tested according to procedures described by Banfill (1990), Hornung (1991) and used in this work (described in Section 5.3.3) are shown in Fig. 5.7. The flow curves were for unmodified mortar with water/cement ratio of 0.6 and 20% SBR 1 modified mortars with water/cement 0.40, and it is evident that all conform to the Bingham model.

Banfill observed that mortar undergoes structural breakdown immediately after starting the Visco-Corder so that the down curves are at a lower torque than the up curves. He also suggested that the structural breakdown is completed at the end of the up curves, i.e. by the time maximum speed is reached.

Hornung (1991) observed that normal mortar will undergo structural breakdown within 4 - 6 minutes after starting the Visco-Corder and running at 120 rpm. He suggested that a minimum of two points were sufficient to construct the flow curves (down curves) to characterise the Bingham model of plastic behaviour. The torques were measured at rotational speeds of 80 and 40 rpm.

In this investigation, the structural breakdown was observed once the constant force was achieved at constant rotational speed of 50 rpm. The speeds were then increased and decreased in a similar way as described by Banfill (1990). The advantage of taking the reading after the second cycle was to ensure no further structural breakdown occurred to the mortar at longer shearing times, hence reducing the scatter of results without causing any segregation.

The present investigations show that, for plain mortar, the procedures adopted in this investigation produced a lower yield value g than the other two procedures. This suggests

that structural breakdown still occurs even after completion of the up curves. For mortar with 20% SBR 1, the yield values obtained were similar within experimental error.

5.4.3 Rheological Behaviour of Mortars M1 Using Sand 1 and SBR 1

The flow curves (down) for unmodified and 5, 10, 20% SBR 1 modified mortars at different water/cement ratio are shown in Figs. 5.8 - 5.9. It is evident that the polymer modified mortars behaved in a similar manner to the unmodified mortar in that they confirmed to the Bingham plastic model of behaviour given by Equation 5.1. It also shows that a small change in the water/cement ratio can be detected by the changes in the values of intercept g. The down curves were good straight lines with correlation coefficients of not less than 0.990 and 0.995 for plain mortars and polymer modified mortars respectively. Selected mixes were replicated five times to demonstrate that the down curves were reproducible. However, correlation coefficients of < 0.990 were obtained when attempts were made to test mixes that were too dry.

Values of intercept g and slope h were found from the plots shown in Figs. 5.8 - 5.9 and using equations (5.10) and (5.11), values of τ_o and μ were calculated in fundamental units. The effect of water/cement ratio on τ_o and μ, at different polymer/cement ratios are shown in Fig. 5.10. It is evident that yield value τ_o and plastic viscosity μ increase roughly exponentially as the water/cement ratio decreases, and this applies to both unmodified and modified mortars.

At low water/cement ratios, the μ values obtained were lower than might be predicted from the general trend. For example, in the case of unmodified mortar, at the lowest water/cement ratio tested (0.45), the value of μ was found to be 2.9 Nsm^{-2} as against 5 Nsm^{-2} predicted from extrapolation of the curve. When this occurred it was noted that during shearing gaps began to appear between the paddle blades/cup walls and mortar

mass providing less resistance to flow. This incident defines the minimum water/cement ratio that can be used to test a given type of mix.

Values of τ_o for unmodified mortar were found to range from 50 to 400 Nm^{-2} for water/cement ratios 0.60 to 0.45. Significant changes occur to the workability in terms of τ_o when SBR 1 was added to the mortar mix. For example at a water/cement ratio of 0.45, the value of τ_o was reduced from 450 to 100 or 50 Nm^{-2} when 5% or 10% SBR 1 was added. Further additions of SBR 1 at this water/cement ratio resulted in mixes so fluid that it was difficult to contain them in the rotating cup. Fig. 5.10(a) also shows that for a given polymer concentration, it is possible to determine the water/cement ratio required to give the same yield value. For example at τ_o of 175 Nm^{-2}, as the polymer concentration increases from 0, 5, 10, to 20%, then the water/cement ratio required decreases from 0.52, 0.44, 0.37 and 0.30. Similar trends were found for changes in plastic viscosity, Fig. 5.10(b). This clearly demonstrates the advantage of adding SBR 1 from a workability point of view. It is evident that significant improvement in workability can be achieved by adding SBR 1 into the mix.

5.4.4 Rheological Behaviour of Mortars M1, M2 and M3 Containing 20% SBR 1

The sand grading and aggregate/cement ratio can have a considerable influence on the values of τ_o and μ obtained as can be seen in Figs. 5.11a & b. Comparing mortar M1 with M2, both had the same sand grading but the aggregate/cement ratio was increased from 1.5 : 1 to 2.5 : 1. It can be seen that both τ_o and μ are significantly increased. A trend similar to that found by Hornung (1991) and Banfill (1994) when using plain mortars with maximum particle size sand of less than 1 mm and 1.18 mm respectively. In contrast, comparing mortar M2 with mortar M3, both have the same aggregate/cement ratio but mortar M3 uses a coarser sand with a maximum particle size of 2.36 mm. It can be seen that both τ_o and μ decreased, but in neither case very significantly.

The results show that the equipment is sensitive enough to determine rheological characteristics of polymer modified mortars typical of those used in practice. The instrument was also sensitive enough to detect changes in both τ_o and μ with variables such as sand grading and aggregate/cement ratios.

5.4.5 Rheological Behaviour of Mortars M3 using Sand 2 and Different Polymers

Flow curves (down) for unmodified mortar M3 and modified with SBR 1, SBR 2, Ac 1 and EVA 1 are shown in Figs. 5.12 - 5.15. The trends are similar to those obtained earlier in that they conformed to the Bingham plastic model of behaviour. The lines have correlation coefficients of between 0.988 - 0.999.

The influence of type of polymer at concentrations of 10% and 20% on τ_o and μ at different water/cement ratios are shown in Figs. 5.16 - 5.17. It can be seen that significant differences in behaviour were found for different polymers. At low water/cement ratios the τ_o values for 10% SBR 1 (w/c 0.4) and 20% EVA 1 (w/c 0.45) deviate from the predicted exponential general trends. Similar deviations were found for changes in μ for unmodified mortar (w/c 0.55), 10% SBR 1 (w/c 0.4 & 0.45), 20% SBR 1 (w/c 0.375 & 0.4), and 20% EVA 1 (w/c 0.45). This confirms the earlier observation (as described in Section 5.4.3) that defined the minimum water/cement ratios needed to test a given type of mix and limitation of the equipment. It is however interesting to note that in the case of the Ac 1, increasing the water/cement ratios appears to result in a limiting value of τ_o at $\approx 150\ Nm^{-2}$.

It is evident that additions of 10% polymers were found to give significant improvement in workability when compared to unmodified mortar. Ac 1 was found to be the most effective, followed by SBR 1 and then EVA 1. In the case of SBR 1 and Ac 1, further improvements were found when concentrations of polymer were increased to 20%. This

was not the case for EVA 1 where little difference was observed. These differences could be due to the differences in chemical and physical properties of polymers. In this respect, it may be necessary to determine the influence of each aspect of formulation, e.g. surface chemistry of the polymer or type of surfactant, on workability.

The effect of SBR 2 carboxylation on workability can be seen by comparing the curve for SBR 1 and points for SBR 2 in Figs. 5.17(a) & (b). It is evident that the points for SBR 2 lie very close to the curve for SBR 1. Thus it may be concluded that carboxylation had little effect on workability of this mix. This is in contrast to the influence of carboxylation on rheology of SBR modified cement pastes where it was found to have a considerable effect. SBR 2 modified cement pastes were found to be anti-thixotropic whilst with mortars behaviour is Bingham. Furthermore there is little difference in the constants obtained for the mortars. A possibility for this difference in behaviour is that the presence of aggregate increases polymer-cement interparticle separation distances and the interaction forces breakdown.

The results obtained show that the methods employed were sensitive enough to show the influence of different polymer systems on workability. They could be used to compare different polymer systems and to determine variations in their formulation.

5.5 CONCLUSIONS

(1) A Visco-Corder has been constructed and calibrated that is capable of determining the rheological parameters of fresh unmodified and polymer modified mortars in fundamental units.

(2) Results suggest that caution is required when testing very dry or very wet mixes. It is essential to perform trial runs in order to gain a basic understanding of the rheological behaviour of a particular mix before starting actual readings. Procedures have been

established to ensure that completion of structural breakdown has occurred before construction of the down curve.

(3) Investigations have confirmed that unmodified and polymer modified mortars conform to the Bingham plastic model of behaviour.

(4) It was found that this Visco-Corder was sensitive enough to detect any changes in the mix e.g. sand grading, aggregate/cement ratio, w/c, type of cement, and different polymer systems on the rheological parameters of mortars.

(5) At a given polymer solids concentration it was found that workability of an unmodified mortar was improved in the following order: Ac 1 > SBR 1 and 2 > EVA 1 > unmodified, although the reasons for this were not elucidated.

(6) No difference in behaviour was found for SBR 1 and SBR 2. Thus it may be concluded that carboxylation had little effect on the workability of the mortar mix. This is in contrast to the influence of carboxylation on rheology of SBR modified cement pastes (see Chapter 4). This difference was attributed to the presence of aggregate particles which increase polymer-cement interparticle separation distances and result in breakdown of the interaction forces.

(7) Use of the Visco-Corder may be preferable to the empirical tests for establishing rheological parameters, when comparisons are being made of the properties of different polymer systems at constant workability.

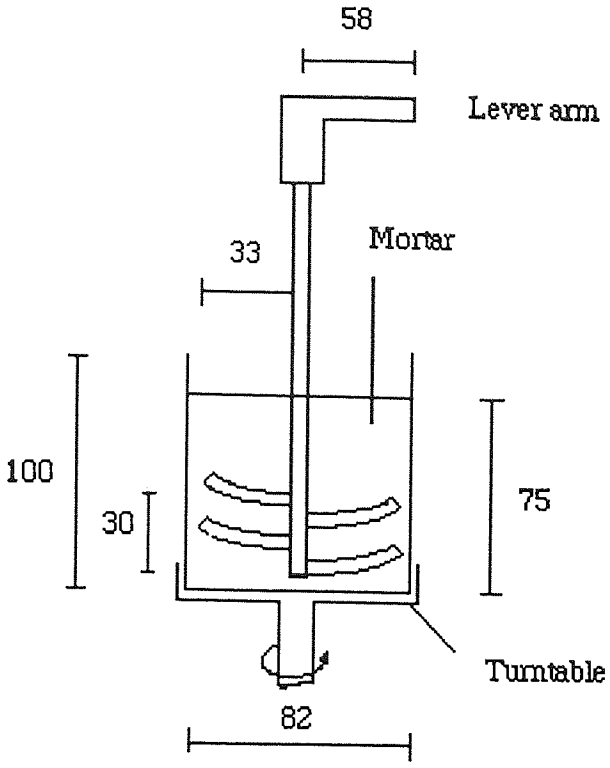

Fig. 5.1: Visco-Corder

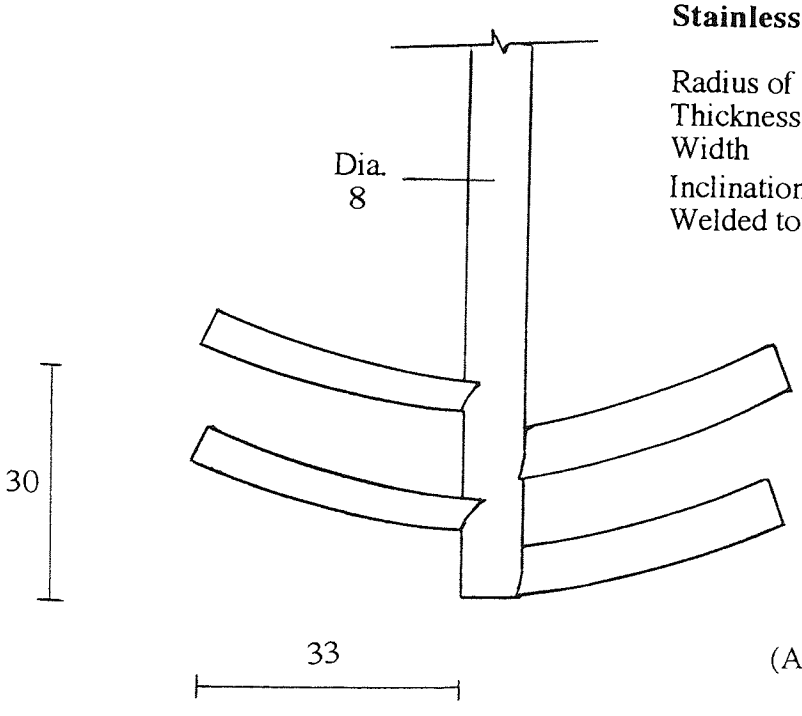

Note:

Stainless steel paddle blade:

Radius of curvature	150 mm
Thickness	1 mm
Width	8 mm
Inclination angle to the shaft	30°

Welded to the shaft @ 7.5 mm c/c

(All dimensions in mm)

Fig. 5.2: Paddle for Visco-Corder

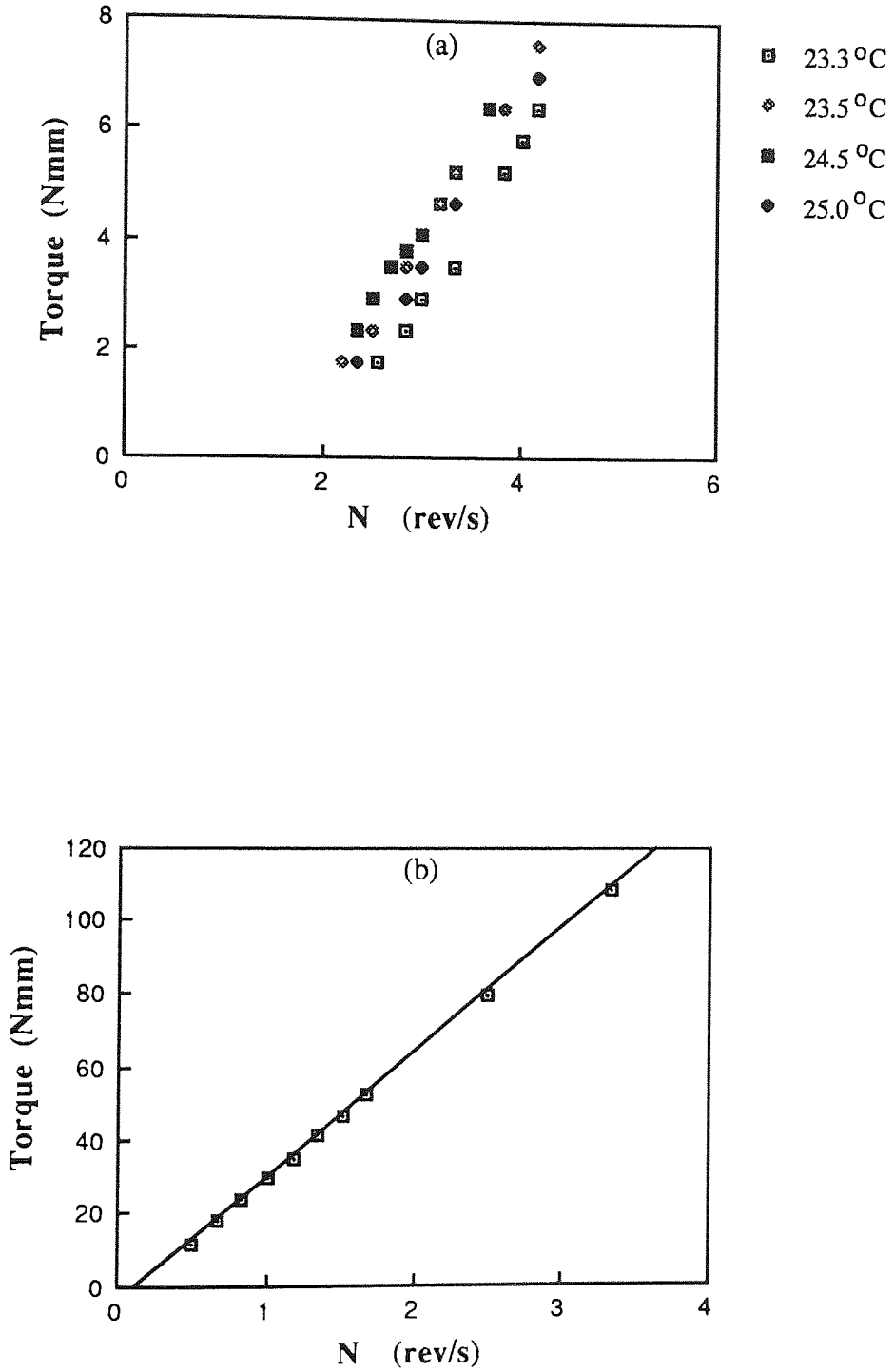

Fig. 5.3: Flow curves of; (a) castor oil at various room temperatures, (b) standard oil in the Visco-Corder at 23.3°C

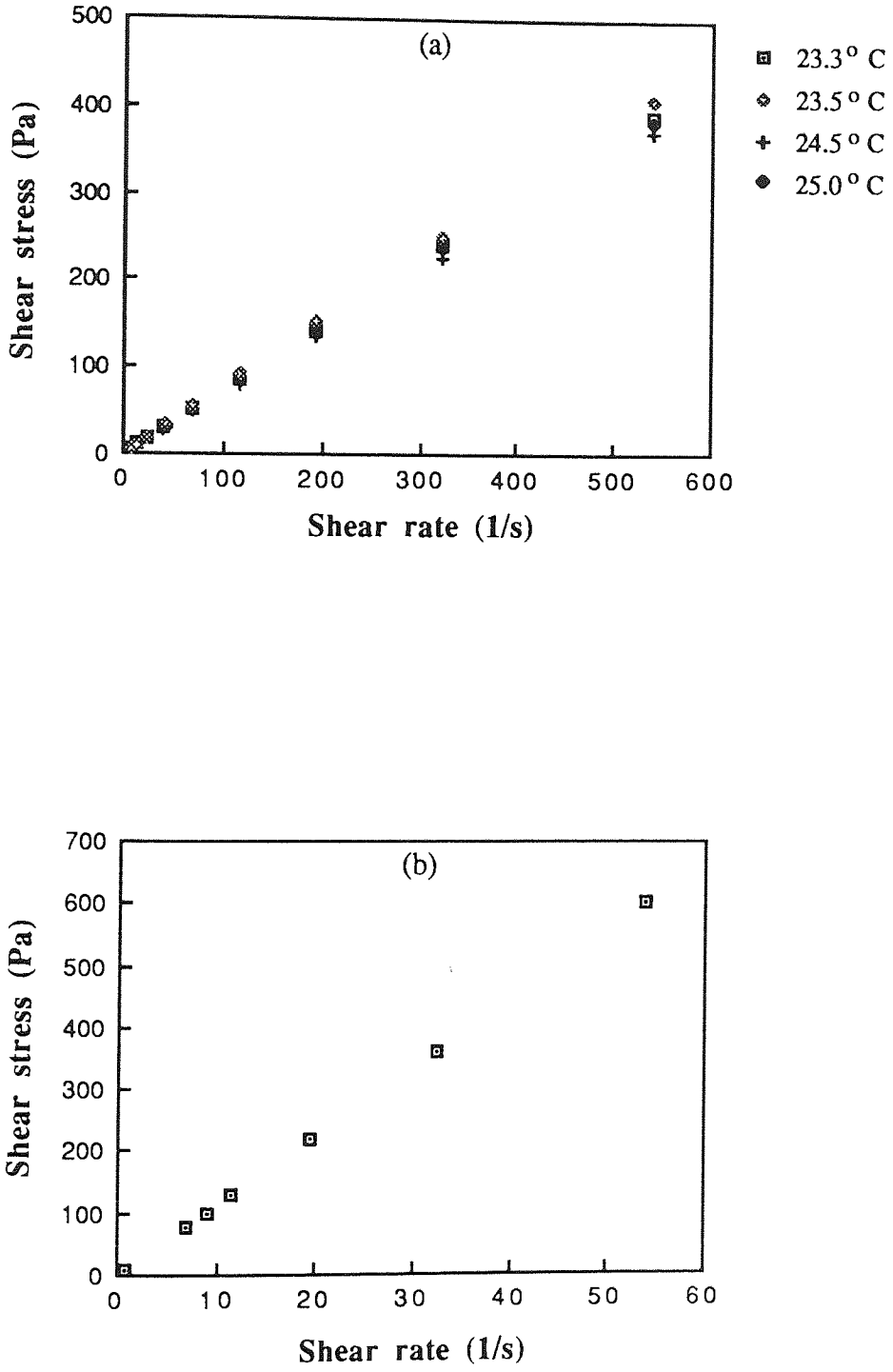

Fig. 5.4: The plot of shear stress against shear rate in the Rotovisco for, (a) castor oil at various room temperatures, (b) standard oil at 23.3°C

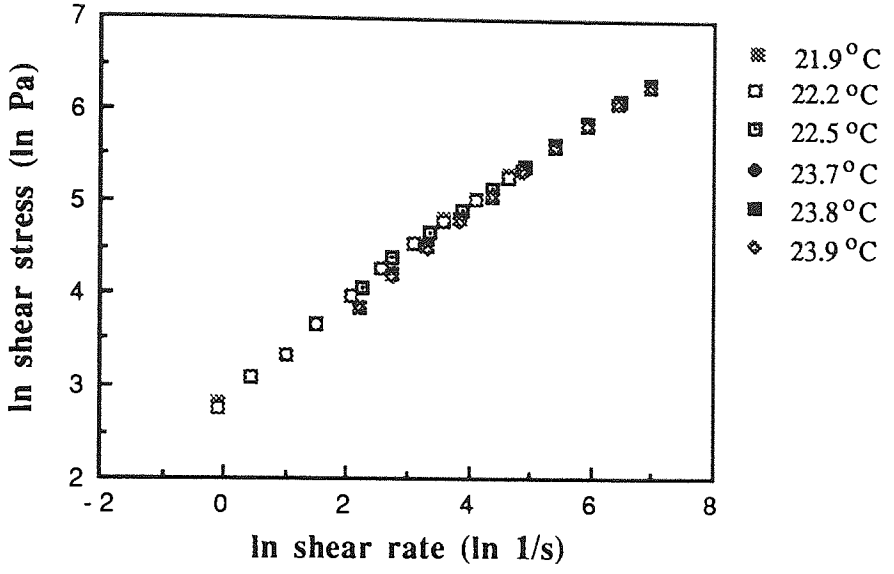

Fig. 5.5: Plot of ln shear stress against ln shear rate (inner cylinder) of carboxymethyl cellulose tested in the Rotovisco at various room temperatures

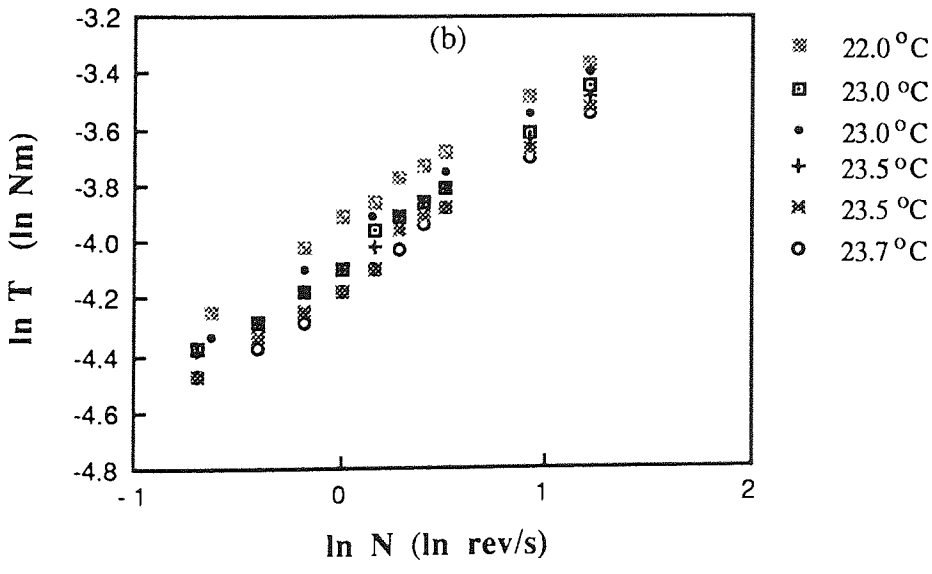

Fig. 5.6: Plot of ln T against ln N for carboxymethyl cellulose tested in the Visco-Corder at various room temperatures

Table 5.1: Summary of results for Newtonian fluids

Liquid	Equations for Visco-Corder	Equations for Rotovisco	T (°C)	Apparatus Constant, G ($x10^3$)
Castor oil	1) T = -5.70 + 2.87N	$\tau = 0.73\gamma$	23.3	3.93
	2) T = -4.97 + 2.85N	$\tau = 0.72\gamma$	25.0	3.96
	3) T = -4.43 + 2.90N	$\tau = 0.69\gamma$	24.5	4.20
	4) T = -4.84 + 2.96N	$\tau = 0.76\gamma$	23.5	3.89
Oil 102	5) T = -4.65 + 33.9N	$\tau = 11.1\gamma$	23.3	3.05

The mean of the apparatus constant G is $3.81 \pm 0.39 \times 10^{-3}$ m^3.

Table 5.2: Summary of power law constants

No	p	q	r	s	1/ (s-1)	(q-1)/ (s-1)	K	K/G
1	0.0182	0.5045	21.55	0.4719	-1.89	0.94	17.0	4.46
2	0.0155	0.5081	15.94	0.5200	-2.08	1.02	16.8	4.41
3	0.0170	0.4866	16.54	0.5130	-2.05	1.05	14.4	3.78
4	0.0159	0.5081	16.02	0.5180	-2.07	1.02	15.9	4.17
5	0.0197	0.4793	17.53	0.5360	-2.15	1.12	13.6	3.57
6	0.0182	0.5063	17.31	0.5360	-2.15	1.06	15.7	4.12

Mean value of $\frac{K}{G}$ is 4.1 ± 0.32

Table 5.3: Mean values of the constants obtained for calibration of the Visco-Corder

Constant	G $x10^3$ m^3	p	q	r	s	(q-1)/ (s-1)	K
Present Work	3.81 ± 0.39	0.017	0.499	17.5	0.516	1.04	15.6
Banfill (1991)	1.29 ± 0.04	0.023	0.396	56.3	0.503	1.22	10.1
Tattersall and Bloomer (1979)*	22.20	2.290	0.280	179.0	0.300	1.02	135.0

* Two-point test for concrete

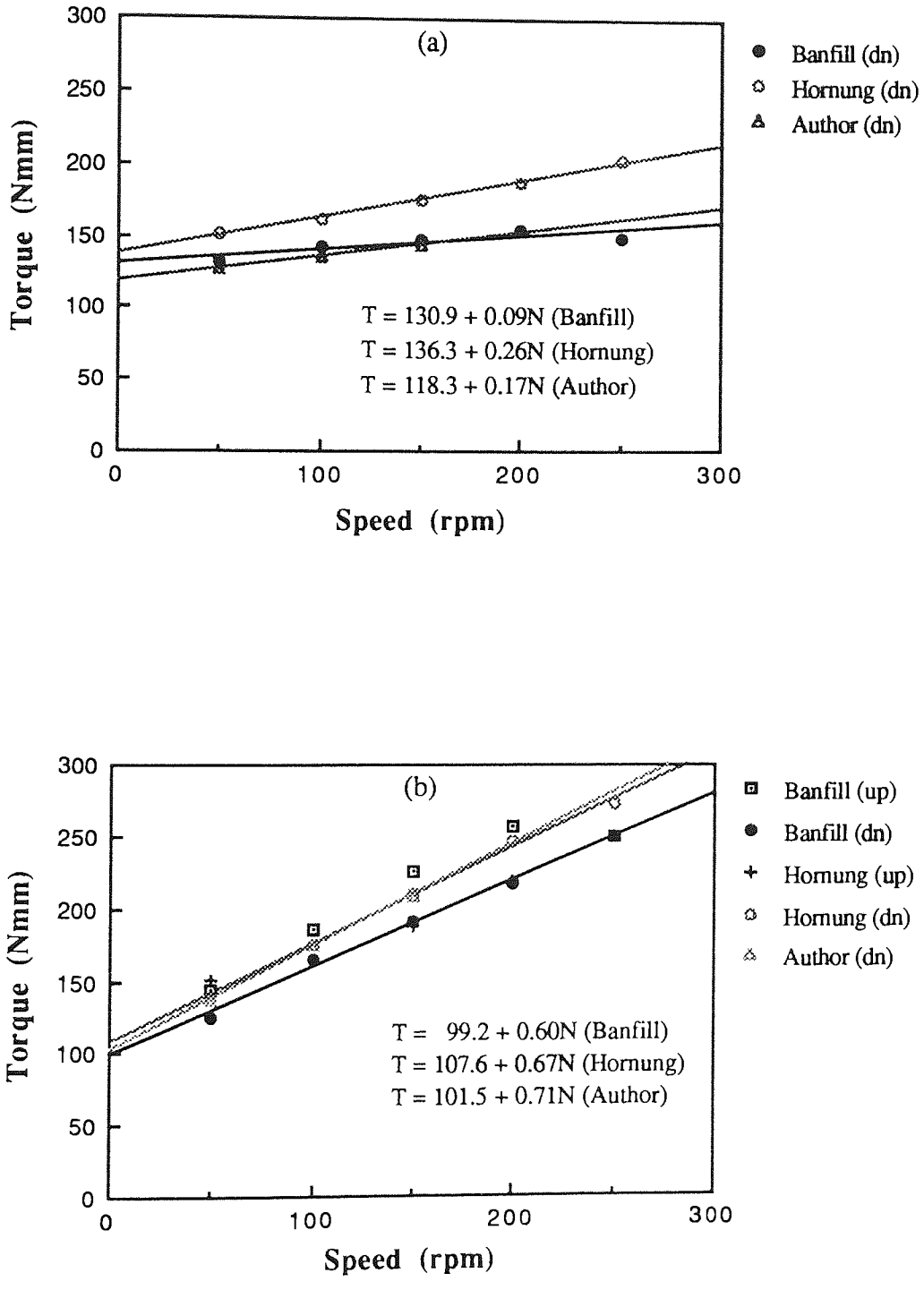

Fig 5.7: Flow curves of mortar M2 using different test procedures; (a) 0% polymer, w/c 0.6, (b) 20% SBR 1, w/c 0.4

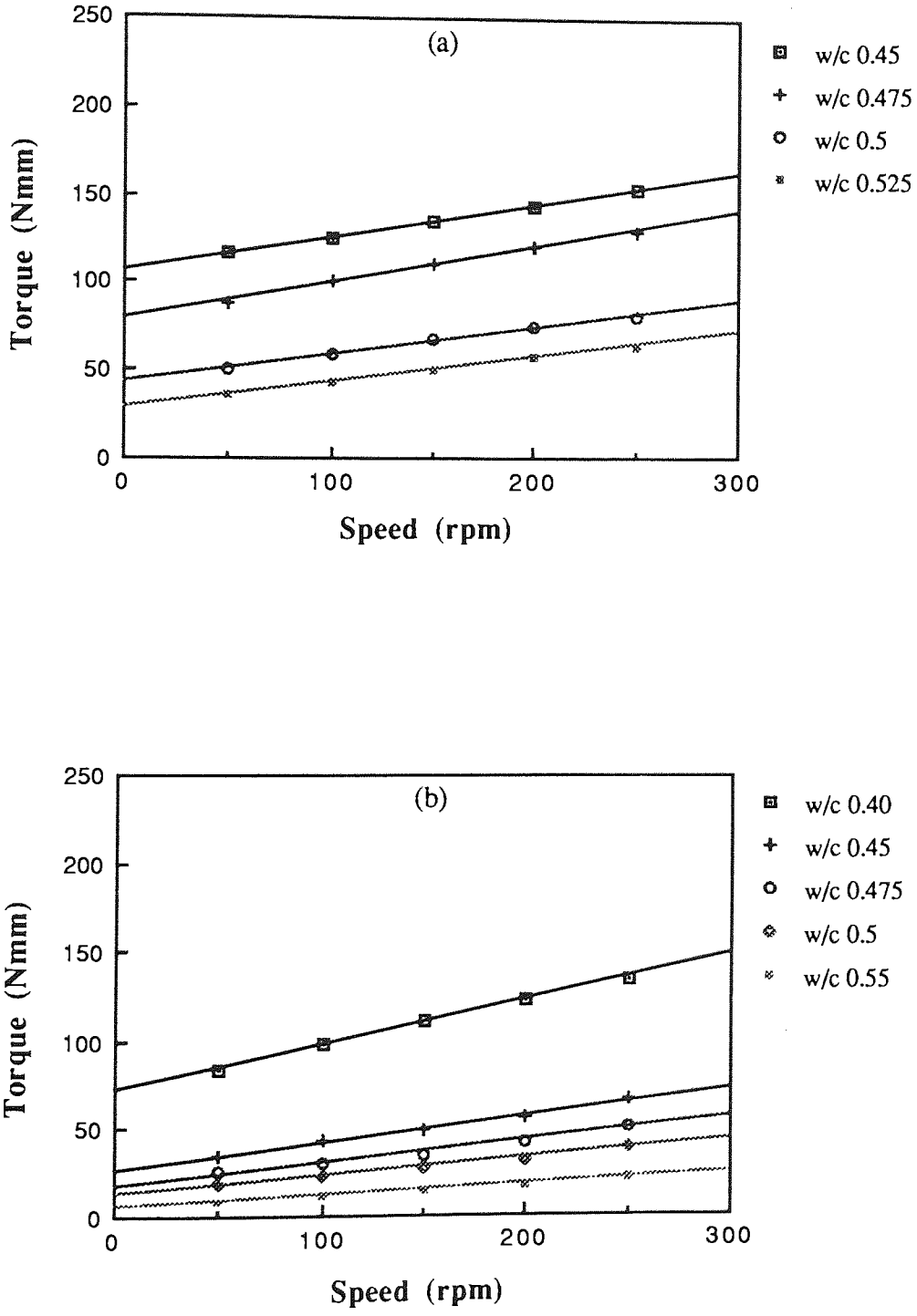

Fig 5.8: Flow curves of mortar M1 with; (a) 0% polymer and (b) 5% SBR 1

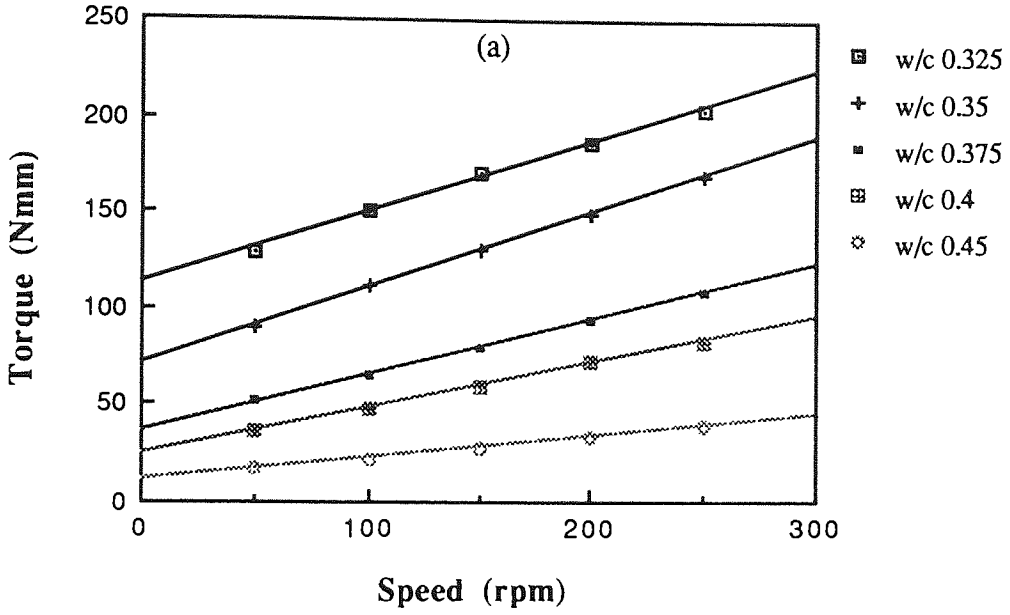

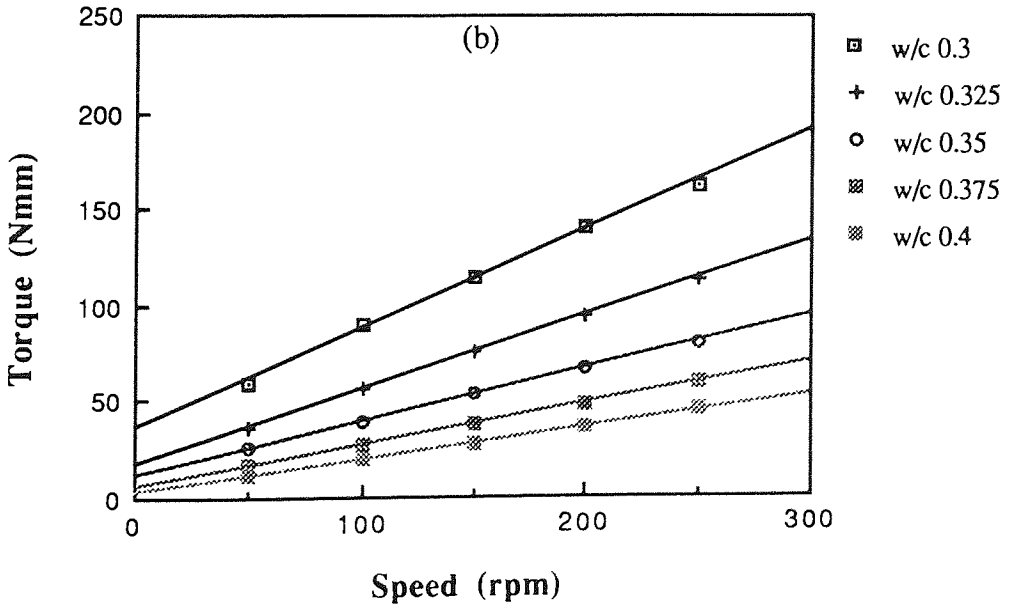

Fig 5.9: Flow curves of mortar M1 with; (a) 10% SBR 1 and (b) 20% SBR 1

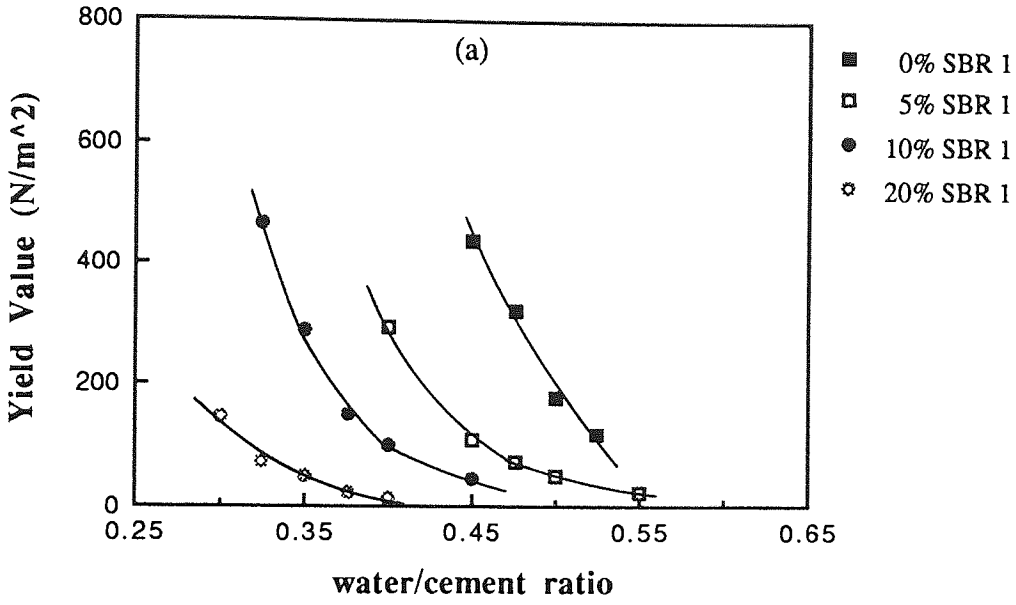

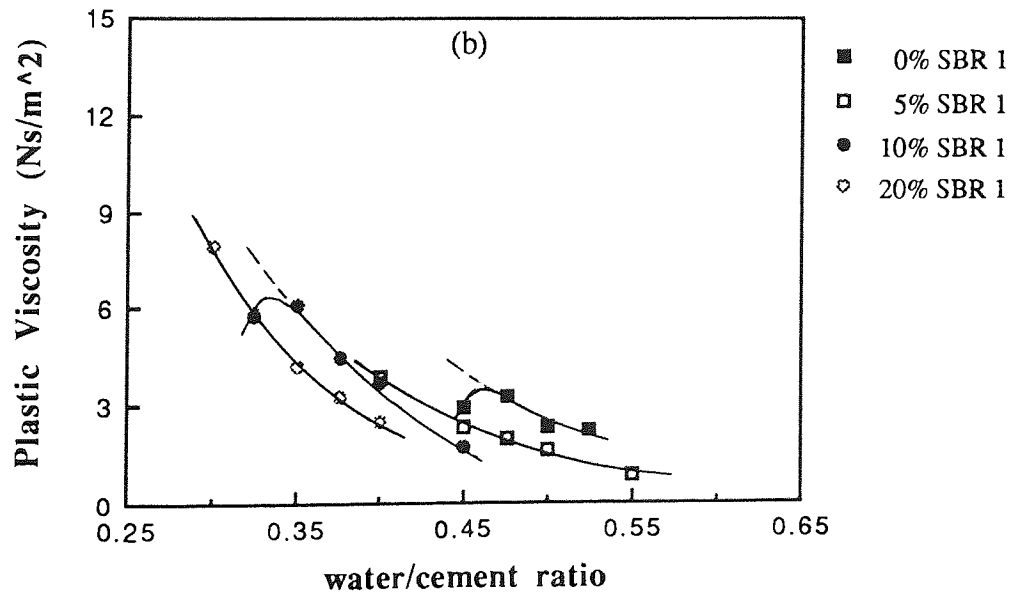

Fig 5.10: The effect of water/cement ratio on (a) τ_o and (b) μ for mortar M1

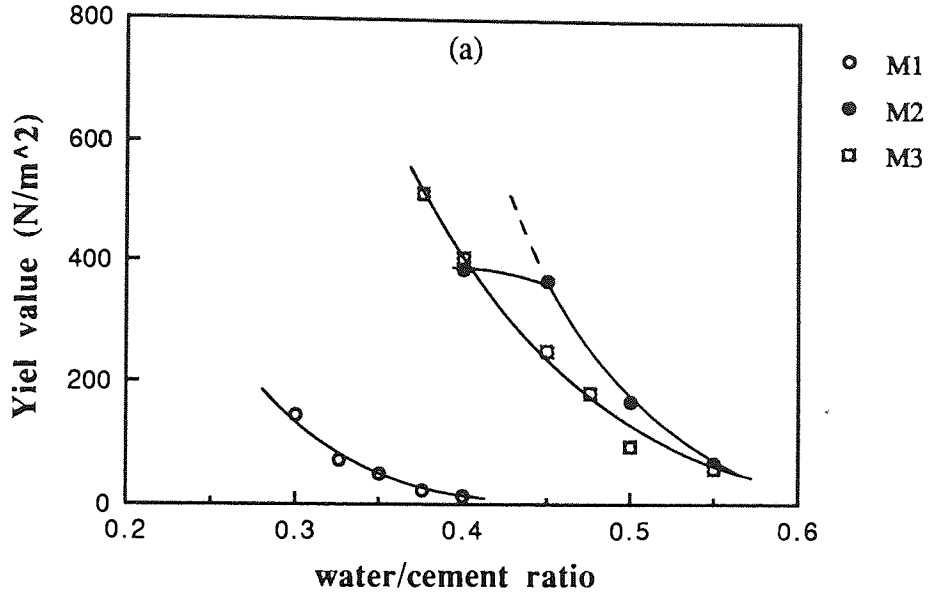

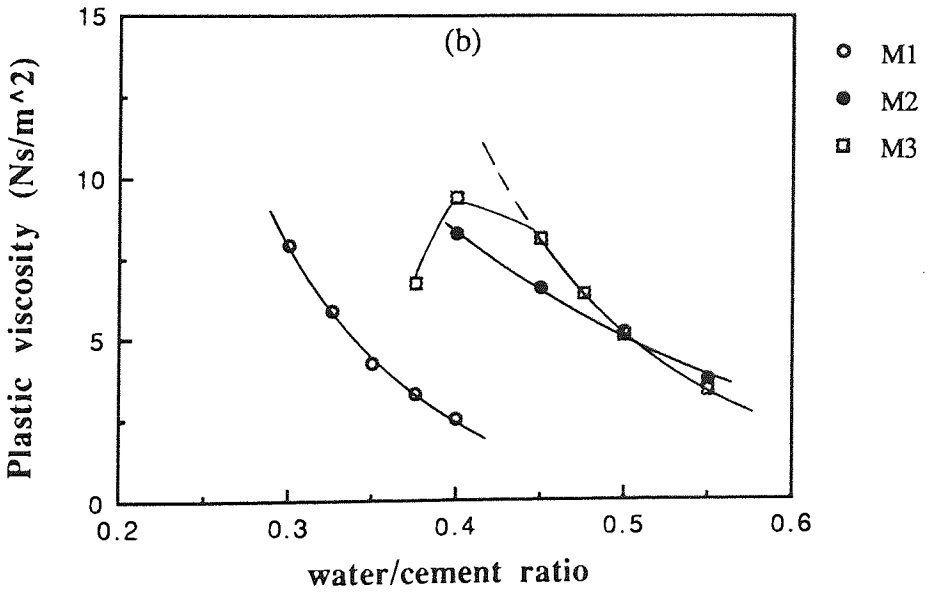

Fig 5.11: The effect of sand content on (a) τ_o and (b) μ for mortars modified with 20% SBR 1

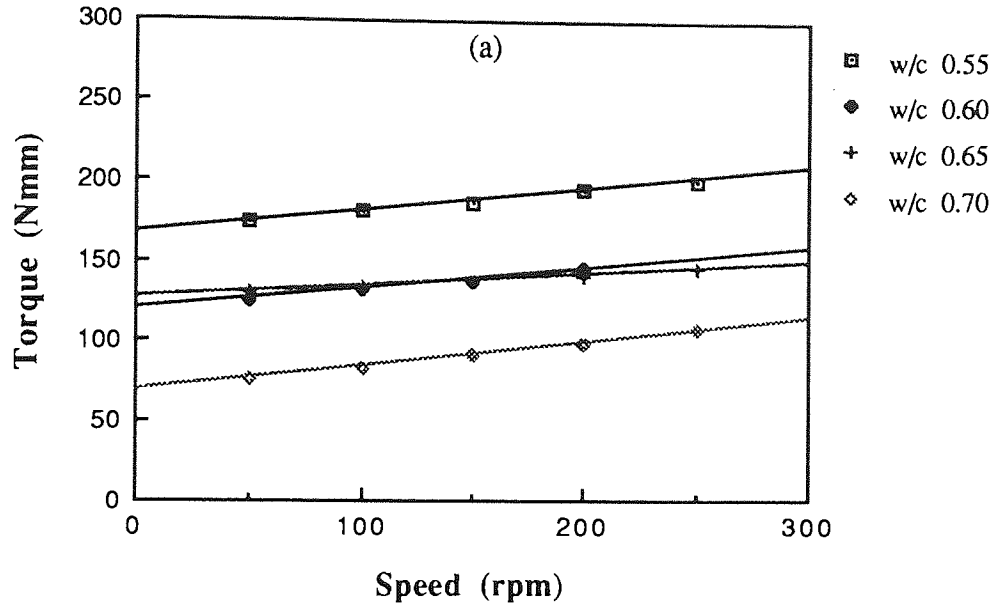

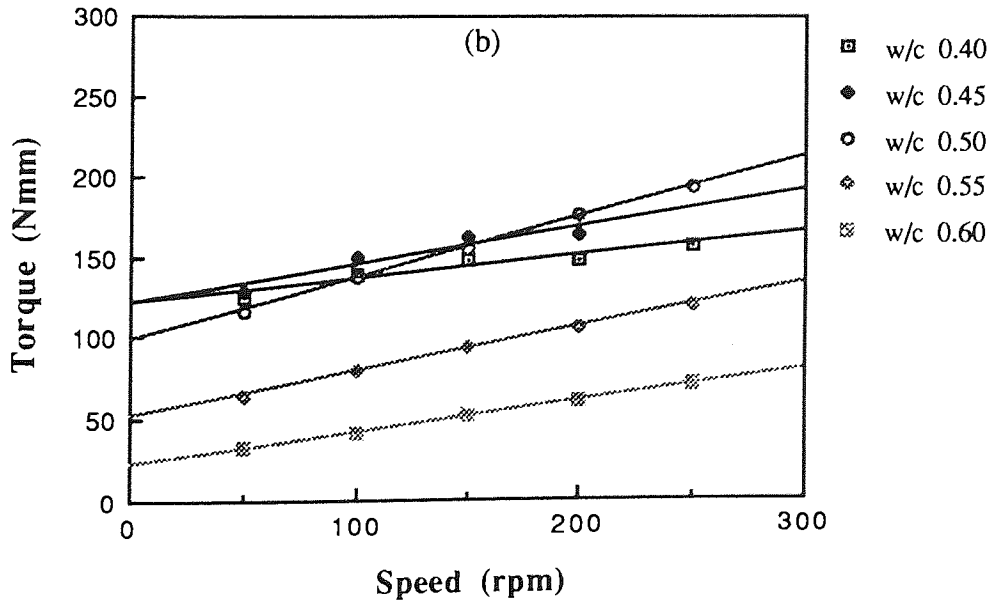

Fig 5.12: Flow curves of mortar M3 with (a) 0% polymer and (b) 10% SBR 1

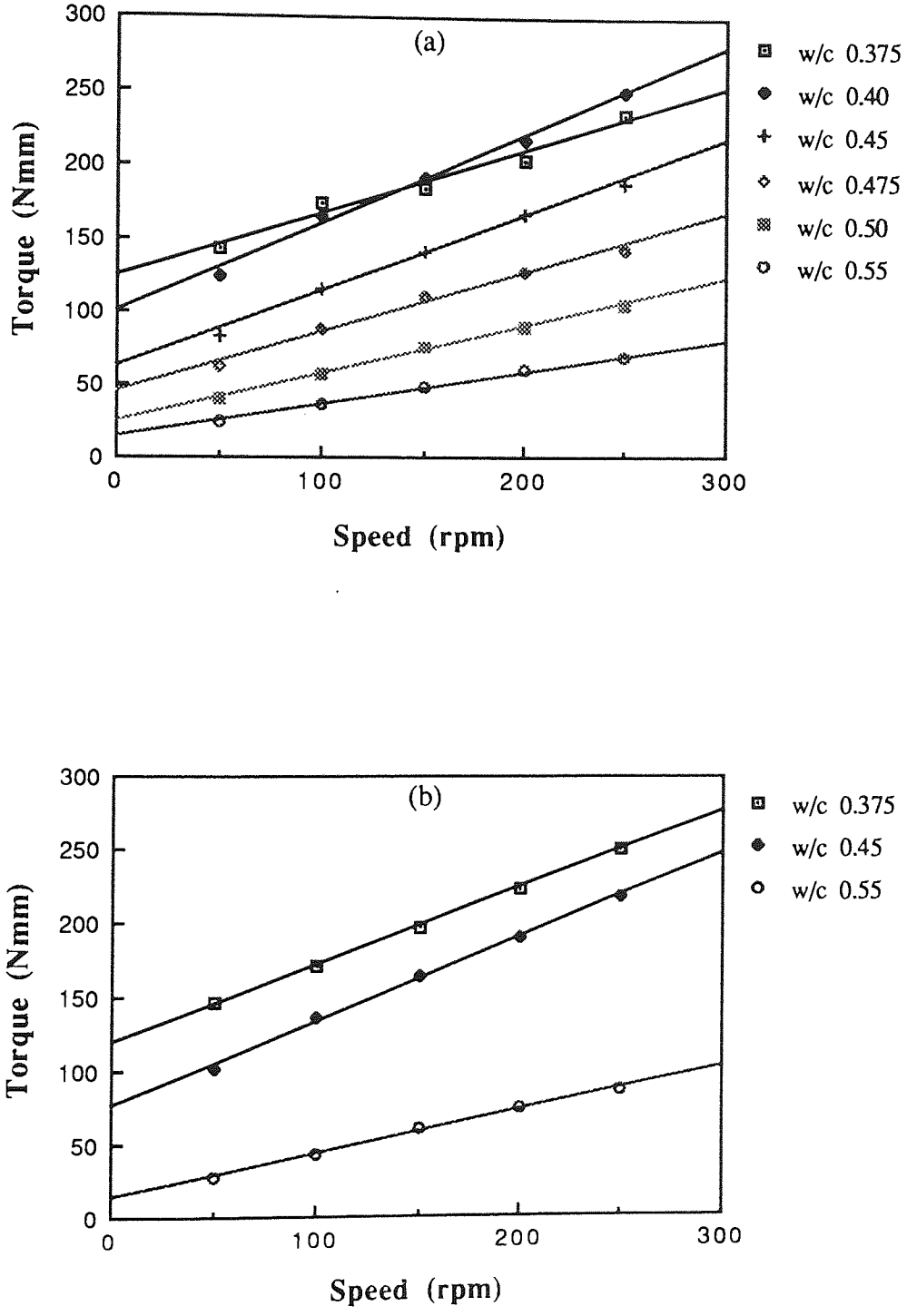

Fig 5.13: Flow curves of mortar M3 with (a) 20% SBR 1 and (b) 20% SBR 2

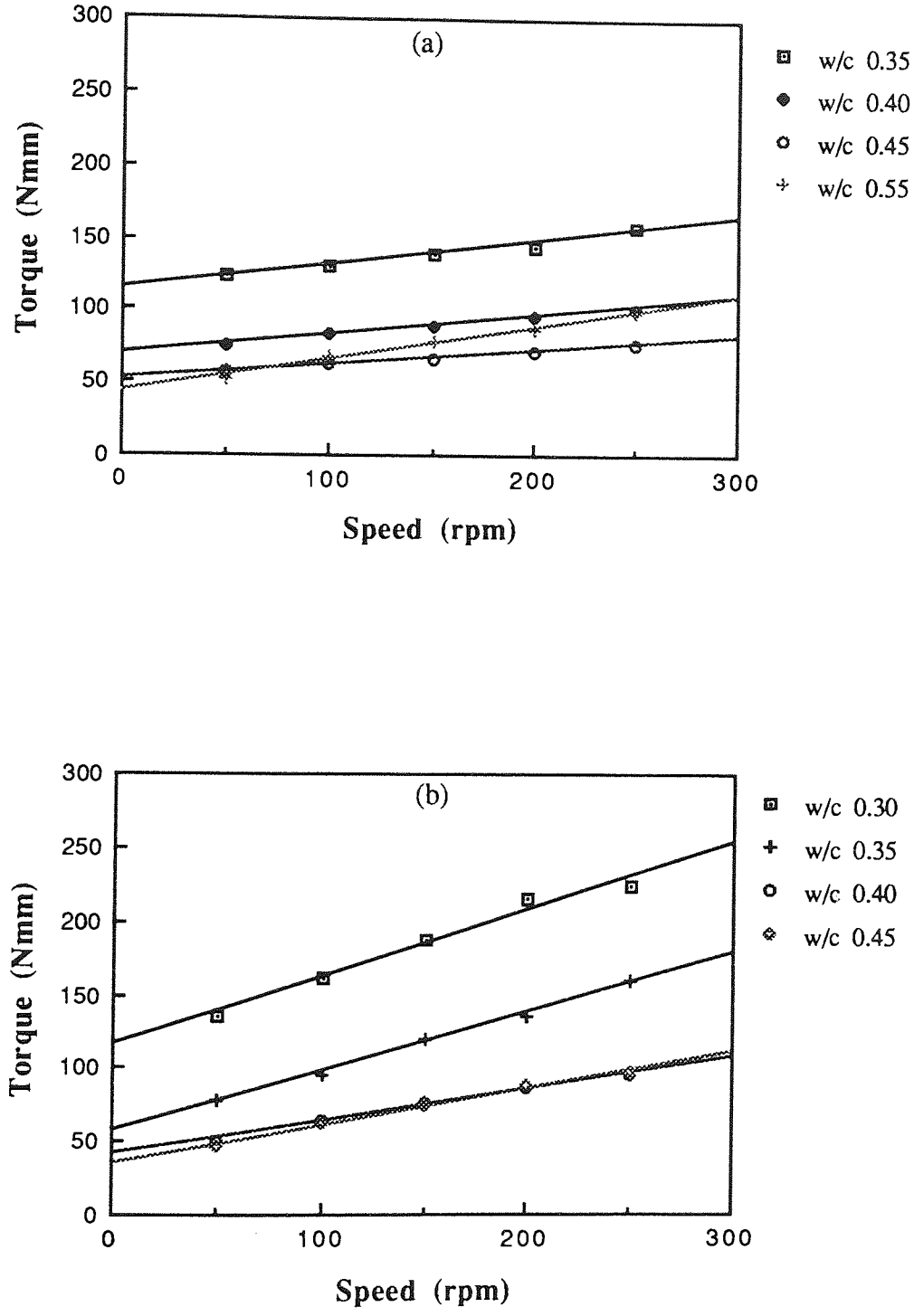

Fig 5.14: Flow curves of mortar M3 with (a) 10% Ac 1 and (b) 20% Ac 1

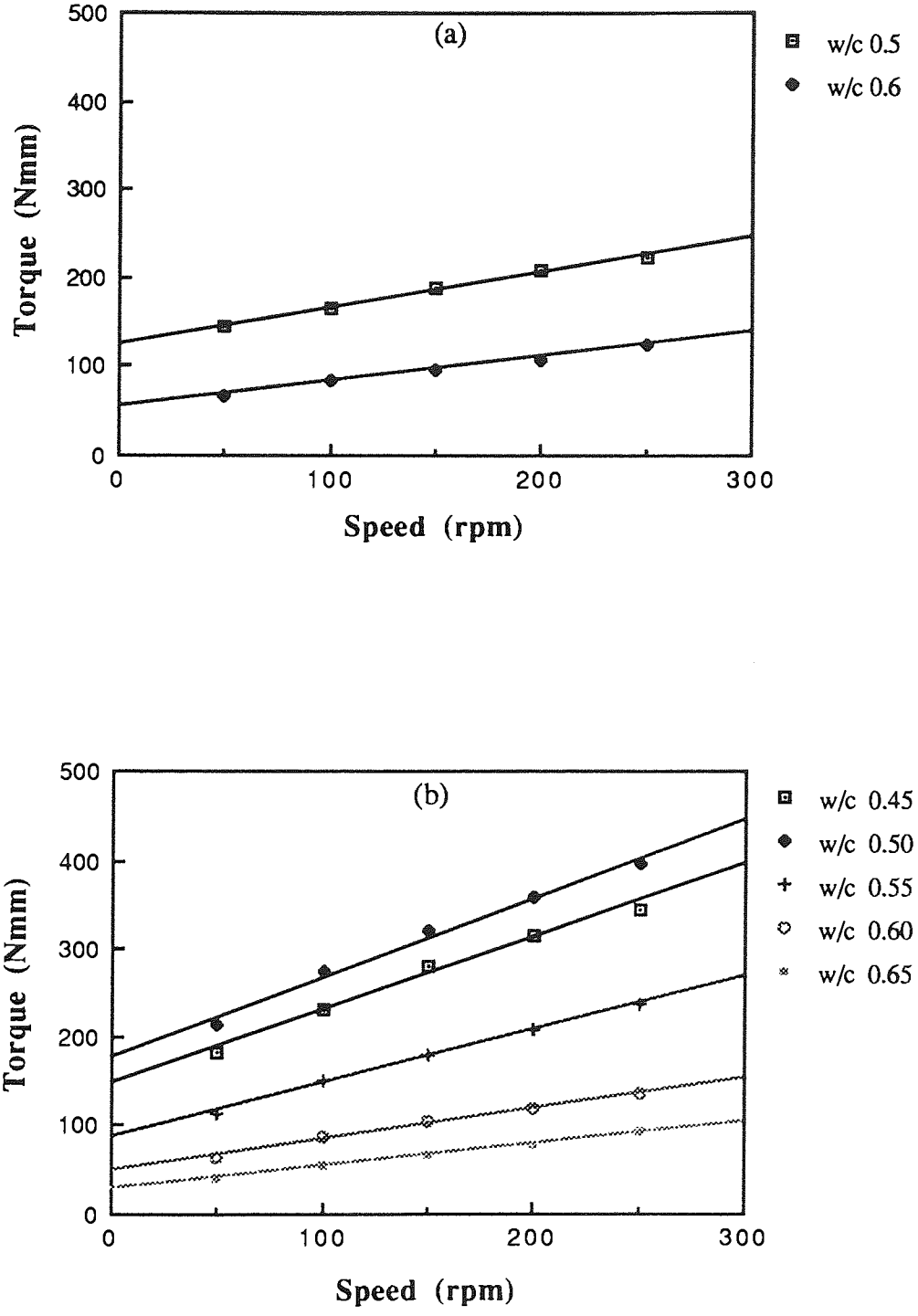

Fig 5.15: Flow curves of mortar M3 with (a) 10% EVA 1 and (b) 20% EVA 1

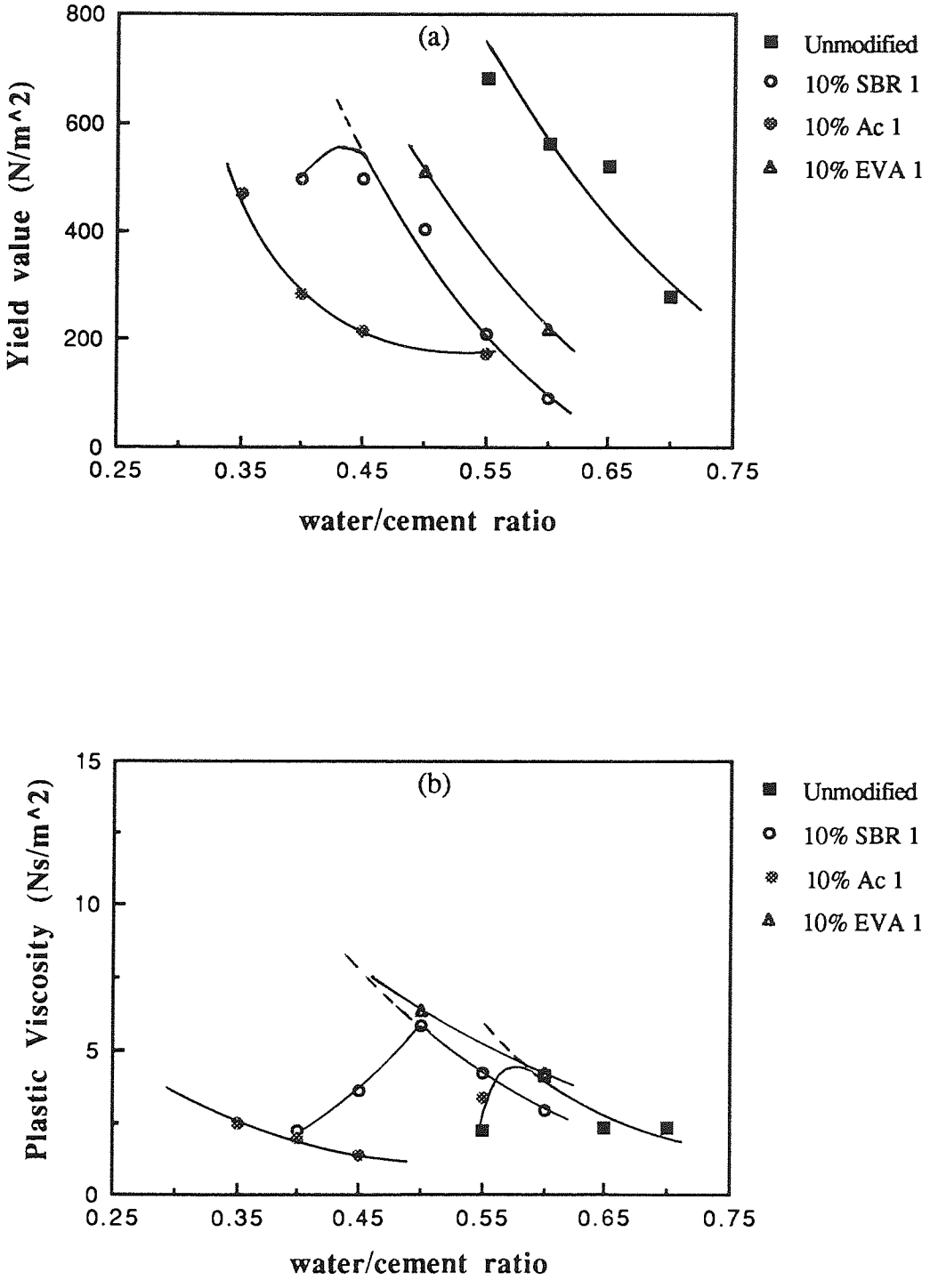

Fig 5.16: The influence of 10% polymer and water/cement ratio on (a) τ_0 and (b) μ for mortar M3

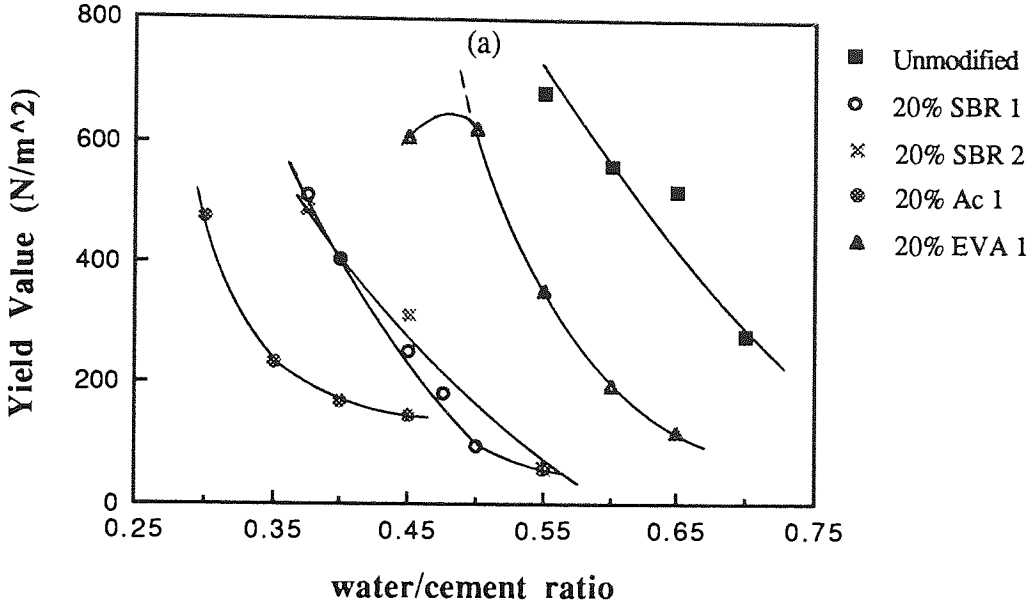

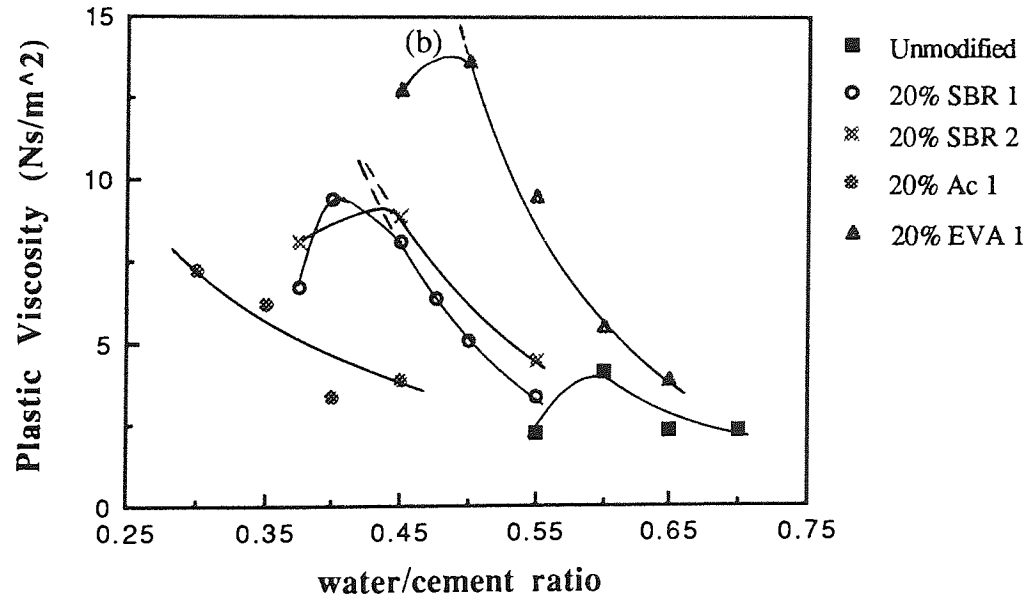

Fig 5.17: The influence of 20% polymer and water/cement ratio on (a) τ_o and (b) μ for mortar M3

6 INFLUENCE OF CURING ON POROSITY AND PORE SIZE DISTRIBUTION OF POLYMER MODIFIED CEMENT PASTES

6.1 INTRODUCTION

The widely recommended curing regime for polymer modified mortars advises that the surface be kept damp for 24 - 48 hours to provide good initial conditions for Portland cement hydration, followed by air-dry curing so that polymer films or strands may form and bind the matrix together. This wet-dry curing regime allows the development of optimum mechanical properties. However, such a curing regime is contrary to that which would be expected for a low porosity surface layer, desirable for e.g. good resistance to chloride ingress.

In other than water-saturated curing, it is thought that the water loss will be most rapid at the outer surface and lowest at some point remote from the surface (Cather, 1994). Sufficient curing for the outermost surface of concrete can be achieved in a > 80% RH environment as recommended by BS 8110 (1985). However, weight loss when drying at 20°C and 60% RH reduced significantly when the initial high humidity (sealed) curing periods increased (Parrott, 1995). This suggests that increased sealed curing periods promote better cement hydration and lead to a reduced capillary porosity in the concrete cover region.

For LMC, drying after initial curing is necessary to allow coalescence of polymer particles (Ohama, 1984). Rate of evaporation during dry curing is lower in LMC compared to unmodified cements. With the increase in latex content, weight loss through evaporation was reportedly lower (Ohama and Kan, 1982). Both weight loss and compressive strength

increase with time indicating that evaporation and cement hydration in latex modified concrete continue during the dry curing period (ACI 548.3R-91, 1991).

The **main aim** of the present work was to determine the influence of curing conditions on the surface porosity of polymer modified cements compared to that in the bulk.

6.2 MERCURY INTRUSION POROSIMETRY

The Mercury Intrusion technique has been widely used to provide information on the pore structure of hardened cement pastes and concrete. A knowledge of total porosity and pore size distribution is extremely important since these factors may influence the properties of concrete such as the strength and durability.

The technique and basic equipment for determining the void spaces and pores in a porous material by use of mercury penetration were reported by Orr (1969). Calculations of specific surface area and particle size distribution were determined from the volume of mercury penetrating the porous material as a function of pressure.

Mercury porosimetry is based on capillary theory governing liquid penetration into small pores of a material. For a non-wetting liquid and assuming cylindrical pores that are not interacting, a form of the Washburn (1921) equation is used:

$$P = -(4\gamma \cos\theta)/d \qquad (6.1)$$

where;

P = applied pressure

d = pore diameter

γ = surface tension of mercury

θ = contact angle between mercury and the pore walls

Early work on mercury porosimetry studies of cement pastes was reported by Winslow and Diamond (1970). The study was conducted on cement pastes with water/cement ratio of 0.4 and 0.6. The pore size distributions were determined at different ages. Elaborate studies were also conducted to determine the contact angle, the effect of mercury compression, compressibility of sample, machine expansion and possibility of mercury expansion due to temperature rise. They reported that the effects of mercury compression, compressibility and temperature rise were negligible.

Arguments on the accuracy of the technique continue, and revolve around the actual value of contact angle used, method of drying, pore shape, damage to the pore during intrusion, expansion of the machine, compression of the mercury and surface tension of mercury. These factors have been reported in detail by Winslow & Diamond (1970), Shi & Winslow (1985), Dexiang & Winslow (1985), Cook & Hover (1993) and Gane *et. al.* (1995).

Measurements of the contact angle between mercury and cement pastes have been reported by Orr (1969), Winslow & Diamond (1970), Shi & Winslow (1985) and Cook & Hover (1991) using hardened cement paste of known cylindrical pore diameter. The contact angle was measured at a certain pressure to effect a certain amount of mercury intrusion. The reported values of contact angle were 117° for oven-dried at 105°C and 130° for P-dried samples (Winslow and Diamond, 1970), 123 - 135° for fly-ash cement (Shi and Winslow, 1985) and 139 - 152° (Cook and Hover, 1991). Orr (1969), however concluded that the value of 130° was the most frequent value used.

Although the actual value for the contact angle between mercury and polymer modified cement paste could be measured, no relevant values have been reported. However the value of 140° was used by Gane *et. al.* (1995) to determine void space structure of compressible polymer spheres used in a paper-coating formulation.

Different methods of drying hydrated pastes were conducted by Feldman and Beaudoin (1991) with the aim of providing an insight into how pre-treatment of samples affect the pore size distribution. The pre-treatments given prior to mercury intrusion included solvent displacement using methanol or isopropanol, vacuum drying, oven and vacuum drying and pre-drying to 11% RH. The results showed that water replacement by isopropanol followed by immediate evacuation and heating to 100°C for 20 hours will result in the least influence on the pore structure of the paste. It was also reported that solvent replacement allows water removal without causing major stress to the pores; thus subsequent evacuation and heating did not affect pore size distribution.

Moukwa and Aitcin (1988) reported that by drying the samples at 105°C, the internal structure may be changed as a result of internal stresses induced by the removal of water from the paste. As expected, they reported that oven-dried samples showed higher intrusion volume than those subjected to drying by other means.

Cook and Hover (1993) reported that the porosimetry data can be processed correctly using associated correction factors. Using mature concrete samples extracted from a 50 years old bridge deck as the reference concrete, they demonstrated that significant differences may occur to the total porosity, the shape of PSD curves and threshold pore size if porosimetry data is not properly processed. The following corrections to the volume data were used:

$$V_{int} = V_o - V_{blank} + V''_{cHg} - V_{cs} \qquad (6.2)$$

where V_{int} is the corrected intrusion volume, V_o is the uncorrected volume, V_{blank} is the volume during blank run, V''_{cHg} is the volume of mercury expansion, V_{cs} is the volume due to sample compression.

The volume of mercury compression and sample compression are given in the following expressions respectively:

$$V''_{cHg} = 0.175(BV_{sample}) \log_{10}(1 + P/1820) \quad (6.3)$$

$$V_{CS} = P(\Psi_{sample})(UV_{sample}) \quad (6.4)$$

where BV_{sample} is bulk volume, P is pressure in MPa, Ψ_{sample} is coefficient of compressibility (reciprocal of bulk modulus, M_{SS}) and UV_{sample} is the unintruded volume.

Equation (6.4) was further expanded by Gane *et. al.* (1995), where the increase in volume due to sample compression (δV_{sample}) is as follows:

$$\delta V_{sample} = V'_{bulk}(1 - \varnothing')(1 - \exp\{(P' - P)/(M_{ss})\} \quad (6.5)$$

where; V'_{bulk} is sample bulk volume, $\varnothing'$ is porosity of sample at atmospheric pressure P', P is pressure at intrusion and is M_{SS} bulk modulus. The work was further expanded to simulate the shape of the pore and demonstrating it graphically using Pore-Core computer programme (Matthews, 1994). The effect due to sample compression was in the range of less than 1% of the bulk volume to 6% for the most compressible sample of polymer system used in the paper coating industry (Gane *et. al.*, 1995).

However, the programme (Gane *et. al.*, 1995) only includes volume change factors for a compressible sample. Its effect on the total porosity is only at high pressure, and even then is very small. These negligible effects were demonstrated earlier by Cook and Hover (1993). The effect of sample compression and differential mercury compression as demonstrated by Cook and Hover (1993) had negligible effect on intrusion volume for pressures below 30 and 20 MPa respectively.

The influence of drying methods on PSD of pure cement pastes aged for 7 days with water/cement ratio of 0.3 and 0.5 were investigated by Zeng (1996). Standard specimens were cast in the UPVC cylindrical moulds as described elsewhere (Page *et. al.*, 1981). Samples were dried by means of (1) propan-2-ol for 48 hours (2) propan-2-ol for 48 hours and dried in the oven at 50°C for 10 hours and (3) oven drying at 105°C until constant weight was achieved. The contact angle used was 117° throughout. For water/cement ratio of 0.3, the PSD of samples dried with methods (1) and (2) were similar. As expected for specimens water/cement ratio of 0.5 and oven dried at 105°C, higher porosity and coarser pores than for specimens dried by other methods were obtained. Drying with method (2) shows only a marginally higher fraction of coarse pores than method (1) but similar total porosity.

In view of possible limitations of this technique, values of total porosity obtained have been checked by comparing with those found using water absorption, solvent exchange and helium pycnometry. Results showed that whilst the different techniques did result in different values for total porosity, these differences were not large and trends in porosity as a result of e.g. using different polymers, curing regimes etc., were the same. It was concluded that MIP was a useful technique for comparing the influence of various parameters on pore size distribution (Zeng, 1996).

For this investigation, the effects of sample compression and machine expansion were not calculated. However, its effects on the total porosity are probably very small and were neglected. Specimens were dried using propan-2-ol and values of surface tension and contact angle were assumed to be 485 dynes/cm and 117° respectively.

6.3 EXPERIMENTAL

Pastes were prepared as described in Chapter 4 (Section 4.3.2). They were then cast into wooden moulds, the sizes of which were either 100 x 50 x 10 mm or 100 x 50 x 30 mm

depending on the specific series of experiment as shown in Table 6.1. The surface was then carefully trowelled. The moulds were placed in a curing box with a minimum of 95% RH, and this is described as Wet (W). They were demoulded after 24 hours, after which all sides, except the top trowelled face were given three layers of a black bituminous paint coating. This was to ensure unidirectional movement of water through the trowelled face only. Once the coating was fully dried (approximately 2 hours), specimens were transferred to their respective curing regimes.

After curing, slices ($\approx$ 2 - 3 mm thick) were taken from top, middle and bottom layers of the hardened cement paste blocks by means of a micro slice diamond cutter (see Fig. 6.1). In the case of the specimens from Series I (10 mm thick), samples were only taken from the top and bottom layers. To avoid any effect from the bituminous coating, approximately 1 mm was discarded from all painted sides.

The sliced samples were cleaned with deionised water and broken into small pieces. These were then immersed in propan-2-ol and given an ultra-sonic bath treatment to displace the water. They were then transferred into clean propan-2-ol and soaked for 72 hours, then filtered and dried by means of cool air. All samples were then stored above silica gel in a vacuum desiccator for at least seven days before being subjected to MIP. This was to ensure the samples were completely dry.

The Pore Size Distributions (PSD) of hardened cement pastes were determined using a Mercury Micromeritics Model 9310 Pore Sizer. This equipment was capable of exerting 207 MPa (30000 psi) pressure.

About 2.5 - 3.5 g of cement paste were placed in the porosimeter sample cell. The cells were then evacuated prior to introduction of mercury. The mercury surrounded samples were then transferred to the high pressure chamber for intrusion. The pressure increments

and intruded volume of mercury were monitored automatically. The pressures that force the intrusion can be converted to equivalent pore diameters using Equation (6.1).

Cumulative intrusion volume versus equivalent pore diameter was then plotted to give the pore size distribution (PSD) curve. The greatest intrusion value on this curve corresponds to the highest pressure and smallest equivalent pore size. The shape of the curve provides an indication of the material's PSD.

Investigations evolved through three series of experiments, see Table 6.1, and as follows:

Series I

Preliminary investigations were carried out to determine whether a wet-dry curing regime produces a surface porosity which is different to that in the bulk of the samples. Specimen thickness was 10 or 30 mm reflecting the range normally encountered in practice, although applications up to 100 mm for floor toppings have been successfully used (Dennis, 1988 & 1992). However, these thick sections are not always suitable for polymer modified mortars, either because of the cost or unacceptably slow drying out process.

Two curing regimes were used:

i) 1 day wet (i.e. exposed to a minimum of 95% RH) then 27 days dry (i.e. exposed to 50 ± 5% RH) - (Code: 1W27D)

ii) 1 day wet then 89 days dry - (Code: 1W89D)

Series II

This series of experiments looked at the influence of polymer/cement and water/cement ratios. Samples were cured:

1 day wet then 27 days dry - (Code: 1W27D).

Series III

This series of experiments were to compare different types of polymer, i.e. SBR 1, Ac 1 and EVA 1 at a constant water/cement ratio of 0.35. Three curing regimes were used:

i) 28 days wet - (Code: 28W)

ii) 1 day wet then 27 days dry - (Code: 1W27D)

iii) 1 day wet, 20 days dry then 7 days wet - (Code: 1W20D7W).

6.4 RESULTS AND DISCUSSION

6.4.1 Series I

The pore size distribution curves for Series I experiments are shown in Figs. 6.2 & 6.3. Values of total intrusion volume and initial pore entry diameter are given in Table 6.2.

The results for 10 mm thick unmodified cement specimens are shown in Fig. 6.2(a). There is a distinct difference between the pore size distributions at the top and bottom of the samples. The top has a greater total porosity, 0.16 cc/g and greater initial pore entry diameter, 1.9 μm compared to the bottom (approximately 8 mm from the surface), 0.12 cc/g and 0.3 μm respectively. This difference is presumably a result of evaporation of water from the surface layers. There is no significant difference in values after dry curing for 27 and 89 days, demonstrating that there is no significant hydration during this part of the curing period.

The results for the 30 mm thick unmodified cement specimens are shown in Fig. 6.3(a). Compared with the 10 mm thick specimens, surface section values are the same. Values for the bottom sections (approximately 28 mm from surface) are only slightly lower. These results show that there is a curing-affected zone (CAZ) for unmodified cement although it is not possible to ascertain the depth.

The results for the 10 mm thick SBR 1 modified cement specimens are shown in Fig. 6.2(b). There is now little difference between top and bottom sections. Both show pore entry diameters of around 1.8 - 2.5 μm and total porosity of about 0.17 - 0.18 cc/g. Compared with unmodified cement, pore entry diameters and total porosity are greater and there is a greater fraction of coarser pores in the range of 0.1 - 1.0 μm.

The results for the 30 mm thick SBR 1 modified cement specimens are shown in Fig. 6.3(b). Compared with 10 mm thick specimens, surface values are about the same but values for the bottom layers are slightly lower, presumably reflecting the greater distance from the water evaporation surface. Compared to unmodified cement a coarser pore structure is still evident.

From the above results it is clear that the most severely affected area for both unmodified and modified cements is the surface layer and small effects may be found at distances of 10 mm from the surface. At distance beyond 10 mm only small changes are found. From a practical point of view, these results suggest that more careful control over curing is required for thin sections compared to thick if a low porosity surface is required.

Modified cement pastes show a much coarser structure compared with unmodified pastes. These large differences can not be attributed to e.g. differences in the contact angle. Differences in the contact angle would result in only small shifts in the curves horizontally either to the left or right (Cook and Hover, 1993). Contact angle differences do not affect the total porosity.

If the further corrections were to be used as suggested by Cook & Hover (1993) and Gane *et. al.* (1995), in particular using equations (6.2) to (6.5), the shape of PSD curves will only deviate at high pressure and at pore diameter of < 0.01 μm. This will only give a slightly lower intrusion volume than shown in the present investigations.

6.4.2 Series II

The pore size distribution curves are shown in Figs. 6.4 & 6.5 and the results of total intrusion volume and initial pore entry diameters are given in Table 6.3.

Influence of Polymer-Cement Ratio

The results for 30 mm thick 0, 10 and 20% SBR 1 modified cement specimens with w/c 0.3, are shown in Fig. 6.4. Porosity was determined in the surface section (top) and at approximately 15 mm (middle) and 28 mm (bottom) sections.

In the case of unmodified OPC, Fig. 6.4(a), there is no distinct difference between the pore size distributions at the middle and bottom layers. However, the pore size distribution at the surface is quite different. The total porosity of the surface layer, 0.13 cc/g, is high compared to 0.10 cc/g for both middle and bottom layers. The top layer also has a greater pore entry diameter (1.0 μm), compared to the others (0.2 μm). Comparing Fig. 6.4(a) with Fig. 6.3(a), it can be seen that the pore size distributions for unmodified OPC with w/c 0.3 at any depth are slightly less than specimens with w/c 0.4.

In the case of 10% SBR 1 modified cement, Fig. 6.4(b), the surface layer is much coarser than the middle and bottom layers. The difference in porosity becomes less as the depth from the surface increases. All layers are coarser than unmodified cement.

It can be seen that for addition of 20% SBR 1, Fig. 6.4(c), the surface layer is less coarse than that for additions of 10% SBR 1, but still coarser than the unmodified cement. There is no difference in the pore size distribution in the middle and bottom layers. Both have same pore entry diameter of 0.65 μm and total porosity of 0.12 and 0.13 cc/g for middle and bottom layers respectively.

Influence of Water/Cement Ratio

The influence of w/c can be seen by comparing Figs. 6.4(b), 6.5(a) & (b), where the w/c were 0.3, 0.35 and 0.4 respectively, for a 10% SBR 1 modified paste. It can be seen that an increase in water content results in coarser pore structure and this applies at any distance from the surface. This also applies when SBR 1 additions are 20%.

Generally

In general, Series II experiments show that:

i) Both 10% and 20% added SBR 1 increase the total intrusion volume and the initial pore entry diameter at any depth and is particularly high at the surface.

ii) The total porosity and the initial pore entry diameter decrease with decreasing water/cement ratio.

iii) The initial pore entry diameter is high at the surface for all specimens but falls rapidly with distance from the surface in the case of OPC but remains high in the case of SBR 1 modified pastes.

iv) The surface porosity is higher than the porosity of the middle and bottom layers regardless of water/cement ratio and polymer content.

6.4.3 Series III

The PSD curves are shown in Figs. 6.6 - 6.9. These series involved unmodified OPC and cement modified with 20% SBR 1, Ac 1 and EVA 1 at constant water/cement ratio 0.35 and 30 mm thick specimens. The results of total intrusion volume and pore entry diameters are given in Table 6.4. The results obtained may be explained as follows:

Unmodified cement

For wet cured unmodified cement, Fig. 6.6(a) there is no difference in pore size distribution through the whole section. Values of total porosity and initial pore entry diameters are same throughout the sections, 0.10 cc/g and 0.20 μm respectively. This suggests that hydration of cement throughout the whole section reduces the porosity at all levels to the same degree.

For dry cured specimens (27D), Fig. 6.6(b), there is no difference in pore size distributions for the middle and bottom sections. Total porosity and initial pore entry diameters are 0.11 cc/g and 0.32 μm respectively, just slightly greater than for the well cured specimen. However, the surface layer is more porous and has total porosity of 0.14 cc/g and initial pore entry diameter of 1.90 μm. This difference is presumably due to insufficient hydration as a result of evaporation of water from the surface layer. These results indicate that exposure to the dry environment did not influence the local humidity at a depth of more than 15 mm from the surface. Thus the curing-affected zone (CAZ) is approximately 10-15 mm.

Exposure to 7 days wet cure (> 95% RH) after a 1 day wet cure followed by 20 days dry cure, Fig. 6.6(c) resulted in a modified pore size distribution of the surface section. This suggests that rehydration takes place giving same total porosity but leaving some coarser pores in the region of 0.03 - 1.0 μm.

OPC + 20% SBR 1

For wet cured paste, Fig. 6.7(a), essentially there is no difference in pore size distribution throughout the section. Compared with unmodified cement, Fig. 6.6(a), SBR 1 modified cements show some coarser pores through the section despite no evidence of severe water loss through evaporation. This suggests that hydration of cement is retarded by the presence of SBR 1 or lack of effectiveness of the de-foaming agent.

For dry cured specimens, Fig. 6.7(b), the surface layer shows coarser pores than the middle and bottom sections. Compared to the unmodified cement, both latter sections still have coarser pores with total porosity of 0.13 and 0.14 cc/g respectively.

In the case of rewetting, Fig. 6.7(c), pore size distributions are very similar to those observed for the wet-dry cure both in shape, total porosity and pore entry diameter. This suggests that there is no evidence of cement rehydration upon rewetting. This may be due to the effectiveness of the hydrophobic nature of the polymer on the surface that prevents ingress of water during the 7 days exposure to moisture.

Comparing Figs. 6.7(b) & (c) with Fig. 6.5(a) suggest that addition of 20% SBR 1 has no significant advantages in term of improving overall porosity. It can be seen that for dry cure SBR 1 modified cement, low fractions of coarser pores may be achieved by reducing its water content (see results from Series II). Alternatively it can be achieved by wet curing but this is not suitable for polymer modified cement as other important properties may be affected.

OPC + 20% Ac 1

The results for cement pastes modified with 20% Ac 1, Fig. 6.8, suggest that there is very little difference in the pore structure between the three curing regimes. Total porosity is in the region of 0.09 - 0.12 cc/g and initial pore entry diameters in the region of 0.8 - 1.1 μm. However, the shapes of pore size distribution curves are slightly different in the region of 0.05 to 1 μm in diameter. The reason for this is not understood.

Compared with SBR 1, Ac 1 modified cement pastes showed a low fraction of coarser pores at any depth and the total porosity is very similar to that of unmodified OPC. There is some evidence to suggest that top layers have a coarser pore structure than bottom layers but the difference is not as marked as in the case of SBR 1. This may be due to Ac 1

preventing loss of water through evaporation or effectiveness of the anti-foaming agents used in reducing the size of entrapped air.

OPC + 20% EVA 1

For OPC modified with EVA 1, Fig. 6.9, the trends of pore size distribution are very similar for all curing conditions. The only exception is for the top layer of the wet cured specimen, Fig. 6.9(a) which shows slightly coarser pores than other sections, the reasons for which are not clear. Total porosity and pore entry diameters for all curing conditions were in the region of 0.07 - 0.11 cc/g and 0.08 - 0.55 μm respectively.

Despite the difference in the pore size distribution of the surface layer, its pore size distribution was almost coincident with other that obtained using the other curing conditions (1W27D and 1W20D7W), see Figs 6.9(b) & (c). The effect of cement rehydration upon rewetting to the pore size distribution was also not very significant. These results indicate that EVA 1 is capable of preventing water loss through evaporation. The polymer layer on the evaporation surface was also capable of preventing ingress of water upon rewetting.

Pore size distribution of top surfaces

As suggested earlier, the top surface is the most severely affected area when exposed to various curing regimes. The influence of different polymers can be compared by superimposing the pore size distribution curves of the surface layers for the various mixes exposed to different curing conditions (as shown in Fig. 6.10).

For wet cured specimens, Fig. 6.10(a), the pore size distributions and total porosity for unmodified cement, Ac 1 and EVA 1 are very similar. Compared with others, SBR 1 shows slightly high fraction of coarser pores and total porosity. Overall, low porosity was attributed to the wet cure environment suitable for cement hydration.

For dry cure, the pore size distribution of SBR 1 was exceptionally different from the others with high fractions of coarser pores in the region of 0.03 - 1.0 μm. For unmodified cement, Ac 1 and EVA 1, pore size distribution curves were very similar except for slight differences in the region of 0.3 - 1.0 μm and in the region of very small pores for Ac 1 and unmodified cement respectively. Low porosity for Ac 1 and EVA 1 was presumably either due to the effects of sealing and filling by polymer particles/film or the polymer prevents evaporation of water. Another possible cause was the effectiveness of the anti-foaming agents added to the Ac 1 and EVA 1.

Upon rewetting after wet-dry curing, the surface porosity of unmodified cement, Ac 1 and EVA 1 is the same, Fig. 6.10(c). For unmodified cement, evidence of cement rehydration can be seen by comparing it with Fig. 6.10(b), where total porosity reduces from 0.14 to 0.11 cc/g upon rewetting. However, no significant cement rehydration occurred to the polymer modified pastes. This can be seen by comparing PSD curves of wet-dry curing, Fig. 6.10(b) with Fig. 6.10(c) both of which were very similar. The difference, if any, only applies to Ac 1 for pore diameters in the region of 0.1 to 1.0 μm.

6.5 CONCLUSIONS

The influence of curing conditions on the porosity and pore size distribution of polymer modified cements has been investigated using mercury intrusion porosimetry. In spite of the limitations of this technique valid comparisons can be made and the following conclusions drawn:

(1) For well cured (28W) unmodified cement there is no difference in porosity throughout the sample. With polymer modified cements there is again little difference throughout the sample but compared with unmodified cements there is a coarser pore size distribution and greater total porosity. This was attributed to the retardation in hydration.

(2) For unmodified cements the wet-dry curing regime (1W27D) results in a curing affected zone (CAZ) extending some 10-15 mm from the surface. With polymer modified cements the process is more severe. There is a coarser pore size distribution and greater total porosity which was attributed to a combination of water evaporation and retardation. The problem is slightly less severe at additions of 20% suggesting a reduction in evaporation at higher levels of polymer.

(3) For all samples, increase in w/c results in a coarser pore structure and greater total porosity, and this applies at any distance from the evaporation surface.

(4) Further wetting after the wet-dry curing regime for unmodified cements results in densification of the pore structure. This was not apparent for SBR 1 modified cements.

(5) In the case of Ac 1 and EVA 1 modified cements, changes in pore structure as a result of the wet-dry curing regime are not as severe as in the case of SBR 1, although a CAZ still exists. The reasons for this have not been elucidated.

Table 6.1: Summary of experiments

Series	Specimen	w/c ratio	Thickness (mm)	Curing
I	OPC	0.4	10 & 30	1W27D and 1W89D
	OPC + 20% SBR 1	0.4	10 & 30	
II	OPC	0.3	30	1W27D
	OPC+10 & 20% SBR 1	0.3	30	
	OPC+10% SBR 1	0.35 & 0.4	30	
III	OPC (Control)	0.35	30	28W, 1W27D and 1W20D7W
	OPC+20% SBR 1	0.35	30	
	OPC+20% Ac 1	0.35	30	
	OPC+20% EVA 1	0.35	30	

Note:

W = 20 ± 1°C, > 95% RH

D = exposed 20 ± 1°C, 50 ± 5% RH

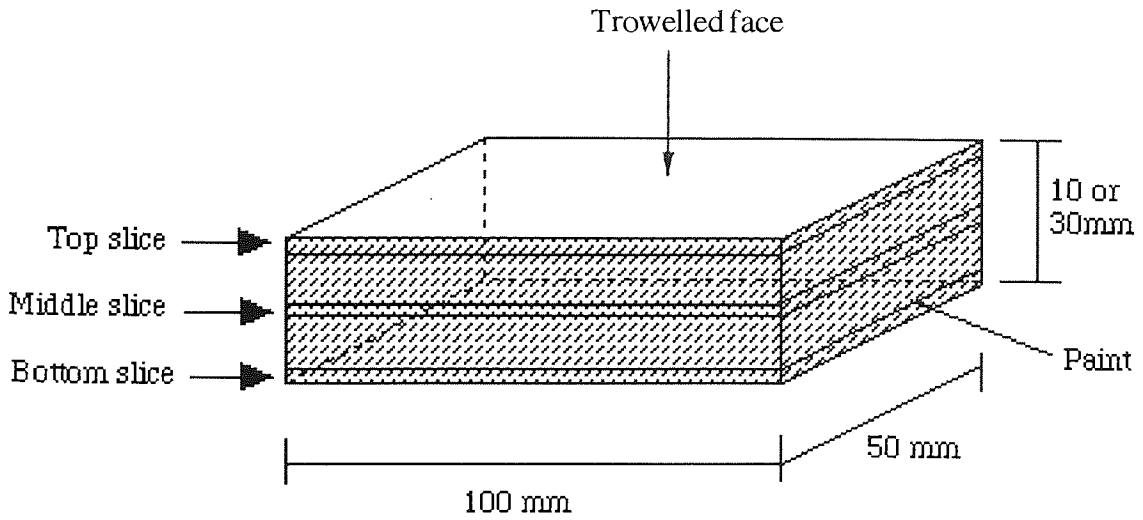

Fig. 6.1: Specimen for MIP experiments

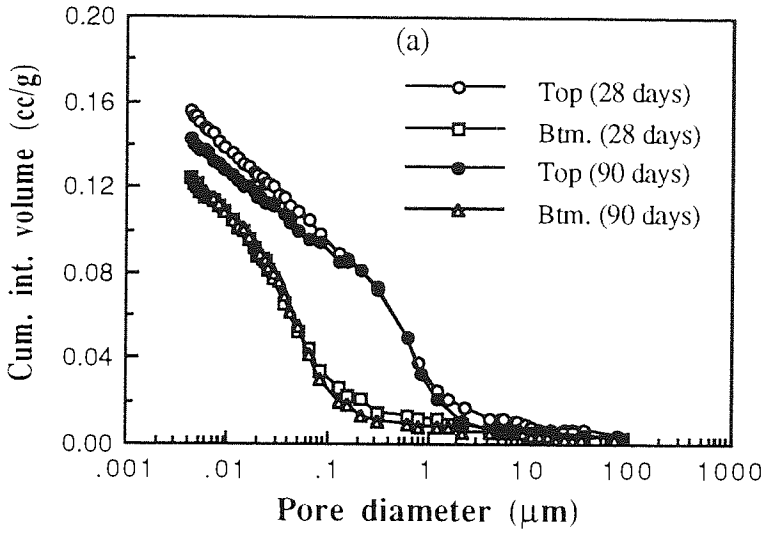

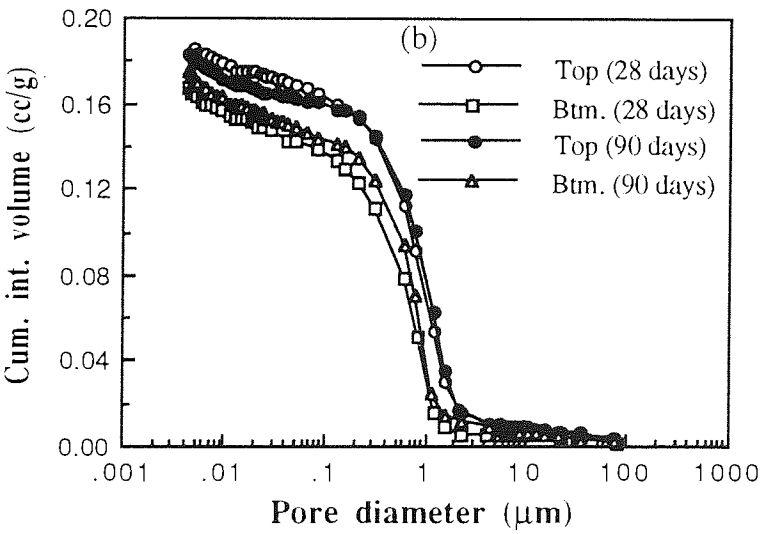

Fig. 6.2: Series I: PSD curves of top and bottom layers for 10 mm thick specimens, w/c 0.4, (a) unmodified OPC, (b) OPC + 20% SBR 1

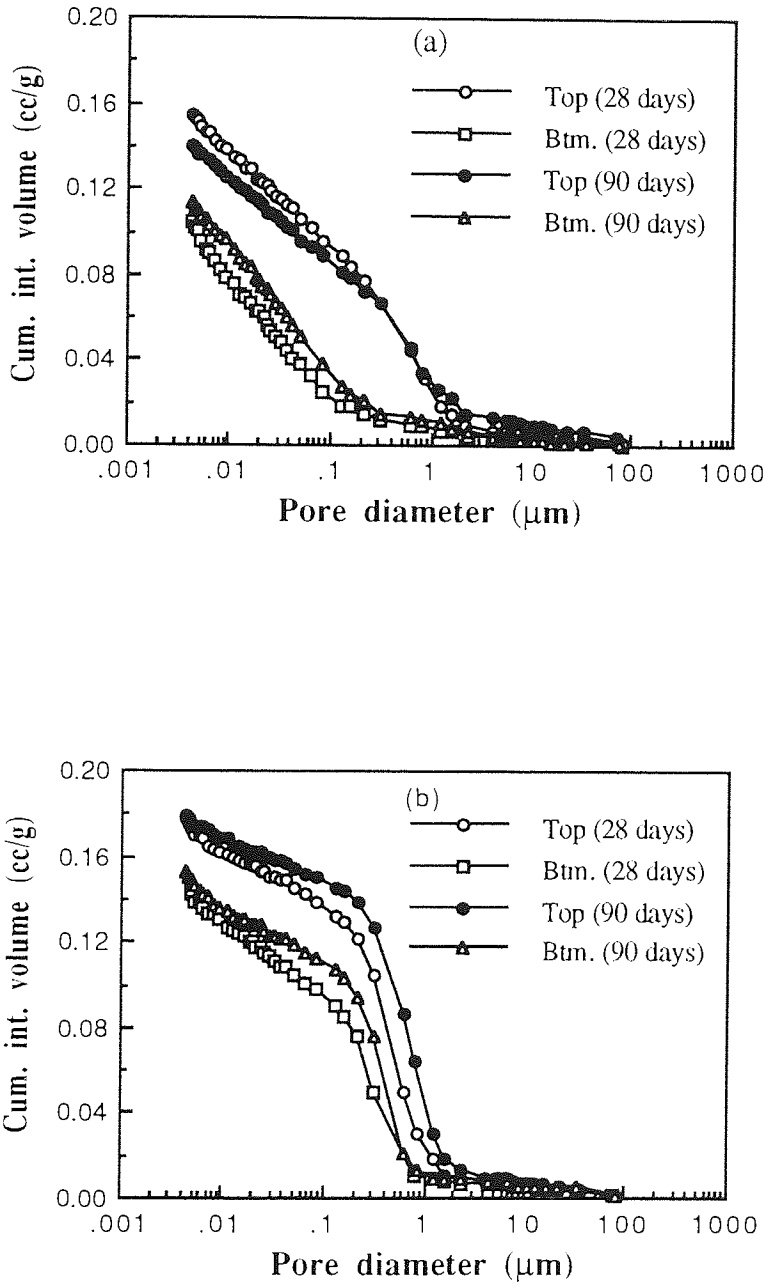

Fig. 6.3: Series I: PSD curves of top and bottom layers for 30 mm thick specimens, w/c 0.4, (a) unmodified OPC, b) OPC + 20% SBR 1

Table 6.2: Series I: Total intrusion volume and initial pore entry diameter

Specimen	Layer	Age (days)	Thickness (mm)	Initial Pore Entry Diameter (μm)	Total Intrusion Volume (cc/g)
Unmodified OPC	Top	28	10	1.9	0.16
	Bottom			0.3	0.12
	Top	90	10	2.2	0.14
	Bottom			0.2	0.12
OPC + 20% SBR	Top	28	10	2.5	0.18
	Bottom			1.8	0.17
	Top	90	10	2.5	0.18
	Bottom			1.8	0.17
Unmodified OPC	Top	28	30	1.5	0.15
	Bottom			0.2	0.10
	Top	90	30	2.0	0.14
	Bottom			0.3	0.11
OPC + 20% SBR	Top	28	30	1.5	0.18
	Bottom			0.9	0.14
	Top	90	30	2.0	0.18
	Bottom			0.9	0.15

Note: w/c 0.4

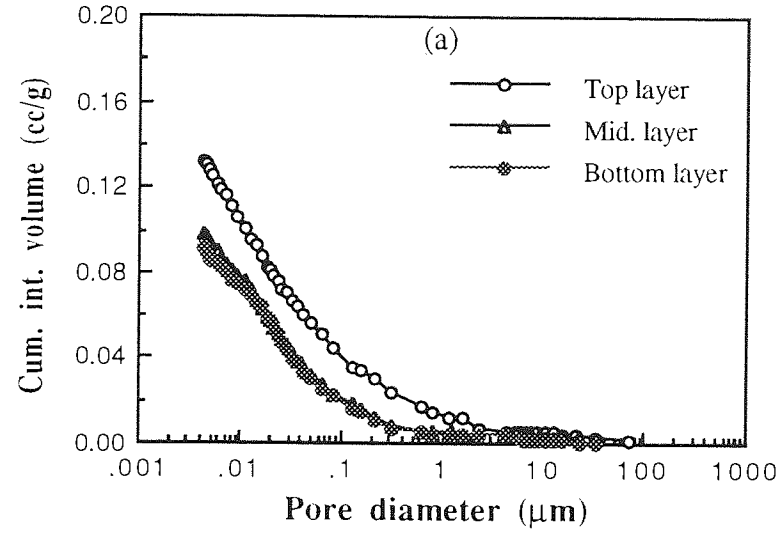

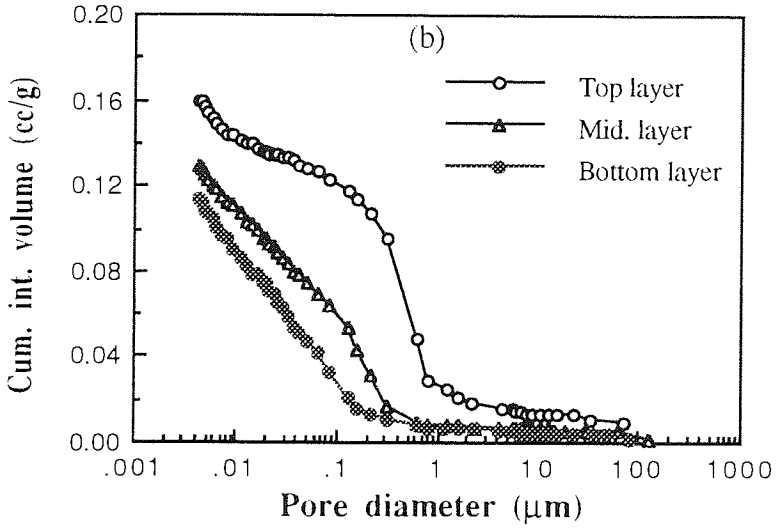

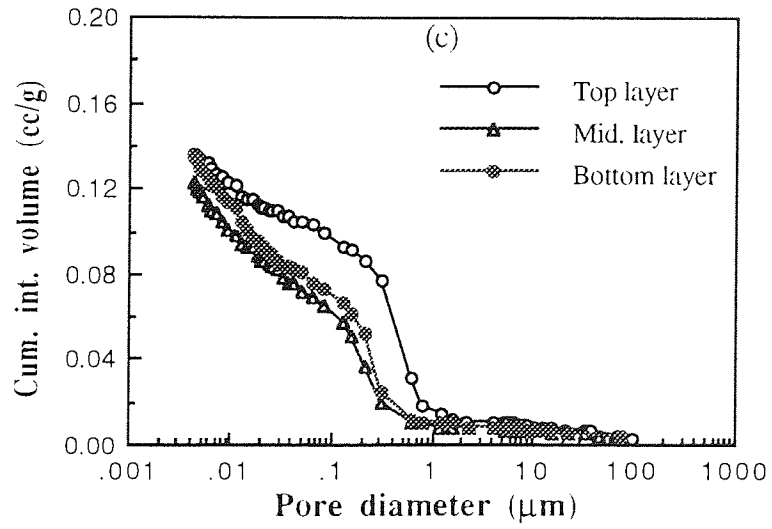

Fig. 6.4: Series II: PSD curves at different distance from surface for 30 mm thick specimens, w/c 0.3, (a) unmodified OPC, (b) OPC + 10% SBR 1 and (c) OPC + 20% SBR 1

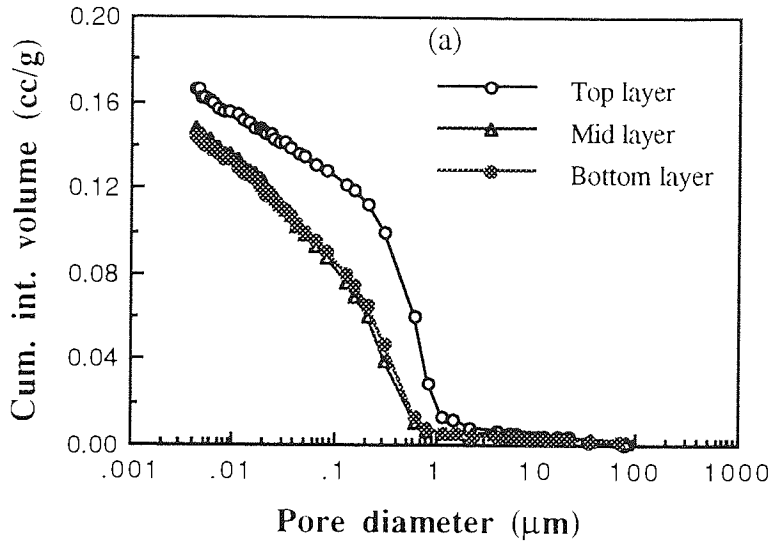

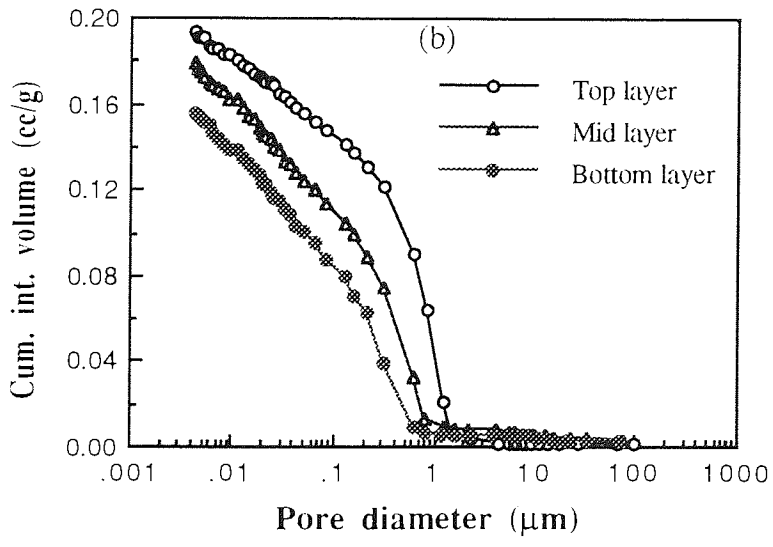

Fig. 6.5: Series II: PSD curves at different distances from surface for 30 mm thick specimens, 10% SBR 1, (a) w/c 0.35 (b) w/c 0.4

Table 6.3: Series II: Total intrusion volume and initial pore entry diameter

Specimen	W/C Ratio	Layer	Initial Pore Entry Diameter (μm)	Total Intrusion Volume (cc/g)
Unmodified OPC	0.3	Top	1.00	0.13
		Mid	0.20	0.10
		Bottom	0.20	0.10
OPC + 10% SBR	0.3	Top	0.80	0.16
		Mid	0.35	0.13
		Bottom	0.30	0.11
OPC + 20% SBR	0.3	Top	0.95	0.14
		Mid	0.65	0.12
		Bottom	0.65	0.13
OPC + 10% SBR	0.35	Top	1.35	0.16
		Mid	0.80	0.15
		Bottom	0.80	0.14
OPC + 10% SBR	0.4	Top	1.70	0.19
		Mid	0.80	0.18
		Bottom	0.65	0.16

Note: Thickness of specimens 30 mm

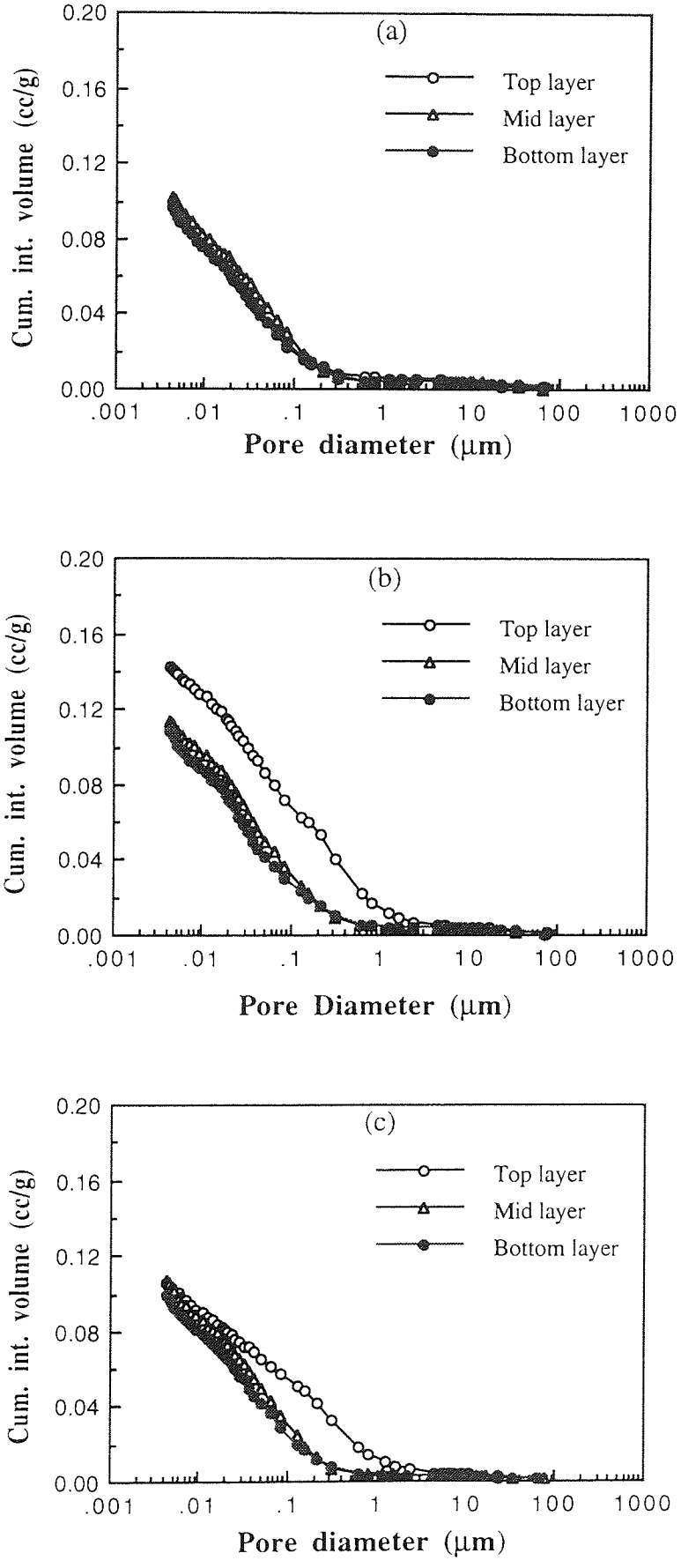

Fig. 6.6: Series III: Effect of curing on PSD curves at different layers for unmodified OPC, (a) 28W, (b) 1W27D and (c) 1W20D7W

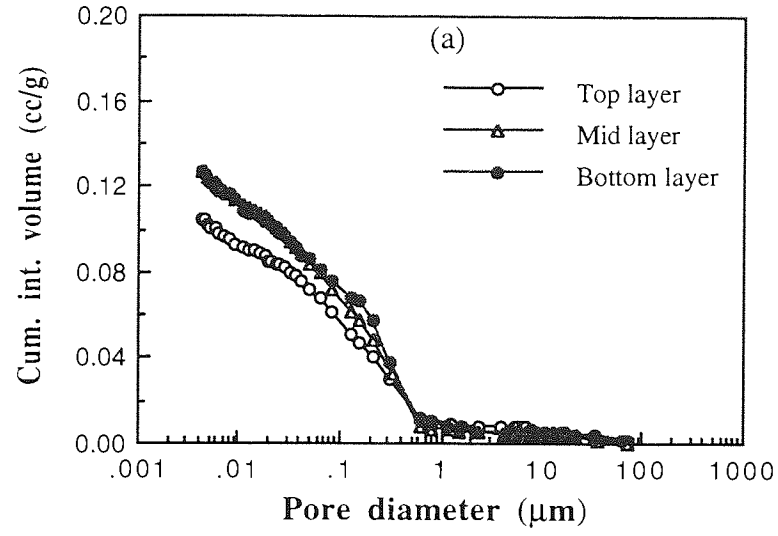

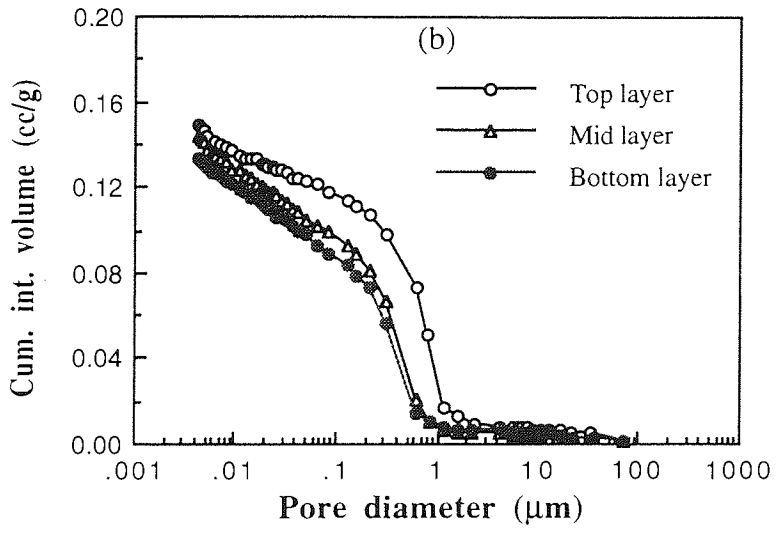

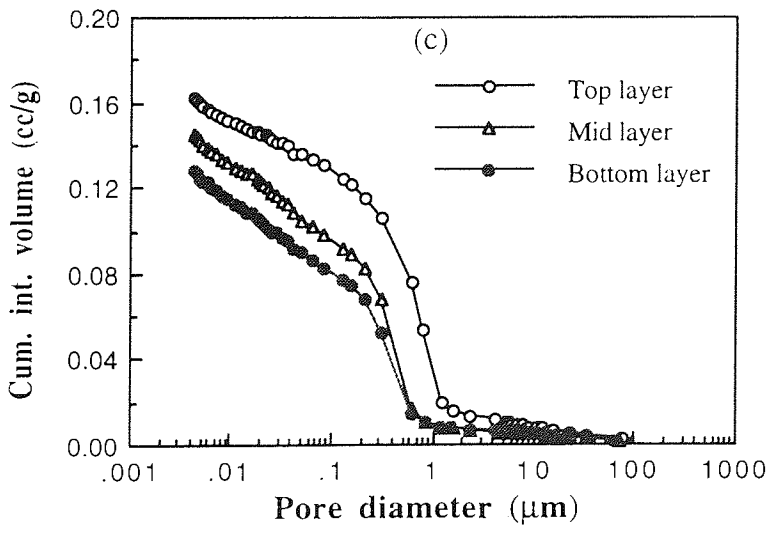

Fig. 6.7: Series III: Effect of curing on PSD curves at different layers for OPC + 20% SBR 1, (a) 28W, (b) 1W27D and (c) 1W20D7W

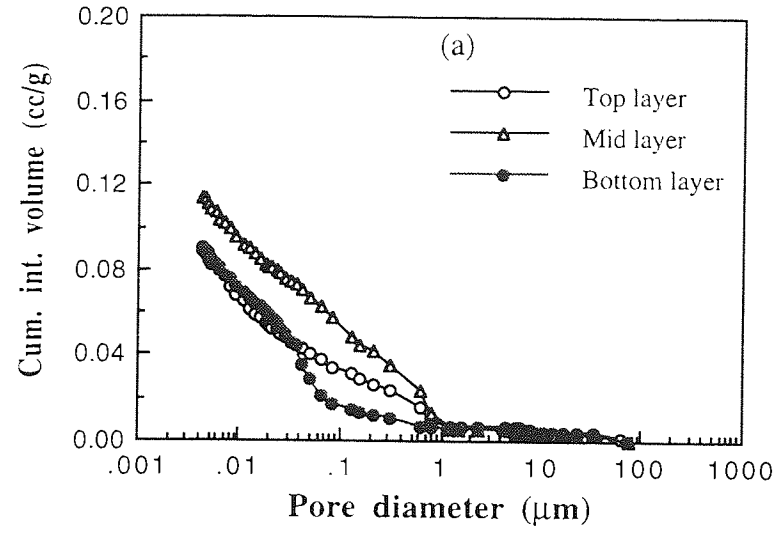

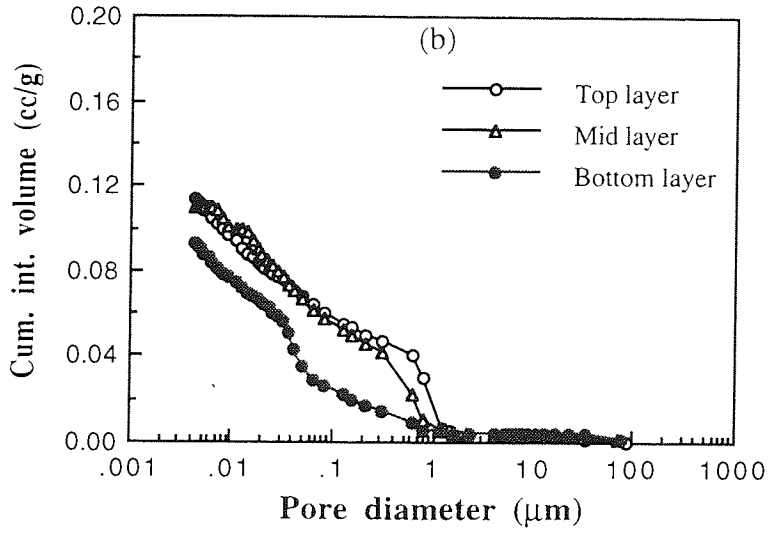

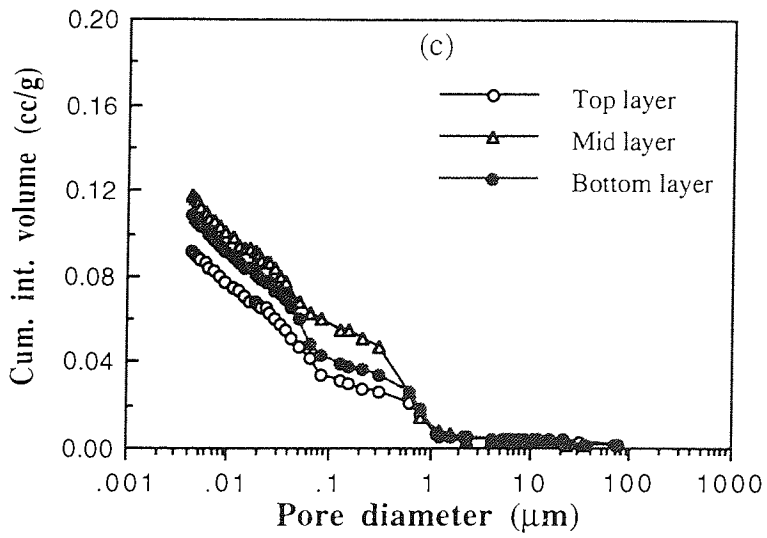

Fig. 6.8: Series III: Effect of curing on PSD curves at different layers for OPC + 20% Ac 1, (a) 28W, (b) 1W27D and (c) 1W20D7W

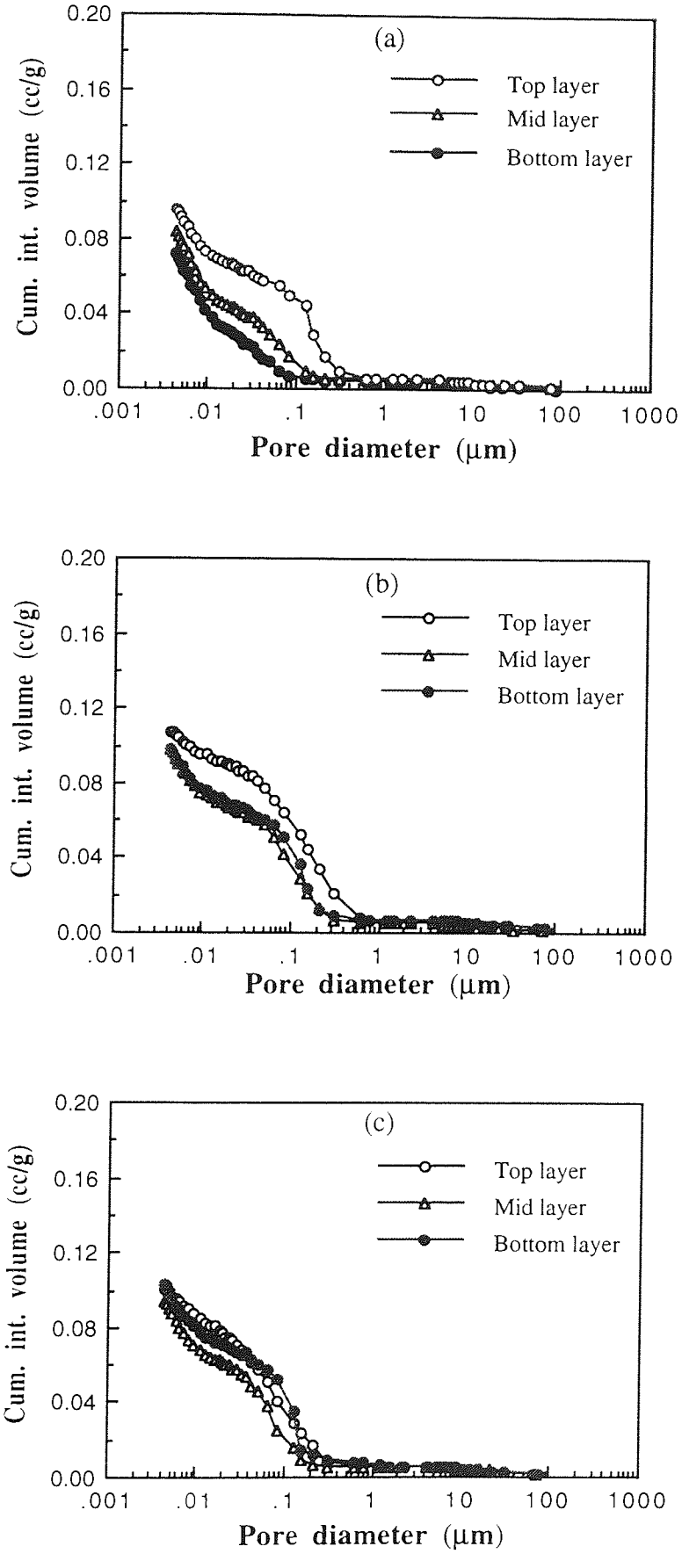

Fig. 6.9: Series III: Effect of curing on PSD curves at different layers for OPC + 20% EVA 1, (a) 28W, (b) 1W27D and (c) 1W20D7W

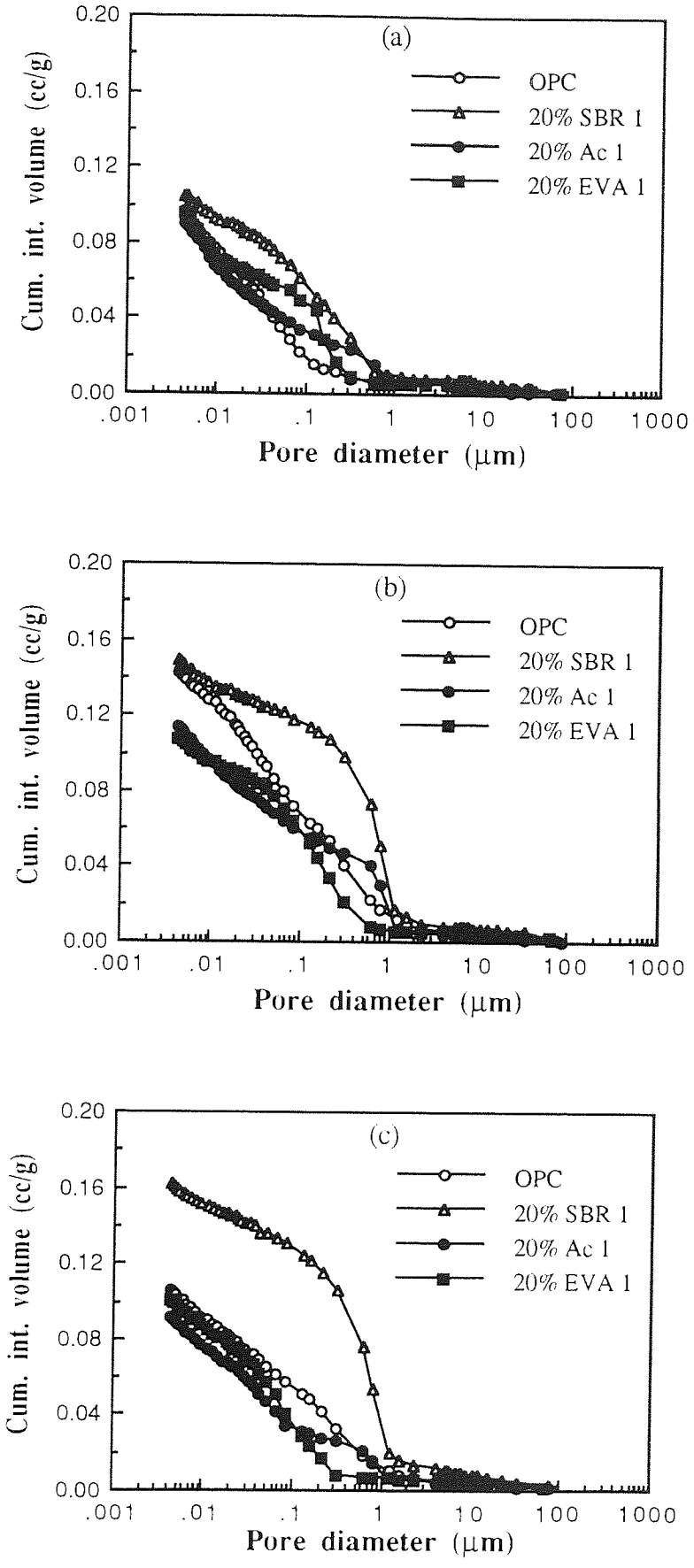

Fig. 6.10: Series III: Effect of curing on PSD curves for top layers of different mixes, (a) 28W, (b) 1W27D and (c) 1W20D7W

Table 6.4: Series III: Total intrusion volume and initial pore entry diameter for different mixes, curing conditions and distance from surface

Specimen	Curing conditions	Layer	Initial Pore Entry Diameter (μm)	Total Intrusion Volume (cc/g)
Unmodified OPC	28W	Top	0.20	0.10
		Middle	0.20	0.10
		Bottom	0.20	0.10
OPC + 20% SBR 1		Top	0.60	0.11
		Middle	0.60	0.13
		Bottom	0.60	0.13
OPC + 20% Ac 1		Top	0.80	0.10
		Middle	0.90	0.11
		Bottom	0.80	0.09
OPC + 20% EVA 1		Top	0.30	0.10
		Mid	0.15	0.08
		Bottom	0.08	0.07
Unmodified OPC	1W27D	Top	1.90	0.14
		Middle	0.32	0.11
		Bottom	0.32	0.11
OPC + 20% SBR 1		Top	1.40	0.15
		Middle	0.80	0.14
		Bottom	0.60	0.13
OPC + 20% Ac 1		Top	1.20	0.11
		Middle	1.00	0.11
		Bottom	0.60	0.09
OPC + 20% EVA 1		Top	0.55	0.11
		Middle	0.20	0.10
		Bottom	0.20	0.10
Unmodified OPC	1W20D7W	Top	1.00	0.11
		Middle	0.25	0.11
		Bottom	0.25	0.10
OPC + 20% SBR 1		Top	1.30	0.16
		Middle	0.60	0.14
		Bottom	0.60	0.13
OPC + 20% Ac 1		Top	1.10	0.09
		Middle	1.10	0.12
		Bottom	1.10	0.11
OPC + 20% EVA 1		Top	0.28	0.10
		Middle	0.17	0.09
		Bottom	0.18	0.10

Note: w/c 0.35

7 DIFFUSION OF CHLORIDE IONS

7.1 INTRODUCTION

Ingress of deleterious ions is one of the major causes of the deterioration of reinforced concrete structures. Penetration of chloride ions in particular is one of the major factors that cause corrosion of the steel reinforcement, eventually leading to cracks and spalling of the cover concrete. A lot of effort has been made to reduce chloride ion mobility into concrete especially in the vicinity of steel reinforcement. This includes coating the reinforcement, surface treatment of concrete, cathodic protection and using cementitious materials that reduce porosity and hence diffusion.

The use of polymer modified cement systems have been reported to improve durability of mortar and concrete. However the performance and mechanism of improvements are very much dependent on the type of polymer, polymer content, water/cement ratio, curing conditions and service conditions. Despite the slightly higher porosity of certain polymer modified cement composites, lower effective diffusivities of chloride ions have been reported compared with the unmodified paste (Diab *et. al.*, 1988, and Jinping *et. al.*, 1990).

The **aims** of the present investigation were:

1. To investigate the effect of wet-dry curing conditions on chloride ion diffusion in SBR 1 modified paste.

2. To compare the effective diffusion coefficients of well cured ethylene vinyl acetates (EVA) from different commercial suppliers and in the form of an emulsion and redispersible powders.

(**Note:** Similar experiments were carried using other types of latexes as part of the project by Zeng, S. (1996)).

7.2 PREVIOUS WORK

Early work on the diffusion of chloride ions in cement pastes was reported by Page *et. al.* (1981). It has been reported that the diffusion of chloride ions in hardened cement paste is strongly influenced by the curing, temperature, water/cement ratio and the type of cement used.

Chloride ion distribution of conventional concrete with water/cement ratio of 0.44 and concrete with acrylic latex, styrene-butadiene latex and epoxy modifier was investigated by soaking in 15% NaCl solution for 21 days. Marusin (1987) reported that all concretes had a high level of chloride ranging from 0.27 to 0.34 percent by weight of concrete at a depth of 0 to 12 mm from the surface whilst concretes with 25% latex contained about 0.02 to 0.03 percent of chloride content in the next depth of 12 to 25 mm. A similar concentration was recorded for conventional concrete but at depth intervals of 25 to 38 mm. Poor performance was exhibited by epoxy modified concrete compared with others even at the lowest water/cement ratio of 0.26. With the exception of epoxy modified concrete, chloride ion penetration is greatly influenced and reduced by the decrease in the water/cement ratio.

The effect of insitu polymerisation on the chloride diffusion of polymer-Portland cement pastes was reported by Bentur *et. al.* (1990). The investigation was conducted on cement pastes and mortars of the same water/cement ratio, consisting of Portland cement, 10% polymer, pozzolanic additives and polymer + 10% silica fume. The polymer used was a vinyl sulphonic acid monomer (25% aqueous solution) which was added to the paste and polymerised insitu using potassium persulfate and sodium bisulfite as initiators. A water/cement ratio of 0.5 was used throughout. The diffusion test was conducted in a similar way as reported by Page *et. al.* (1981). It was reported that the coefficient

of chloride diffusion obtained was in the following order; OPC > polymer + PFA > polymer + silica fume. Reduced coefficient of diffusion of polymer modified paste was attributed to the formation of a dispersed film (supported by SEM observations) in the paste matrix. In an earlier investigation, Diab *et. al.* (1988) suggested that there was a possibility of chemical interactions between calcium ions and vinylsulphonic polymer during the diffusion test.

Al-Qaser *et. al.* (1990) measured the diffusion of various ions through OPC, sulphate resisting Portland cement and polyacrylamide cement pastes using ASTM sea water as a salt solution. Chloride analysis was determined by taking a 1 ml aliquot from the solution and titrating it with silver nitrate. Sulphate analysis was carried out gravimetrically using barium chloride as a precipitating reagent after diffusion had taken place. The concentration of sodium, calcium, potassium and magnesium ions were estimated using Atomic Absorption Spectrophotometry. They reported that polymer modified pastes were only partially effective in reducing the diffusion rate of the various ions.

Another technique of measuring chloride ion diffusion was reported by Jinping *et. al.* (1990). Similar experimental principle as reported by Page *et. al.* (1981) was used but the chloride ion concentration was measured by withdrawing a 25 ml aliquot in compartment 2 and titrating it with $AgNO_3$. The cumulative amount of diffused Cl^- ions was calculated after n sampling at time t. They reported that the effective diffusion coefficients of Cl^- in acidic cationic polychlorobutadiene emulsion and carboxylic styrene-butadiene latex (XSBR) cement pastes are only 1/3 - 1/10 of those in ordinary cement paste with the same water/cement ratio (0.35). It has been suggested that a lower diffusion coefficient in polymer-modified pastes compared with ordinary cement was attributable to their high volume of pores with a radius smaller than 0.05 μm.

7.3 EXPERIMENTAL

7.3.1 Preparation of specimens used to investigate the influence of a wet-dry curing regime: SBR 1 modified cement

Mixing of cement pastes was carried out in a similar way to that described in Section 4.3.2. Cement pastes modified with 20% SBR 1 and w/c ratio of 0.35 were cast into six cylindrical UPVC containers, 30 mm in height x 49 mm in diameter. Each container was filled with cement paste and compacted by means of a vibrator until no visible air bubbles came out to the top surface. The topmost layer was scrapped off and a small piece of polythene sheet was placed over the exposed surface. A cap was forced on the top of the container, thus tightly sealing it and preventing loss of water during the initial set.

The pot was labelled and subjected to a continuous rotation for 48 hours to prevent segregation. After 48 hours, the cap and polythene sheet were removed. The cylinders were then placed above saturated LiCl in a desiccator giving ~ 11% RH. The temperature was maintained at 20° C for 60 days. After 60 days, discs approximately 3 mm thick were cut from the top (evaporation surface) and bottom of the cylinders (see Fig. 7.1a).

Four discs were used for diffusion experiments and two discs were used for MIP. Porosity and pore size distribution were determined before and after diffusion.

7.3.2 Preparation of well cured specimens: EVA modified cement

Specimens of modified cement pastes were made up with a w/c ratio of 0.35, and polymer/cement ratio of 0.1. The polymers used were EVA 1, EVA 2 and EVA 3, all with 1% defoamer added during mixing. For EVA 2, an additional specimen without defoamer was also cast. Unmodified OPC was cast as a control specimen.

The cement paste was poured into cylindrical plastic containers, 75 mm in height x 49 mm in diameter. Each container was filled with cement paste in three layers and compacted by means of a vibrator until air bubbles no longer came to the surface of the paste. The process was continued until the container was overflowing. The topmost layer was scrapped off and a small piece of polythene sheet was placed over the exposed surface. A cap was forced on the top of the container, thus tightly sealing it. The pot was labelled and subjected to a continuous rotation for 48 hours to prevent segregation. After 48 hours, the cylinders were transferred into a curing room at 20°C for 60 days before slicing.

After 60 days, the pastes were demoulded and from the central part of the cylinders, six circular discs approximately 3 mm thick were cut by means of a diamond saw (see Fig. 7.1b). The discs were then lightly ground on grade 600 emery paper, rinsed with distilled water and dried with lens tissue paper. Four discs were then fitted into diffusion cells and the other two were used for Mercury Intrusion Porosimetry (MIP). Porosity and pore size distribution were determined before diffusion only.

Preparations of MIP samples and testing were carried out in a similar way as described in Chapter 6.

7.3.3 Chloride ion diffusion test

The experimental arrangements for the diffusion test are shown in Fig 7.2. For each set four replicate cells were placed in a water bath at constant temperature of 25°C. Compartment 1 was filled with 1M NaCl and 0.0325M NaOH. Compartment 2 was filled with 0.0325M NaOH. This concentration was chosen to prevent leaching of calcium hydroxide. The volume of each compartment was recorded in cm^3. The concentrations of chloride ion in compartment 2 of the cells after various diffusion times were determined by withdrawing 100 µl aliquots of solution and analysing them using a standard spectrophotometry technique as described by Page *et. al.* (1981).

Samples were tested this way for a period of up to four weeks. On completion of each set of measurements, the discs were removed from the cells and their thicknesses and diameters of diffused area were determined by means of micrometer gauge and vernier calliper respectively.

Chloride diffusion across the thickness of the disc becomes established after an induction period of t_o. In theory, the concentration of chloride in compartment 2 (C_2) increases linearly with time, whilst that in compartment 1 (C_1) remains constant over the period of measurement.

For the quasi-steady-state diffusion across the disc, the flux (J) in mol/cm^{2}s^{-1} of chloride ion entering compartment 2 is given by the following expression (Page *et. al.* 1981):

$$J = \frac{V}{A}\frac{dC_2}{dt} = \frac{D}{l}(C_1 - C_2) \qquad (7.1)$$

where D is the effective diffusivity of chloride ion through the disc in cm^{2}s^{-1}, V is the volume of solution in compartment 2, A is the cross-sectional area in cm^2, l is the thickness of the disc in cm and C_1 and C_2 are the concentrations in compartment 1 and 2 respectively.

The effective diffusivity of chloride ion may be determined by using the following equation:

$$\log_e\left(1 + \frac{C_2}{C_1 - C_2}\right) = \frac{DA}{Vl}(t - t_0) \qquad (7.2)$$

For $t > t_o$, and $C_1 >> C_2$:

$$C_2 = \frac{DAC_1}{l}(t - t_0) \qquad (7.3)$$

Thus a plot of C_2 against time will produce a straight line and D may be calculated calculated from the slope.

7.4 RESULTS AND DISCUSSION

7.4.1 Effect of wet-dry curing regime: SBR 1

Typical plots of chloride ion concentration versus time are shown in Fig. 7.3 for discs taken from; (a) the top of the cylinders (i.e. evaporation surface) and (b) bottom of cylinders.

In the latter case, the relationship is linear over the whole period of diffusion and the average value of D for four discs was $2.41 \pm 0.88 \times 10^{-8}$ cm^2s^{-1}. From the pore size distribution curves before and after diffusion, Fig. 7.4, a small densification of paste during the test was evident as shown by reduction in porosity for pores in the region of 5 nm to 0.5 μm. Initial porosity reduces from 0.09 cc/g to 0.08 cc/g, and the initial pore entry diameter before and after diffusion reduces from 0.35 μm to 0.2 μm respectively. These reductions were probably as a result of some further hydration of cement paste.

However, for discs from the top of the cylinder, the plots of chloride concentration, Fig. 7.3a were only linear in the initial stages of diffusion, i.e. approximately up to 11 days, giving the average value of D for four discs of $9.47 \pm 1.30 \times 10^{-8}$ cm^2s^{-1}. This is about four times higher than the value of D from the bottom of the cylinders. The difference in the diffusion coefficient values was attributed to the higher total porosity and coarser pore structure. The value of total porosity for top layers was approximately 50% higher than bottom layers for both before and after diffusion.

If values of chloride concentration versus time after 11 days are approximated to a straight line, the average value of D is now $5.49 \pm 0.75 \times 10^{-8}$ cm^2s^{-1}. This approximately 42% reduction in D with time is probably as a result of continuous hydration of cement paste

which occurred during the diffusion test. This observation is confirmed by large changes in the pore size distribution before and after diffusion. Total porosity before and after diffusion is 0.15 cc/g and 0.10 cc/g respectively.

It is clear from these results that surface evaporation at the top of the cylinders results in the disruption of cement hydration compared to the bottom of the cylinders. This also suggests that for cement modified with SBR 1, good curing for 48 hours by means of sealing the evaporation surface was not sufficient for cement hydration. This also suggests that SBR 1 severely delays cement hydration (as explained in Chapter 4) and any polymer film formed is unable to prevent water loss through evaporation when exposed to the dry environment.

Weight losses during initial stages of uniaxial drying of concrete were observed by Parrot (1995). This was due to water lost from the capillary pores in the cover concrete. Weight lost was monitored when specimens were exposed to 20°C and 60% RH for 4 days and 6 months after concrete cubes had been sealed cured for 1, 3 and 28 days. A marked reduction in weight loss was observed as the initial curing period increased (see Fig. 7.5).

In the case of LMC, Ohama and Kan (1982) reported that after 2 days wet cure (100% RH), rapid weight loss occurred during the subsequent 28 days exposure to 50% RH. They reported that weight loss reduced as the polymer/cement ratio increased.

However, the average value of D ($2.41 \pm 0.88 \times 10^{-8}$ cm^2s^{-1}) obtained for bottom layer was very reasonable compared with Zeng (1996) who reported the value of 1.26×10^{-8} cm^2s^{-1} and 3.92×10^{-8} cm^2s^{-1} for the same type of SBR 1 (20%) and cement with w/c ratio of 0.3 and 0.5 respectively, but the paste was prepared in a standard manner and well-cured for 90 days in sealed plastic moulds as described in Section 7.3.2. At 10% SBR 1 the values of D were 1.23×10^{-8} cm^2s^{-1} (w/c 0.3) and 4.28×10^{-8} cm^2s^{-1} (w/c 0.5). The values of D were very much lower compared to the unmodified OPC, 2.19×10^{-8} cm^2s^{-1} and 10.10×10^{-8} cm^2s^{-1} for w/c of 0.3 and 0.5 respectively.

The results also suggest that good curing is extremely important for reducing the effective diffusivity for SBR 1 compared with that of well-cured unmodified OPC at the same water/cement ratio. However, results from Chapter 6, Series III showed that the porosity for well-cured SBR 1 is higher than well-cured unmodified OPC. The results do not agree with the usual trends of high porosity leading to high diffusion coefficients. Similar results were reported by Page *et. al.* (1981) where pastes with 30% PFA were more porous than OPC but the value of D for OPC/30% PFA was one-third of OPC. This shows that some forms of surface activity or interactions probably occurred to OPC + SBR 1 paste during diffusion test. It is recognised, however, that in view of differences in e.g. contact angle and compressibility of the modified and unmodified samples that it may be difficult to make a true comparison.

The delay in the formation of $Ca(OH)_2$ when C_3S is mixed with vinyl sulfonic acid and p-styrene sulfonic acid was reported by Ben-Dor *et. al.* (1985). This was demonstrated by DTA-TG, IR and XRD. The retardation was the result of an interaction between Ca^{2+} with the sulfonic groups of the polymer and water being absorbed by the sulfonic groups. These chemical effects were thought to be correlated with the changes in porosity or pore size distribution of polymer modified cement that result in reduction of the chloride diffusion coefficient (Diab *et. al.*, 1988).

7.4.2 Diffusion through well cured EVA

The effective diffusivities recorded for OPC and OPC + 10% EVA, Table 7.2, are not significantly different from each other when the standard deviations are taken into consideration. The lowest effective diffusivity was probably from EVA 2 (emulsions) with 1% defoamer added but this was only very marginally lower than without defoamer.

It is also obvious that at the same w/c of 0.35 and curing condition, the effective diffusivities of chloride ion for cement pastes modified with different ethylene vinyl

acetates were not significantly different from the unmodified OPC. The marginal difference in values recorded was within experimental error. For EVA 2, addition of 1% defoamer gives no significant effect compared to the one without defoamer presumably due to the effectiveness of vibration. These findings were very similar to the results obtained by Zeng (1996) but using acrylic latex of Ac 1. At 10% Ac 1 and w/c 0.3, the values of D with 0% and 1% defoamer were similar, i.e. 2.07 and 2.08 x 10^{-8} cm^2s^{-1} respectively. However, with the increase of defoamer content to 2%, the value of D for 10% Ac 1 reduces to 1.04 x 10^{-8} cm^2s^{-1}. It is important to note that the function of defoamer is to break small entrapped air bubbles in the mix into bigger air bubbles which subsequently move to the surface. Without vibration, it is very difficult to remove air bubbles and obtain discs from the central part of cylinders that are free from obvious voids or pinhole.

The result of unmodified cement (3.59 x 10^{-8} cm^2s^{-1}) compared reasonably well with the values reported by Page *et. al.* (1981), who obtained a value of 2.6 x 10^{-8} cm^2s^{-1} and 4.4 x 10^{-8} cm^2s^{-1} for OPC paste cured in $Ca(OH)_2$ solutions with w/c ratio of 0.4 and 0.5 respectively. The result for plain OPC also compared reasonably well with the values reported by Ngala *et. al.* (1995) who obtained values of 3.95 x 10^{-8} cm^2s^{-1} and 7.80 x 10^{-8} cm^2s^{-1} for well cured OPC immersed in 35mM NaOH solution and stored in a curing room at a temperature of 38 ± 2°C for 10 weeks with w/c ratio of 0.4 and 0.5 respectively.

The pore size distribution curves of the unmodified OPC and OPC + 10% EVA before diffusion, Fig. 7.6, show that the pore structures of the pastes were very similar. This was reflected by the total porosity values, Table 7.2, and the same initial pore entry diameters. It is therefore reasonable to conclude that due to these similarities, the effective diffusivities of chloride ions obtained for different EVAs were not significantly different.

7.5 CONCLUSIONS

(1) Curing conditions had a marked effect on the diffusivity coefficients of chloride ions in polymer modified cement paste. Initial 48 hour sealed cure for SBR 1 was not sufficient to promote proper hydration of cement and subsequent dry curing resulted in an increased diffusion coefficient. This was a result of the coarsening of surface porosity.

(2) Significant pore structure modification occurred to the improperly cured polymer modified cement paste during the diffusion test probably as a result of continuing hydration of cement.

(3) The effective diffusion coefficients and pore size distributions of well-cured unmodified cement and a range of 10% EVA modified cements were very similar. EVA from the same source but in emulsion (EVA 2) and redispersible powder (EVA 1) forms gave the same results. Similarly EVA in the same form but from different sources also gave the same results. Since vibration of samples was required during preparation it was not really possible to test the effectiveness of the defoamer at the 1% level.

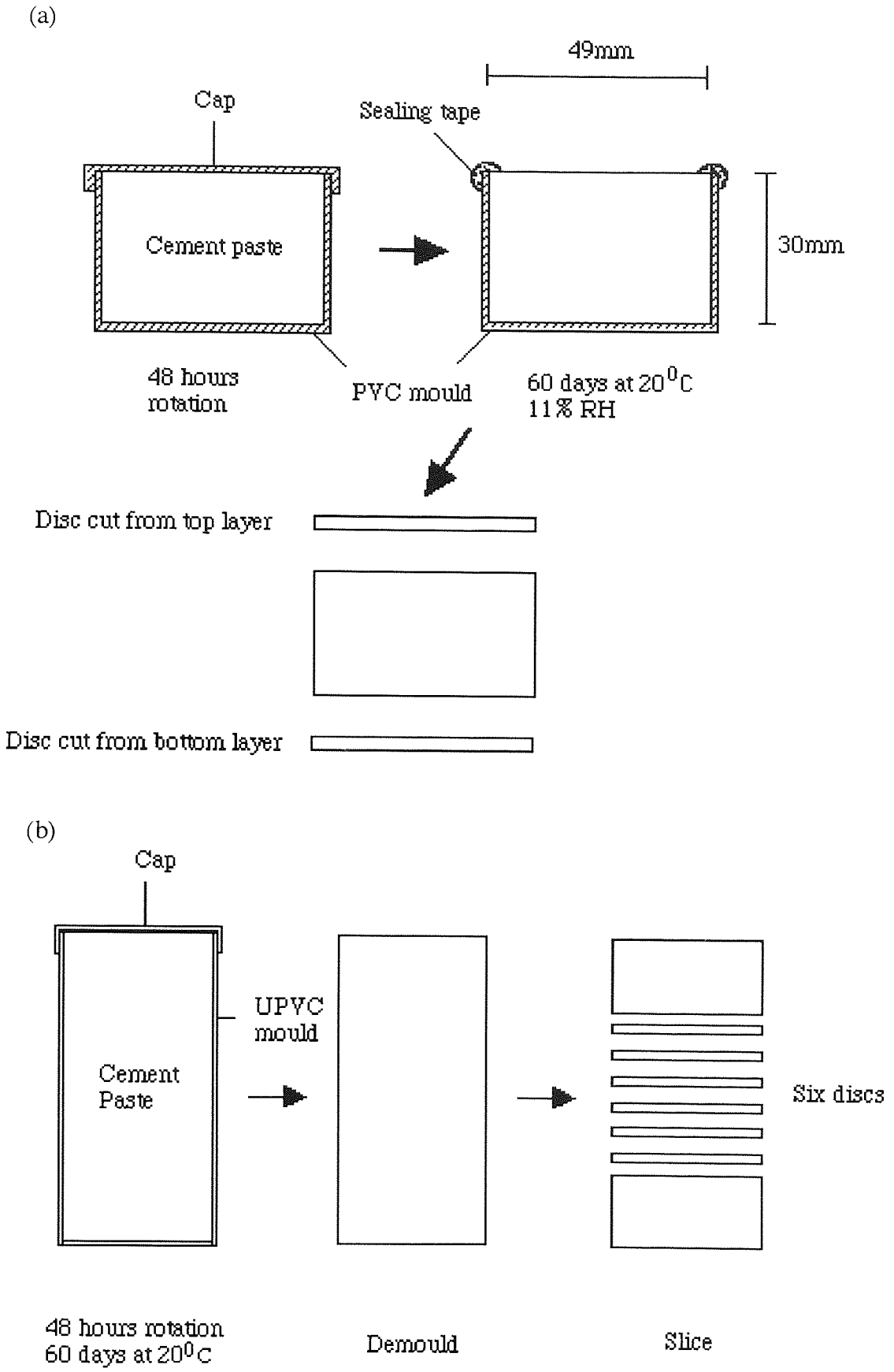

Fig. 7.1: Specimens for chloride diffusion, (a) Wet-Dry curing, (b) Standard

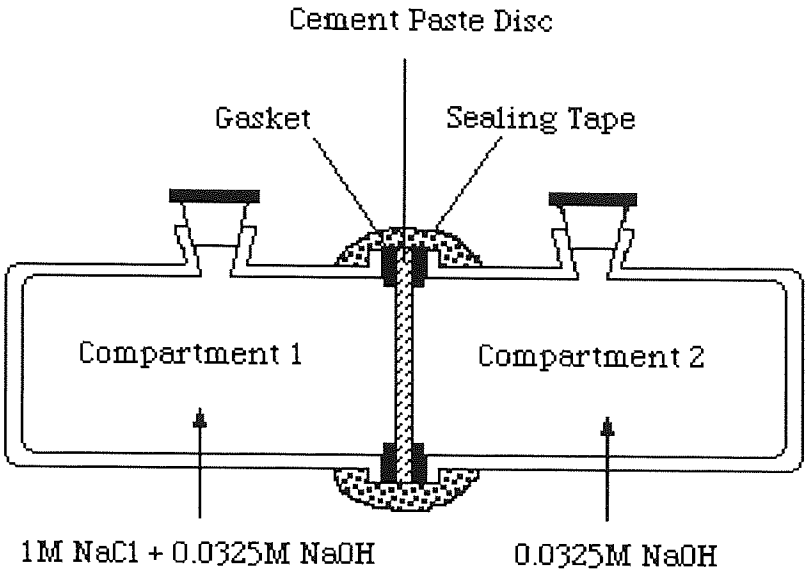

Fig 7.2 : Diffusion cell

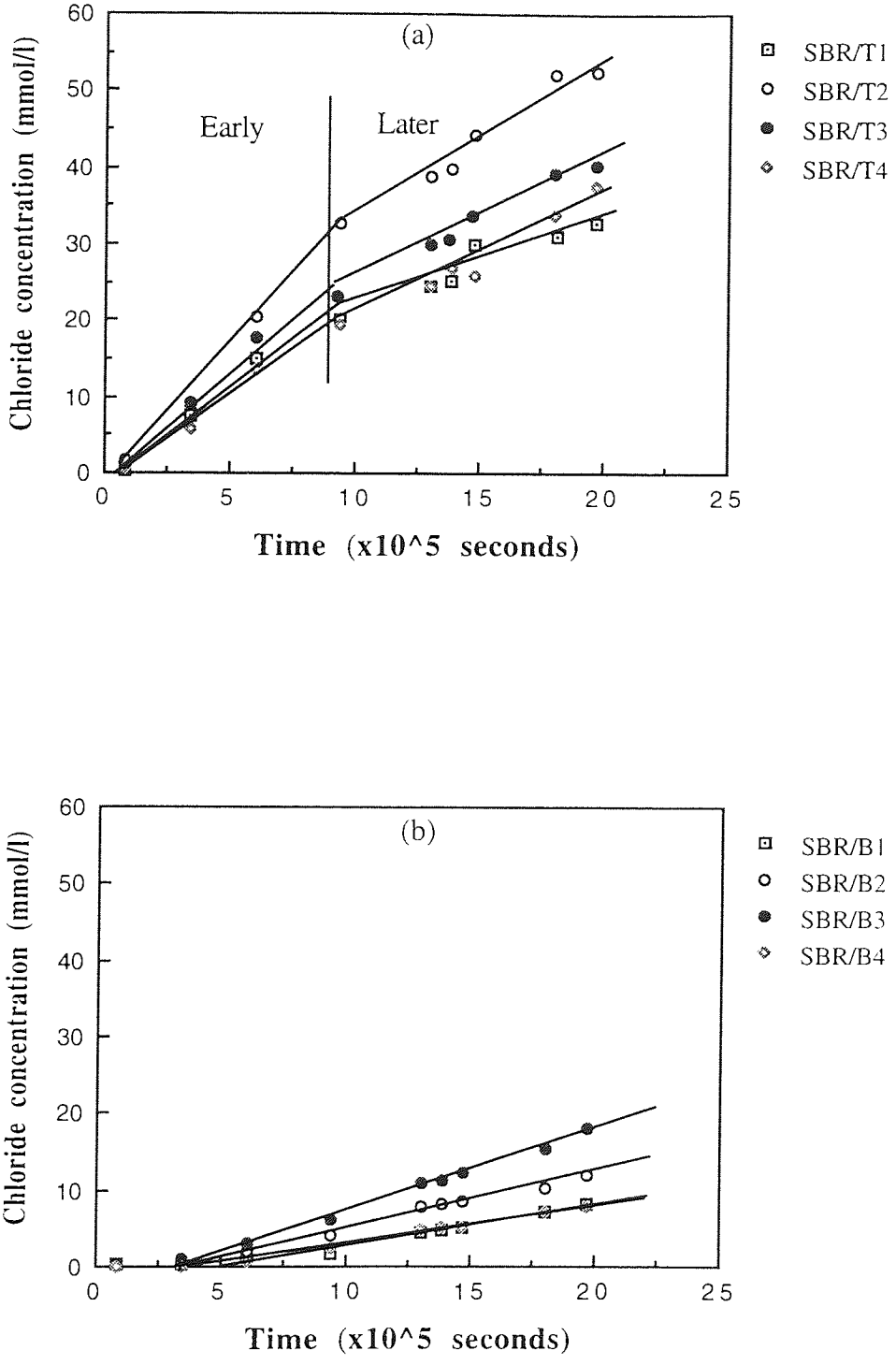

Fig. 7.3: Chloride diffusion through OPC + 20% SBR 1 discs taken from, (a) Top and (b) Bottom of four wet-dry cured cylinders

Table 7.1: Effective diffusivity of chloride ions and total porosity for discs taken from top and bottom sections of wet-dry cured SBR 1

Sample	Layer	D (x 10^8 cm^2s^{-1})	Total porosity (cc/g)
OPC + 20% SBR 1	Top	9.47 ± 1.30 (early) 5.49 ± 0.75 (later)	0.15† 0.10*
	Bottom	2.41 ± 0.88	0.09† 0.08*

Note:

† Before diffusion

* After diffusion

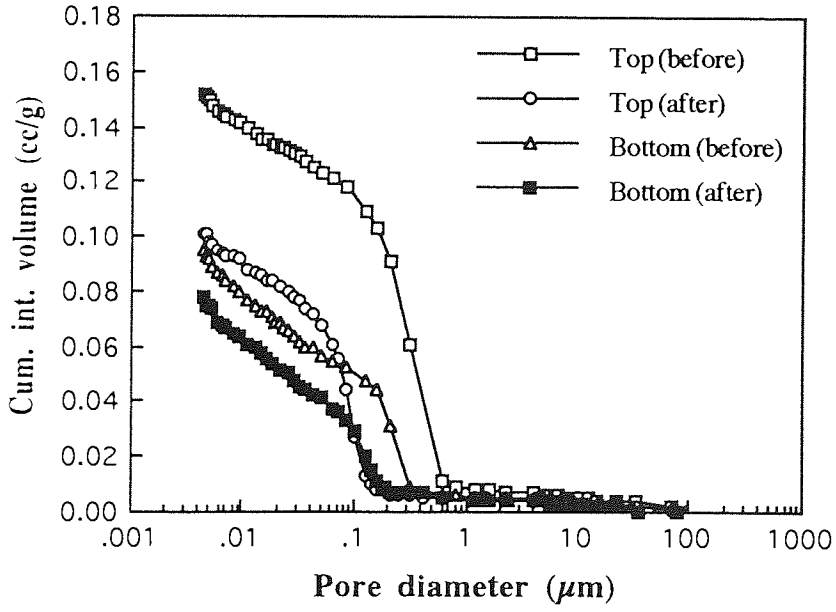

Fig. 7.4: Pore size distribution for OPC + 20% SBR 1 before and after diffusion

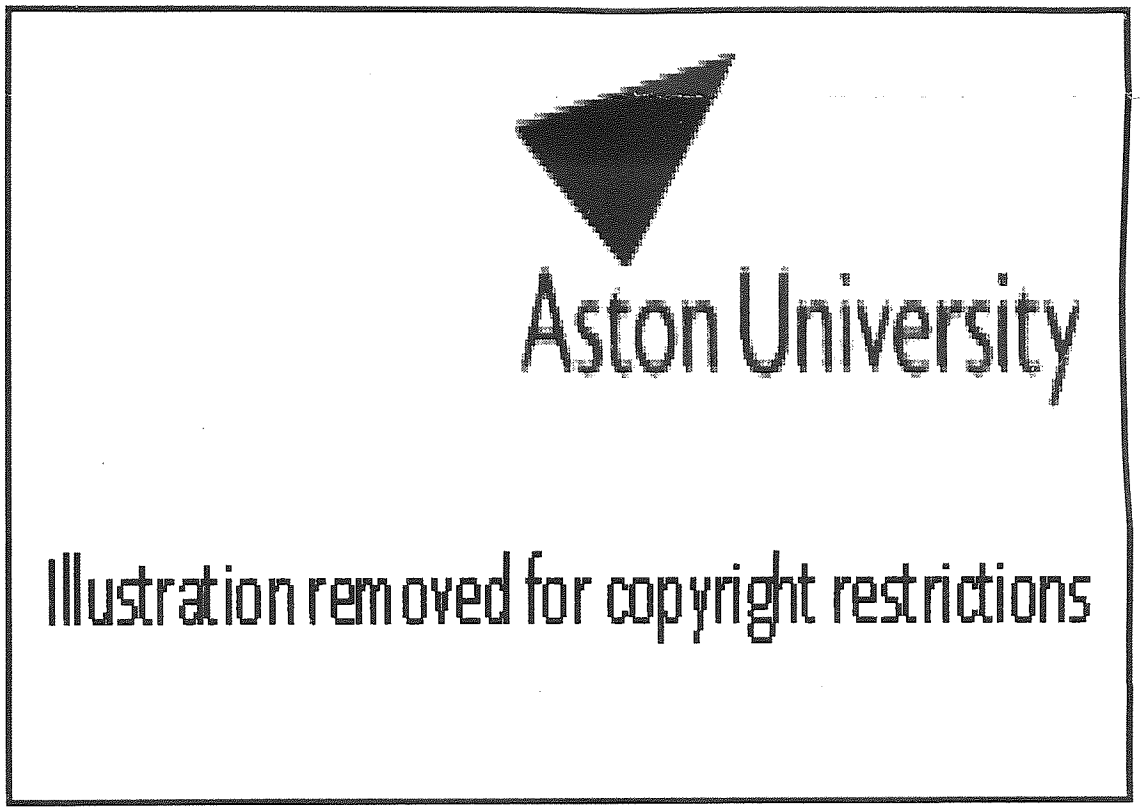

Fig. 7.5: Weight loss for the unmodified concrete during uniaxial drying after initial sealed cure (Parrott, 1995).

Table 7.2: Average Effective diffusivity of chloride ions and total porosity before diffusion for well cured cylinders.

Sample	D ($\times 10^{8}$ cm^2s^{-1})	Total Porosity (cc/g)
OPC	3.59 ± 0.55	0.09
OPC + 10% EVA 1 (1% De)	3.85 ± 0.92	0.09
OPC + 10% EVA 2 (0% De)	3.14 ± 0.48	0.09
OPC + 10% EVA 2 (1% De)	2.70 ± 0.28	0.08
OPC + 10% EVA 3 (1% De)	3.45 ± 0.64	0.08

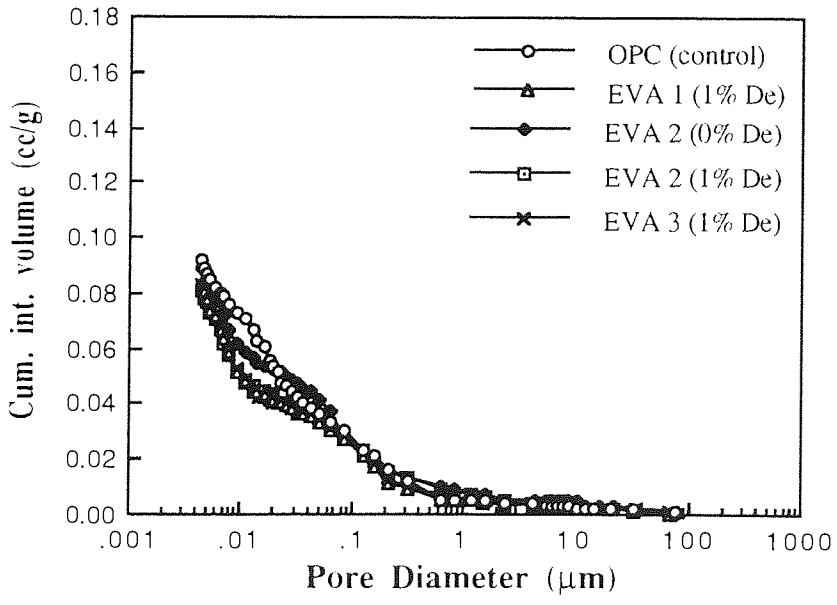

Fig. 7.6: Pore size distribution before diffusion for well cured OPC and EVAs

8 BOND STRENGTH AND MICROSTRUCTURE OF INTERFACES

8.1 INTRODUCTION

A important aspect of the cementitious materials used to repair damaged concrete is their ability to adhere to the concrete being repaired. The primary cause of failures in patch repair is normally attributed to the quality of bond between new patch material and old concrete. These failures are often associated with the types of repair material, quality of substrate and repair procedures employed. Other associated factors are exposure and loading conditions .

Polymer modified cement mortars are known to offer much better adhesion than normal unmodified mortars. They have been widely used for small patch repairs where the thickness of application is normally between 5 to 30 mm. As well as better adhesion to substrates, polymer modified cement mortars are considered to have better durability than conventional cement mortars.

The present investigations were conducted with the following **aims**:

1) To determine the effect of curing conditions on adhesion strength.
2) To determine the locus of failure at the patch-substrate interface.
3) To determine the adhesion strength of cements modified with different polymer systems.
4) To investigate the bulk and interfacial microstructures of polymer modified cement repairs in relation to curing conditions.

Two types of test configurations were used to determine the strength and locus of failure, i.e. pull-off and flexural tests. Comparison of different patch materials was made on the basis of approximately constant workability as defined by the yield value determined in the rheology tests (described in Chapters 4 & 5). A microstructural approach was then used to evaluate the bond mechanisms at the interface and the microstructure of polymer modified cement composites.

The microstructure at the interfaces of SBR modified cement/mortar patch materials and mortar substrates have been studied using scanning electron microscopy (SEM). Carefully selected spots were analysed using energy dispersive X-ray analysis (EDXA). The SEM examinations were carried out on both sides of the patch-substrate interface. SEM was also carried out on the fracture surfaces of bulk cement and mortar patch repair materials.

A microscopic study was made on the thin sections of samples using a transmitted light polarising microscope. Specific examination was made of the bulk and the bond interface in order to gain further information regarding the nature of bond between patch cement paste and mortar to the substrate.

8.2 PREVIOUS WORK

8.2.1 Bond Test

Since good adhesion is of primary importance, a number of tests have been developed to assess bond strength both quantitatively and qualitatively. Direct comparisons of bond test results often give considerable differences in strength. These differences have been attributed to alternative methods employed, polymer systems, curing conditions and quality of substrates.

The development of bond test methods often results in different test configurations. Despite these differences, the types of test can be divided into four categories; 1) tension, 2) flexure, 3) shear, and 4) combination of compression and shear (slant-shear).

The slant shear test (BS 6319, Part 4, 1984) has been widely used and utilises a specimen size of 55 x 55 x 150 mm and a bond line of 30° to the vertical axis. Judge *et. al.* (1986) used the slant shear, Elcometer pull-off and tensile strength (BS 6319, Part 7, 1984) of repaired 'dog bone' specimens to test the bond strength of various systems. These included acrylate, SBR slurry and epoxy resin which were primed to the concrete substrate, left until tacky, prior to placing Fosroc mortars. Rapid setting repair mortars without polymers were also tested. The composite plaques were cured for 14 days at 20°C and 65% RH, and cut to a standard size prior to test. It was concluded that the repaired 'dog bone' tensile test was the most suitable to measure direct bond strength of patch repairs. The failure line of this test normally occurs at the narrowest section of the specimen, which is also along the bond line of patch and substrate.

The influences of different test methods, curing and polymer systems on adhesion strength of patch repairs were investigated by Ohama *et. al.* (1986). Patch repair mortars were prepared according to JIS A 1171. Polymers used were SBR, EVA and polyacrylic ester (PAE). The amount of water was adjusted to give approximately a constant flow of 175 ± 5% using flow table test. Curing was 2 days moist at 80% RH, 20°C, 5 days in water at 20°C followed by 21 days dry at 20°C, 50% RH. Slant shear tests show much higher strength values compared with other test methods irrespective of the polymer content and curing conditions. These results suggested that the slant shear test did not measure the bond strength at the interface but a combination of compression and shear strength. Despite the differences in test methods, the trend of bond strength results were similar. However the failure mode at the failure interface varied significantly due to the differences in method of load application and test geometry.

Assessment of different patch repairs using slant shear, core pull-off and friction transfer (torsion) was reported by Naderi *et. al.* (1987). Patch repair slabs 600 mm x 300 mm and 50 or 100 mm thick were prepared and tested at 14 days old. Repair systems consisted of plain mortar, SBR, fibre reinforced acrylic and acrylic. Residual strength after cyclic temperature changes was also investigated for core pull-off and torsion specimens. The temperature cycle used involved heating at 80°C for 7 hours, followed by air cooling at 0 - 10°C for 17 hours. This was continued for 150 cycles, followed by 50 cycles of cooling between room temperature and - 20°C. For core pull-off and torsion tests, a 50 mm aluminium probe was glued to the patch surface prior to the test. It was reported that bond strength of acrylic modified mortars show superior performance than SBR and plain mortars. Residual tensile bond strengths of modified mortars show a steady decrease between 80 and 150 cycles but plain mortar had negligible strength.

Patch repair systems have also been evaluated for use in marine environments. Patch repair prisms with artificial spalls were specially developed for this test (Treadaway *et. al.*, 1988). Cox *et. al.* (1989) subsequently evaluated the repair systems of ordinary mortar, SBR modified mortar, glass-fibre-reinforced SBR, glass-fibre-reinforced mortar, epoxy and rapid setting mortar. Evaluation was made for a period of up to 10 years based on the ease of application, visual appearance, bond to substrate, dimensional stability and protection of steel. It has been shown that rapid setting repair systems are only effective for short term repairs (< 2 years). The investigation showed that for long term repairs of up to 10 years, the unmodified and SBR modified mortars were effective in protecting the steel from corrosion. However, this type of repair prism was only suitable for visual assessment of patch repairs.

Statistical data from a 3 year study of bond has been presented by Kuhlman (1990). SBR modified mortar 76 mm in diameter and 36 mm thick was cast onto a 76 mm diameter concrete substrate. Three types of surface preparation were used, 1) saw cut, 2) sanded and 3) sandblast. The specimens were pulled-off at 1, 3, 7, 14, 28 and 90 days after dry cure at

20°C and 50% RH. The study showed that surface preparation did not significantly affect the tensile pull-off results. The failure generally occurred at the bond surface.

Marosszeky *et. al.* (1991) evaluated the bond strength of five patch repair systems: normal mortar, SBR, terpolymer, EVA, and acrylic. Slant shear (BS 6319, 1984) and core pull-off tests were used. For the pull-off test, a 50 mm thick patch was cast at the top of a concrete slab 400 mm x 400 mm x 50 mm. Cores of 55 mm diameter were drilled through the patch ending at a depth of 10 mm into the concrete substrate. It was reported that the surface roughness did not significantly affect the pull-off strength, but when using the slant shear test, the strength increased with increase in surface roughness.

The behaviour of shallow concrete patch repairs was reported by Austin and Robins (1993). The primary aim was to develop a suitable patch test specimen that could be loaded in compression, flexure and pre-loading in tension. The behaviour of repaired prisms under various loading conditions were investigated and this can be used in relation to the actual service conditions of repaired concrete structures. However, the specimen configurations required extensive preparation such as cutting, chiselling and needle-gunning. Later, the work was extended (Robins & Austin, 1995, Austin *et. al.*, 1995) and the results were compared with core tensile pull-off and slant shear tests. The effects of surface roughness and moisture conditions were also investigated. They reported that the patch prisms, core pull-off tests and slant shear tests all showed a dependency on surface roughness.

8.2.2 Microstructure of polymer cement composites

Early work by Isenburgh and Vanderhoff (1974) suggested that a polymer film forms an interpenetrating network throughout the hardened cement paste. The fracture surfaces of mortar modified with vinylidene chloride and SBR latexes were examined using SEM. The micrographs suggest that polymer film in the form of microfibres bridged the microcracks

which were observed in the microstructure of unmodified mortar. There was no additional evidence for the presence of a polymer film.

A Backscattered Scanning Electron (BSE) imaging technique was used by Johnson (1988) to analyse quantitatively cement hydration products. Optical microscopy was also used to determine any important features of the hydration products. Polished samples of OPC, epoxy resin and SBR modified mix were used. Micrographs obtained suggest that three distinct phases of CSH gel, $Ca(OH)_2$ and unreacted materials could be identified and quantified using this technique. The image was analysed and presented in the form of histogram peaks which consisted of three phases namely carbon, calcium and gold. Epoxide resin can easily be detected by polymer phase separation but the presence of SBR was difficult to detect and it did not appear to be separated. Although the BSE technique is very useful, the presence of voids in mortar and concrete will also give a dark image, which in turn could be misinterpreted as polymer.

Distribution of the polymer phase and spot analysis of polymer in the matrix were conducted using thin section microscopy and SEM/EDXA respectively (Oye, 1989). Analysis for carbon of the polymer suggested that a distinct polymer phase occurred in the matrix. In the case of polyvinyl chloride (PVC), the presence of chlorine made it easier to detect the polymer in the matrix.

Pareek *et. al.* (1990) conducted an extensive SEM study on the fracture interfaces between the bonded mortars and polymer dispersion coated mortar substrates. Attempts were made to explain the mechanism of improved adhesion. Improved bond strength was attributed to the micro-mechanical interlocking of polymer film at the adhesive interfaces.

The morphology of SBR latex modified concrete was examined by Lewis and Lewis (1990) using SEM and EDXA. Fracture specimens, from the fragments of cubes and tensile splitting cylinders which had been tested, were selected from plain concrete with 12 and

15% SBR content. The presence of polymer phase in the matrix was very difficult to detect. Bromine was used as a tagging agent which is capable of bonding to the carbon-carbon double bond in the butadiene repeat units. Tagging was carried out either by suspending polished samples above liquid bromine or immersed in a 5% aqueous solution for 2 days, followed by washing and drying. A high concentration of bromine was detected at the aggregate-cement matrix interface. This observation was supported with 'dot maps' showing the location of bromine. However at 12% polymer content, the polymer was not well distributed in the matrix.

Another way of revealing the polymer phase is by etching the polymer cement composites and observing them microscopically. These observations can then be supported by elemental analysis of interesting features or X-Ray mapping of elements such as carbon, calcium, silica and oxygen. Acid etching followed by SEM investigations were reported by Wagner (1965), Bentur *et. al.* (1990) and Justnes & Oye (1990b). Cement paste was treated with diluted HCl to reveal the gross structure of polymer. In the case of mortar, Wagner (1965) used a concentration of 10% HCl and 10% HF successively to etch the cementitious paste and aggregate.

Micrographs of etched mortars suggest that the coalesced polymer was confined within the hardened sand-cement composition. Wagner (1965) observed that poly (vinylidene and vinyl chloride) did not coalesce within the mortar matrix. Justnes and Oye (1990b) observed that a continuous network of polymer film in mortar could be achieved when the polymer dosage is between 5 - 10 % and water/cement ratio of 0.55. However, in the case of epoxy mortars the polymer appeared to be separated in the form of polymer clusters that were easily identified within the matrix.

When using a vinyl acid monomer starting material, Bentur *et. al.* (1990) observed that the polymer phase was in the form of either a continuous or discontinuous film. A discontinuous polymer phase, poor bonding to sand grains, and polymer bridging of cracks

were observed in cement mortars. A continuous polymer phase with film thickness of $\approx$ 1 μm was found in etched cement paste + silica fume + 10% polymer. These films were not analysed to see if they consisted only of polymer.

The presence of polymer in a threadlike structure was confirmed by using EDXA (Justnes & Oye, 1990b). However the secondary electrons from EDXA also detect other elements like calcium and silica near the area of analysis. This appears to be not a distinct polymer film but polymer with CSH gel.

The interfacial microstructure between polymer modified cement paste and aggregates were investigated by Su and Bijen (1990). Samples were fabricated by casting polymer modified cement pastes onto the polished surface of limestone and granite. Acrylate and VVC were used with polymer contents of 8, 15 and 25% with w/c 0.35 and 0.45. The samples were cured at 20°C, 65% RH for a period of up to 180 days. It was suggested that polymer appears to accumulate at the interfacial region. The presence of polymer was confirmed by the high concentration of Cl^- at the interface. A microhardness study of the transition zone between aggregate and cement paste, showed that hardness was less at the interface compared to the bulk.

Further work, Su *et. al.* (1991a & b) confirmed that a relatively high polymer content is present at the polymer modified cement-aggregate interface. From the SEM/EDXA analyses it was suggested that good adhesion between SA and VVC polymer modified cement pastes and aggregate was due to improved particle packing compared with the unmodified paste. In the case of unmodified cement, the 'wall effect' and bleeding lead to a water rich interfacial layer which contributed to a porous and weak bond.

8.3 EXPERIMENTAL

8.3.1 Adhesion Tests

Investigations were carried out in three series of experiments:

Series I: SBR 1 modified cement paste patch repairs subject to pull-off and flexural adhesion tests.

Series II: SBR 1 modified mortar patch repairs subject to pull-off and flexural adhesion tests.

Series III: SBR 1/EVA 1/Ac 1 modified mortar patch repairs subject to flexural adhesion tests.

Mortar Substrates

The same mix design for the mortar substrates was used in all three series of experiments:

Sand (max. size 5 mm) : cement	-	2.5 : 1
Water/cement ratio	-	0.5
Mean 28 days compressive strength	-	49 Nmm^{-2}

For pull-off tests, mixes were cast into cylindrical UPVC moulds 50 mm in diameter x 70 mm depth.

For flexural tests, mixes were cast into steel prisms moulds 40 mm x 40 mm x 160 mm.

In both cases samples were then covered with wet hessian, demoulded at 1 day and cured for a further 27 days under water at 20°C. The prisms were then cut in half to give sections 40 mm x 40 mm x 80 mm.

All bonding surfaces of mortar substrates used in Series I & II were wire brushed and cleaned with water. For Series III, the bonding faces were sand blasted and cleaned with a jet of water to remove loose particles.

Patch Repair Materials

Materials cast were:

Series I:

Cement pastes containing 0, 10 and 20% SBR 1

Surface preparation - wire brush

Curing:

WET = 2 days > 95% RH, 26 days in water @ 20°C (Code: 28W)

DRY = 2 days > 95% RH, 26 days at 20°C @ 65% RH (Code: 2W26D)

Series II:

Sand : Cement - 1.5 : 1

Sand Grading - Sand 1

Surface preparation - wire brush

Curing:

WET = 2 days > 95% RH, 26 days in water @ 20°C (Code: 28W)

DRY = 2 days > 95% RH, 26 days at 20°C @ 65% RH (Code: 2W26D)

Series III:

Sand : Cement - 2.5 : 1

Sand Grading - Sand 2

Surface preparation - Sand blast

Curing:

WET = 2 days > 95% RH, 26 days in water @ 20°C (Code: 28W)

DRY = 2 days > 95% RH, 26 days at 20°C @ 65% RH (Code: 2W26D)

Mixing of patch repair materials was carried out in a similar way to that described for the workability experiments in Sections 4.3.2 and 5.3.3. The w/c used were chosen to give the same workability at polymer contents of 0, 10 and 20%. These are given in Table 8.1 and were determined from the workability tests.

Test Configurations

Tensile Pull-off Adhesion Tests

For tensile pull-off specimens, 50 mm diameter and 30 mm thick, UPVC moulds were placed on top of the substrate cylinders and held together by means of ring clips prior to casting the patch materials, see Fig. 8.1a.

The patch mix was then cast into the moulds and the surface was trowelled smooth. The moulds were covered with damp hessian leaving a small gap between the surface of the patch and the hessian. Mould and the hessian were then wrapped in cling film for 48 hours. This procedure ensured that specimens cured at a minimum of 95% RH. After 48 hours they were carefully demoulded and further cured at the various curing conditions described above.

After curing, circular steel dollies were glued with rapid set epoxy to the both ends of the tensile pull-off specimens. For wet cure specimens, both ends were dried by means of heat from a hair drier and the specimens, with the glued circular steel dolly, were left in the laboratory overnight prior to the tensile pull-off tests. This was because the epoxy required a dry environment to set. This ensured that the epoxy bond strength was stronger than the bonding joint of the specimens.

Tensile pull-off tests were carried out by fixing the specimens in a Hounsfield Tensometer.

Flexural Adhesion Tests

For flexural adhesion test specimens, the half prism substrates were placed in the steel moulds and patch material was cast into the other half, making a prism of 40 mm x 40 mm x 160 mm, see Fig. 8.1(b).

The specimens were then cured in a similar way as described earlier. After curing the load and support positions on the prisms were clearly marked. They were then carefully fixed to a test jig which was attached to the Hounsfield Tensometer.

Flexural adhesion tests were carried out according to JIS A 1172 using the same Hounsfield Tensometer. The adhesion strength of the specimens was calculated by dividing the failure load by the area of the bonded surface. The interfaces / failed cross sections were then examined for type and loci of failures.

8.3.2 Thin Section Microscopy (TSM)

Thin sections were prepared from patch repair prisms of mortar containing 0% polymer and 20% SBR 1. The specimens examined are given in Table 8.2. The prisms were prepared in a similar way to that described in Section 8.3.1 *(Flexural Adhesion Tests)*. The prisms

were cut by means of a circular saw, leaving a middle section with dimensions of 40 mm x 40 mm x 50 mm. The blocks were sliced, parallel to a casting face, see Fig. 8.2, to give blocks of dimensions 40 x 50 x 15 mm. The blocks were cleaned with deionised water followed by drying in the oven at 36°C for 72 hours. They were then vacuum impregnated with fluorescent resin. One side was polished, flattened and glued to a glass slide. The blocks were subsequently cut to approximately 2 - 3 mm thickness and then ground down to a thickness of 9 μm. Finally a cover slip was glued to the thin sections and they were then ready to be examined with an optical microscope.

The thin section was analysed using a normal transmitted light polarising microscope. Examination should provide information on bonding interface, distribution of air voids, cracks and distribution of polymer film in the matrix by employing plane and polarised light. Features of significant interest were taken and examined. From these observations, a good basis could be made on the nature of bond between old concrete and new patch material.

8.3.3 Scanning Electron Microscopy (SEM)

The scanning electron microscopy (SEM) was carried out on (a) the fracture surface of patch material and (b) at the debonded interface between substrate and patch. Samples were prepared in a similar way to that described earlier. The samples examined are shown in Table 8.3.

The prisms were broken into two using the Hounsfield Tensometer and the load was recorded. The failure faces along the bonding line of both substrate and patch were sliced by means of diamond circular cutter to give sections approximately 3 - 4 mm thick, see Fig. 8.3. Both sections were cut to a size approximately 5 x 5 mm, representing the same location (mirror image). Samples were also taken well away from the interface to represent the structure in the bulk of the specimens.

All samples were rinsed with deionised water, immersed in propan-2-ol and then given an ultrasonic bath treatment to remove any loose dirt and water. This was followed by drying in an oven at 36°C for 72 hours. After 72 hours the samples were placed above silica gel where a small amount of carbosorb was also placed in the desiccator and stored at 20°C prior to SEM analyses. This was to minimise the risk of carbonation.

Selected samples of small pieces from polymer modified cement paste were also subjected to an acid etch treatment before being examined in the SEM. The chunks were immersed in a solution of 1% HCl + 1% HNO_3 for 5 - 7 minutes to lightly dissolve the cement components and expose the polymer phase. The samples were carefully washed with deionised water and dried by means of cool air from a hair dryer. The samples were placed above silica gel in a desiccator (as described earlier) for at least 10 days.

The samples were glued to SEM stubs and a layer of gold deposited on the sample surface under vacuum. The samples were then fitted to the SEM holder and examined. The examination was carried out using a Cambridge Stereoscan 90 scanning electron microscope. The microscope was equipped with an Link Systems EDXA that is capable of plotting the energy spectrum of detected elements. The area for the spot analysis was about 4 μm^2 and the accuracy of compositional analysis depends on e.g. surface topography. It is therefore very difficult to determine the exact percentage of the elements present at a particular spot. In spite of this limitation the semi-quantitative analyses do give a good indication of the phases present.

Photomicrographs and spot analyses of the features of significant interest were taken. For the etched samples, SEM/EDXA dot maps of carbon were performed on the polymer rich area. The purpose of this investigation was to reveal the polymer in the matrix in order to verify the role it plays in the paste.

8.4 RESULTS AND DISCUSSION

8.4.1 Bond strength

Adhesion strength of cement and mortar patches for Series I, II and III are shown in Tables 8.4 - 8.6. The pull-off and flexural adhesion strengths were calculated by dividing the failure load by the area of the bonded surface. The results shown are the mean of three tests with values for standard deviation. Typical loci of failure for the flexural adhesion test of cement and mortar patches are shown in Figs. 8.4 & 8.5. Interpretation of failure modes were made according to the CIRIA Technical Note 139 (McLeish, 1993).

Considering first the Series I experiments, unmodified cement pastes, wet cured, showed better bond strength compared with dry cured samples, 2.2 against 0.8 Nmm^{-2} for pull-off and 1.8 against 0.3 Nmm^{-2} for flexural adhesion. This is presumably because the wet curing conditions allow development of cement hydration products which is probably not the case when curing dry. The mode of failure for wet cure pull-off test samples was predominantly cohesive through the substrate whilst that for flexural adhesion specimens was cohesive through the patch (see Fig. 8.4a). In the case of dry cure, adhesive bond failure was recorded for all specimens either in pull-off or flexural adhesion tests.

The bond strength of dry cured SBR 1 modified paste was better than that of the wet cured paste. Furthermore, the bond strength of 20% SBR 1 modified pastes was better than that of the 10% SBR 1 modified paste, but this trend was reversed when the specimens were cured wet. Results from Series I show that polymer addition does not greatly improve bond over the well cured unmodified paste. The mode of failure for all wet cured specimens was adhesive (see Fig. 8.4b) and for dry cured polymer modified patch were 80 - 90% cohesive through the substrates (Fig. 8.4c).

Results from Series II show that bond strengths of dry cured polymer modified mortar increased as the polymer content increased. The bond strength of wet cured pull-off specimens were less than those which had been dry cured, for both 10 and 20% polymer content. However, this was not obvious for wet cured flexural specimens, particularly at 10% polymer content. The strength obtained was similar to the well cured plain mortar but the failure mode was generally 50 - 70% adhesive.

Results from Series III show that the flexural bond strength of dry cured polymer modified mortars, at 20% polymer content, are better than well cured unmodified mortars on the basis of the same workability. The bond strengths obtained when using different polymers was in the order of Ac 1 > EVA 1 > SBR 1. This trend does not appear to be related to the water/cement ratio and may therefore be related to the chemical properties of the polymer.

The failure modes of these samples are shown in Fig. 8.5. In each case significant porosity at the surface of the patch materials can be seen. In the case of the EVA 1 sample, the failure was adhesive. With Ac 1 some small sand particles are attached to the surface of the patch showing a degree of cohesive failure through the substrate. The SBR 1 sample showed about 70% cohesive failure through the substrate as evidenced by larger sand particles attached to the patched surface. For the unmodified mortar, the failure mode was adhesive.

It is obvious that polymer modified materials require a wet-dry curing regime in order to gain good bond strength. The initial wet curing at 100% RH for a period of 48 hours is very important to allow proper hydration of cement paste. A dry curing period should follow to allow coalescence of polymer particles. Other curing periods such as 7 days wet followed by 21 days dry give a similar effect, Ohama *et. al.* (1986).

As part of the SEM investigation one specimen of cement modified with 20% SBR 1 (Series I) and one specimen of mortar modified with 20% SBR 1 (Series III) were

re-wetted for a period of 110 days. The aim was to determine whether long term exposure to a wet environment resulted in a change in the nature of interfacial structures (bond). Results showed that for the modified cement paste, flexural adhesion strength reduced from 1.5 Nmm^{-2} to 0.5 Nmm^{-2} and for the modified mortar patch strength reduced from 1.2 Nmm^{-2} to 0.8 Nmm^{-2}. Whilst only one specimen was tested in each case, the results suggest that significant deterioration in bond occurred when exposed to prolonged wet environments. Similar effects were found by Oye & Justnes (1991b) and Justnes & Oye (1992b) who reported that compressive and flexural strengths of polymer modified mortars reduced when exposed to: i) 2 days wet - 14 days dry - 7 wet - 7 dry, and ii) 2 days wet - 21 days dry - 7 days wet. According to Justnes and Oye (1990b) surfactants may re-emulsify the polymer, partly perforate the film or entrain water and hence weaken the polymer film. However, Zeng (1996) showed that immersion of these polymer films in an alkali environment over long periods of time did not result in re-emulsification although considerable swelling did occur. The reason for this effect is still not fully resolved.

8.4.2 Thin Section Microscopy (TSM)

Observations of the microstructure were carried out at X100 magnifications. Unmodified cement shows a microstructure consisting of well hydrated paste with a small amount of unhydrated clinker, Fig. 8.6. Portlandite crystals were not evident. The existence of a good bond along the interface between patch and substrate made it difficult to differentiate between their microstructures in the interfacial area. Microcracks along the bond line were not observed.

In the case of SBR 1 modified paste a different microstructure was observed (Fig. 8.7). Well developed Portlandite crystals with different orientations and unhydrated clinker were evident and dominate the appearance of the paste microstructure. Such well developed Portlandite crystals are observed since retardation of cement hydration allows sufficient space within the structure for them to grow without hindrance from CSH gel. Further

growth of CSH gel probably was interrupted due to the limited amount of water available. A good bond along the interface was observed. The two different microstructures observed between polymer modified cement paste and the mortar substrate can easily be determined. Microcracks and polymer separation were not observed either along the bond line or within the bulk structure.

Similar observations were obtained for unmodified mortar patches, Fig. 8.8, compared with unmodified cement patches, Fig. 8.6. With SBR 1 modified mortar, Fig. 8.9, well defined Portlandite crystals are not evident compared with SBR 1 modified cement, Fig. 8.7. This is probably due to the higher w/c (0.42 compared with 0.28).

8.4.3 SEM Examination of Samples from Series I Flexural Adhesion Tests

8.4.3.1 Microstructure of fracture surface through cement paste patch

Typical bulk microstructures for wet cured unmodified cement paste, wet cured 20% SBR 1 modified paste and dry cured 20% SBR 1 modified paste are shown in Fig. 8.10. Elemental analyses of important features marked in Fig. 8.10 are given in Table 8.7. The tabulated major elements shown were obtained from spot analyses which covered areas of approximately 4 μm^2. In addition elements will be detected at the depths of about 1 μm below the surface.

The fracture surface of unmodified cement paste (Fig. 8.10a) shows a structure consisting of $Ca(OH)_2$, featureless gel and microcracks. Analyses on locations 1 and 2 showed that both areas have similar compositions. Visually these areas appear to be $Ca(OH)_2$ but this may well encapsulate CSH gel thus showing the presence of silicon in the analyses.

A typical microstructure of wet cured 20% SBR 1 modified paste is shown in Figs. 8.10b & c. The structure is not unlike that found for the unmodified paste except for the presence of large voids. Within the voids hexagonal shaped crystals are clearly evident and these were confirmed as being $Ca(OH)_2$ by analysis at location 3 and given in Table 8.7. Presumably during wet curing the voids were filled with water allowing precipitation of Portlandite. Analyses at locations 4 and 5 reveal significant amounts of carbon. At these concentrations the carbon must be from the polymer and demonstrates that this phase is probably polymer in conjunction with, or close to, $Ca(OH)_2$.

The microstructure of dry cured 20% SBR 1 modified paste, Fig. 8.10d appears to be quite different from the previous two samples. The hydration products are more featureless, there are a lot of small voids and well developed $Ca(OH)_2$ crystals with different orientations confirming the TSM observation (Fig. 8.7). Analysis of the featureless hydration products at location 6 suggest the presence of CSH gel together with a high concentration of polymer. There is no evidence for a distinct polymer film and it again appears that the polymer is intimately combined with hydration products.

When samples of dry cured 20% SBR 1 modified cement were rewetted for 110 days consolidation of the structure was apparent and it was now very similar to the microstructure of wet cure 20% SBR 1 modified paste.

A fracture surface of dry cured 20% SBR 1 modified cement paste was lightly acid etched in an attempt to locate the polymer film in the hardened microstructure. Micrographs of a typical area are shown in Figs. 8.11a & b with an EDXA dot map for carbon covering the same area, Fig. 8.11c. From Figs. 8.11a & b it is evident that the acid etch has selectively dissolved some areas e.g. locations 1 and 2 leaving a more resistant network. The EDXA analysis shows this network to be rich in carbon, and suggests polymer is not uniformly distributed through the matrix.

8.4.3.2 Interfacial microstructure between cement patch and substrate

Unmodified cement patch and substrate

The mode of failures for wet cured unmodified cement patch systems were generally 80% cohesive through the cement paste and 20% adhesive. Therefore the SEM micrographs on these surfaces only reveal bulk microstructure of either the cement patch or mortar substrate. Cohesive failure through the patch suggests that a good bond at the contact surface was achieved. Cohesive failure of the patch also suggests that the adhesion strength at the interface exceeds the tensile strength of cement paste.

Wet cured SBR 1 modified cement patch and substrate

Adhesive failure was observed for almost all specimens (see Figs. 8.12a & b). This is confirmed by the rather flat surface shown in the micrographs. It is also noticeable that this interfacial zone is very porous. Spot analyses of interesting features are summarised in Table 8.8. Analysis of location 1 showed only calcium and carbon suggesting the presence of calcium hydroxide and polymer. Analysis of location 2 showed only calcium, although this looks like CSH gel (see Ben-Dor, 1983 and Jennings, 1983). This contradiction demonstrates the difficulty of interpreting EDXA analysis on fracture surfaces.

Dry cured SBR 1 modified cement patch and substrate

Generally the failure mode was more than 70% cohesive failure through the substrate. Fig. 8.13a shows the patch side of the failure and aggregate / mortar matrix which has pulled-off from the substrate and covers part of the patch area is clearly visible.

An area of the failure surface of the patch not covered by substrate is shown in Fig. 8.13b showing a rather porous microstructure. Analyses of locations 3, 4 and 5 show the presence of a high concentration of carbon, oxygen, silicon and calcium. This suggests that CSH gel, $Ca(OH)_2$ and polymer are present together. It is not possible to distinguish clearly between separate phases.

An area of the failure surface of the substrate not pulled-off is shown in Figs. 8.13c & d. Analyses of locations 6 and 7 are very similar to those found on the patch. This suggests that a discontinuous film of patch material remains on the substrate. The strength of the bonding layer here was not high enough to pull-off substrate matrix. Microcracks of approximately 1 μm in width were also visible. Needle-like products appear to bridge the crack but elemental analysis on this area was not possible because of its size. It is possible that this may be polymer film.

8.4.4 SEM Examination of Samples from Series III Flexural Adhesion Tests

8.4.4.1 Microstructure of fracture surface through mortar patch

Whilst it was easier to compare unmodified and modified cement microstructures of the cement pastes, some interesting observations have been made on the mortars. Some typical morphologies of wet cured unmodified mortar, and wet & dry cured SBR 1 modified mortars are shown in Fig. 8.14. Elemental analyses of important features marked in Fig. 8.14 are given in Table 8.9.

The unmodified mortar shows the presence of microcracks, layers of calcium hydroxide and amorphous C-S-H gel. Analysis of location 1 suggests that this feature is $Ca(OH)_2$

covering C-S-H gel. However, the low calcium and high oxygen and silicon contents at location 2 suggests the presence of sand particles.

A more dense morphology was observed with wet cured SBR 1 modified mortar. Well developed calcium hydroxide crystals dominate the voids, see Fig. 8.14b & c. Analyses of locations 3, 4 and 5 again confirm that polymer is well dispersed within the matrix and intimately combined with other hydration products.

The morphology of dry cured SBR 1 modified mortar, Fig. 8.14d, was also rather featureless. Layers of hydration products were covered by featureless layers rich with polymer. Microcracks were not visible compared with the unmodified mortar. Analyses of locations 6 and 7 showed that significant amounts of carbon were detected. High oxygen and silicon contents at location 6 suggests that the polymer probably covered an aggregate surface. Analysis of location 7 confirmed that polymer is intimately combined with other hydration products.

8.4.4.2 Interfacial microstructure between mortar patch and substrate

Unmodified mortar patch and substrate

The modes of failure for wet cured unmodified mortar and substrate were generally adhesive, i.e. bond failure at the interface. There were no significant differences in morphology between these two surfaces, Fig. 8.15. Microcracks are visible both on the unmodified mortar patch, Fig. 8.15a & b, and substrate, Fig. 8.15c & d. Layers of $Ca(OH)_2$ crystals were not visible. However, some needle shaped crystals (possibly ettringite, see Ben-Dor, 1983 and French, 1991) can be seen on the mortar substrate, Fig. 8.15d.

Analyses at locations A1, A2, A3 and A4 given in Table 8.10 suggest that the hydration products at the interface are rich with CSH gel. From the analyses, traces of carbon were detected at all locations. This could be attributed to carbonation but from the TSM micrograph, Fig. 8.8, carbonation at the interface was not detected. Furthermore, every care was taken during the preparation and drying of specimen in order to reduce risk of possible carbonation.

Wet cured SBR 1 modified mortar patch and substrate

Micrographs of wet cured 20% SBR 1 modified mortar and substrate, Fig 8.16 show that the failure was adhesive. Clear featureless lumps with a lot of small voids are visible both on the patch and substrate. This morphology was very similar to the adhesive failure of the dry cured 20% SBR 1 modified cement patch (see Fig. 8.13c). Spot analyses of locations B1, and B5 suggest that polymer may well be covering aggregate particles. Analyses of locations B2, B3 and B4 suggest that polymer is intimately combined with other hydration products.

Dry cured SBR 1 modified mortar patch and substrate

Micrographs of dry cured SBR 1 modified mortar (Fig. 8.17a & b) showed that the failure was mainly cohesive through the modified mortar patch, leaving some of this material adhered to the substrate. Spot analysis of location C1 confirmed that a high percentage of carbon (polymer) was present with other hydration products possibly CSH gel. A high percentage of silicon at location C2 suggests that polymer is covering sand particles.

Micrographs of the substrate surface after fracture (Fig. 8.17c) showed essentially patch material with a few areas where the substrate has broken away. Polymer rich hydration products and cracks are visible. Spot analysis on location C3 suggests that polymer is

intimately combined with CSH gel. Analyses of location C4 and C5 suggest polymer free areas.

Rewetted, Dry cured SBR 1 modified mortar patch and substrate

Micrographs of failure interface for dry cured and then rewetted SBR 1 modified patch and substrate are shown in Fig. 8.18a - d, and the mode of failure was adhesive. The fracture surface of the SBR 1 modified mortar patch shows that fully developed $Ca(OH)_2$ and ettringite were evident. This suggests that hydration continued allowing CSH and $Ca(OH)_2$ to grow within any voids. Elemental analyses on locations D1 to D5, given in Table 8.10, again showed that polymer intimately combined with other hydration products.

The substrate fracture surface showed that polymer rich hydration products were deposited on its surface. Fully developed $Ca(OH)_2$ crystals and ettringite were evident. This possibly suggests that as a result of prolonged wet curing, hydration proceeds and hydration products continue to grow within the available space. The polymer film / clusters are now confined to the gaps and voids between hydration products. This in turn reduces physical bond between polymer and hydration products.

8.5 CONCLUSIONS

(1) With an unmodified patch repair material wet curing is required for a good bond. In contrast for a polymer modified repair material very little bond is obtained with wet curing alone and a wet-dry curing regime is required. Bond strength increases with increasing polymer content.

(2) On the basis of equivalent workability the bond strengths obtained when using different polymers was in the order Ac 1 > EVA 1 > SBR 1. This trend does not appear

to be related to water/cement ratio and may therefore be related to the chemical properties of the polymer.

(3) Petrographic and SEM examination of the bulk microstructure of polymer modified material showed very little evidence for the formation of a distinct polymer film phase as identified by Isenburgh and Vanderhoff (1974). It was found that a non-uniform distribution of polymer exists forming a discontinuous network. It was not possible to show how this phase is bound with CSH gel and $Ca(OH)_2$.

(4) The structure at the interface between the polymer modified material and the mortar substrate was found to depend on the type of curing employed. With wet curing (adhesive failure) a porous interfacial layer was found. At the actual interface, solid material consisted of calcium hydroxide and polymer. A wet-dry curing regime resulted in essentially (70%) cohesive failure and it is thus difficult to examine the interface itself. Examination of areas where the interface was exposed showed the presence of a combined CSH gel and polymer similar to that found in the bulk microstructure. There was little evidence of a distinct polymer film as identified by Isenburgh and Vanderhoff (1974) at the interface, except where emulsion may have penetrated existing cracks. A clear understanding of the limitations of SEM is required for correct interpretation of results.

(5) Re-wetting a wet-dry cured polymer modified repair shows a reduction in bond strength (and a return to adhesive failure). Microstructural examination suggested that further hydration had taken place and calcium hydroxide and ettringite were much more evident. It is not clear why this process disrupts the interfacial bond rather than consolidating it, but it may have something to do with swelling of the polymer phase.

Table 8.1: Mix proportions of patch materials

(i) OPC patch for pull-off and flexural adhesion tests (Series I)

Type of patch	SBR 1 content (%)	W/C	Curing
OPC	0	0.40	28W
	10	0.30	or
	20	0.28	2W26D

(ii) Mortar patch for pull-off and flexural adhesion tests (Series II)

Type of patch	SBR 1 content (%)	W/C	Curing
Mortar	0	0.53	28W
	10	0.40	or
	20	0.30	2W26D

(iii) Mortar patch for flexural adhesion tests (Series III)

Type of patch	Polymer content (%)	W/C	Curing
Mortar	0	0.60	28W
Mortar + 20% SBR 1	20	0.42	2W26D
Mortar + 20% Ac 1	20	0.35	
Mortar + 20 % EVA 1	20	0.55	

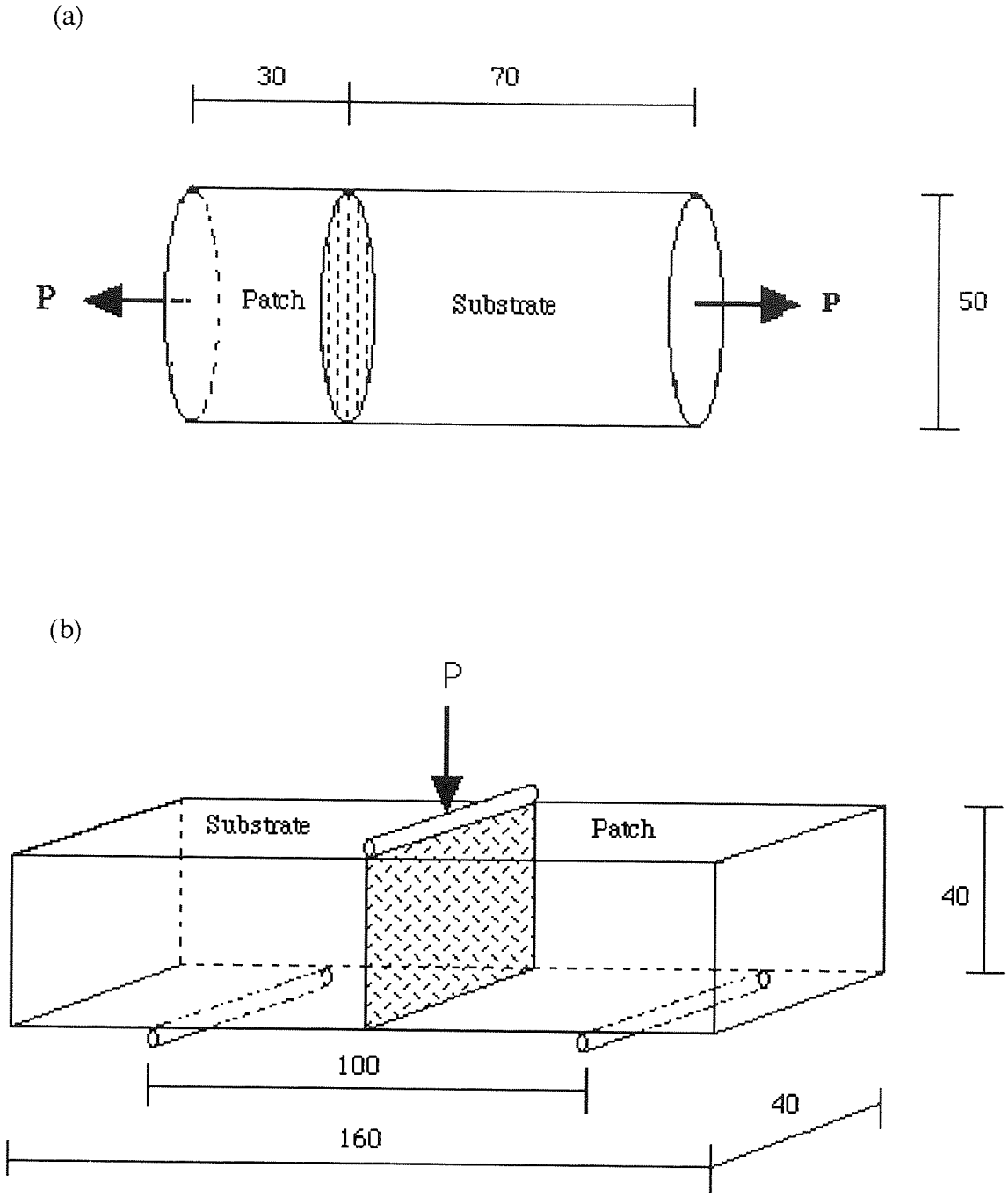

(All dimensions in mm)

Fig. 8.1: Bond test specimens: (a) Tensile pull-off, (b) Flexural adhesion

Table 8.2: Specimens for the Thin Section Microscopy (TSM)

Type of patch	Polymer content (%)	Water/Cement ratio	Curing
OPC	0	0.40	28W
OPC + 20% SBR 1	20	0.28	2W26D
Mortar	0	0.60	28W
Mortar + 20 % SBR 1	20	0.42	2W26D

Table 8.3: Specimens for Scanning Electron Microscopy (SEM)

Type of patch	Polymer content (%)	Water/Cement ratio	Curing
OPC	0	0.4	28W
OPC + 20% SBR 1	20	0.28	28W, 2W26D, 2W26D110W
Mortar	0	0.6	28W
Mortar + 20 % SBR 1	20	0.42	28W, 2W26D, 2W26D110W

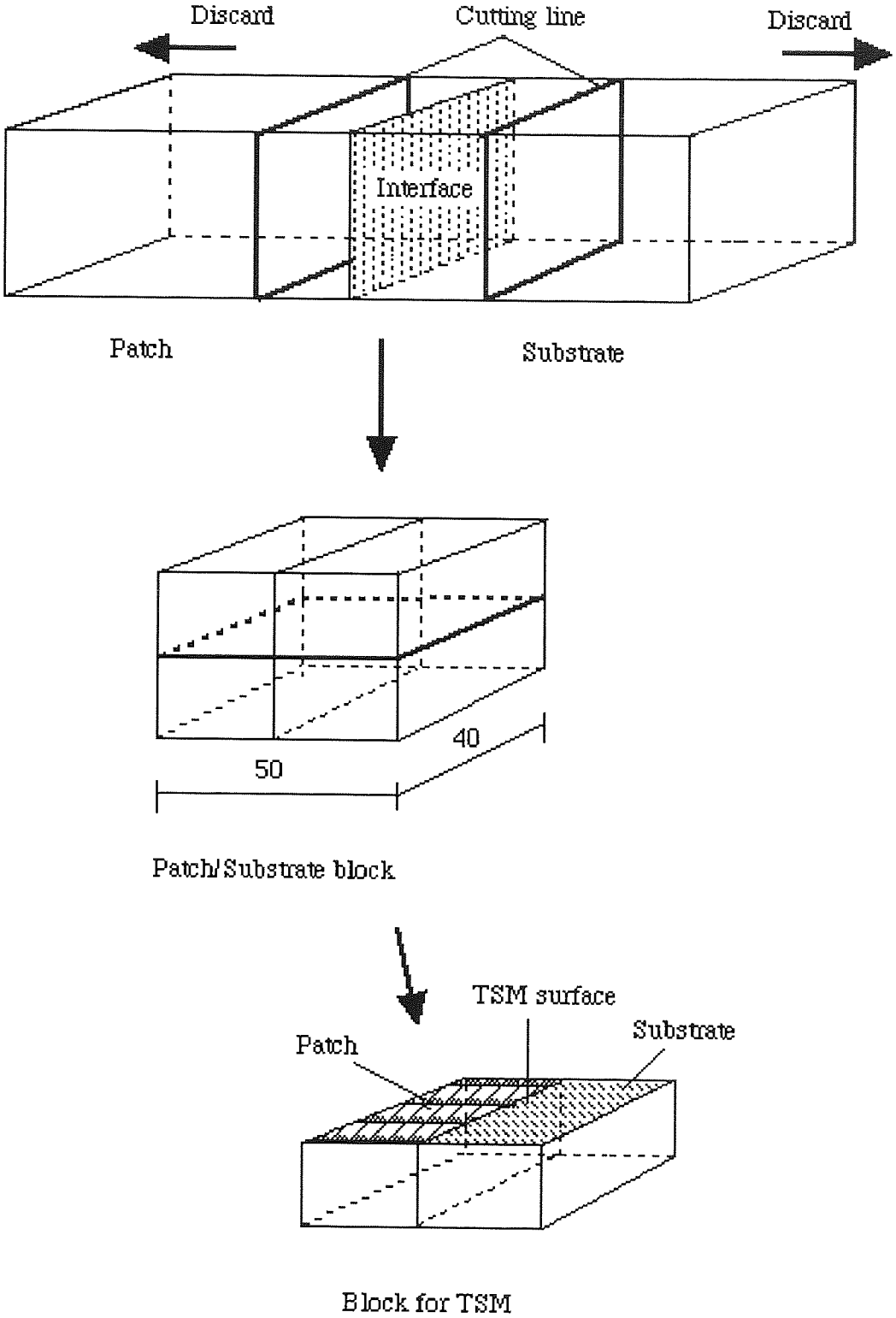

Fig. 8.2: Specimen preparation for Thin Section

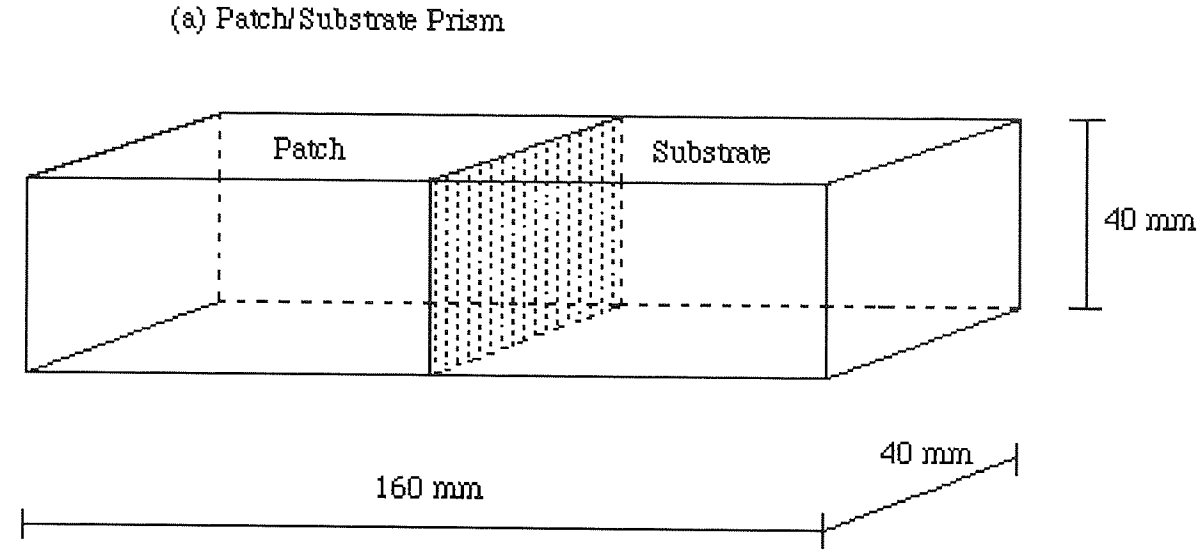

Fig. 8.3: Preparation of SEM specimen

Table 8.4: Adhesion Strength of OPC Patch (Series I)

Specimen	w/c ratio	Curing	Tensile Pull-off Strength (N/mm^2)	Flexural Adhesion Strength (N/mm^2)
OPC	0.40	WET	2.2 ± 0.3	1.8 ± 0.1
OPC + 10% SBR 1	0.30		1.5 ± 0.2	0.05 ± 0.01
OPC + 20% SBR 1	0.28		0.0	0.0
OPC	0.40	DRY	0.8 ± 0.1	0.3 ± 0.1
OPC + 10% SBR 1	0.30		1.7 ± 0.1	1.2 ± 0.1
OPC + 20% SBR 1	0.28		2.7 ± 0.2	1.5 ± 0.1

Table 8.5: Adhesion Strength of Patch Mortar (Series II)

Specimen	w/c ratio	Curing	Tensile Pull-off Strength (N/mm^2)	Flexural Adhesion Strength (N/mm^2)
Mortar	0.53	WET	1.8 ± 0.2	1.4 ± 0.3
Mortar + 10% SBR 1	0.40		0.8 ± 0.1	1.4 ± 0.1
Mortar + 20% SBR 1	0.30		2.4 ± 0.1	1.4 ± 0.1
Mortar	0.53	DRY	1.3 ± 0.2	0.6 ± 0.1
Mortar + 10% SBR 1	0.40		2.2 ± 0.1	1.4 ± 0.2
Mortar + 20% SBR 1	0.30		4.6 ± 0.3	1.8 ± 0.1

Table 8.6: Flexural Adhesion of Patch Mortar with Different Polymers (Series III)

Specimen	w/c ratio	Curing	Flexural Adhesion Strength (N/mm^2)
Mortar (Control)	0.60	WET	1.0 ± 0.1
Mortar + 20% SBR 1	0.42	DRY	1.2 ± 0.2
Mortar + 20% EVA 1	0.55		1.5 ± 0.1
Mortar + 20% Ac 1	0.35		2.2 ± 0.1

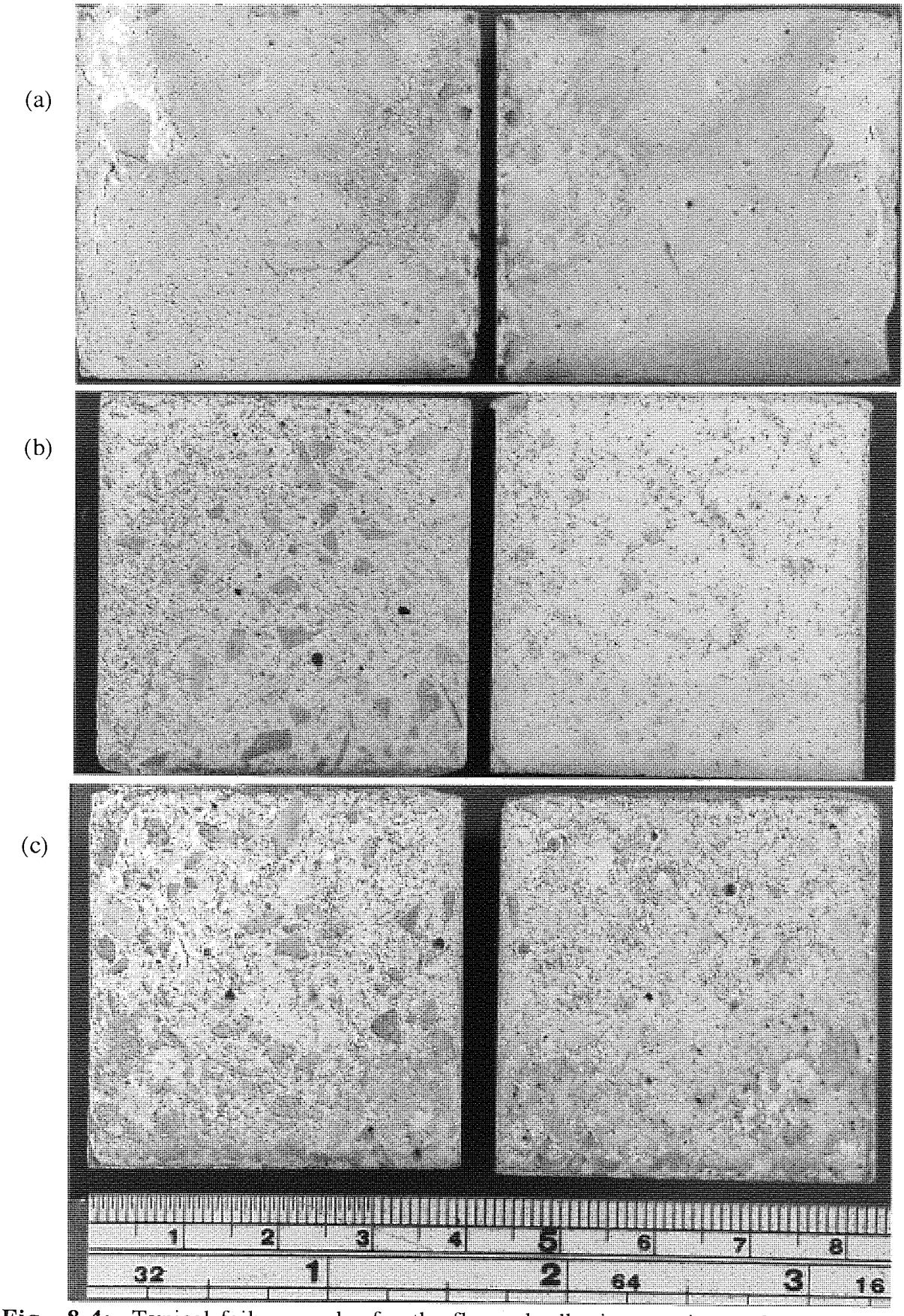

Fig. 8.4: Typical failure modes for the flexural adhesion specimens from Series I, Substrate (left), Patch (right); (a) Cohesive failure through unmodified cement patch, (b) Adhesive bond failure for the wet cured 20% SBR 1 modified cement, (c) Cohesive failure through substrate for the dry cured 20% SBR 1 modified cement.

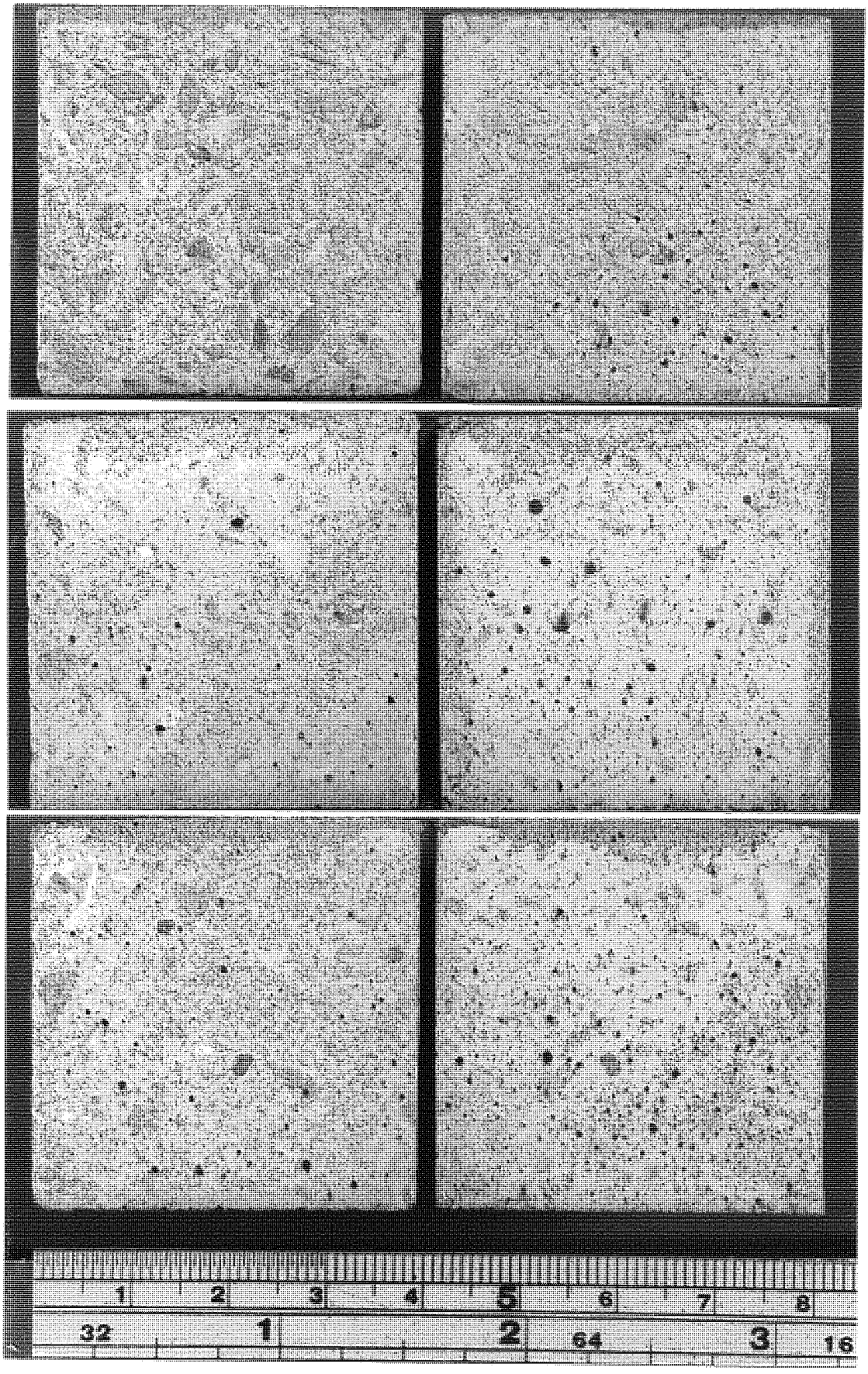

Fig. 8.5: Typical failure modes for the flexural adhesion specimens from Series III, Substrate (left), Patch (right); (a) Cohesive failure through the substrate of the dry cured 20% SBR 1 modified mortar (b) Adhesive bond failure for the dry cured 20% EVA 1 modified mortar, (c) Cohesive failure through substrate for the dry cured 20% Ac 1 modified mortar.

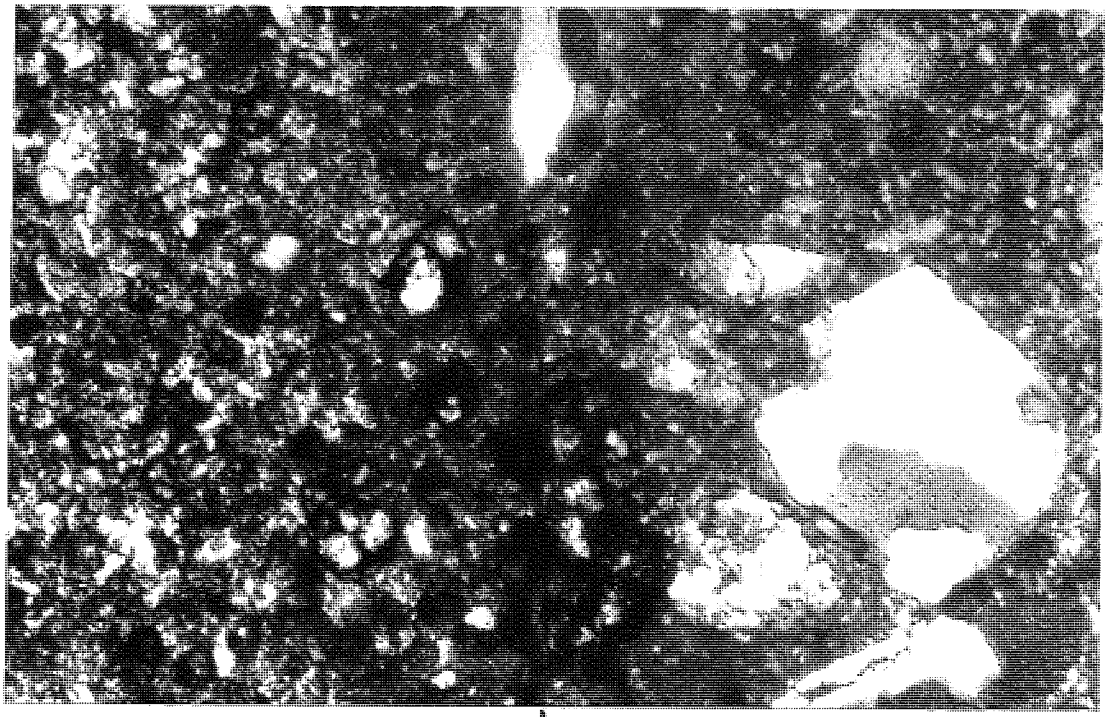

Unmodifed Cement Patch, w/c 0.4
Well hydrated paste with a small
amount of unhydrated clinker

INTERFACE
(good bond)

Mortar Substrate

Fig. 8.6: Micrograph of thin section for the interface between unmodified cement patch, wet cured (left) and substrate (right). (x100)

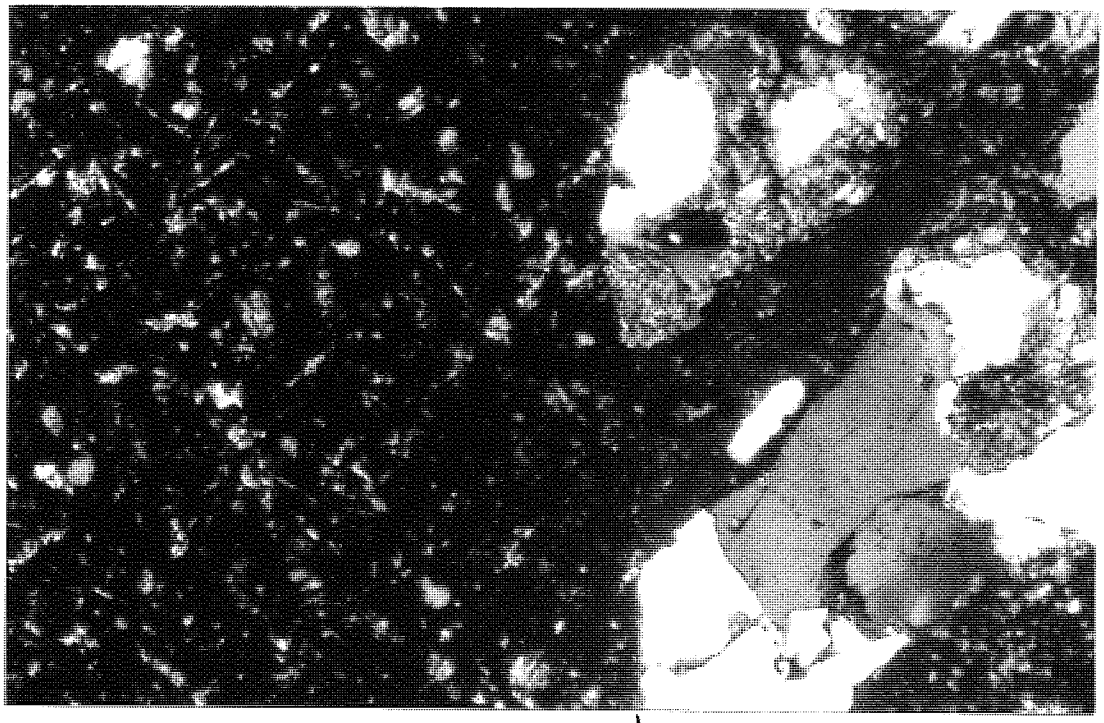

SBR 1 modified Cement Patch, w/c 0.28
Well defined crystals of Portlandite
+ unhydrated clinker

INTERFACE
(good bond)

Mortar Substrate

Fig. 8.7: Micrograph of thin section for the interface between 20% SBR 1 modified cement patch, dry cured (left) and substrate (right). (x100)

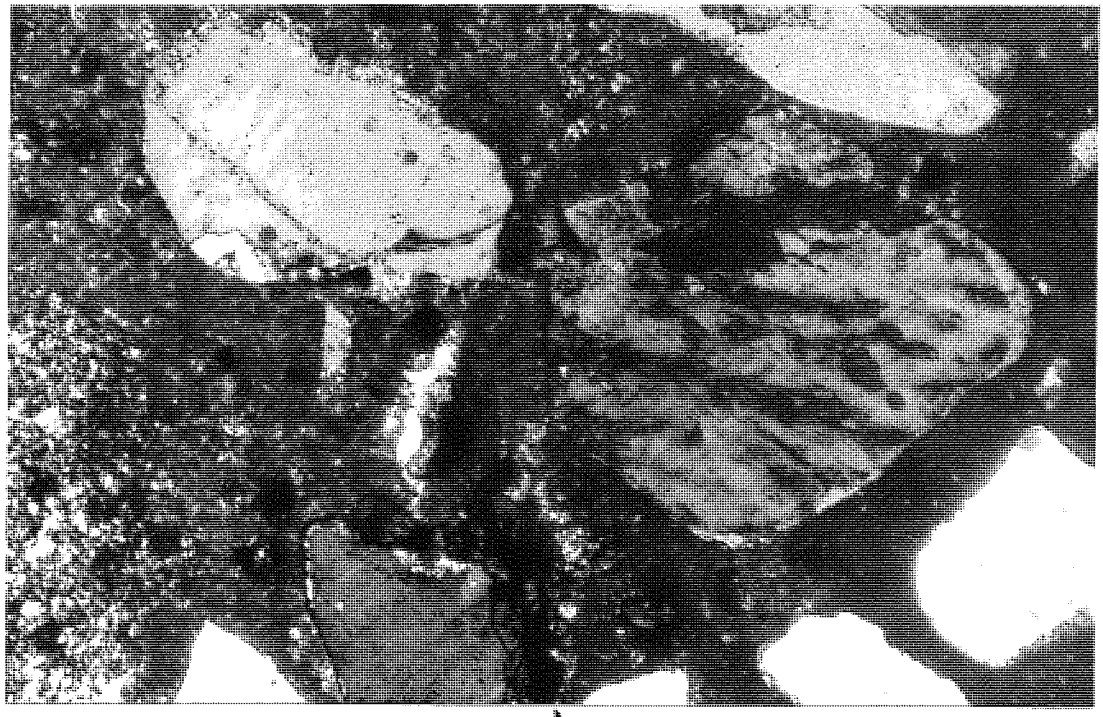

Fig. 8.8: Micrograph of thin section for the interface between unmodified mortar patch, wet cured (left) and substrate (right). (x100)

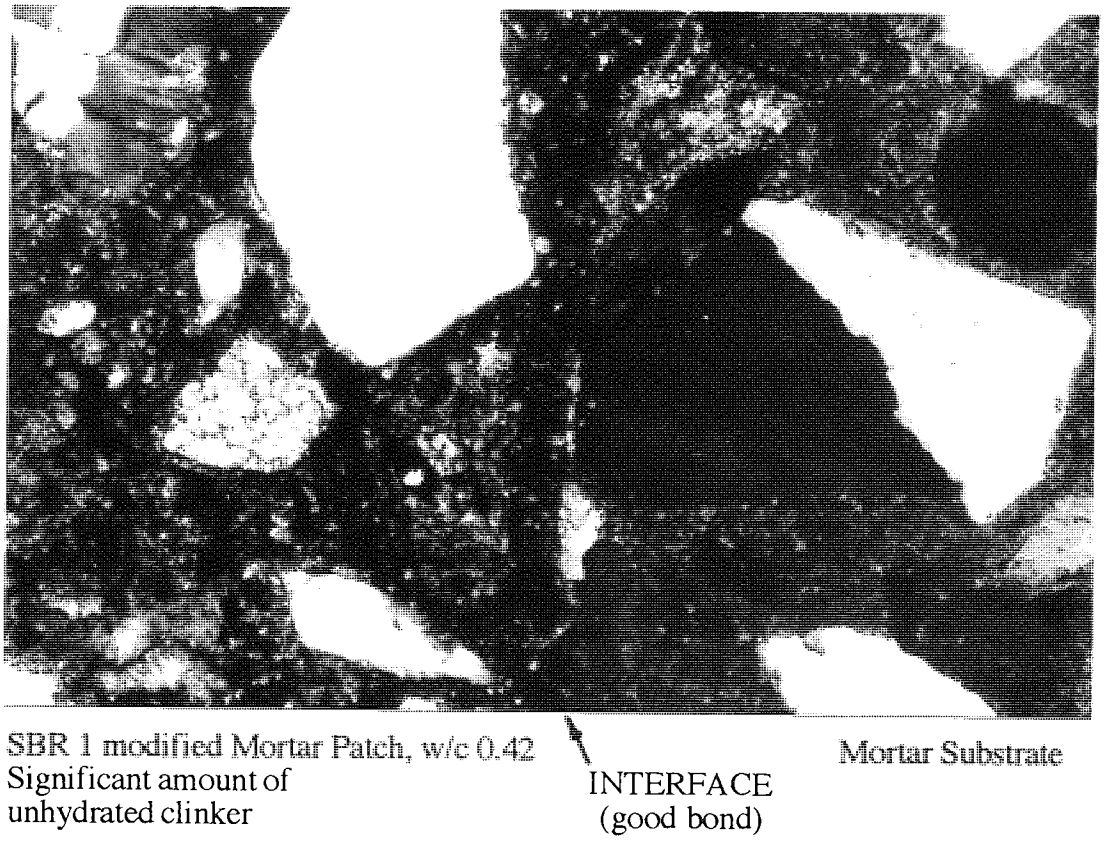

Fig. 8.9: Micrograph of thin section for the interface between 20% SBR 1 modified mortar patch, dry cured (left) and substrate (right). (x100)

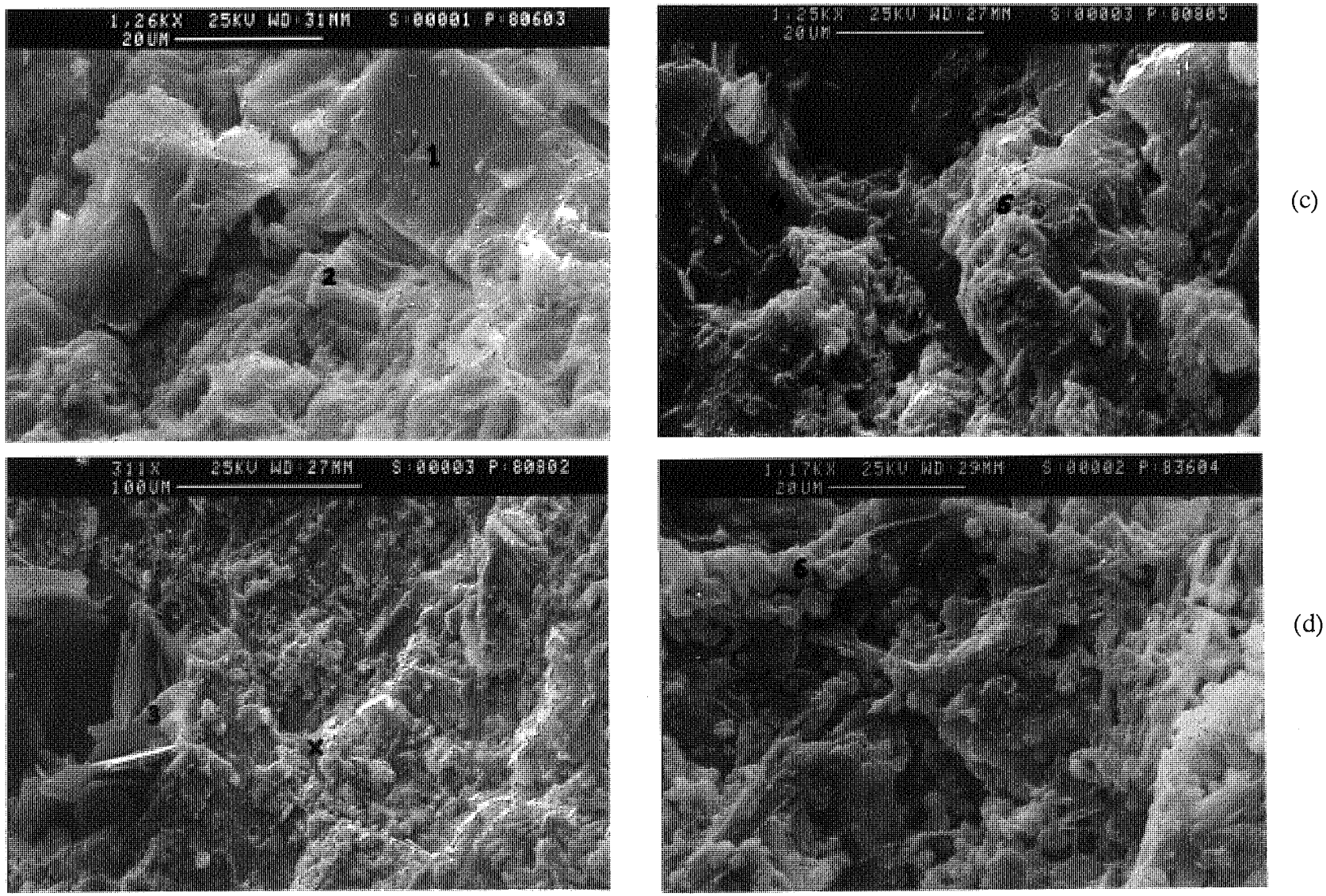

Fig. 8.10: SEM micrographs of fracture surface through; (a) Unmodified cement paste, (b) Wet cured 20% SBR 1 modified cement paste, (c) Higher magnification of area X and (d) Dry cured 20% SBR 1 modified cement paste.

Table 8.7: Spot analyses on fracture surface of cement pastes

Specimen	Figure 8.10 (Location)	Major Element (% Total)							
		C	O	Al	Si	S	K	Ca	Fe
OPC	1	0.0	17.2	2.7	9.7	0.0	0.0	65.0	1.0
	2	0.0	11.9	3.9	12.4	0.0	0.0	65.6	1.4
OPC + 20% SBR 1 (WET)	3	0.0	1.5	0.0	0.0	0.0	0.0	97.1	0.0
	4	14.8	15.0	0.9	2.7	0.0	0.0	65.2	0.0
	5	27.1	12.9	4.7	5.5	1.9	0.0	44.9	2.0
OPC + 20% SBR 1 (DRY)	6	31.0	7.0	4.1	5.2	0.0	1.3	47.5	2.0

(a)

(b)

(c)

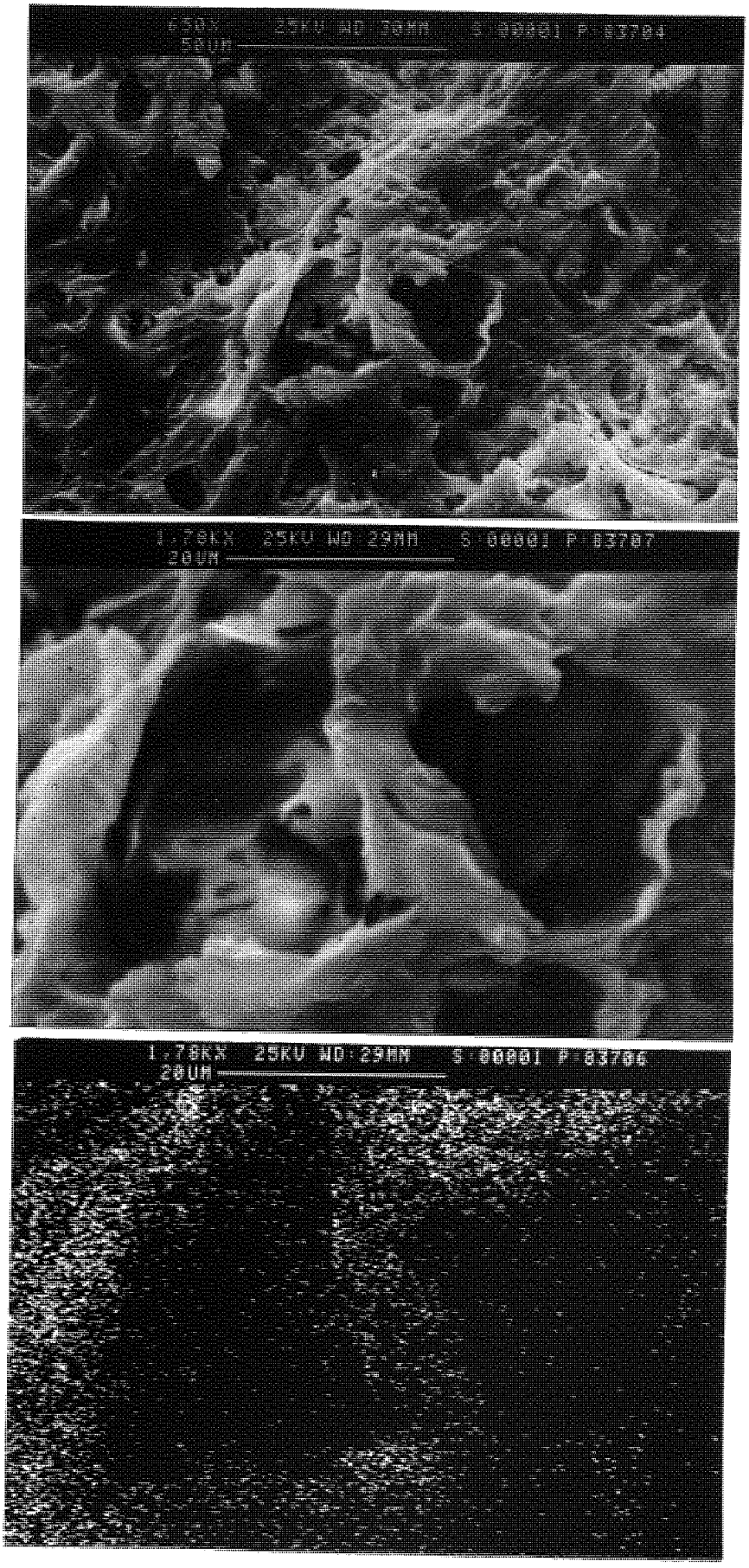

Fig. 8.11: SEM micrographs of acid etched (a) 20% SBR 1 modified cement, (b) Higher magnification around area X and (c) SEM/EDXA carbon dot map of (b)

(a)

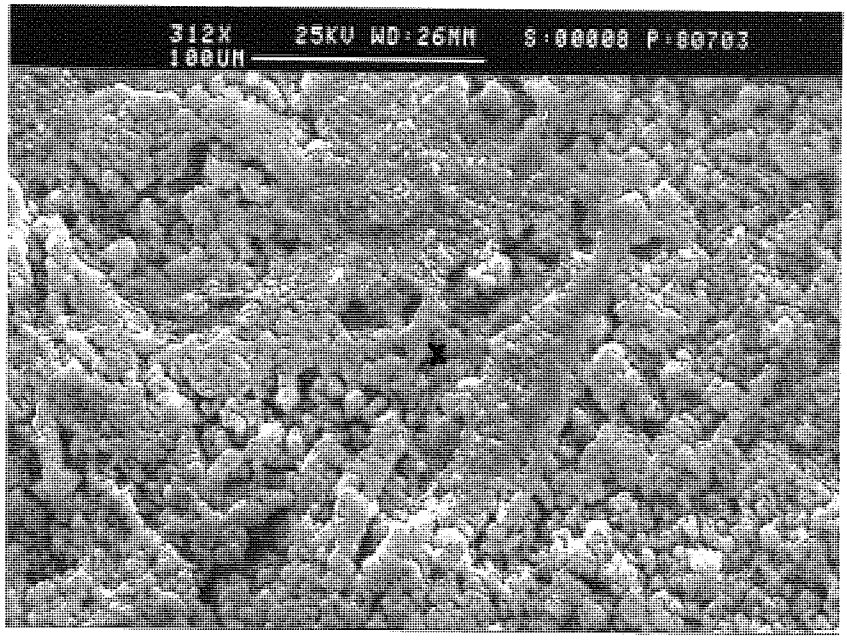

(b)

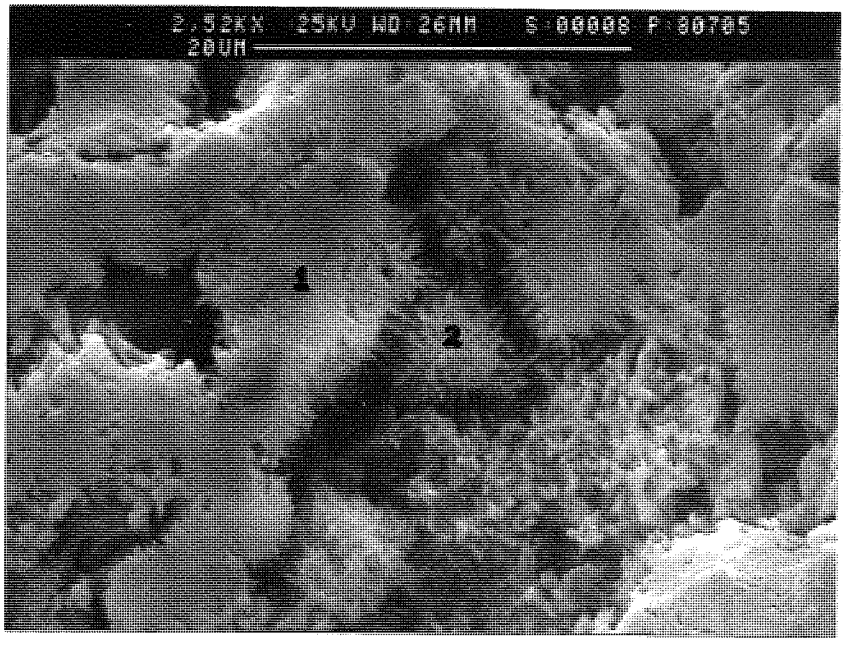

Fig. 8.12: SEM micrographs of adhesive bond failure at the surface of wet cured 20% SBR 1 modified cement patch, (a) Featureless appearance and massive small voids, (b) Higher magnification of area X.

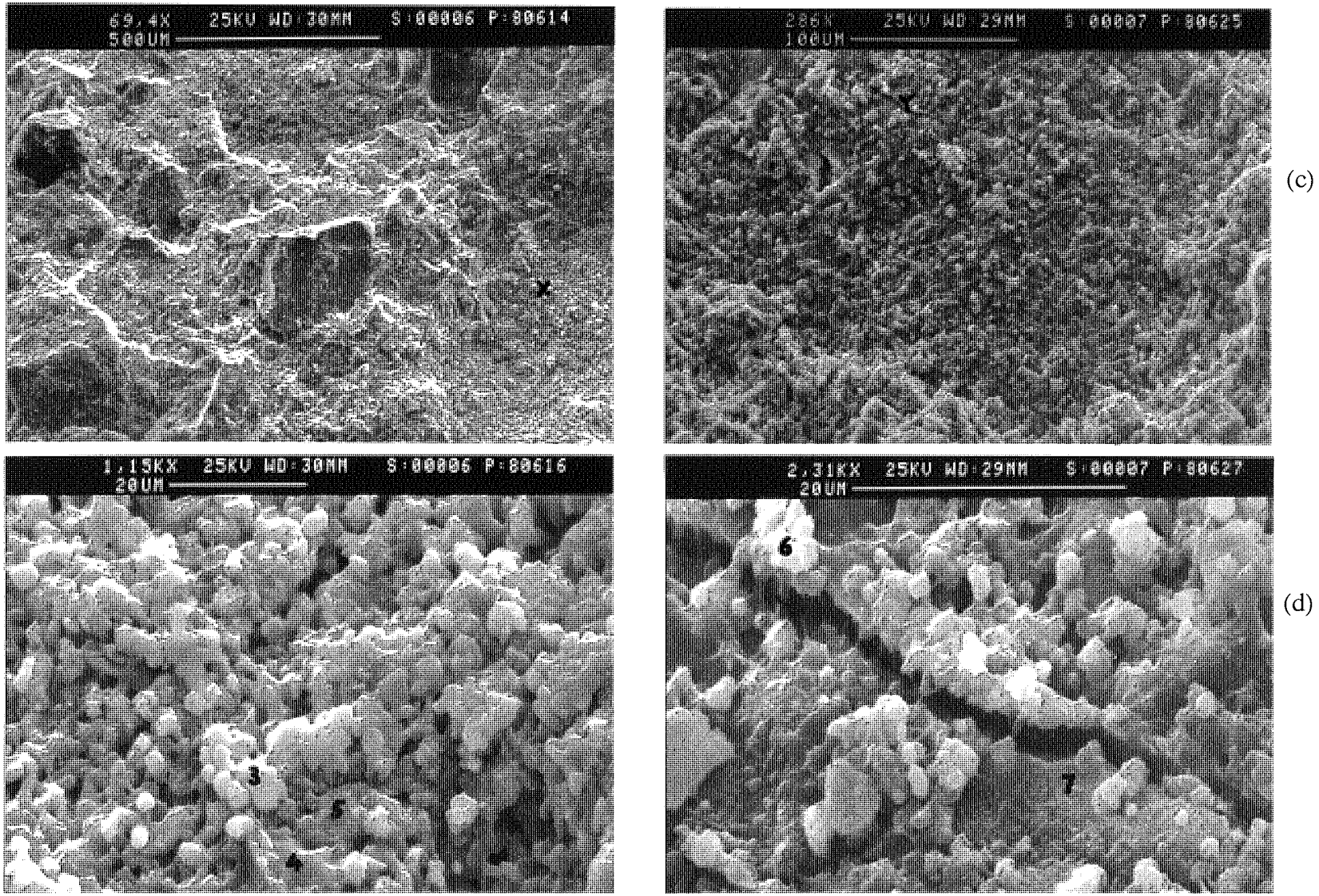

Fig. 8.13: SEM micrographs at the interface of the dry cured 20% SBR 1 modified cement patch; (a) Cohesive failure through substrate, (b) Higher magnification of area X showing adhesive failure on patch surface, (c) Failure surface of substrate, (d) Higher magnification of area Y showing needle-like products bridging microcracks on substrate.

Table 8.8: Spot analyses at the failure interface

Specimen	Figs 8.12 & 8.13 (Location)	Major Element (% Total)							
		C	O	Al	Si	S	K	Ca	Fe
Patch OPC + 20% SBR 1 (WET)	1	17.4	15.1	0.0	0.0	0.0	0.0	64.9	0.0
	2	3.1	1.8	0.5	0.8	0.0	0.0	93.4	0.0
Patch OPC + 20% SBR 1 (DRY)	3	41.7	14.4	2.0	5.7	0.0	0.0	32.4	0.9
	4	30.3	6.9	6.0	4.4	0.0	0.0	46.6	3.4
	5	17.7	9.7	2.2	5.1	0.0	0.0	58.6	2.1
Substrate OPC +20% SBR 1 (DRY)	6	35.3	18.7	2.4	4.7	0.0	1.8	34.4	0.9
	7	10.9	14.1	4.7	9.3	0.0	3.2	50.6	3.7

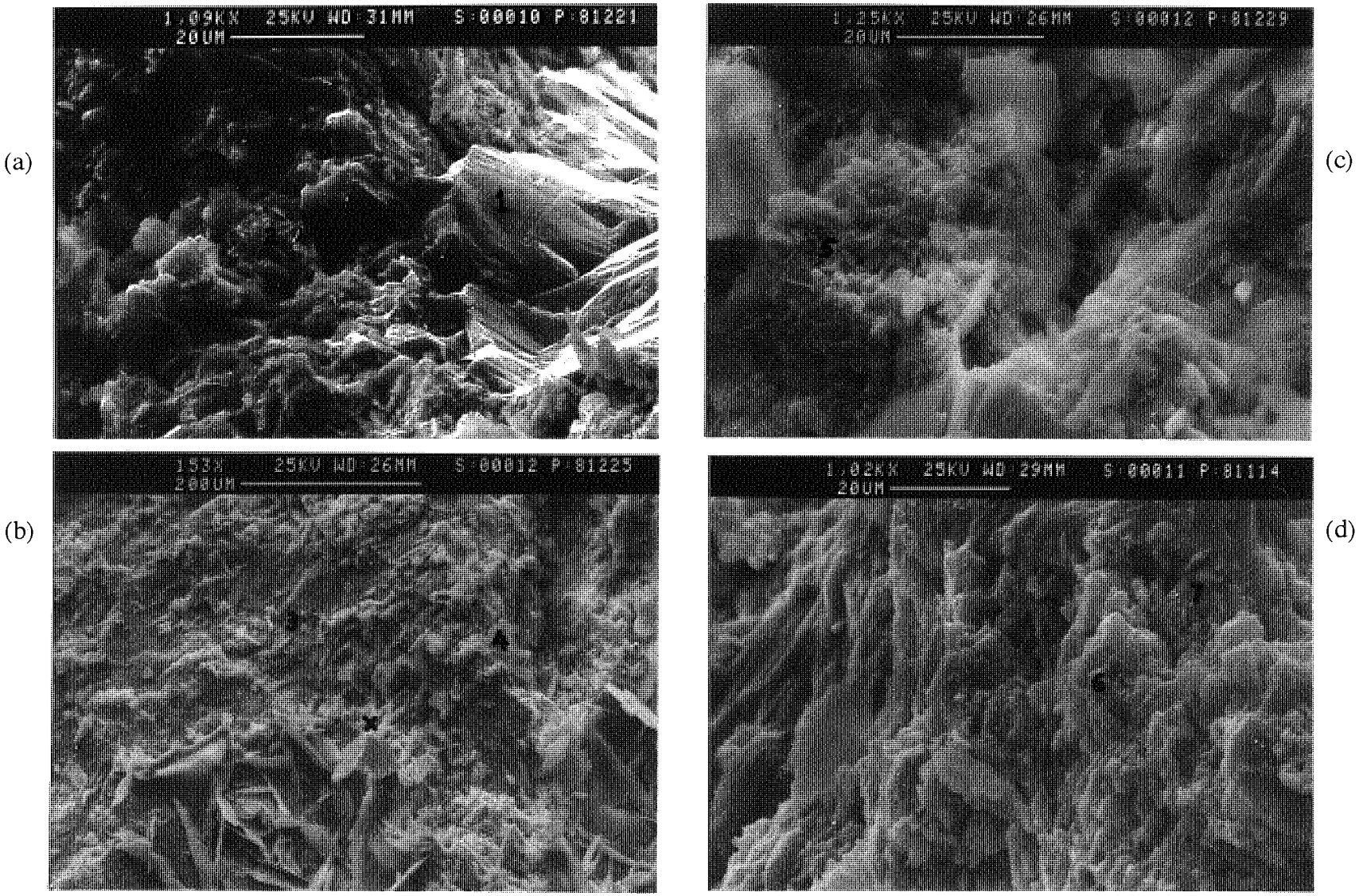

Fig. 8.14: SEM micrographs of fracture surface through; (a) Wet cured unmodified mortar, (b) Wet cured 20% SBR 1 modified mortar, (c) Higher magnification of area X showing featureless morphology, (d) Dry cured 20% SBR 1 modified mortar.

Table 8.9: Spot analyses on fracture surface of mortars

Specimen	Figure 8.14 (Location)	Major Element (% Total)							
		C	O	Al	Si	S	K	Ca	Fe
Unmodified Mortar	1	-	26.7	2.4	11.2	-	-	54.3	0.6
	2	-	43.5	0.1	50.3	-	-	8.3	0.1
Mortar + 20% SBR 1 (WET)	3	9.2	17.3	-	67.9	-	-	5.0	0.4
	4	22.5	12.8	3.1	8.3	0.8	0.7	48.1	2.1
	5	10.0	10.9	4.2	7.7	1.4	0.6	63.4	0.7
Mortar + 20% SBR 1 (DRY)	6	19.0	31.0	0.3	43.3	-	-	5.2	0.6
	7	27.5	17.4	2.9	7.2	1.0	1.3	39.8	1.1

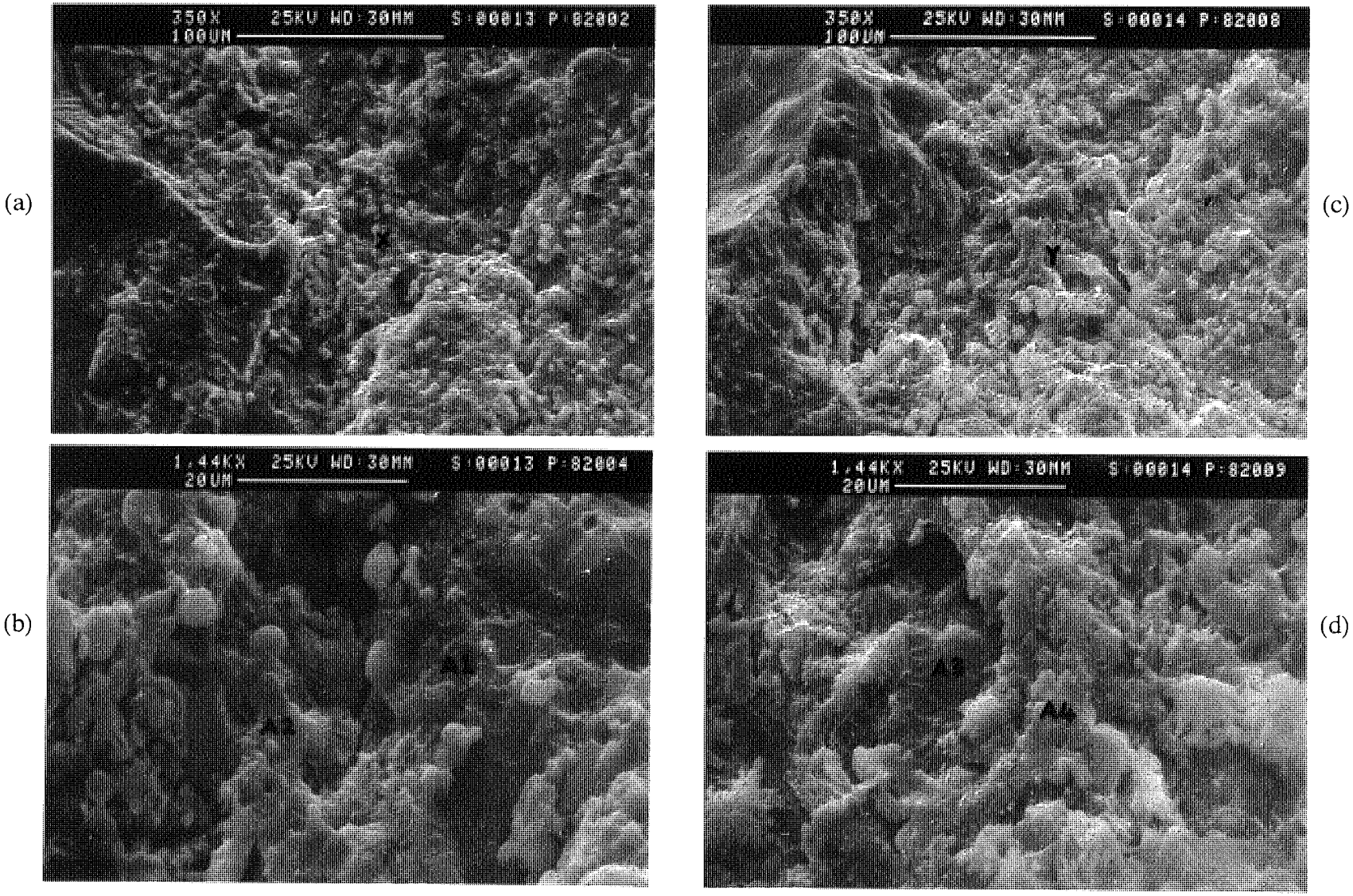

Fig. 8.15: SEM micrographs at the interface of the unmodified mortar patch; (a) Adhesive failure at the patch surface, (b) Higher magnification of area X, (c) Adhesive failure at the substrate surface, (d) Higher magnification of area Y.

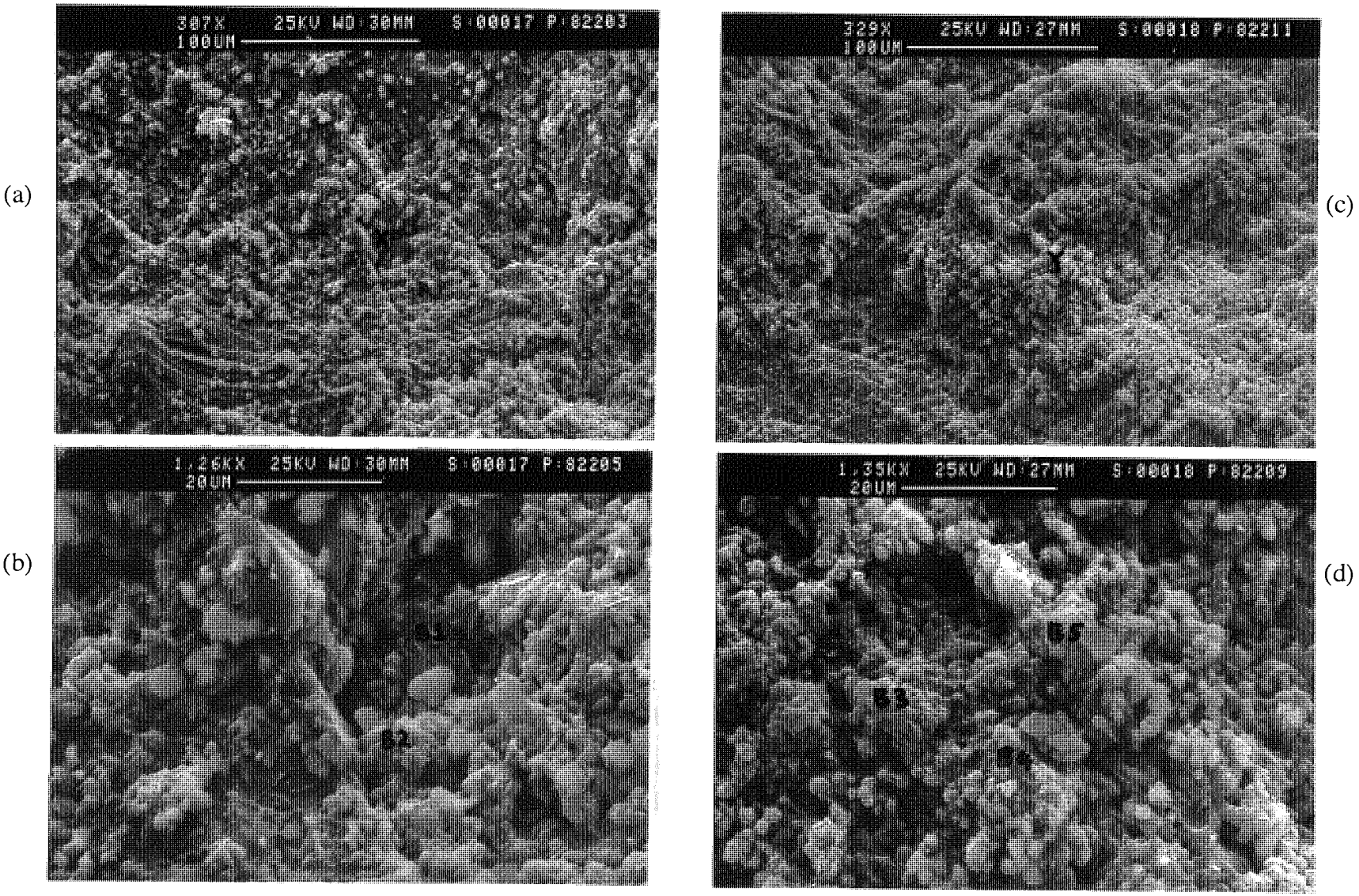

Fig. 8.16: SEM micrographs at the interface of the wet cured 20% SBR 1 modified mortar patch; (a) Adhesive failure at the patch surface, (b) Higher magnification of area X, (c) Adhesive failure at the substrate surface, (d) Higher magnification around area Y.

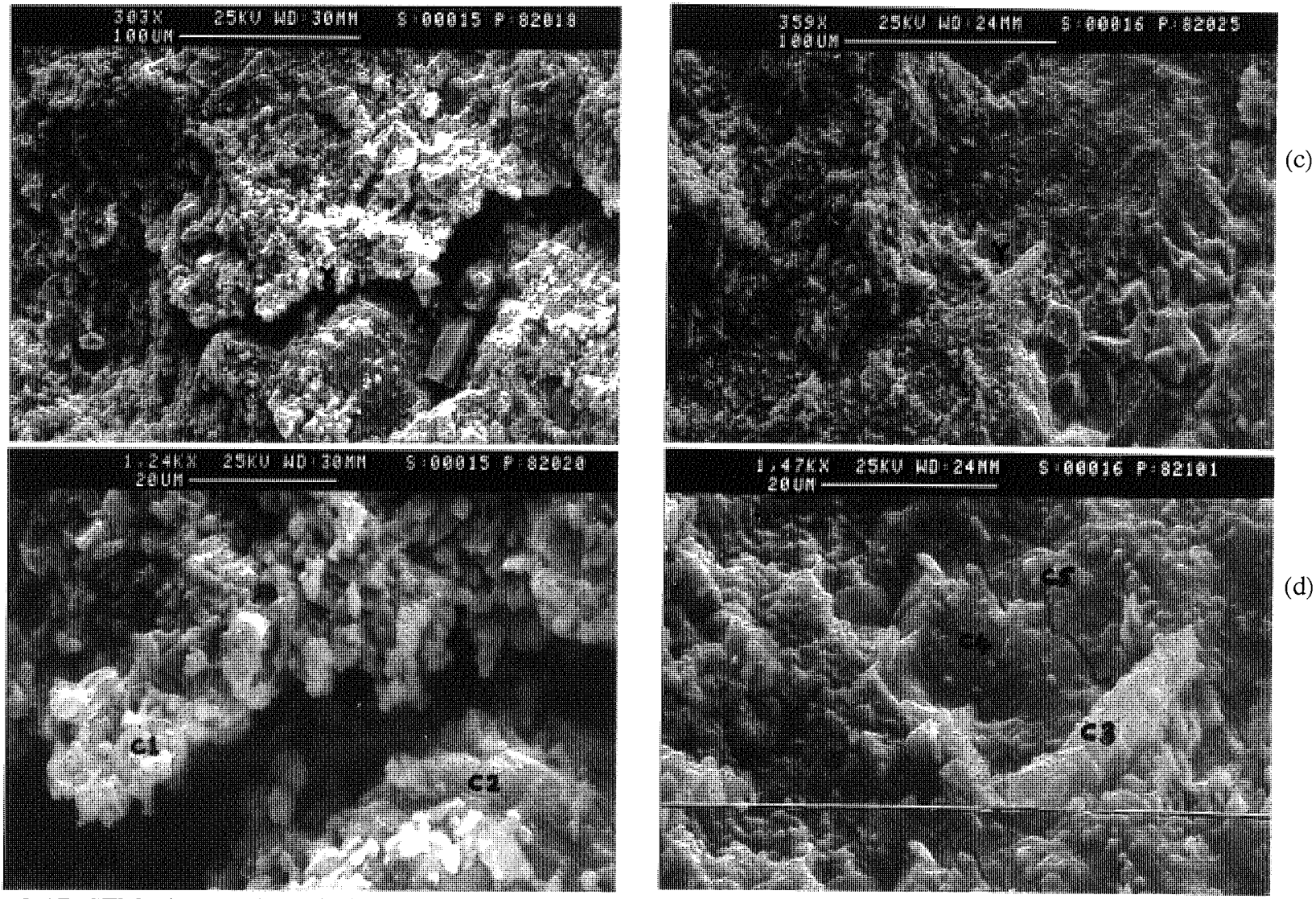

Fig. 8.17: SEM micrographs at the interface of the dry cured 20% SBR 1 modified mortar patch; (a) Cohesive failure through the patch, (b) Higher magnification of area X showing crack and polymer rich clusters, (c) Cohesive failure of the substrate surface, (d) Higher magnification of area Y.

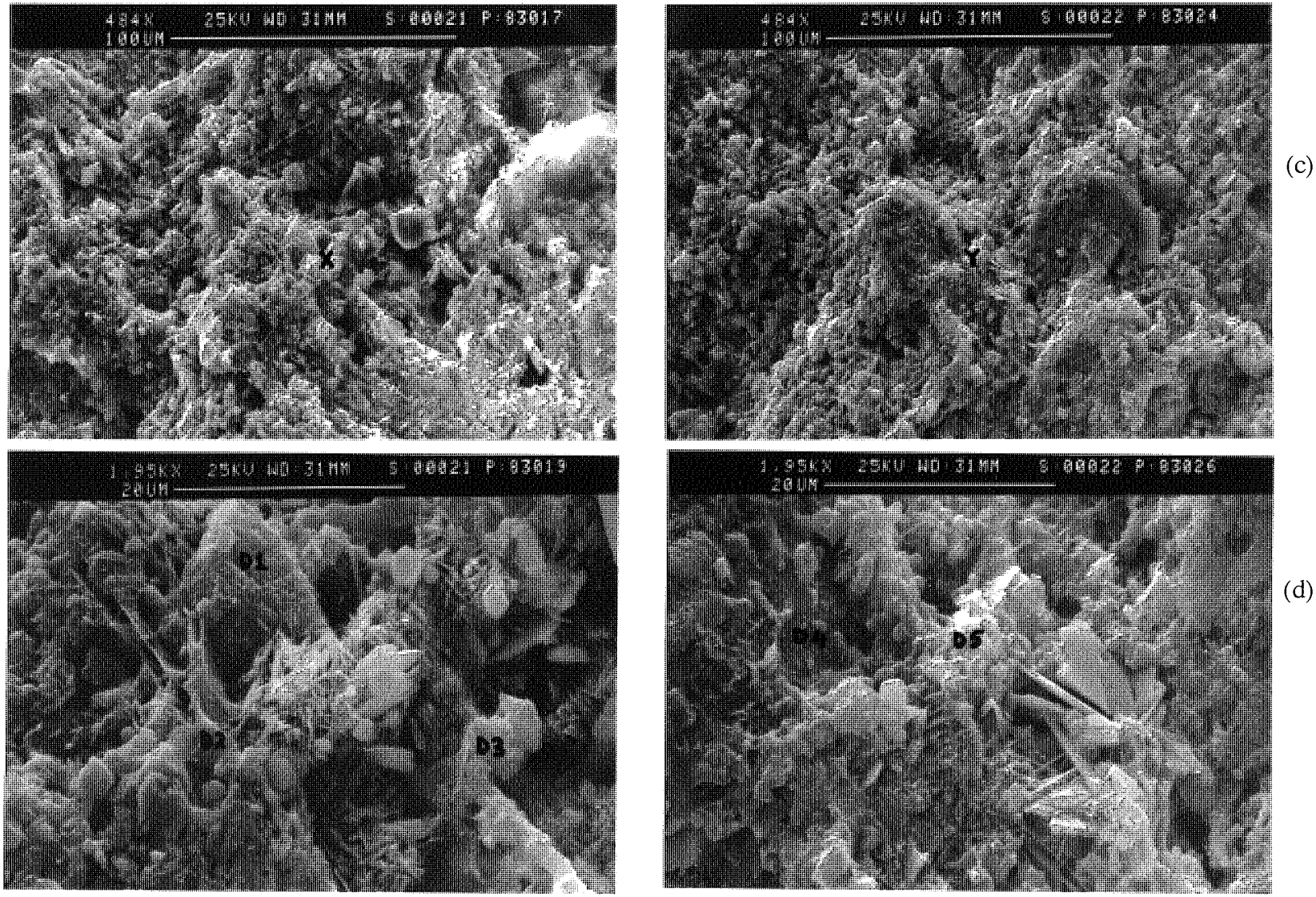

Fig. 8.18: SEM micrographs at the interface of the Dry / Wet cured 20% SBR 1 modified mortar patch; (a) Adhesive failure of the patch, (b) Area X showing polymer intimately combined with well-developed hydration products, (c) Adhesive failure of the substrate surface, (d) Area Y, well-developed hydration products and polymer rich clusters.

Table 8.10: Spot analyses at the patch and mortar substrate.

Specimen	Figure (Location)	Major Element (% Total)							
		C	O	Al	Si	S	K	Ca	Fe
Patch Unmodified Mortar	A1	3.5	12.3	5.0	7.8	2.7	0.5	66.0	1.0
	A2	3.3	11.5	1.6	5.6	-	-	76.0	0.5
Substrate	A3	1.6	15.9	2.0	14.9	0.4	-	63.2	0.6
	A4	7.9	21.5	3.2	7.8	0.7	0.8	54.5	2.5
Patch Mortar + 20% SBR 1 (WET)	B1	23.6	10.2	3.5	53.8	-	0.7	7.1	0.4
	B2	29.0	12.7	1.1	12.0	-	0.3	42.9	0.7
Substrate	B3	27.0	11.9	2.1	9.3	1.3	0.7	45.4	1.4
	B4	5.5	17.1	-	71.4	-	-	5.2	-
	B5	20.8	14.6	0.7	48.0	-	-	14.6	-
Patch Mortar + 20% SBR 1 (DRY)	C1	26.0	12.2	4.9	11.5	-	2.2	38.5	2.7
	C2	10.4	6.7	1.4	73.6	-	-	7.1	0.3
Substrate	C3	22.9	16.9	1.7	8.9	-	2.3	45.0	0.8
	C4	0.9	1.9	0.6	3.3	-	3.5	86.2	2.5
	C5	1.5	4.6	1.6	10.7	-	3.3	75.1	1.1
Patch Mortar + 20% SBR 1 (DRY/WET)	D1	10.6	2.6	4.0	12.7	1.8	0.4	64.2	2.6
	D2	23.9	10.7	3.9	14.3	-	-	43.9	1.3
	D3	37.2	12.1	6.4	14.9	-	5.0	22.6	0.9
Substrtate	D4	8.4	3.5	3.6	11.6	-	-	66.9	4.6
	D5	30.9	10.0	5.1	11.5	-	0.9	36.8	2.3

9 GENERAL DISCUSSION, CONCLUSIONS AND FUTURE WORK

9.1 GENERAL DISCUSSION

9.1.1 Rheological properties of polymer modified cement pastes and mortars

Increasing interest in the use of polymers to modify the properties of cement and concrete has led to more active research being conducted throughout the world. A large number of proprietary polymer systems have been used in recent years and new materials are continuously being introduced for concrete repairs. A large number of methods have been used to test the increasing number of polymer systems.

Investigation on the rheological properties of polymer cement involves certain practical difficulties. The more familiar empirical techniques may no longer be suitable when polymer is added into cement, mortar or concrete. Various procedures and configurations have been used in the past with the hope that a simple rheological technique could be used to assess workability of different polymer systems.

The present studies were carried out on the three groups of polymers namely SBR, Acrylics and Ethylene Vinyl Acetates (EVA). Within the groups, aqueous dispersions and redispersible powdered polymers were compared. In order to limit other variations, only one type of cement was used throughout.

Since the property of mortar or concrete is influenced by its cement phase, the rheological properties of this phase were investigated (Chapter 4). Different amounts of polymers,

water/cement ratios, anti-foaming agent, aqueous component and time were some of the factors investigated that could influence rheological properties.

The rheological properties of cement pastes mixed with polymers have been revealed. Properties such as yield values, plastic viscosity and structural breakdown of different systems have been characterised. The technique could also be used to study the setting time and stiffening behaviour of different polymer systems.

Transient behaviour of cement paste during the dormant period showed that the initial information on setting time and useful working life of different polymer systems could be used as additional information on the hydration mechanisms of polymer modified mixes. The technique could be used to determine early age interactions such as early setting and retarding effects of different polymer systems.

The typical behaviour of mortar compositions and different sands were extensively investigated using the two-point workability apparatus, namely the Visco-Corder (Chapter 5). A suitable paddle was designed and fabricated, and later the apparatus was calibrated using appropriate techniques and theories. The results obtained were comparable to those reported by earlier workers.

The rheology of fresh mortars was found to be typical of a Bingham plastic material and could be measured in fundamental units. The behaviour of the different systems has been determined. The technique was suitable to reveal effects such as the effect of polymer content, particle size of aggregate, aqueous component and w/c on the yield values and plastic viscosity.

The tests clearly showed that not all polymers have the ability to give improved workability at lower w/c. SBR 1 and Ac 1 systems give highly workable mixes in which the workability increases with the increase in polymer content. However, for EVA 1 and

unmodified mortar the workability can only be increased with increase in water content. The technique also confirmed that the amount of water needed to achieve any required workability could be extrapolated or determined quantitatively. This should provide more reliable methods of determining workability of a mix instead of relying on the supplier's normal recommendation to use a "suitable amount of water" to achieve the required workability.

Notwithstanding its limitations, the technique is very useful for determining the influence of parameters such as sand grading, aggregate/cement ratio and type of cement on the workability of polymer modified mortars. It could form the basis of comparing properties such as shrinkage, diffusion resistance and strength of mortars modified with different polymer systems, at constant workability.

The viscometer is only suitable to determine the rheology of cement paste. For practical applications, the rheological properties of polymer modified mortars can be measured using the Visco-Corder. However, the limitations of this technique should be taken into considerations.

9.1.2 The influence of curing, w/c and polymers on pore size distribution and diffusion of chloride ions

Porosity of cement pastes mixed with polymer and the effects of curing conditions were extensively investigated (Chapter 6). Porosity and pore size distribution at different depths from the surface were investigated using the MIP technique. The effects of curing conditions, w/c and polymer content on the pore size distribution were also investigated.

The formation of polymer films and strands within the voids and microcracks exert an influence upon the growth of calcium silicate hydrates and other hydration products. In theory, the presence of polymer in the voids or pores improves hydrated cement pastes'

water-tightness and resistance to the ingress of any deleterious agents. A marked reduction in the number of large pores and an increase in the fine pores will result in the reduction of overall pore volume.

For polymer modified cement pastes, coarser fractions of smaller pores were obtained at the surface of all dry cured specimens. This leads to higher porosity for up to 10 mm or more from the surface. Upon rewetting, the surface layer will rehydrate due to availability of water resulting in the low fraction of smaller pores. However, the porosity of the surface layer of SBR 1 remained higher than those associated with the other layers and polymers. Wet curing for 28 days showed that low porosity can be achieved for all systems. However, wet curing for 28 days may be unrealistic for practical applications of polymer systems despite taking full advantage of cement hydration.

It was expected that with other than water-saturated curing, the water loss through evaporation at the outer surface will be most significant compared with that at some point below the surface. The reduction in the amount of water in the surface layer has an adverse effect on hydration of cement paste. The possibility of a thin layer of hydrophobic polymer film formed at the surface that prevents the water loss or ingress of water was not proven, judging from the pore size distribution results.

As far as polymer modified systems are concerned, the use of low water/cement ratios and dry curing may have advantage over conventional cement provided that proper hydration is uninterrupted at the early part of curing. It is possible to achieve low porosity for polymer modified cement at low water/cement ratio without experiencing difficulty in handling the mix. However, it has been shown that for all polymer systems a curing affected zone (CAZ) of about 10 mm is formed although it does not go beyond 30 mm from the surface.

High surface porosity has been confirmed by the MIP test on the SBR 1 samples before and after the diffusion test (Chapter 7). Although the specimens and curing were different from

the earlier MIP results (Chapter 6), water loss at the surface layer was evident. This suggests that dry curing at low humidity (11% RH) may not necessarily improve the water retention ability of polymer modified systems in which the polymer film may prevent water loss through evaporation.

An improved diffusion coefficient was obtained for SBR 1 modified paste at a depth of 27 mm below the surface. However, the value was only marginally better than the well-cured unmodified paste. This was attributed to the well-hydrated paste and more refined pore size distribution.

The effects of different EVAs on the PSD and diffusion coefficient of chloride ions were not significantly better compared with the unmodified cement paste. In general the performances of EVA, either in the form of emulsions or redispersible powdered were in fact very similar. The present results however revealed that the performance of well-cured EVA 1 & 3 in terms of chloride diffusion only marginally better than the well-cured unmodified paste.

The results for diffusion coefficients, D should be treated with caution as the pore structure may be altered during diffusion test. It was difficult to confirm that reduced diffusivity coefficients were due to either the presence of inter-connecting polymer film or pore structure modification during the diffusion test.

9.1.3 Bond performance of polymer modified cement and mortars

Bond strength of patch repair materials has been examined in this investigation (Chapter 8). The influence of curing, surface preparation and the types of polymer were also investigated. Modes of failure at the bonding interface were examined visually and microscopically. The simple way of assessing the modes of failure at the interface is by

examining it visually. The observation at failure surfaces of the samples can determine the weakest component of the new patch and old substrate.

It has been shown that the tensile pull-off tests were less convenient to perform than the flexural adhesion tests. The adhesive used to glue the dolly to the substrate surface and patch needs to be very reliable, strong and fast to set. A wet surface was found to be unsuitable for most adhesive materials. The flexural adhesion test is relatively simple to prepare and carry out compared with the tensile pull-off.

The results revealed that the optimum bond strength of the polymer modified patch can be obtained in the dry environment. Rewetting the polymer modified systems will lead to much reduced bond strength. Surface treatment and mortar compositions did not significantly influence the mode of failures and adhesion strength compared with the effects of curing conditions, w/c, polymer content and the type of polymers.

9.1.4 Bond mechanisms at the interfaces

The interactions and bonding mechanisms between the new polymer modified patch and the old mortar substrates have not been fully explained. The influence of polymer content, the types of polymer, water/cement ratio and curing conditions on mechanical and physical properties of mortars were investigated. The present investigation was not too successful in revealing the bond mechanisms at the interface.

Improved mechanical bond between polymer and substrate was attributed to the drying out process in which polymer particles coalesce and form a mechanical contact on the surface of substrate. During hydration, chemical interactions do occur between new cement compositions and solid phases of substrate. Therefore two kinds of bonds at the interface can be expected, 1) physical attraction between solid surfaces and 2) chemical bonds. On the basis of visual examinations of the modes of failure, the improved bond mechanism

is reflected by the loci of failure, that is cohesive either through patch or substrate. This is illustrated and shown in Fig. 9.1.

In a wet environment, polymer particles remained in deflocculated forms and unable to coalesce and form a polymer film. Chemical bonds between "new cement" and old solid phases do not proceed well in the presence of dispersed polymer systems, which consist of polymer particles, surfactants and other ingredients.

Theoretically, the micro-mechanical interlocking at the contact zone or the interface can be improved by, 1) increasing the contact area of the substrate and 2) increasing the amount of impermeable polymer network that can penetrate the contact area. However, these two factors do not necessarily guarantee excellent bond and performances of polymer modified patches.

9.1.5 Microstructure of polymer cement composites

The use of the SEM / EDXA technique showed certain interesting features that were in fact very useful to further understand the morphology of polymer modified cement / mortar. However, owing to limitations of the technique results require careful interpretation. The investigation has shown that the morphology of polymer modified cement paste was relatively easy to differentiate compared with the polymer modified mortar. A distinct polymer film similar to that observed by Isenburgh and Vanderhoff (1974) was not detected despite the distinct difference in microstructure compared with the unmodified cement / mortar. Spot analyses were able to locate polymer rich areas in the hardened microstructure.

SEM / EDXA with x-ray dot maps were also very successful in revealing the polymer rich inter-connecting network of the lightly acid etched polymer modified cement. The continuous interconnections of polymer film together with the cement hydrates have been

revealed by lightly etching SBR 1 modified paste. Spot analyses were again useful to support the presence of polymer in the cement paste. However, the analyses indicate that other elements such as oxygen, silicon, calcium and iron were also presence in the carbon rich morphology. This suggests that polymer was intimately combined with other hydration products.

The effect of curing conditions was best explained by the difference in the morphological features of both cement pastes and mortars. The microstructures of wet cured polymer modified cement paste and mortar were more dense than the dry cured. It was also revealed that polymer modified mortar continued to hydrate when the water was available and polymer rich area was more difficult to locate.

9.1.6 Microstucture of the failure interface

The microstructure at the interfaces which reflected performances under different curing conditions has been revealed (Chapter 8). The differences in the morphological features of cement pastes were relatively easy to differentiate compared with mortars.

Wet curing was proven not suitable for polymer modified systems, i.e. SBR 1 latex. The microstructure of a wet cured patch reveals that a micro-mechanical bond was lacking between the patch and substrate. The lack of bond may be attributed to; 1) polymer unable to coalesce and the systems remaining in dispersed forms and 2) lack of chemical interactions between cement and water in the presence of polymer particles and its stabilising systems which form a protective barrier around cement particles. Delayed setting time of SBR 1 was revealed in the rheological studies (Chapter 4).

Upon rewetting, there is a possibility of cement phases rehydrating in the presence of water that changes the morphology of polymer rich hydration products. At the same time water penetrates the gaps or porous hydrates through the capillary suction. This results in further

rearrangements and development of hydration products such as C-S-H and $Ca(OH)_2$ crystals and creating internal stresses at the contact zone. For polymer systems, the surfactants and carboxylic acids may react to form other product in the presence of water. Furthermore, weakening of micro mechanical interlocking at the contact zone may occur as a result of polymer swelling, and this may be simplified as shown in Fig. 9.2. The changes to the more dense morphology of wet cured polymer modified paste has been confirmed by SEM.

9.2 CONCLUSIONS

As well as the conclusions given at the end of each chapter, the main points may be summarised as follows:

(1) Rheological techniques using a viscometer can be used to study the rheological behaviour and early interactions of polymer modified cement pastes.

(2) The Two-point workability test can be used to study performances of polymer modified mortars on the basis of the same workability.

(3) The most severely affected curing zone of the polymer modified cement paste is about 10 mm, although it is unlikely to give any effects at a depth of 30 mm from the surface. Surface porosity of the dry cured polymer modified cement pastes are no better than the well-cured unmodified cement paste.

(4) The effective diffusion coefficients of polymer modified cement paste are not significantly lower than those of well-cured unmodified cement paste.

(5) The optimum bond between polymer modified patch and substrate can only be achieved after moist curing for 24 - 48 hours, followed by exposure to drying at ambient temperature and relative humidity.

(6) The bond strength could be maximised by using a high workability mix but low water/cement ratio.

(7) The micro-mechanical interlocking mechanisms and chemical interactions between polymer and substrate at the interfaces are difficult to reveal and the mechanisms shown are only speculative based on the results of TSM and SEM investigations.

(8) A distinct polymer film was not detected but inter-connecting polymer intimately combined with other hydration products can be revealed.

(9) The role of the polymer network in the cement systems and its effect on general performances of polymer modified cement and mortar are difficult to reveal microscopically.

9.3 FUTURE WORK

The present work has revealed a number of aspects concerning the performance of different polymer systems reviewed from published literature and studied experimentally. In this project it was established that the performances of different groups of polymers vary, and within the group, the performance of latex dispersion and powdered polymers are also likely to vary.

Although the project has revealed certain aspects of the general performances of different polymer systems, its scope and findings may be limited as only laboratory work was undertaken. Furthermore the relative differences in performance of polymer cement

composites are probably dependent on chemical aspects of the polymers. Little could be done regarding the chemistry of polymers simply because not much information was given by the suppliers.

Attempts to reveal interfacial interactions between polymer modified patches and mortar substrates by the mechanical test and microscopic examinations proved to be not very successful. The reason for significant loss of bond in the wet environment was not fully revealed. However, it would appear that application of polymer modified systems should preferably be restricted to dry environments. Several questions remained unsolved from the results of the present project.

The present project could be expanded as follows:

1) A study of the transient behaviour of polymer modified cement pastes using other variables such as a different group of polymers and different types of cements.

2) The optimum w/c and polymer contents based on the same workability could be determined for other types of polymer systems not currently used in patch repair applications.

3) The performance of polymer modified mortars could be studied based on equivalent workability in relation to other physical properties such as long term stress, strain and load carrying capacity on a typical test repair applications.

4) A study could be undertaken of the effects of longer early wet curing of 4 - 5 days at > 95% RH instead of the usual 24 - 48 hours on durability properties such as porosity, PSD, oxygen diffusion, carbonation, chloride ions diffusion and water permeability. This could establish the optimum curing conditions applicable to the polymer modified systems.

5) SEM / EDXA and Backscattered Electron investigations using selective dissolution or acid etching to reveal polymer phase / network in the bulk and at the interface between the new polymer modified patch and old substrate may be useful. However, such a study would require a clear understanding of the limitations of this technique and would probably need to be undertaken with polished, as opposed to fractured, specimens.

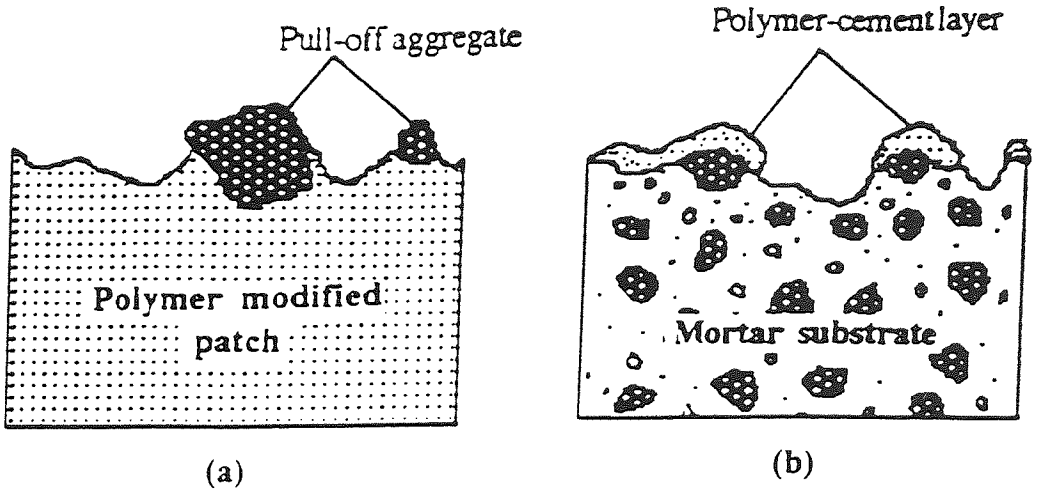

Fig. 9.1: Cohesive failure at the interface; (a) polymer modified patch and (b) mortar substrate

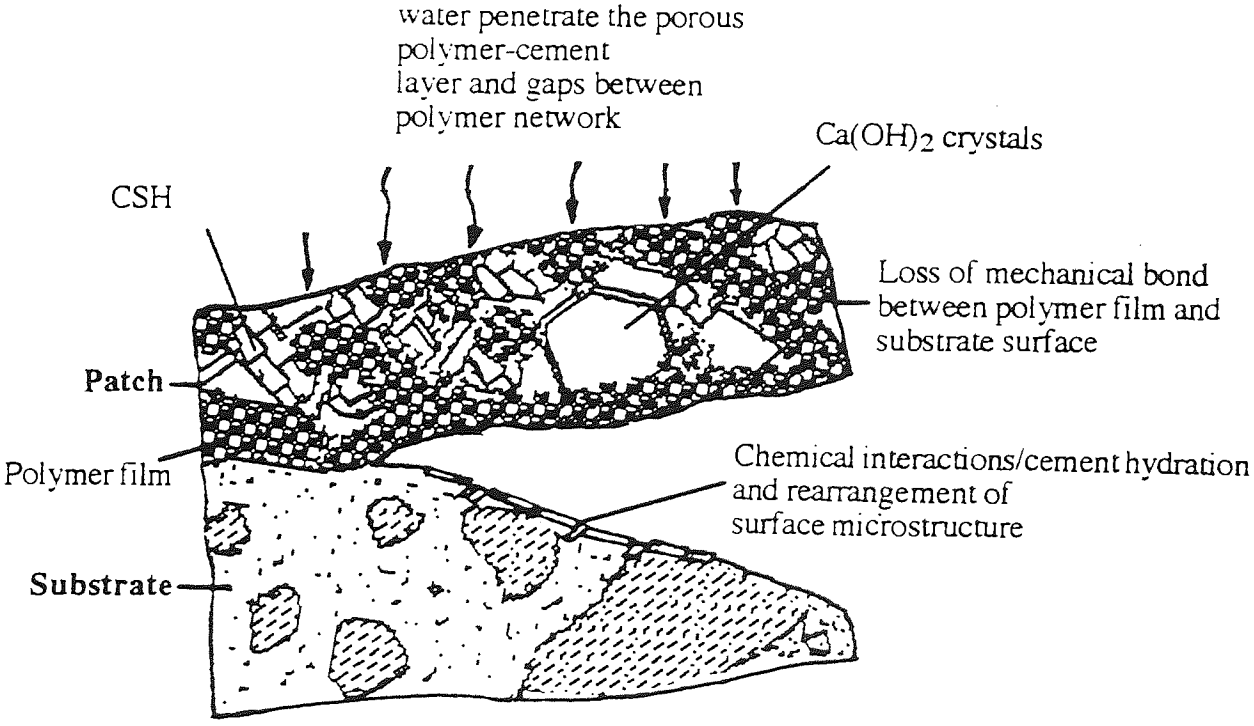

Fig. 9.2: Simplified debonding mechanisms between polymer modified cement patch and substrate

REFERENCES

ACI 548.3R-91 (1991), "State-of-the-art Report on Polymer-Modified Concrete", *American Concrete Institute*, Reported by Committee 548.

ACI 503.5R (1992), "Guide for the Selection of Polymer Adhesives with Concrete", *ACI Materials Journal*, **89**, No. 1, pp. 90-105.

Afridi, M. U. K, Chaudhary, Z. U., Ohama, Y., Demura, K. and Iqbal, M. Z. (1994), "Strength and Elastic properties of powdered and aqueous polymer-modified mortars", *Cement and Concrete Research*, **24**, No. 7, pp. 1199-1213.

Al-Qaser, A. N. F., Griffiths, D. L. and Mangabhai, R. J. (1990), "Diffusions of various ions from sea water into polymer-modified cement paste", in Page, C. L., Treadway, K. W. J. and Bamforth P. B.(eds), *Corrosion of Reinforcement in Concrete*, Elseviour Applied Science, pp. 266-277.

ASTM C939-87: Standard Test Method for Flow of Grout for Pre-placed-Aggregate Concrete (Flow Cone Method).

Atzeni, C., Massida, L. and Sanna, U. (1985), "Model for thixotropic behaviour of cement pastes", *Industrial & Engineering Chemistry Product Research and Development*, **25**, No. 3, pp. 499-504.

Atzeni, C., Massida, L and Sanna, U. (1989), "Rheological behaviour of cements mixed with polymeric lattices", *The International Journal of Cement Composites and Lightweight Concrete*, **II**, No. 4, pp. 215-219.

Austin, S.A. and Robins, P.J. (1993), "Development of patch test to study behaviour of shallow concrete patch repairs", *Magazine of Concrete Research*, **45**, No. 164, pp. 221-229.

Austin, S.A., Robins, P. J. and Pan, Y. (1995), "Tensile bond testing of concrete repairs", *Materials and Structures*, **28**, pp. 249-259.

Banfill, P. F. G. (1980), "Workability of flowing concrete", *Magazine of Concrete Research*, **32**, No. 110, pp. 17-27.

Banfill, P. F. G. (1981), "A viscometric study of cement pastes containing superplasticizers with a note on experimental techniques", *Magazine of Concrete Research*, **33**, No. 114, 1980, pp. 37-47.

Banfill, P. F. G. (1987), "Feasibility study of Coaxial cylinders viscometer for mortar", *Cement and Concrete Research*, **17**, No. 2, pp. 329-339.

Banfill, P. F. G. (1990), "Use of the ViscoCorder to study the rheology of fresh mortar", *Magazine of Concrete Research*, **42**, No. 153, pp. 213-221.

Banfill, P. F. G. (1991), "The rheology of fresh mortar", *Magazine of Concrete Research*, **43**, No. 154, pp. 13-21.

Banfill, P. F. G. (1994), "Rheological methods for assessing the flow properties of mortar and related materials", *Construction and Building Materials*, **8**, No. 1, pp. 43-50.

Banfill, P. F. G., Bellagraa, L. and Benaggoun, L. (1993), "Properties of polymer-modified mortars made with blended cements", *Advances in Cement Research*, **5**, No. 19, pp. 103-109.

Banfill, P. F. G. and Sounders, D.C. (1981), "On the viscometric examination of cement pastes", *Cement and Concrete research*, **11**, No. 3, pp. 363-370.

Barnes, P. and Ghose, A. (1983), "The Microscopy of Unhydrated Portland Cement", in Barnes, P., (ed), *Structure and Performance of Cements*, Applied Science Publishers Ltd. England, pp. 109-203.

Ben-Dor, L., (1983), "Electron and Optical Microscopy", in Ghosh, S. N., (ed), *Advances in Cement Technology*, Pergamon Press Ltd, Headington Hill Hall, Oxford OX3 OBB, England, pp. 733-792.

Ben-Dor, L., Heitner-Wirguin, C. and Diab, H. (1985), "The effect of ionic polymers on the hydration of C_3S", *Cement and Concrete Research*, **15**, No. 4, pp. 681-686.

Bentur, A., Diab, H., Ben-Dor, L. and Heitner-Wirguin, C. (1990), "The effect of in-situ polymerisation on the chloride diffusion and microstructure of polymer-Portland cement pastes and mortars", *Advances in Cement Research*, **3**, No. 9, pp. 1-9.

Berg, W. V. (1979), "Influence of specific surface and concentration of solids upon the flow behaviour of cement pastes", *Magazine of Concrete Research*, **31**, No. 109, pp. 211-216.

BS 882 (1992): Aggregates from natural sources for concrete.

BS 1881 (1983): Testing of concrete:
Part 102: Method of determination of slump.
Part 103 Method of determination of compacting factor
Part 104: Method for determination of Vebe time
Part 105: Method for determination of flow

BS 4551 (1980): Methods of testing mortars, screeds and plasters.

BS 6319 (1984): Testing of resin compositions for use in construction , Part 4: Method for measurement of bond strength (Slant shear method).

BS 6319 (1985): Testing of resin compositions for use in construction , Part 7: Method for measurement of tensile strength.

BS 6319 (1990): Testing of resin and polymer/cement compositions for use in construction , Part 3: Methods for measurement of modulus of elasticity in flexure and flexural strength.

BS 8110 (1985): Part 1; Code of Practice for Design and Construction.

Carther, B. (1994), "Curing : The true storey?", *Magazine of Concrete Research*, **46**, No. 168, pp. 157-161.

Chandra S. and Flodin, F. (1987a), "Interactions of polymers and organic admixtures on Portland Cement hydration", *Cement and Concrete Research*, **17**, No. 6, pp. 875-890.

Chandra S. and Flodin, F. (1987b), "Interactions of polymer with Calcium Hydroxide and Calcium Trisilicate", *American Concrete Institute Special Publication*, SP 119-14, Ottawa Conference, pp. 263-268.

Chappuis, J. (1991), "Rheological measurements with cement pastes in viscometers: A comprehensive approach", in Banfill, P. F. G. (ed), *Rheology of Fresh Cement and Concrete*, E & FN Spon, London, pp. 3-12.

Comite Euro-International Du Beton (CEB) (1992), *Durable Concrete Structure, Design Guide*, Thomas Telford Ltd., England.

Concrete Society Technical Report (1984), "The Repair of Concrete Damaged by Reinforcement Corrosion", *Concrete Society Technical Report No 26*, The Concrete Society, 3 Etongate, 112 Windsor Road, Slough SL1 2JA, England.

Concrete Society Technical Report (1994), "Polymers in Concrete", *Concrete Society Technical Report No 39*, The Concrete Society, 3 Etongate, 112 Windsor Road, Slough SL1 2JA, England.

Cook, R. A. and Hover, K. C. (1991), "Experiments on the contact angle between mercury and hardened cement paste", *Cement and Concrete Research*, **21**, No. 6, pp. 1165-1175.

Cook, R. A. and Hover, K. C. (1993), "Mercury Porosimetry of Cement-Based Materials and Associated Correction Factors", *ACI Materials Journal*, **90**, No. 2, pp. 152-161.

Cox, R. N., Coote, A. T. and Davies, H. (1989), "Results of exposure tests to evaluate repairs to reinforced concrete in marine conditions", *BRE Information Paper*, Garston, Watford WD2 7JR, England.

Cresson, L. (1923), *British Patent* 191,474; January 12.

Dennis, R. (1985), "Latex in the Construction Industry", *Chemistry and Industry*. No. 15, pp. 505-511.

Dennis, R. (1988), "Polymer Dispersions or Lattices", in Hewlett, P. (ed), *Cement Admixtures, Uses and Applications*, Longman Scientific & Technical, 2nd. Edition 1988, Chapter 9, pp. 130-143.

Dennis, R. (1992), "Polymer Dispersions", in Doran, D. K. (ed), *Construction Materials Handbook*, Butterworth-Heineman Ltd, Linacre House, Jordan Hill, Oxford OX2 8DP, pp. 39/1-39/12.

Department of Transport (1986), "Materials for Repair of Concrete Highway Structures", *Departmental Standard BD 27/86*, Department of Transport, London.

Dexiang, S. and Winslow, D. N. (1985), "Contact angle and damage during mercury intrusion into cement paste", *Cement and Concrete Research*, **15**, No. 4, pp. 645-654.

Diab, H., Bentur, A., Hetner-Wirguin, C. and Ben-Dor, L. (1988), "The diffusion of Cl^- ions through Portland cement and Portland cement-polymer pastes", *Cement and Concrete Research*, **18**, No. 5, pp. 715-722.

Domone, P. L. and Thurairatnam, H. (1991), "The relationship between early age property measurements on cement pastes", in Banfill P. F. G. (ed), *Rheology of Fresh Cement and Concrete*, E & FN Spon, London, pp. 181-191.

Emberson, N. K. and Mays, G. C. (1990a), "Design of Patch Repairs: Measurements of physical and mechanical properties of repair systems for satisfactory performance, Protection of concrete", in Dhir, R. K. and Green, J. W. (eds), *Proceedings of Int. Conference*, held at the University of Dundee, Scotland, U.K., 11-13 September 1990, E & F.N. Spon, pp. 937-954.

Emberson, N. K. and Mays, G. C. (1990b), "Significance of property mismatch in the patch repair of structural concrete, Part 1: Property of Repair Systems", *Magazine of Concrete Research*, **42**, No. 152, pp. 147-160.

Eyre, J. R. and Domone, P. L., (1985), "The slant shear testing of bond of repair materials for concrete structures", *The Second International Coference on Structural Faults and Repairs*, 30 April - 2nd May, 1985, organised by The Institution of Civil Engineers, London.

Eyring, Y., (1936), *Journal of Chemical Physics*, American Institute of Physics, **4**, pp. 283.

Feldman, R. F. and Beaudoin, J. J. (1991), "Pretreatment of hydrated cement pastes for mercury intrusion measurements", *Cement and Concrete Research*, **21**, pp. 297-308.

French, W. J., (1991), "Concrete Petrography: A review", Quarterly Journal of Engineering Geology", **24**, No. 1, pp. 17-48.

Gane, P. A. C., Kettle, J. P., Mathews, G. P., and Ridgway, C. J. (1995), "*Void space structure of compressible polymer spheres and consolidated calcium carbonate paper-coating formulations*", University of Plymouth, Plymouth PL4 8AA, UK, Private communication,

Gregory, T. and O'Keefe, S. J. (1991), "Rheological measurements with cement pastes in viscometers: A comprehensive approach", in Banfill, P. F. G. (ed), *Rheology of Fresh Cement and Concrete,* E & FN Spon, pp. 69-79.

Helmuth, R. A. (1980), "Structure and rheology of fresh cement paste", *7th. International Congress on the Chemistry of Cement*, Paris, **III**, Editions Septima, 14 rue Falguiere, 75015 Paris, pp. VI-0/016-VI-0/30.

Herschel, W. H. and Bulkley, R. (1926), "Measurement of consistency as applied to rubber-benzene solutions", *Proceedings of the American Society for Testing Materials*, **26**, No. 82, pp. 24.

Hornung, F. (1991), "The use of the Brabender ViscoCorder to study the consistency of fresh mortar by Two-Point Tests", in Banfill P. F. G. (ed), *Rheology of Fresh Cement and Concrete*, E & FN Spon, London, pp. 227-307.

Isenburgh, J. E. and Vanderhoff, J. W. (1974), "Hypothesis for Reinforcement of Portland Cement by Polymer Latexes", *Journal American Ceramic Society*, **57**, No. 6, pp. 242-245.

Jawed, I., Skalny, J. and Young, J. F. (1983), "Hydration of Portland Cement", in Barnes, P., (ed), *Structure and Performance of Cements,* Applied Science Publishers Ltd. England, Chapter 6, pp. 237-317.

Jennings, H. M., (1983), "The Developing Microstructure in Portland Cement", in Ghosh, S. N., (ed), *Advances in Cement Technology*, Pergamon Press Ltd, Headington Hill Hall, Oxford OX3 OBB, England, pp. 349-396.

Jinping, L., Liping, X. and Xueli, W. (1990), "Diffusion of chloride ions in polymer modified cement paste", in Huang, Y, Wu, K. and Chen, Z. (eds), *Proceeding of Sixth International Congress on Polymers in Concrete* International Academic Publishers, Beijing, China, pp. 268-274.

JIS A 1172: Method of Test for Strength of Polymer-Modified Mortars, *Japanese Industrial Standards.*

Johnson, D. I. (1988), "Further investigations of the properties of polymer modified cements for use in the immobilisation of ILW", *United Kingdom Atomic Energy Authority, Materials Development Division, Harwell Laboratory*, Oxfordshire, England

Jones, T. E. R. and Taylor, S. (1977), "A mathematical model relating the flow curve of a cement paste to its water/cement ratio", *Magazine of Concrete Research*, **29**, No. 101, pp. 207-212.

Judge, A. I., Cheriton, L. W. and Lambe, R. W. (1986), "Bonding systems for concrete repair- An assessment of commonly used materials", *Proceedings of an International Symposium organised by RILEM Technical Committee 52-Resin Adherence to Concrete*, Paris, 16-19 September, pp. 661-681.

Justnes, H. and Dennington, S. P. (1988), "Designing latex for cement and concrete", *Nordic Concrete Research*, Norske Betongforening, Oslo, Publication No. 7, pp. 188-206.

Justnes, H. and Øye, B. A. (1990a), "Protecting concrete against chloride ingress by latex additions", in Huang, Y, Wu, K. and Chen, Z. (eds), *Proceeding of Sixth International Congress on Polymers in Concrete,* International Academic Publishers, Beijing, China, pp. 261-267.

Justnes, H. and Øye, B. A. (1990b), 'The microstructure of polymer cement mortars", *Nordic concrete Research*, Publication No. 9, Norske Betongforening, Oslo, pp. 69-80.

Justnes, H. and Øye, B. A. (1992a), "A microstructural approach to an evaluation of factors affecting the performance of polymer cement concrete and mortars (PCC)", in Paturoev, V. V. and Serykh, R. L. (eds). *Polymers in Concrete, VII International Congress on Polymers in Concrete* , Moscow, pp. 184-192.

Justnes, H. and Øye, B. A. (1992b), "Chloride penetration in mortars modified with different Acrylic latexes", in Paturoev, V. V. and Serykh, R. L. (Eds). *Polymers in Concrete, VII International Congress on Polymers in Concrete* , Moscow, pp. 124-134.

Kirkpatrick, S. M. (1925), *British Patent* 242,345; November 6.

Krieger, I. M. and Maron, S. H. (1951), "Rheology of synthetic latex. I. Test of some flow equations", *Journal of Colloid Science*, **6**, No. 5, pp. 528-538.

Kuhlmann, L. A. (1987), "Application of Styrene-Butadiene Latex Modified Concrete", *Concrete International*, **9**, No. 12, pp. 48-53.

Kuhlmann, L. A. (1990), "Styrene-Butadiene Latex-Modified Concrete: The ideal concrete repair material?", *Concrete International*, **12**, No. 10, pp. 59-65.

Lapasin, R., Papo, A., and Rajgelj, S. (1983), "Flow behaviour of fresh cement pastes: A comparison of different rheological instruments and techniques", *Cement and Concrete Research*, **13**, No. 3, pp. 349-356.

Larbi, J. A. and Bijen, J. M. J. M. (1990), "Interaction of polymers with Portland cement during hydration: A study of the chemistry of the pore solution of polymer-modified cement systems", *Cement and Concrete Research*, **20**, No. 1, pp. 139-147.

Lavelle, J. A. (1988), "Acrylic latex-modified Portland cement", *ACI Materials Journal*, **85**, No. 1, pp. 41-48.

Leeming, M. B. (1993), "Standard tests for repair materials and coatings for concrete, Part 2: Permeability tests", *CIRIA, Technical Note 140*, Construction Industry Research and Information Association, 6 Storey's Gate, Westminster, London SW1P 3AU.

Lees, T. P. (1992), "Deterioration mechanisms", in Mays, G., *Durability of concrete structures, investigation, repair, protection*, E & FN Spon, Chapter 2, pp. 10-36.

Lefebure, V. (1924), *British Patent* 217,279; June 5.

Lenk, R. K. (1978), *Polymer Rheology*, Applied Science Publishers Ltd., London.

Lewandowski, R. and Wolter, G. R. (1981), "Early stiffening behaviour of cement and concrete", *Betonwerk + Fertigteil-Technik*, Heft 5.

Lewis, W. J. and Lewis, G. (1990), "The influence of polymer latex modifiers on the properties of concrete", *Composites*, **21**, No. 6, pp. 487-494.

Marosszeky, M., Yu, J. G. and Ng, C. M. (1991), "Study of bond in concrete repairs", *ACI Special Publication*, SP 126-70, Part 2, pp. 1331-1354.

Marusin, S. L. (1987), "Microstructure, Pore Characteristics, and Chloride Ion Penetration in Conventional Concrete and Concrete Containing Polymer Emulsions", *American Concrete Institute Special Publication* SP 99-9, pp. 135-150.

Mathews, G. P. (1994), "A new dimension in mercury porosimetry", *The Micro Report*, Micromeritics Instrument Corporation, One Micrometics Drive, Norcross, G. A. 30093-1877, USA, **5**, No. 3, pp. 1-4.

McCurrich, L. H. (1993), "International Developments in Polymer Cements", *International Symposium on Innovative World of Concrete*, Rotterdam, **Vol. 1**, pp. KN101-KN125.

Mcleish, A. (1993), "Standard tests for repair materials and coatings for concrete, Part 1: Pull-off tests", *CIRIA, Technical Note 139*, Construction Industry Research and Information Association, 6 Storey's Gate, Westminster, London SW1P 3AU.

Moukwa, M. and Aitcin, P. C. (1988), "The effect of drying on cement pastes pore structure as determine by mercury porosimetry", *Cement and Concrete Research*, **18**, No. 5, pp. 745-752.

Naderi, M., Cleland, D. J. and Long, A. E. (1987), "Polymer modified repair materials-strength and durability", *5th. International Congress on Polymer in Concrete*, Brighton, England, pp. 335-341.

Neville, A. M. (1993), *Properties of Concrete*, Longman Scientific & Technical, U.K., 3rd. Edition.

Ngala, V. T, Page, C. L., Parrott, L. J. and Yu, S. W. (1995), "Diffusion in Cementitious Materials: II. Further investigations of chloride and oxygen diffusion in well-cured OPC and OPC/30% PFA pastes", *Cement and Concrete Research*, **25**, No. 4, pp. 819-826.

Ohama, Y. (**1984**), "Polymer-Modified Mortars and Concretes", in Ramachandran, V.S. (ed), *Concrete Admixture Handbook, Properties, Science and Technology,* Noyes Publications, Mill Rd., Park Ridge, New Jersey, 07656 USA, 1984, Chapter 7, pp. 337-429.

Ohama, Y. (**1987**), "Principle of Latex Modification and some Typical Properties of Latex Modified Mortars and Concretes", *ACI Materials Journal,* **84**, No. 6, pp. 511-518.

Ohama, Y., Demura, K., Nagao, H. and Ogi, T. (**1986**), "Adhesion of polymer-modified mortars to ordinary cement mortar by different test methods", in Sasse, H.R.(ed), *Adhesion between polymers and concrete, Proceedings of International Symposium Organised by RILEM Technical Committee 52,* Chapman and Hall, pp. 719-729.

Ohama, Y. and Kan, S. (**1982**), "Effects of specimen size on Strength and Drying shrinkage of polymer-modified concrete", *The International Journal of Cement Composites and Lightweight Concrete*, **4**, No. 4, pp. 229-233.

Orr, C. (**1969**), "Review paper: Application of Mercury Penetration to Mercury Analysis", *Powder Technology*, **3**, pp. 117-123.

Øye, B. A. (**1989**), *Repair Systems for Concrete - Polymer Cement Mortars, An evaluation of some polymer systems,* PhD Thesis, Institutt For Uorganisk Kjemi, Norges Tekniske Hogskole, Universitetet I Trondheim.

Øye, B. A. and Justnes, H. (**1991a**), "Carbonation resistance of polymer cement mortars (PCC)", in Malhotra, V. M. (ed), *Second International Conference on Durability of Concrete*, American Concrete Institute SP-126-55, Montreal, Canada, **II**, pp. 1031-1046.

Øye, B. A. and Justnes, H. (**1991b**), "Microstructure and performance of polymer cement mortars (PCC) based on latex", in Schorn, H. H. and Middel, M. (Eds), *International Symposium on Concrete Polymer Composites*, Bochum, Germany, pp. 9-17.

Page, C. L., Short, N. R. and El Tarras, A. (**1981**), "Diffusion of chloride ions in hardened cement pastes", *Cement and Concrete Research*, **11**, No. 4, pp. 395-406.

Pareek, S. N., Ohama, Y. and Demura, K. (**1990**), *Adhesion of Bonded Mortar to Polymer-Cement Paste Coated Mortar Substrates*, Interfaces in Cementitious Composites, RILEM, Edited by J.C. Maso, E & FN Spon, pp. 89-98.

Parrott, L. J. (1995), "Influence of cement type and curing on the drying and air permeability of cover concrete", *Magazine of Concrete Research*, **47**, No. 171, pp. 103-111.

Plum, D. R. (1990), "The behaviour of polymer materials in concrete repair and factor influencing selection", *The Structural Engineer*, **88**, No. 17, 4 Sept. 1990, pp. 337-345.

R. Critchley Ltd. and Bond, A. E. (1932), British Patent 369,561; March 17.

Riley, V. R. and Razl, I. (1974), "Polymer additives for cement composites: A review", *Composites*, **5**., No. 1, January, pp. 27-33.

Robins, P. J. and Austin, S. A. (1995), " A unified failure envelope from the evaluation of concrete repair bond test", *Magazine of Concrete Research*, **47**, No. 170, pp. 57-68.

Sasse, H. R. and Fiebrich, M. (1983), "Bonding of polymer materials to concrete", *Materials and Structures*, **94**, pp. 293-301.

Shaw, I. M. (1989), " Interactions between Organic Polymers and Cement Hydration Products", *PhD Thesis*, The University of Aston in Birmingham.

Sherman, P. (1970), *Industrial Rheology*, Academic Press, London and New York, Chapter 1 and 2, pp. 1-96.

Shi, D. and Winslow, D. N. (1985), "Contact angle and damage during Mercury intrusion into cement paste", *Cement and Concrete Research*, **15**, No. 4, pp. 645 - 654.

Su, Z. and Bijen, J. M. J. M. (1990), "The effect of polymer dispersions on the interface between cement paste and aggregate", in Huang, Y., Wu, K. and Chen, Z.(eds), *Proceeding of Sixth International Congress on Polymers in Concrete*, International Academic Publishers, Beijing, China, pp. 474-481.

Su, Z., Bijen, J. M. J. M. and Larbi, J. A. (1991a), " The influence of polymer modification on adhesion of cement pastes to aggregates", *Cement and Concrete Research*, **21**, No. 5, pp. 727-736.

Su, Z., Bijen, J. M. J. M. and Larbi, J. A. (1991b), " The interface between polymer-modified cement paste and aggregates", *Cement and Concrete Research*, **21**, No. 6, pp. 983-990.

Tabor, L. J. (1992), "Repair materials and techniques", in Mays, G. (ed), *Durability of Concrete Structures, Investigation, repair, protection*, E & FN Spon, Chapter 4, pp. 82-129.

Tattersall, G. H. (1973), "The rationale of a two-point workability test", *Magazine of Concrete Research*, **25**, No. 84, pp. 169 -172.

Tattersall, G. H. (1991), *Workability and Quality of Concrete*, E & FN Spon, London 1st. Edition.

Tattersall, G. H. and Bloomer, S. J. (1979), "Further development of the two-point test for workability and extension of its range", *Magazine of Concrete Research*, **31**, No. 109, pp. 202-210.

Wagner, H. B. (1965), "Polymer-modified hydraulic cements", *Industrial and Engineering Chemistry Product Research and Development*, **4**, No. 3, pp. 191-196.

Wagner, H. B. (1966), "Compressive strength of polymer-modified hydraulic cements", *Industrial and Engineering Chemistry Product Research and Development*, **5**, No. 2, pp. 149-152.

Wagner, H. B. and Grenley, D. G. (1978), "Interphase effects in polymer-modified hydraulic cements", *Journal of Applied Polymer Science*, **22**, No. 3, pp. 813-822.

Wallevik, O. H. and Gjorv, O. E. (1990), "Modification of the two-point workability apparatus", *Magazine of Concrete Research*, **42**, No 152, pp. 135-142.

Walters, D. G. (1990), "Comparison of Latex-Modified Portland Cement Mortars for Concrete", *ACI Materials Journal*, **87**, No. 4, pp. 371-377.

Washburn, E. W. (1921), "Note on a Method of Determining the Distribution of Pore Sizes in a Porous Material", *Proceedings of the National Academy of Sciences*, **7**, No. 3, pp. 115 -116.

Winslow, D. N. and Diamond, S. (1970), "A Mercury Porosimetry Study of the evolution of porosity in Portland cement", *Journal of Materials*, **5**, No. 3, pp. 564-585.

Wolter, G. R. (1985), "Measuring relative viscosity in cement mortars: measuring principle and fields of application", *Betonwerk + Fertigteil-Technik*, Heft 12, pp. 816-824.

Zeng, S. (1996), "Polymer Modified Cement: Hydration, Microstructure and Diffusion Properties", *PhD Thesis*, The University of Aston in Birmingham.

Zeng, S., Short, N. R., and Page, C. L. (1996), "Early age hydration kinetics of polymer modified cement, *Advances in Cement Research* , **28**, No. 29, pp. 1-9.